frontiers | Research Topics

New insights in sepsis pathogenesis and renal dysfunction: Immune mechanisms and novel management strategies

Edited by
Alessandra Stasi and Patrick M. Honore

Published in
Frontiers in Immunology
Frontiers in Medicine

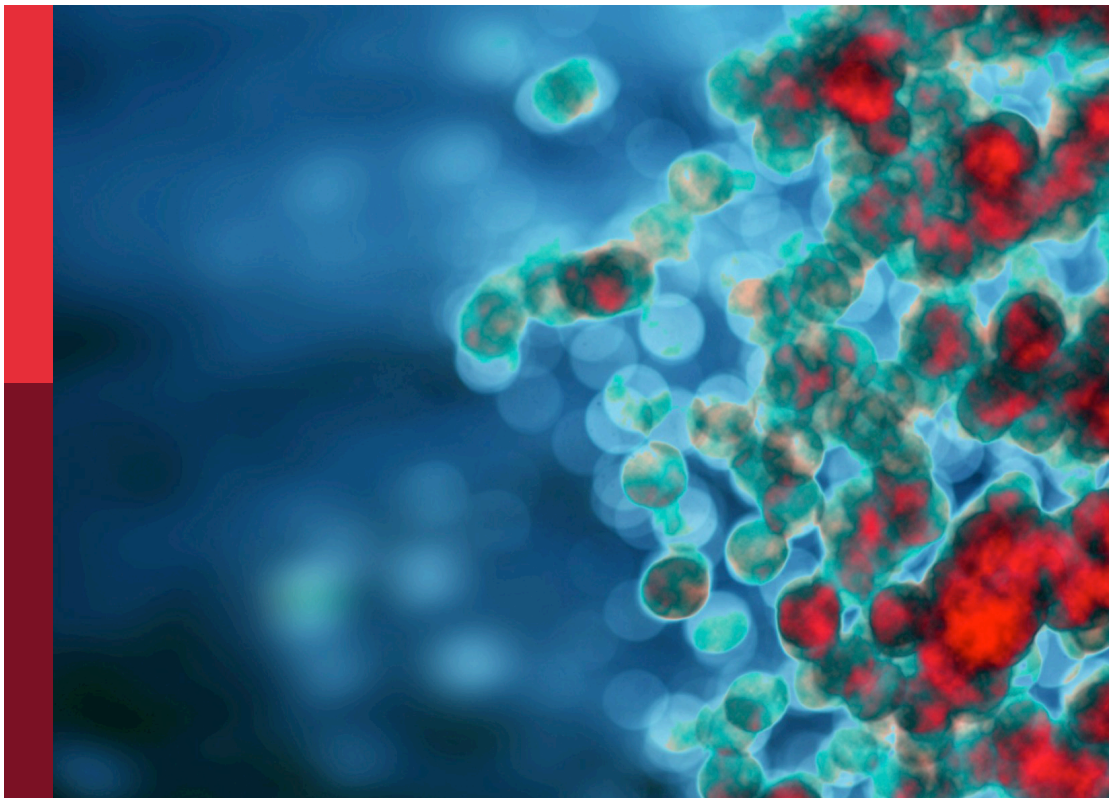

ISSN 1664-8714
ISBN 978-2-83251-985-1
DOI 10.3389/978-2-83251-985-1

About Frontiers

Frontiers is more than just an open access publisher of scholarly articles: it is a pioneering approach to the world of academia, radically improving the way scholarly research is managed. The grand vision of Frontiers is a world where all people have an equal opportunity to seek, share and generate knowledge. Frontiers provides immediate and permanent online open access to all its publications, but this alone is not enough to realize our grand goals.

Frontiers journal series

The Frontiers journal series is a multi-tier and interdisciplinary set of open-access, online journals, promising a paradigm shift from the current review, selection and dissemination processes in academic publishing. All Frontiers journals are driven by researchers for researchers; therefore, they constitute a service to the scholarly community. At the same time, the *Frontiers journal series* operates on a revolutionary invention, the tiered publishing system, initially addressing specific communities of scholars, and gradually climbing up to broader public understanding, thus serving the interests of the lay society, too.

Dedication to quality

Each Frontiers article is a landmark of the highest quality, thanks to genuinely collaborative interactions between authors and review editors, who include some of the world's best academicians. Research must be certified by peers before entering a stream of knowledge that may eventually reach the public - and shape society; therefore, Frontiers only applies the most rigorous and unbiased reviews. Frontiers revolutionizes research publishing by freely delivering the most outstanding research, evaluated with no bias from both the academic and social point of view. By applying the most advanced information technologies, Frontiers is catapulting scholarly publishing into a new generation.

What are Frontiers Research Topics?

Frontiers Research Topics are very popular trademarks of the *Frontiers journals series*: they are collections of at least ten articles, all centered on a particular subject. With their unique mix of varied contributions from Original Research to Review Articles, Frontiers Research Topics unify the most influential researchers, the latest key findings and historical advances in a hot research area.

Find out more on how to host your own Frontiers Research Topic or contribute to one as an author by contacting the Frontiers editorial office: frontiersin.org/about/contact

New insights in sepsis pathogenesis and renal dysfunction: Immune mechanisms and novel management strategies

Topic editors

Alessandra Stasi — University of Bari Aldo Moro, Italy

Patrick M. Honore — CHU UCL Namur Site Godinne, Belgium

Citation

Stasi, A., Honore, P. M., eds. (2023). *New insights in sepsis pathogenesis and renal dysfunction: Immune mechanisms and novel management strategies*. Lausanne: Frontiers Media SA. doi: 10.3389/978-2-83251-985-1

Table of contents

frontiers | Frontiers in Immunology

TYPE Editorial
PUBLISHED 08 March 2023
DOI 10.3389/fimmu.2023.1176620

OPEN ACCESS

EDITED AND REVIEWED BY
Pietro Ghezzi,
University of Urbino Carlo Bo, Italy

*CORRESPONDENCE
Alessandra Stasi
alessandra.stasi@uniba.it

SPECIALTY SECTION
This article was submitted to Inflammation, a section of the journal Frontiers in Immunology

RECEIVED 28 February 2023
ACCEPTED 01 March 2023
PUBLISHED 08 March 2023

CITATION
Stasi A and Honore PM (2023) Editorial: New insights in sepsis pathogenesis and renal dysfunction: Immune mechanisms and novel management strategies. *Front. Immunol.* 14:1176620. doi: 10.3389/fimmu.2023.1176620

Editorial: New insights in sepsis pathogenesis and renal dysfunction: Immune mechanisms and novel management strategies

Alessandra Stasi[1]* and Patrick M. Honore[2]

[1]Nephrology, Dialysis and Transplantation Unit, Department of Precision and Regenerative Medicine and Ionian Area, University of Bari "Aldo Moro", Bari, Italy, [2]Intensive Care Unit (ICU) Department, Université Catholique de Louvain (UCL) Louvain Medical School, Centre Hospitalier Universitaire (CHU) UCL Godinne Namur, Yvoir, Belgium

KEYWORDS

sepsis, molecular mechanism, omics, animal model, therapeutic strategy, immunology & infectious diseases, acute kidney injury

Editorial on the Research Topic

New insights in sepsis pathogenesis and renal dysfunction: Immune mechanisms and novel management strategies

Sepsis is one of the main causes of admission in Intensive Care Units (ICU) with an estimated 13.7 million of deaths globally for 2019 (1). Sepsis is a complex disease characterized by a systemic inflammatory response that arises during infection. Gram negative bacteria are considered the common pathogens involved in sepsis disease (2). The host response includes pro-inflammatory and anti-inflammatory mechanisms that are necessary for pathogen clearance, but in this context, they could become impaired and lead to systemic organ damage (3). There is currently no cure for this disease which affects a broad set of population starting from infants to elderly people. Nevertheless, there were some treatment attempts targeting either the endotoxin inactivation/elimination or some cytokines which are supposedly keys in the detrimental cytokine storm induced by either bacterial or viral (like the recent sars-Cov-2) infections and which is the hallmark of sepsis.

Therefore, more efforts have to be addressed to better understand the pathogenesis of this disease and discover novel targeting candidates for innovative therapeutic approaches.

We, as co-guest editors, are pleased to present the first volume of the Research Topic collection "*New Insights in Sepsis Pathogenesis and Renal Dysfunction: Immune Mechanisms and Novel Management Strategies*" in Frontiers in Immunology. This volume aimed to cover the multiple mechanisms associated with the dysfunctional immune response and life-threatening organ dysfunction that commonly includes acute kidney injury (AKI). The first study submitted and accepted for the current Research Topic details the controversial role and heterogeneity of Treg in sepsis, defined as angels or demons and possible target for new therapeutic approaches (Gao et al.).

Several original research articles accepted in this collection report new insights into the molecular mechanisms that exacerbate the renal injury during sepsis. The study by Zhang

et al. presented a systematic single cell transcriptomic atlas of AKI by dissecting the key cellular player and molecular mechanisms associated with AKI onset. In particular, the authors identified pre-injured proximal tubule cells (PTC) subtypes and their pro-inflammatory and pro-fibrotic signature.

Interestingly, Chen et al. clarified the exact role of STAT3 activation in sepsis-induced AKI, introducing a new intriguing mechanism that could display remarkable protective effect and could offer a new therapeutic target to prevent acute tubular damage.

In line with recent literature, animal models such as murine and rat models are valuable and extensively used for the investigation of pathogenesis and verification of potential treatment in sepsis associated immunosuppression. Wang et al. summarized the current knowledge of murine models to investigate sepsis disease, highlighting their advantages and limitations, proposing new directions in refining murine sepsis models to increase the clinical relevance and optimizing their value of meeting research and translational demands. In addition, Cao et al. successfully developed a standardized model of urinary sepsis in rats that could have a great relevance in the translational research.

Actually, the research is strongly involved in finding new injury or stress markers that could guide clinicians to recognize the first signs of renal injury and to avoid disease progression. The early diagnosis of AKI in sepsis, together with the use of antibiotics and appropriate fluid therapy may provide an optimal strategy to counteract renal injury progression and worsen outcome associated with poor survival (4). In this context, Qiao and Cui introduced the application of multiple "omics" techniques to discover new mechanisms in the pathophysiology of SI-AKI and to find more effective biomarkers that could accelerate diagnosis and provide the possibility of individualized treatment. Interestingly, Xiao et al. presented several statistical methods, such as competing risks models and double robust estimation, to evaluate the association between the ratio of neutrophils to lymphocytes and platelets (N/LP) with the incidence of S-AKI and severe AKI in sepsis patients. Then, enhanced monitoring of UO and N/LP would be more helpful in guiding clinical decisions about S-AKI. Finally, Wang et al. established a risk prediction model to assess the probability of developing AKI in Hemophagocytic lymphohistiocytosis (HLH) patients. The occurrence of this clinical syndrome, caused by an uncontrolled immune response, as in sepsis, is associated with a higher percentage of multiorgan failure, including kidney failure and death.

Sex-stratified medicine is an important aspect of precision medicine. Previous studies are mainly about the effect of sex on mortality of SI-AKI patients, and data on the association between sex and the incidence, risk factors and clinical impact of SI-AKI are not exhaustive. In a large retrospective study, Peng et al. provided evidences that sex-related effects may play a minor role in the incidence and the clinical course of SI-AKI, and the association between sex and the clinical management was insignificant in the full-adjusted model.

Current treatment protocols for septic patients are based upon source control,hemodynamic resuscitation, supportive therapy and adequate antibiotic therapy. However, in most critically ill patients, these measures are not enough to prevent sepsis-related organ dysfunction and the onset of AKI. In the study by Anter et al. the authors demonstrated for the first time the effect of menthol on an experimental model of sepsis (cecal ligation and puncture model). They found that menthol improved the survival of rats after induction of sepsis and protected the lung and kidneys, showing an ameliorative effect against enhanced oxidative stress induced by sepsis. Finally, the authors explored the pathways mediating the protective effect of menthol, and they introduced anti-proliferating cell nuclear antigen (PCNA) as a new target for sepsis therapy.

Since other investigations have to be carried out to identify other potential multi-protective mediators that could regulate a broad spectrum of events that occurred in sepsis pathogenesis, we are pleased to launch the volume II of this Research Topic.

Author contributions

AS compiled first and final version of the manuscript. PMH revised the manuscript. All authors contributed to the article and approved the submitted version.

Conflict of interest

The authors declare that the research was conducted in the absence of any commercial or financial relationships that could be construed as a potential conflict of interest.

Publisher's note

References

1. Rudd KE, Johnson SC, Agesa KM, Shackelford KA, Tsoi D, Kievlan DR, et al. Global, regional, and national sepsis incidence and mortality, 1990–2017: Analysis for the global burden of disease study. *Lancet* (2020) 395:200–11. doi: 10.4161/viru.27024

2. Ramachandran G. Gram-positive and gram-negative bacterial toxins in sepsis: A brief review. *Virulence* (2014) 5:213–8. doi: 10.4161/viru.27024

3. Jarczak D, Kluge S, Nierhaus A. Sepsis–pathophysiology and therapeutic concepts. *Front Med (Lausanne)* (2021) 8:628302. doi: 10.3389/fmed.2021.628302

4. Wang K, Xie S, Xiao K, Yan P, He W, Xie L. Biomarkers of sepsis-induced acute kidney injury. *BioMed Res Int* (2018) 2018:6937947. doi: 10.1155/2018/6937947

frontiers in Immunology

REVIEW
published: 25 February 2022
doi: 10.3389/fimmu.2022.829210

Regulatory T Cells: Angels or Demons in the Pathophysiology of Sepsis?

Yu-lei Gao[1], Ying Yao[1], Xiang Zhang[2], Fang Chen[1], Xiang-long Meng[1], Xin-sen Chen[1], Chao-lan Wang[1], Yan-cun Liu[1], Xin Tian[3], Song-tao Shou[1] and Yan-fen Chai[1]**

[1] Department of Emergency Medicine, Tianjin Medical University General Hospital, Tianjin, China, [2] Department of Emergency Medicine, Rizhao People's Hospital of Shandong Province, Rizhao, China, [3] Department of Medical Research, Beijing Qiansong Technology Development Company, Beijing, China

Sepsis is a syndrome characterized by life-threatening organ dysfunction caused by the dysregulated host response to an infection. Sepsis, especially septic shock and multiple organ dysfunction is a medical emergency associated with high morbidity, high mortality, and prolonged after-effects. Over the past 20 years, regulatory T cells (Tregs) have been a key topic of focus in all stages of sepsis research. Tregs play a controversial role in sepsis based on their heterogeneous characteristics, complex organ/tissue-specific patterns in the host, the multi-dimensional heterogeneous syndrome of sepsis, the different types of pathogenic microbiology, and even different types of laboratory research models and clinical research methods. In the context of sepsis, Tregs may be considered both angels and demons. We propose that the symptoms and signs of sepsis can be attenuated by regulating Tregs. This review summarizes the controversial roles and Treg checkpoints in sepsis.

Keywords: sepsis, regulatory T cells, pathophysiology, checkpoints, secondary infections

OPEN ACCESS

Edited by:
Alessandra Stasi,
University of Bari Aldo Moro, Italy

Reviewed by:
Charles E. McCall,
Wake Forest Baptist Medical Center, United States
Lixin Xie,
People 's Liberation Army General Hospital, China

****Correspondence:***
Yan-fen Chai
chaiyanfen2012@126.com
Yu-lei Gao
gaoyulei828@126.com

Specialty section:
This article was submitted to Inflammation, a section of the journal Frontiers in Immunology

Received: *05 December 2021*
Accepted: *07 February 2022*
Published: *25 February 2022*

Citation:
Gao Y-l, Yao Y, Zhang X, Chen F, Meng X-l, Chen X-s, Wang C-l, Liu Y-c, Tian X, Shou S-t and Chai Y-f (2022) Regulatory T Cells: Angels or Demons in the Pathophysiology of Sepsis? Front. Immunol. 13:829210. doi: 10.3389/fimmu.2022.829210

INTRODUCTION

A study of the global burden of disease from 1990 to 2017 showed that an estimated 48.9 million (38.9-62.9) sepsis cases were recorded globally and 11.0 million (10.1-12.0) sepsis-related deaths were reported in 2017, representing 19.7% (18.2-21.4) of global deaths (1). In China, one-fifth of patients admitted to intensive care units (ICU) have sepsis and their 90-day mortality rate is 35.5%. It is estimated that the annual medical costs of the 230,000 septic patients admitted to China's ICUs are about US $4.6 billion, which is a huge medical and social burden (2). In 2015, over 1.9 million deaths occurred in 605 disease-surveillance points in mainland China, and the standardized sepsis-related mortality incidence was 66.7 deaths per 100,000 population (3). Despite the 37% (11.8-54.5) decrease in age-standardized sepsis and the 58% (47.7-57.5) decrease in mortality from 1990 to 2017, aggressive infection source control, early appropriate antibiotic treatment, titration, compression therapy, and improved organ support measures, sepsis remains one of the major causes of global mortality (1–7).

Regulatory T cells (Tregs) are a subset of CD4+ T lymphocytes with negative immunomodulatory functions. They maintain peripheral immune tolerance to control immune responses to prevent exaggerated responses to infections and harmless antigens, and prevent autoimmunity. Due to the extensive regulatory role that Tregs play in the immune system, they have considerable potential as treatment for various diseases (8–10). The discovery that forkhead box P3

(Foxp3) is a key transcription factor in the differentiation and function of Tregs has multiple implications for understanding how the immune system functions and for developing therapeutic interventions for autoimmune diseases, infectious diseases, and malignancies (11–13).

Over the past two decades, Tregs have been a focus in sepsis-induced immune-inflammatory dysfunction research and the hotspot strategy in immunotherapy and checkpoint inhibition (14, 15). In sepsis, reduced T cell function is associated with increased expression of Foxp3 (16–18). CD4+ T helper 17 cells (Th17) represent the pro-inflammatory subpopulation, while Tregs promote anti-inflammatory effects (19–22). This review explores the current controversial, and sometimes conflicting, conclusions about Tregs in the pathophysiology of sepsis. Both laboratory and clinical research methods and models need to be considered to begin to understand the precise role of Tregs throughout the stages of sepsis (**Figure 1**).

SEPSIS

Research on the epidemiology, prevention, and management of sepsis is an important topic for critical care medicine, surgery, and anesthesiology, where clarification of the complex pathophysiological mechanism of sepsis is a fundamental problem (14, 23, 24). Since 1992, the definitions of sepsis, severe sepsis, and septic shock, as well as associated clinical and laboratory studies have relied on the presence of infection and the characteristics of systemic inflammatory response syndrome (SIRS) (1, 24–28). However, efforts to inhibit this hyper-inflammatory response syndrome by blocking pro-inflammatory cytokines, such as interleukin (IL)-1β and tumor necrosis factor (TNF)-α, ultimately fail to yield survival benefits (26, 27). Physicians have emphasized the evaluation of sepsis-induced organ dysfunction when they conduct the diagnosis and treatment of sepsis, especially based on the sequential (sepsis-related) organ failure assessment (SOFA), national early warning score and modified early warning score, rather than quick SOFA (qSOFA) (4–6, 24, 28–32).

Antagonism between the host and pathogenic microorganisms is a complex pathophysiological reaction: pathogens seek an advantage by incapacitating various aspects of host defenses while the host seeks to control the bacterial invasion and initiate repair of injured tissues (33, 34) (**Figure 2**). Compared with Sepsis 3.0 criteria, the definition of Sepsis 2.0 and 1.0, as well as guidelines for the diagnosis and treatment of sepsis, focus more on pathophysiological mechanisms (4, 25, 26, 29, 35). The first three days of sepsis are defined as the early stage; in these cases, more than 80% of patients first seek emergency medicine according to their clinical manifestations of the biological systemic immune-inflammatory response (26, 36–43). As sepsis management techniques continue to improve,

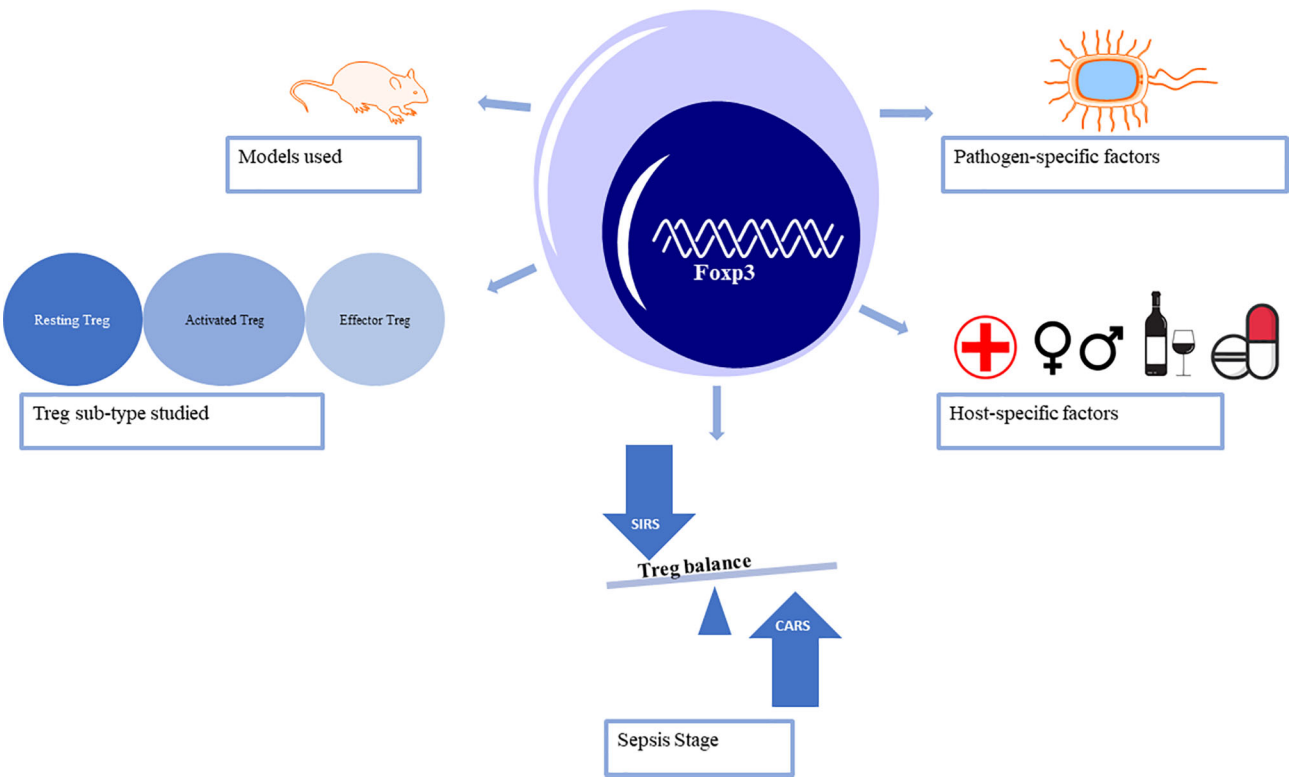

FIGURE 1 | Factors that lead to the controversy surrounding the role of regulatory T cells in sepsis.

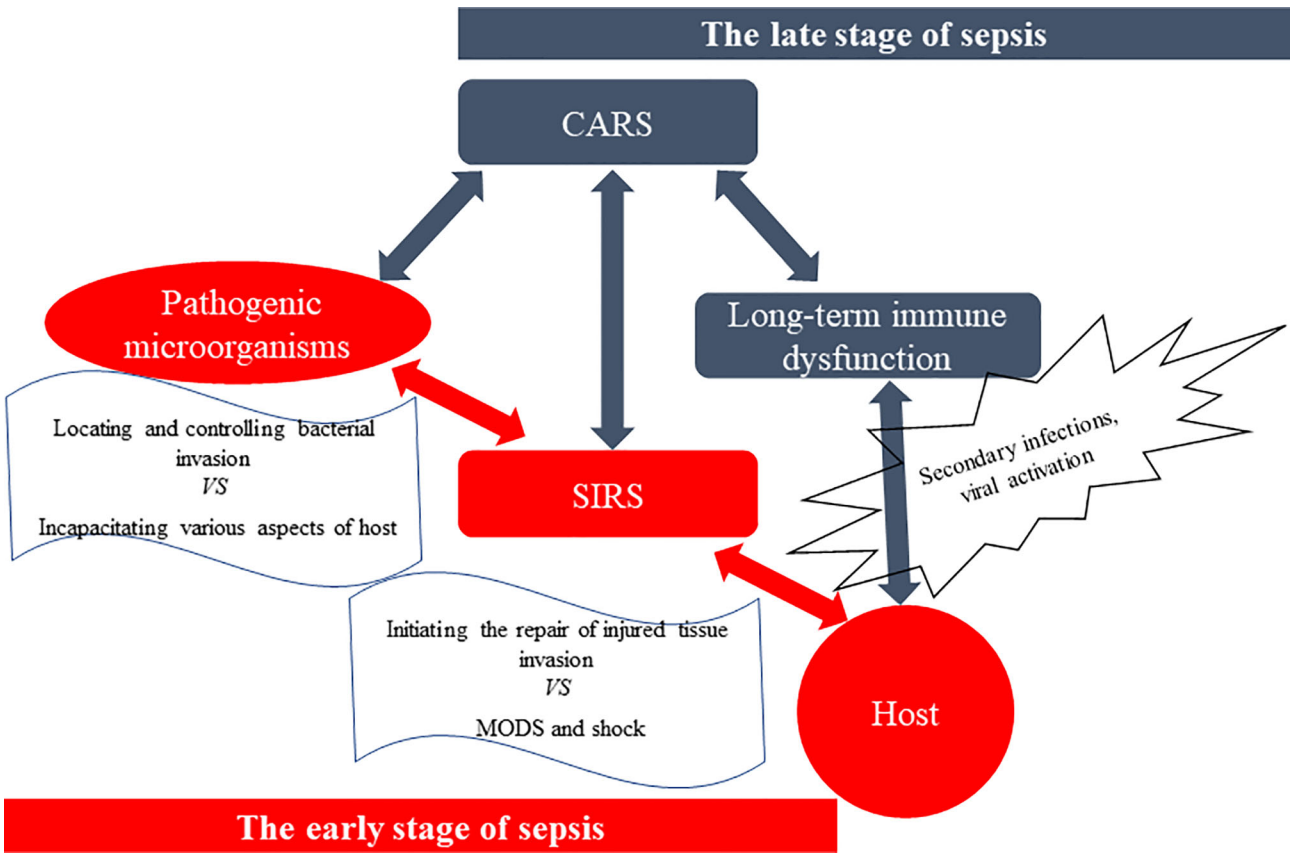

FIGURE 2 | The antagonism between the host and pathogenic microorganisms. The spread of pathogens, especially Gram-negative bacteria, and their products [such as lipopolysaccharide (LPS), etc.] causes systemic inflammatory response syndrome (SIRS), which leads to multiple organ dysfunction syndromes (MODS) and shock, and even death. However, surviving patients suffer from a stage of compensatory anti-inflammatory response syndrome (CARS), especially immunosuppression, and experience a long-term immune dysfunction called immuno-paralysis. And they are more susceptible to secondary infections, increased viral activation, and reduced 5-year survival rate, compared to those who do not have sepsis.

most patients survive the SIRS-induced "cytokine storm" in the early stage of sepsis and begin the late stage dominated by compensatory anti-inflammatory response syndrome (CARS) (44–46). Compelling experimental and clinical evidence has indicated that SIRS and CARS occur early and simultaneously in sepsis, and immunosuppression may persist for months or even longer from the onset of sepsis (4, 15, 26, 45–51). Importantly, immunosuppression is the cause of such aggravation, which increases the chance of secondary infections and viral activation. This complicates multiple organ dysfunction syndromes (MODS), extends hospital length of stay, and may even leads to death (15, 45, 46, 49).

Approximately 60-70% of septic deaths occur in the late stage (≥3 days) and most deaths were associated with ICU-acquired complications, including nosocomial infections (52). T cell apoptosis and dysfunction contributes to sepsis-induced immunosuppression (15, 26, 46, 53, 54). Intervention strategies, such as anti-programmed cell death (PD)-1/PD-L1 mAb, blocking cytotoxic T lymphocyte antigen (CTLA)-4, and blocking 2B4, have improved survival in experimental models of sepsis and recent clinical trials through improved T cell-induced immunosuppression (46, 55–58). The degree of sepsis-induced inflammation, including the level of immunosuppression, is defined by specific host factors (such as age, gender, alcoholism, repeated nosocomial infection, frequency in hospital, chronic comorbidities, immunosuppressant use, malignant tumor, site of infection, splenectomy, trauma, and stress state) (59–66), pathogen status (such as multiple drug-resistant organisms, malaria, SARS-CoV-2) (7, 26, 67, 68), and the duration of sepsis (6, 28, 35, 44, 46, 61, 69, 70).

TREG HETEROGENEITY IN SEPSIS

Combined single-cell, TCR, and other analyses of Tregs and conventional CD4+Foxp3– T cells (Tconv) demonstrate that Tregs are highly heterogeneous cells in homeostasis and disease (71–73). Treg cells can be either thymus-derived or peripherally induced by naive CD+ T cells. Phenotypically, Tregs are identified by markers they possess such as the transcriptional regulator Forkhead box (Foxp3). Based on the expression levels of Foxp3,

Tregs can be either resting Tregs with weak inhibitory potential, activated Tregs with strong inhibitory potential, or cytokine secreting non-suppressive Tregs also called effector Tregs (74). Sepsis influences the heterogeneous characteristics of Tregs from the aspects of percentage (22, 74), absolute number (67, 75), phenotypes (15, 47, 50, 58, 75–79), cytokine and chemokine secretion (80–82), and stability (12, 13, 60) (**Tables 1**–**4**). Coordination between the innate and adaptive immune systems plays a crucial role in the host's responses to infection. Even after sepsis recovery, the mechanism and cellular characteristics of the immune system change due to the different characteristics of host immune and pathogen status (23, 59–65, 84, 105, 120, 121).

Over the past decade, evidence from many compelling experiments and clinical trials indicates that sepsis increases the heterogeneous characteristics of Tregs. They act on both the innate and adaptive immune systems, dampening immune functions, causing immuno-paralysis, and eventually leading to MODS and death in sepsis (14, 18, 122–125). Intervention strategies (**Tables 3** and **4**), such as human recombinant cytokines (IL-15 and IL-36) (59, 101), blocking phenotypes or chemokines [neuropilin (Nrp)-1, CTLA-4, lymphocyte activation gene (LAG)-3, and chemokine (C-X-C motif) ligand (CXCL) 4)] (50, 58, 77, 82), nutrients (glutamine) (107), inhibiting molecules [sema3A, tissue-nonspecific alkaline phosphatase (TNAP), Sirtuin1, P2Y12, COX-2, and poly ADP-ribose polymerase (PARP)] (48, 51, 102, 111–113), as well as even clinical therapeutics (high-volume hemofiltration, immunoglobulin, fresh frozen plasma, stem cells, and ulinastatin) (41, 114, 115, 117, 118) and traditional Chinese medicine (TCM) (electroacupuncture and tanshinone IIA) (103, 106), can increase the chance of survival by inhibiting the heterogeneous characteristics of Treg-induced immunosuppression. Alternatively, other studies have shown improved outcomes in sepsis by increasing the heterogeneous characteristics of Tregs to inhibit sepsis-induced SIRS through intervention strategies such as human recombinant cytokines (IL-38 and IL-7) (96, 97), blocking phenotypes or cytokines (CD28 and IL-3) (81, 95), nutrients (arginine and fiber cellulose) (108, 109), and others (bilirubin, ITK inhibitor, miR-126, maresin1, excretory-secretory products of Trichinella spiralis adult worms, and adipose-derived mesenchymal stem cell-derived exosomes) (19, 20, 70, 98, 99, 116), as well as even clinical therapeutics (enteral nutrition and pre-and post-dilution during continuous veno-venous hemofiltration) (22, 42, 119) and TCM (baicalin, rhubarb, Xuebijing injection, and curcumin) (21, 100, 104, 105). Establishment of sepsis models such as the "memory mouse" (57, 95), "two- or three-hit mouse" (70, 118), and "gene recombination mouse" models (78, 79, 94) have begun to shed light on additional heterogeneous immune characteristics in sepsis, including the presence of IL-10+ regulatory B cells (Bregs) and lipopolysaccharide-responsive beige-like anchor protein (LRBA)-deficient patients (97, 126, 127).

TREG CHECKPOINTS IN SEPSIS

Multiple co-stimulatory molecules (CD28, CD27, OX40, and 4-1BB) (128–130) and co-inhibitory receptors [B– and T–lymphocyte attenuator (BTLA), T cell immunoglobulin and mucin domain-containing-3 (TIM-3), CTLA-4, T cell immunoreceptor with immunoglobulin and ITIM domains (TIGIT), LAG-3, PD-1, and Nrp-12] (15, 50, 57, 77, 93, 131) that transmit various secondary signals play a pivotal role in the heterogeneous characteristics of Tregs and may contribute to Tregs-induced dysfunction of the whole immune system in sepsis, especially imbalanced Tregs/Tconvs (15, 74–77, 83, 132, 133). Although the innate immune system is dominant in the early stage of sepsis, Tregs are thought to be the link between the innate and adaptive immune systems (37, 40).

The percentage of Tregs, OX40+ Tregs, and 4-1BB+ Tconvs were higher in the early stage of CAP-associated septic patients. The percentage of CD4+CD27+, CD4+CD28+, and CD4+OX40 + CD27-CD28- T cells were positively correlated with SOFA and predicted 28-day mortality, respectively (40). In addition, these data indicated that imbalanced expression of OX40 and 4-1BB may contribute to evaluate the imbalance of Tregs/Tconvs. The absolute number of CD4+TIM-3+, CD4+PD-1+, and CD4 +CTLA-4+ T cells were positively correlated with the severity of sepsis, especially CD4+PD-1+ T cells, which may be a risk factor for sepsis (93). BTLA is a co-inhibitory receptor that is constitutively expressed on IL-10+Tregs, which can effectively inhibit the function of CD4+ T cells (15). BTLA expression on Tregs remained high in patients with sepsis, compared to healthy controls from day 1 to 7, especially in non-survivors (75). GPR174, a member of the G-protein-coupled receptor family, plays a negative role in the development and functionality of Tregs which is highly expressed on the surface of Tregs in the early stages of sepsis and closely associated with adverse sepsis outcomes (79). A decrease of Human Leukocyte Antigen-DR (HLA-DR) expression on monocytes has proved to be a reliable indicator of immunosuppression in sepsis (37, 41, 60). From day 1 to 28 after sepsis diagnosis, both Foxp3 and RORC, the specific transcription factor of Tregs and Th17 cells, respectively, were significantly more highly expressed in survivors than in non-survivors. The lack of a linear correlation with HLA-DR may be due to the influence of sample size and other patient-specific factors (60). Thymus Stromal Lymphopoietin (TSLP) has been identified as a crucial inflammatory cytokine in immune homeostasis and promoted Tregs differentiation (134). The percentage of IL-10+ Tregs significantly increased in septic patients with high TSLP levels (80). A comprehensive study on the expression of co-stimulatory molecules and co-inhibitory receptors in different stages of sepsis induced Tregs would contribute to the systematic understanding of Tregs in sepsis and help people identify the most effective immune checkpoints for Tregs.

HOST-DEPENDENT TREG PATTERNS IN SEPSIS

Compelling experimental and clinical evidence has indicated that sepsis is a multi-dimensional heterogeneous syndrome, which is reflected in the host's variable immune responses (23, 135, 136).

TABLE 1 | Observational studies using animal models focused on the characteristics of T_{regs} in sepsis.

Observational study	Species	Model	Observation time	Specimen Source	T_{regs}	Immunological characteristics	Outcome
He, et al. (23)	Mouse	Recurrent sepsis (Three LPS stimulations, once every 5 ds)	5 ds after the last LPS injection	Spleens Lung	Percentage and absolute number↑	percentage and number of $CD4^+$ T cells↓ Percentage of $CD8^+$ T cells↓ CD69 and CD28 of $CD4^+$ T cells↓ PD-1 and Tim-3 of $CD4^+$ T cells↑ MHC-II of antigen-presenting cells↓	Antiviral immune responses (secondary virus infection) ↓
		Acute sepsis (One LPS stimulations)	12, 24, and 48 hs after LPS injection		Percentage↑	Percentage and number of total T cells↓ percentage and number of $CD4/8^+$ T cells↓ CD69 at 12hs↑, 24, and 48 hs↓ MHC-II of antigen-presenting cells↑	Antiviral immune responses (secondary virus infection) →
Gaborit, et al. (83)	Mouse	*Pseudomonas aeruginosa* induced "two-hit" model	Day 3 for T cell phenotype Day 4 for lung injury in the double-hit model	Spleens Lung	Activation↑ $TNFR2^{pos}$ Tregs↑ *Gizmo, Mki67* (Ki67), *Irf4*, *Prdm1* (Blimp 1) and *Havcr2* (TIM-3) ↑ CD62, CD25, CTLA-4 and IL-10↑ percentage↑	Number of splenic $CD4^+$T cells↓	Susceptibility to secondary pneumonia↑
Saito, et al. (84)	Mouse	CS-induced model SAE	24hs, 6, 8 10, and 30 ds after induced	Brain Blood Spleen and other lymph nodes	Percentage and absolute number (brain)↓	Microglia, neuroinflammation, and neutrophil infiltration (brain)↑ astrocytes (brain)↓ $CD4/8^+$ T cell accumulation (brain)↑ T cell (blood and spleen)↓	The brain-blood barrier was disrupted (24hs) Anxiety-like behaviors↑ Marble burying test↑ Open-field test↓ Forced swimming test↓ Depression
George, et al. (17)	Mouse	Acute *DenV* infection and 7 days later followed with *listeria monocytogenes* induced "two-hit" sepsis	3, 7,10,15 ds after induced	Spleen Blood	Proliferation (number and percentage)↑ GITR, CTLA-4, Foxp3, CD40L, CD44, CD62L, and CD69↑ IL-10, and TGF-β↑	$CD4/CD8^+$ T cell responses↓ IFN-γ↓	Susceptibility↑ Attenuates DHF/DSS
Baek, et al. (85)	Preterm pigs	LPS stimulated Staphylococcus epidermidis challenge	6, 12, and 24 hs, day 5, 7, and 9 after stimulated or challenged	Cord blood Blood	Percentage and absolute number↑	Genes related to both innate and adaptive immunity↓ Blood neutrophil and platelet counts↓ Neutrophil phagocytosis capacity↓	Severe septic responses↑ 9-ds incidence and severity of spontaneous infections↑ Overall birth weight↓
Shrestha, et al. (86)	Neonatal mouse	LPS stimulated once daily on postnatal days (PNDs) 3–5	PND7 or PND14	Lung	Percentage and absolute number↓	*CCL2, CCL3, CXCL1, IL-1β*, and *TNF-α*↑ *IL-10*↑	Survival↓ Body weight↓ Alveolar simplification↑

(Continued)

TABLE 1 | Continued

Observational study	Species	Model	Observation time	Specimen Source	T_{regs}	Immunological characteristics	Outcome
							Pulmonary vascular simplification↑ Lung cell proliferation↓, and apoptosis↑
Qiu, et al. (79)	*G protein-coupled receptor 174-* KO Mouse	LPS stimulated CLP	24 hs after stimulated or challenged	Thymus Lung	*Ctla-4, Pdcd-1, and IL-10*↑ CTLA-4 and IL–10↑	M2 macrophages↑ IL-6 and TNF-α↓	2 and 7-ds survival↑ Resistant to inflammatory shock↑ Lung injury↓
Zhou, et al. (87)	$PTEN^{M-K}$ Mouse	LPS-induced ALI	24 hs after induced	Blood Lung BALF	Percentage and absolute number↑ Foxp3 and TGF-β↑	TGF-β↑ Neutrophil accumulation↓ RORγt, IL-17A, TNF-α, and IL-1β↓	6-ds survival↑ Lung injury↓ Weight↑
Andrade, et al. (88)	Mouse	Received LPS injection each day for 5 days, and followed with CLP	4 hs after CLP	Spleen Blood	Absolute number (received LPS injection) ↑ Absolute number (after CLP) ↓	IL-2, IL-6, TGF-β, and INF-γ (received LPS injection)↑ Th17(received LPS injection)↑ Th17(after CLP) ↓	72-hs survival↑
Cao, et al. (89)	$TLR4^{-/-}$ mouse	CLP	24 hs after CLP	Lung Liver Spleen Blood	Percentage and absolute number↓ Apoptosis↓ *Foxp3* and *Tlr4*↓	IL-10 and IL-4↓ IL-2 and TNF-α↑	72-hs survival↑ Lung, liver injury↓
Fay, et al. (78)	$CD43^{-/-}$ mouse	CLP	24 hs after CLP	Spleens	Percentage ↓	Number of $CD4^+$ T cells↓ Numbers of $CD4/8^+$ central memory and effector memory cells↓ Apoptosis of central memory T cells↑ IL-2-secreting CD4+ T cells↓ IL-4-secreting CD4+ T cells↑ Th17↓	7-ds survival↓
Bomans, et al. (69)	Mouse	CLP	3 months after CLP	Spleens Blood Bone marrow	Percentage (spleens)↑	Enlarged spleens with higher weights↑ $CD11b^+$ $F4/80^-$ splenic monocytes↑ $Ly6C^+$ inflammatory monocytes↑ $Ly6C^-$ alternative monocytes↓ $CD11b^+$ $F4/80^+$ macrophages↑	There is no long-term impact of sepsis on the systemic immune response in mice 12 weeks after CLP.
Ahmadi, et al. (64)	Tumor mouse	Induction of systemic *candidiasis*	8 ds after induction	Blood Spleens Renal Liver	Percentage (spleens and tumor) ↑	ratio of IFN-γ/IL-4↓ IL-10↑	Relative tumor volume↑
Hu, et al. (90)	Mouse	Injected with PC61 before a two-hit model	24 hs two-hit	Lung BLFC Spleens	Percentage and absolute number↓	IL-1β, IL-6, and IL-17A↑ IL-10↓	3 and 7-ds survival↑ Bacterial colonies↓ Lung injury↓

Compared with the control group, "↑" represents up-regulation, increase or enhancement ; "↓" represents down-regulation, decrease or inhibition, and "→" represents no change.

TABLE 2 | Observational studies using septic patients or combined animal models focused on the characteristics of T_{regs} in sepsis.

Observational study	Species	Model	Observation time	Specimen Source	T_{regs}	Immunological characteristics	Outcome
Yin, et al. (74)	Humans	Severe sepsis/septic shock patients with severe neutropenia	Day of PICU admission	Blood	Percentage↑	CRP, PCT, IL-6, IL-10, and IFN-γ↑	28-ds survival↓
Jiang, et al. (76)	Humans	Septic patients	Day of ICU admission	Blood	PD-1↑↑ CD28, PD-L1, and CD86↑	No data	SOFA scores↑ 28-ds survival↓
Youssef, et al. (91)	Neonates	Vitamin D deficiency	After enrolled	Cord blood	Percentage ↓	Total lymphocytes, $CD3^+$ T lymphocytes, $CD4^+$ T-helper, $CD8^+$ T-cytotoxic lymphocytes, and $CD4^+CD45RA^+$ naïve T cells↓	16.27% of infants with a 25-OHD deficiency were admitted with sepsis No cases of sepsis in the normal 25-OHD group
Carvelli, et al. (37)	Humans	Septic shock patients	24 and 72 hs after admission	Blood	Percentage↓	Lymphocytes ($CD3^+$ T cells and $CD3^-CD56^+$ NK) ↓ HLA-DR↓ Innate lymphoid cells 1 count↑ Innate lymphoid cells 2 count↓ Innate lymphoid cells 3 count↓ Innate lymphoid cells 3 percentage↑	secondary infections↑
Arens, et al. (92)	Humans	Abdominal sepsis	Over 5 ds	Blood	No distinguishable trends in the percentage	B and NK cell counts↓ IL-8↓ Th17 cells↑	Day 21, 5/26 patients showed no *candida* colonization or invasive candidiasis (IC), 13/26 patients colonization was detected, and 8/26 patients were diagnosed with IC.
Xu, et al. (60)	Humans	Septic patients	Days 1, 3, 5, 7, 10, 14, 21 and 28 after sepsis	Blood	Foxp3 (survivors)↑	HLA-DRA (survivors)↑ Th1 and Th2 cells(especially non-survivors)↓ Th17 (survivors)↑ T-bet (Th1) and GATA-3 (Th2) had a linear correlation with HLA-DRA 59 survivors, 19 non-survivors	
Yu, et al. (80)	Humans	Septic patients	After admission	Blood	The ratio of $IL\text{-}10^+$ Tregs to total Tregs↓	TSLP↑ Number of Th1 cells↑ IL-1β, IL-6, IFN-γ, and TNF-α↑	134 patients had hyperleukocytosis and a high neutrophil ratio Mortality↑ Stays in the intensive care unit↑
Liu, et al. (75)	Humans	Septic patients	Ds 1 and 7	Blood	Day 1, absolute number (non-survivors) ↓ Day 7, percentage and absolute number(non-survivors) ↑ Day 7, percentage↓↓ and absolute number(survivors) ↑↑		BTLA expression on Tregs (non-survivors) ↑↑ Day 1, BTLA on $CD4^+$ T cells was in patients with severe sepsis↓ day 7, BTLA on $CD4^+$ T–cells in both survivors and non-survivors↑ BTLA/Tregs were positively correlated with SOFA
Greenberg, et al. (93)	Humans	*Staphylococcus aureus*	After positive S. aureus blood culture	Blood	Associated with immunosuppressive medications	Neutrophil-to-lymphocyte count ratio↑ IL-6 and IL-17A↑ Th17↑ Th1↓ Th17 score-to-Th1 score ratios↑	90-ds survival↓
Lu, et al. (40)	Humans	Septic shock	Within 3 ds	Blood	Percentage↑ OX40↑	CD28, CD27, OX40 on $CD4^+$ T cells↑ OX40 on $CD4^+CD27^-CD28^-$ T cells↑ $CD4^+CD27^-CD28^-$ T cells↓ 4-1BB on $CD4/8^+$ T cells↓	28-ds survival↓ SOFA↑

(Continued)

TABLE 2 | Continued

Observational study	Species	Model	Observation time	Specimen Source	T_{regs}	Immunological characteristics	Outcome
Li, et al. (67)	Humans	Pneumonia induced sepsis	Day of ICU admission	Blood	Percentage and absolute number↓	Th17/Treg, Th1/Th2, and M1/M2 cell radios↑	No data
	SD rats	Pneumonia-derived sepsis rat was induced with *Klebsiella pneumonia*	12 hs after induced	Blood Lung		IL-6, TNF-α, IL-1β, and IL-18↑ HMGB1, RAGE, and IL-17A↑	
Willers, et al. (94)	Infants (newborns and during infancy)	Follow-up observation was conducted for 2 years	First-year of life (ds 1, 3, 10, 30, 90, 180, and 360)	Stool samples Intestine biopsies	A low level of S100 proteins in infants' fecal samples associated with the development of sepsis and obesity by age 2 years.		
	Newborn S100a9$^{-/-}$ mouse	Infected with *Staphylococcus aureus*	24hs after infection	Blood Intestine Mesenterial Celiac lymph nodes Colon contents	Percentage and absolute number (brain)↓	CX3CR1 protein, and *Il10* and *Tgfb1* mRNAs↓	fatal sepsis↑

Compared with the control group, "↑" represents up-regulation, increase or enhancement ; "↓" represents down-regulation, decrease or inhibition.

There is significant inter–study heterogeneity among a large number of sepsis-related studies: male sex, increased age, organ dysfunction acquired during ICU stay, recurrent sepsis, and presence of comorbidities are independently associated with increased sepsis–related mortality, especially in ICUs (2, 3, 137). Seymour and colleagues demonstrated that patients with the α phenotype (33%) have the lowest administration of a vasopressor; Patients with the β phenotype (27%) are the oldest age with the most chronic illness and renal dysfunction; Patients with the γ phenotype (27%) have the most inflammation and pulmonary dysfunction; Patients with the δ phenotype (n = 2667; 13%) have more liver dysfunction and septic shock. Their cumulative 28-day mortality rates are 5%, 24%, 13%, and 40%, respectively (135).

Studies of immune responses to sepsis usually exclude patients who have immune disorders or receive immunosuppressive medications (40, 76, 80); therefore, these studies do not fully reflect the heterogeneous characteristics of sepsis (91, 135). An increased Th17/Treg response throughout infection is most strongly associated with increased mortality among patients who are not immunocompromised; a decreased Th1/Treg response is most common among immunocompromised patients. Unexpectedly, patients who have immunocompromising comorbidities or take immunosuppressive medications do not have increased 90-day mortality, contrary to previous studies (138, 139). Immunocompromised patients with malignancies, especially those treated with chemotherapies that have adverse effects on immune function, have broadened the types and risks of drug-resistant multi-pathogenic infections (140). For example, systemic infection with *Candida albicans* (candidiasis) in tumor-bearing mice does not significantly increase the percentage of Tregs compared to the tumor group, but it significantly increases the proportion of Tregs in the spleen of the non-tumor bearing mouse. Surprisingly, systemic infection with *C. albicans* promotes the rapid growth of tumors, and the percentage of tumor-infiltrated Tregs in the tumor/candidiasis group is significantly higher than these in the tumor only group (64). This demonstrates that candidiasis could promote the growth of tumors by expanding Tregs: tumors and candidiasis promote each other through increased Treg activity. On the other hand, research on common variable immunodeficiency (CVID) and autoimmune diseases, both of which are characterized by loss of Treg function, show that the heterogeneity in sepsis due to host factors has become more prominent (127, 141). Autoimmune diseases are associated with a lower risk of 30-day death (27% reduction) for sepsis through a mechanism unrelated to the chronic immunomodulation medications (141). LRBA deficiency leads to different types of congenital immune deficiencies, such as CVID, autoimmune lymphoproliferative syndrome (ALPS) with recurrent infections, and even sepsis. Low expression of CTLA-4, Foxp3, and CD25 in LRBA-deficient patients leads to a partial loss of the regulatory effects of Tregs on T/B cell activation and causes an inappropriate increase in T and B cell activation (127).

Some evidence demonstrates that ICU-acquired infections contribute to the overall mortality of septic patients. Patients with septic shock who have secondary infections are at a 5.8 times higher risk of late-stage death than those without because

TABLE 3 | Intervention studies using animal models focused on the target of T_{regs} in sepsis.

Intervention study	Species	Model	Intervention	Intervention time	Observation time	Specimen Source	T_{regs}	Immunological characteristics	Outcome
Sun, et al. (57)	Mouse	Memory mouse (56 ds antigen-experienced) and CLP	TIGIT (αTIGIT Ab)	12 and 24 hs after CLP	48 hs after CLP	Spleens Blood	Activation↓ Differentiation↓ Helios↓ CTLA-4↓ IL-10↓	Apoptosis of memory T cells↑ T cell function↓ IL-10, IL-6,and MCP-1↓	7-ds survival↓
Sun, et al. (95)			CD28 (agonistic anti-CD28 Ab)	Immediately after CLP and at ds 2, 4, and 6 post-CLP	24 hs after CLP		Proliferation and activation↑ IL-10↑ CD127, CD69, Helios and CTLA-4↑	Apoptosis of $CD44^{hi}$ memory $CD4^+$ T cells↓ IL-10↑	7-ds survival↑
Tran, et al. (70)	Mouse	Injected with LPS, and 24 hs latter CLP induced "Two-Hit" Model	Bilirubin	Immediately after CLP	24 hs after CLP	Lung Blood	Percentage↑	TNF-α, IL-6, and IFN-γ↓ IL-10, and TGF-β↑ T cell activation↓ IFN-γ-producing cells↓	14-ds survival↑ Lung injury↓
Ge, et al. (96)	Mouse	CLP	IL-38 (rmIL-38)	2 hs before or after severe CLP	48 hs after CLP	Spleens	Immunosuppressive activity↑ IL-10 and TGF-β1↑ Foxp3 and CTLA-4↑	Th2 response (IL-4)↑ Proliferative ability of T cells↓	7-ds survival↑
Zhao, et al. (81)	Mouse	CLP	IL-3 (siRNA, IL-3 Ab)	2, 6, and 12 hs after CLP	48 hs after CLP	Spleens, lung, and liver	Foxp3, CTLA-4, IL-10, and TGF-β↑ Suppressive activity↑ Percentage↑	Hyper-inflammatory response (TNF-α and IFN-γ)↓ Anti-inflammatory response (IL-10)↑	5-ds survival↑ Lung and liver injury↓
Kulkarni, et al. (97)	Mouse	Stool suspension	IL-7	Daily from day 5–9	3.5 months after sepsis	Spleen	Percentage and absolute number (within 1 week after sepsis) ↑	$IL\text{-}10^+$ B cells (Bregs)↑ $CD3^+CD4^-CD8^-$ T cells↑ IFN-γ and IL-10↑	No data
Nadeem, et al. (98)	Mouse	LPS-induced ALI	ITK (inhibitor)	Once 30 min before and then 3 times after LPS administration at 12 hourly intervals	48 hs after LPS	BAL	Percentage↑	Total leukocytic and neutrophilic numbers↓ $\%IL\text{-}17A^+ CD4^+$ T cells↓	Lung injury↓
Zou, et al. (19)	SD rats	CLP	miR-126 (mimic)	Immediately after CLP	48 hs after CLP	Blood	Percentage and absolute number↑	TNF-α, IL-6, and IL-17↓ IL-10↑ lymphocyte of apoptosis↓ Number of Th17↓	No data
Xia, et al. (20)	Mouse	CLP	Maresin1	1 h after CLP	24 hs after CLP	Lung BALF	Percentage and absolute number↑	IL-1β, TNF-α, IL-6, and IL-17↓ IL-10 and TGF-β↑ Th17/Tregs↓	7-ds survival↑ Lung injury↓
Li, et al. (99)	Mouse	CLP-induced ALI	Excretory secretory products of *Trichinella spiralis* adult worms	Immediately after CLP	12 hs after CLP	Lung Blood	Percentage↑	IL-10 and TGF-β↑ TNF-α, IL-6, IL-1β↓ HMGB1, TLR2, and MyD88↓	3-ds survival↑ Lung injury↓
Liu, et al. (21)	Mouse	CLP-induced pancreatic injury	Baicalin	Immediately after CLP	72 hs after CLP	Blood Spleen Pancreatic tissue	Percentage and absolute number↑ Foxp3 (pancreatic tissue)↑	Th1 and Th17 cells↓ T bet and RORγt (pancreatic tissue)↓ IFN-γ and IL-17↓ IL-10↑	Pancreatic injury↓
Liu, et al. (100)	Rats	Burning model	Rhubarb	Immediately after model	12, 24, and 72 hs after CLP	Liver Blood	Percentage and absolute number↑	$CD4^+$T cell percentage↓ $CD8^+$ T cell percentage↑ $CD19^+$B cell percentage↓ NK cell percentage↑	No data
Saito, et al. (59)	Young mouse	day 0, 4, 7, and 10 to inject CS	IL-15	Day 3, 7 and 10	Within 50 days	Blood Spleens Peritoneal lavage fluids	Percentage and absolute number↓	Naïve $CD4^+$ T cell↑ $PD\text{-}1^+CD4^+$ T cells↓ $CD8^+$ T cell↑	Prevent the initial reduction of body weight (Day 3) ↑ Survival ↑
	Aged mouse						Percentage and absolute number↓	$CD4^+$ T cells↑ Naïve $CD4^+$ T cell↑ $PD\text{-}1^+CD4^+$ T cells↓ Naïve $CD8^+$ T cells↑ $PD\text{-}1^+CD8^+$ T cells↓	Survival ↑
Ge, et al. (101)	Mouse	CLP	IL-36 (IL-36β)	2 hs before or after CLP	48 hs after CLP	Spleens	Tregs were required IL-10 and TGF-β1↓ Foxp3 and CTLA-4↓	$CD4^+CD25^-$T cell proliferation↑ The ratio of IL-4 to IFN-γ↓	7-ds survival (2 hs before CLP) ↑
Gao, et al. (50)	Mouse	CLP	Nrp-1 (siRNA, Nrp-1 Ab)	Immediately after CLP	24 hs after CLP	Spleens and renal	Stability and activity (Foxp3, CTLA-4, TGF-$\beta1^{m+}$, IL-10, and TGF-β1)↓	IL-10, IL-4, and TGF-β1↓ IFN-γ↑	Renal injury↓
Lou, et al. (77)	Mouse	CLP	LAG-3 (KO, LAG-3 Ab)	Immediately after CLP	24 hs after CLP	Blood Spleens	Percentage and absolute number↓	Cytokines (TNF-α, IL-6, and IL-10) and T cells apoptosis↓ IFN-γ, the absolute number and proliferative ability of $CD4/8^+$T cells↑	7-ds survival↑ Bacterial clearance↑

(Continued)

TABLE 3 | Continued

Intervention study	Species	Model	Intervention	Intervention time	Observation time	Specimen Source	T_{regs}	Immunological characteristics	Outcome
Xu, et al. (82)	Mouse	CLP	CXCL4 (CXCL4 Ab)	Immediately after CLP	72 hs after CLP	Urine Blood Spleens	Percentage and absolute number↓	IL-6, IL-10and TNF-α↓	Urine creatinine and urea nitrogen↓
Gao, et al. (48)	Mouse	CLP	Sema3A (EGCG, a strong inhibitor of Sema3A)	Immediately after CLP	24 hs after CLP	Spleens Blood	Foxp3↓	IL-4↓ IFN-γ↑ Apoptosis of $CD4^+$ T cells↓ Proliferative ability of $CD4^+$ T cells↑	liver, lung, and renal injury↓
Brichacek, et al. (102)	Mouse	CLP	Inhibitor of TNAP (SBI-425)	Daily for 7 days after CLP	24 hs after the final injection	Plasma Brain Bone Spleens	$CD4/8^+Foxp3^+$ splenocyte T-cell populations↓	Did not affect 7-ds clinical severity outcomes Loss of barrier function in BBB endothelial cells↑ 48-hs Survival↓ Severity scores↑	
Martin et al. (51)	Mouse	CLP	Sirtuin1 (EX-527-an inhibitor)	24 hs after CLP	30 hs after CLP	Spleen	Percentage↓ CTLA-4↓	TGF-β, IL10↓ IFN-γ↑	7-ds survival↑
Gao, et al. (103)	Mouse	CLP	Tanshinone IIA		24 hs after CLP	Blood Lung Liver Renal Spleens	Percentage↓	$CD3^+CD4^+$ and $CD3^+CD8^+$ lymphocytes percentages↑, and apoptosis↓ IFN-γ and IL-2↑ IL-4 and IL-10↓ Macrophage phagocytotic activities↑	7-ds survival↑ Lung, liver, and renal injury↓ Intraperitoneal bacterial counts↓
Chen, et al. (104)	Mouse	CLP	Xuebijing injection	Immediately after CLP	36 hs after the CLP	Spleens Lung Renal	Percentage and absolute number↑ Differentiation↑ IL-10↑	Th17↓ IL-17, IL-6, and TNF-α↓	5-ds survival↑ Renal and lung injury↓
Chen, et al. (105)	Mouse	CLP	Curcumin	12 hs after CLP	Day 1, 3, 5, and 7 after CLP	Spleen Blood Renal Lung	Percentage and absolute number↑	TNF-α and IL-6↓ The proliferation of CD4 +CD25– T cells↓ IL-10↑	Renal and lung injury↓ 7-ds survival↑
Xie, et al. (106)	Rats	CLP	Electroacupuncture	Immediately after CLP	48 hs after CLP	Spleens Intestinal lymph nodes	Percentage↓	TNF-α and IL-10↓ $CD3^+CD4^+$ cell↑	D-LA and DAO↓
Hou, et al. (107)	Mouse	CLP	Glutamine	2 weeks before CLP	72 h after CLP	Blood Spleens Renal	Percentage↓	Percentages of T and $CD4^+$ T cells↑ IL-6 and IL-4↓ Bcl-2↑	Renal injury↓
Yeh, et al. (108)	Mouse	CLP	Arginine	1 h after CLP	12 and 24 hs after CLP	Blood Para-aortic lymph nodes Liver	Percentage↑	Percentages of $CD4^+$T cells↑ Th1/Th2 ratio↑ Th17/Tregs ratio↓ IL-1β, IL-6, and TNF-α (liver) ↓	Liver injury↓
Di Caro, et al. (109)	Mouse	Injected with LPS	Dietary fiber (fiber cellulose)	2 weeks before injected with LPS	24 and 72 hs post LPS injection	Blood Liver Spleens	Suppressive function↑ Percentage (72 hs) ↑	Number and activation of splenic macrophages and DCs↓ Pro-inflammatory cytokines↓ Chemokines↓ Anergy in T cells↑ Hepatic DNA binding activity of NF-κB↓	4-ds survival↑ (110)
Albayati, et al. (111)	Mouse	CLP	P2Y12 antagonism (clopidogre)	2 hs before CLP	24 hs after CLP	Blood Spleens Hearts Renal	Percentage and absolute number (spleens)↓	Platelets and $CD4^+$ T cells interactions↓	7-ds survival↑ Splenomegaly and spleen damage↓ Renal and cardiac injury↓
Sun, et al. (112)	Mouse	CLP	COX-2-specific inhibitor (parecoxib)	20 min after CLP	24 hs after CLP	Blood Spleens	Percentage↓	IgM and IgG↑ IL-1β, IL-10, and TNF-α↓	7-ds survival↑ Spleen injury↓
Ahmad, et al. (113)	Mouse	CLP	Poly (ADP-ribose) polymerase inhibitor (Olaparib)	30 min and 8 hs after CLP	24 hs after CLP	Spleens Blood	Percentage and absolute number↓	Number of $CD4/8^+$ lymphocytes↑ Th17/Treg ratio↓ TNF-α, IL-1α, IL-1β, IL-2, IL-4, IL-6, and IL-12p40↓	48-hs survival (young, males) ↑ Multiorgan dysfunction↓ Bacterial CFUs↓
Cao, et al. (114)	Mouse	CLP	Ulinastatin	1 h before and 6 hs after CLP	24 hs after CLP	Spleens Blood Lung Liver Renal	Foxp3 and CTLA-4↓	Teff apoptosis↓ Teff proliferation↑ TNF-α, IL-1β, IL-2, and IL-10↓	72-hs survival ↑ Lung, liver, and renal injury↓

(Continued)

TABLE 3 | Continued

Intervention study	Species	Model	Intervention	Intervention time	Observation time	Specimen Source	T_{regs}	Immunological characteristics	Outcome
Topcu, et al. (115)	SD rats	CLP	Human dental follicle stem cells	Immediately or 4 hs after CLP	24 hs after CLP	Ileal tissue Spleens	Percentage↓	TNF-α↓	Ileal tissue injury↓
Chang, et al. (116)	SD rats	CLP	Adipose-derived mesenchymal stem cell-derived exosomes	3 hs after CLP	6, 16, 24, 48, and 72 hs after CLP	Blood Brain Cerebrospinal fluid	Percentage↑	TNF-α and IL-6↓ MMP-9, GFAP, F4/80 and CD14↓ $L6Gy^{+}/CD11^{b/c+}$ inflammatory cells↓ $CD3^{+}/CD4^{+}$cells↓ CD3+/CD8+ cells↓ Early/late apoptotic cells↓	Brain injury↓
Zhang, et al. (117)	Mouse	Infected with *E. coli* 0111: B4	Fresh frozen plasma	After severe sepsis (trembles, high fever, and difficulty breathing)	Recovered from endotoxemia	Blood	Differentiation and expansion↓	Galectin-9↓ The proliferation of Th1 and Th17↑ IL-1β, IL-6, and IFN-γ↑ IL-10↓	Recovered from endotoxemia↑
Kyvelidou, et al. (118)	Mouse	5 ds injection of LPS	IgG and IgM	Day 1 of LPS injection	Day 6 after LPS	Blood Spleens	CD25 and Foxp3↓	CRP↓ IL-6 and TNF-α↓ IL-18↑	7-ds survival ↑ MSS scoring↓

Compared with the control group, "↑" represents up-regulation, increase or enhancement ; "↓" represents down-regulation, decrease or inhibition.

TABLE 4 | Intervention studies using septic patients focused on the target of T_{regs} in sepsis.

Intervention study	Species	Model	Intervention	Intervention time	Observation time	Specimen Source	T_{regs}	Immunological characteristics	Outcome
Liu, et al. (42)	Humans	Septic Patients with mechanical ventilation	Enteral nutrition	Treated within 48 hs after admission	D 1 and 7 after admission to the ICU	Blood	Percentage↑	Th17 cells and endotoxin↓	Duration of mechanical ventilation, lengths of ICU stay, hospital stay, And the incidence of ICU-AW↓
Sun, et al. (22)	Humans	Septic Patients	Enteral nutrition	Treated within 48 hs after admission	7 ds after admission	Blood	Percentage↑	Th17 percentages↓ Th17/Tregs ratios↓ IL-17, IL-23, and IL-6↓	Duration of mechanical ventilation↓ ICU stay↓
Chihara, et al. (119)	Humans	Septic shock patients with acute kidney injury	Pre-and post-dilution during continuous venovenous hemofiltration	24 hs within obtaining informed consent	6 and 24 hs after continuous venovenous hemofiltration	Blood	Induction rate↑	IL-6 and IL-10↓ Neutrophil phagocytic activity↓	No data
You, et al. (41)	Humans	Severe burn	High-volume hemofiltration	Within 3 days after burn	Days 1, 3, 5, 7, 14, 21 and 28 post-burn	Blood	Percentage↓	TNF-α, IL-1β, IL-6, IL-8, and PCT↓ HLA-DR↑	Incidence of sepsis, septic shock↓ Vasopressor↓ 90-ds survival ↑

Compared with the control group, "↑" represents up-regulation, increase or enhancement ; "↓" represents down-regulation.

of their unique immunosuppressive status, especially T cell exhaustion caused by aging and recurrent sepsis (2, 23, 52, 59, 142). In a clinically relevant cecal slurry (CS) induced model of recurrent sepsis, increased T cell exhaustion and poor prognosis (including reduced survival rate and body weight) was observed in aged (18-24 months old) compared with young (5 week old) female or male C57BL6/J mice. Their symptoms persisted for over 50 days and were associated with increased PD-1 expression on Tregs (59). Olaparib, a competitive PARP inhibitor used in the field of oncology that inhibits the binding of NAD+ to the catalytic sites of PARP, showed significant protective effects on cecal ligation perforation (CLP)-induced sepsis in young (8 weeks old) male adult mice compared with aged (72 week old) female mice (143). These age-and sex-selective protective models were associated with olaparib reducing the Treg and Th17 populations, and the Th17/Tregs ratio, by regulating intracellular miRNA levels (113).

In infants, especially preterm infants, early-onset sepsis (EOS) increases the risk of death or neurodevelopmental disorders (144). In a multi-centric clinical study of 326 neonatal intensive care units, 0.8% of infants suffered from EOS, where many factors reduced lymphocyte activation and the percentage of Tregs, including low Apgar score, caesarean delivery, small gestational age, prenatal antibiotic exposure, vitamin D deficiency, and positive maternal group B streptococcus screening results (145, 146). Intraperitoneal injection of *Escherichia coli* O55: B5 LPS in neonatal mice reduced survival and growth rates, including lung development, in a dose-dependent manner. These effects were associated with decreases in the percentage of anti-inflammatory CD4+TCRβ+Foxp3+ Tregs (86).

In addition, multiple clinical studies show that amplification of CD4+CD25+ Tregs and increased Foxp3 levels may increase risks of nosocomial infections or secondary infections in sepsis (61, 68, 147). Using a "two-hit" CLP model with intratracheal injection of *Pseudomonas aeruginosa*, which mimics clinical conditions of secondary infection, Hu *et al.* demonstrated that the absolute number of Foxp3+ Tregs in both spleen and lungs increased 24 hours after secondary *P. aeruginosa* infection. After injection of PC61 (depletion of Tregs *via* CD25), the absolute numbers of Tregs in the spleens and lungs of septic mice were reduced by 50% and 60%, respectively. Partial Treg depletion increased IL-17A, IL-1β, and IL-6 secretion, and decreased IL-10 secretion, in septic mice infected with *P. aeruginosa*, thereby reducing the bacterial load and lung injury, and improving 7-day survival (90). On the other hand, 8-week-old male C57 mice with simulated repeat infection by repeated subcutaneous injection of LPS were able to resist CLP-induced sepsis and hyper inflammatory response. These mice had an increased absolute number of Tregs and Th17 and decreased ratio of Th17/Tregs (88). However, ICU studies with critically ill lymphocytopenia patients suggested that the first three days of septic shock may be characterized by a skewed distribution of circulating innate lymphoid cells (ILC), with an excess of ILC1 and a lack of ILC3. At the same time, there was a significant decrease in the absolute number of circulating Tregs (37). These conflicting studies in both mice and humans highlight the heterogeneous nature of Tregs in sepsis that vary upon host conditions.

TISSUE-SPECIFIC TREG PATTERNS IN SEPSIS

In addition to the role Tregs play in maintaining immune homeostasis in dedicated lymphoid tissues, these cells exist in other tissues such as the lung, liver, renal, muscle, brain and myocardium (73, 87, 98, 99, 102, 148). Many tissue-specific Treg functions go beyond our initial understanding of Tregs as immune inflammation-specific inhibitors (70, 99, 133). However, most previous interventional and observational studies on sepsis have focused on the functions and characteristics of Tregs in the peripheral circulation and spleen (41, 48, 76, 96, 101). Splenectomy improved 28- day survival in a secondary sepsis CLP mouse model from 62% to 92%, which was concurrent with the lower release of inflammatory cytokines (IL-6, CXCL-1, and MCP-1) and a 41% increase in Tregs within 48 hours (65). This indicates that induced circulating Tregs (iTregs), rather than natural Tregs (nTregs) originating in the spleen, may play a role in improving sepsis survival. Sepsis has tissue-specific pathophysiological characteristics due to anatomical and histological constraints: the structure, morphology, and composition of the vasculature system vary across different organs (149–151). In mice infected with *Pseudomonas aeruginosa*, the absolute number of Foxp3+ Tregs in lung tissue increased nearly 2-fold on the third day, then gradually decreased and returned to normal on the seventh day. However, the absolute number of Foxp3+ Tregs in the spleen increased 1.6-fold on the third day and continued to increase (90).

Acute lung injury (ALI) or acute respiratory distress syndrome (ARDS) is a type of respiratory failure caused by trauma, infection (sepsis), or intoxication (152, 153). The pathophysiological mechanism of ALI/ARDS is characterized by rapid onset of widespread lung inflammation (87, 135, 154). A growing body of evidence shows that CD4+CD25+Foxp3+Tregs play a positive role in alleviating sepsis-induced rapid onset inflammation and improving the outcome of ALI/ARDS through both TGF-β-dependent and independent pathways (20, 22, 42, 81, 87, 98, 155). In a mouse model of sepsis-induced ALI, blocking HMGB1 or myeloid-specific PTEN KO (PTEN M-KO) increased TGF-β production, inhibited Rorγt and IL-17 expression, and promoted the β-catenin signalling pathway. The increased CD4+CD25+Foxp3+ Tregs in the lungs improved survival and weight outcomes. However, the opposite result was obtained with myeloid-specific β-catenin ablation (β-catenin M-KO). Furthermore, *in vitro*, the destruction of macrophage HMGB1/PTEN or activation of β-catenin significantly increased CD4+CD25+Foxp3+ Tregs (87). This also suggests that infiltration of macrophages could inhibit lung tissue-specific CD4+CD25+Foxp3+ Tregs *via* HMGB1/PTEN/β-catenin axis in sepsis-induced ALI.

The pathophysiology of sepsis-associated encephalopathy (SAE) is complex, multifactorial, and tissue-specific. Combining intertwined processes, SAE is promoted by countless alterations and dysfunctions resulting from the early and late stages of sepsis. Additionally, some patients experience chronic "sepsis brain" after sepsis recovery, such as inflammation, neuro-inflammation, oxidative stress, reduced

brain metabolism, and injuries to the integrity of the blood brain barrier (BBB) (84, 156, 157). In the early stage of sepsis, some corresponding interventions are effective in alleviating the uncontrolled hyper-inflammatory (IL-1β, IL-6 IL-18, and TNF-α, etc.) and immune (CD3+CD4+ cells and CD3+CD8+ cells, etc.) responses associated with altering the BBB and amplifying the inflammatory responses of SAE (116, 156–158). Mesenchymal Stem Cell (MSC)-derived exosomes significantly increased the percentage and absolute number of Tregs, which ameliorated brain injury in the early stage of sepsis by mitigating the hyper-inflammatory and immune responses (116). As sepsis management techniques continue to improve, SAE is characterized as chronic "sepsis brain", which is associated with long-lasting cognitive deficits and psychological impairments such as anxiety and depression (159, 160). Using a CS-induced sepsis mouse model and focusing on chronic "sepsis brain", Saito *et al.* demonstrated that infiltrated Tregs and Th2 cells attenuate SAE and alleviate SAE-induced mental disorders by resolving neuroinflammation in the chronic phase of sepsis (84).

PATHOGEN-SPECIFIC TREG PATTERNS IN SEPSIS

Many previous induced sepsis models focused on Gram-negative bacteria and their products, such as LPS (50, 51, 101, 103, 118, 121, 161). A recent experimental LPS-induced endotoxemia study in humans showed that pro-inflammatory Th1 (IFN-γ, IL-2, and TNFα) and Th17 (IL-17A) cells were suppressed, while the Tregs and their ability to produce anti-inflammatory IL-10 were not affected (162). In addition, glycolipids and diacylglycerols from *Streptococcus pneumoniae*, which cause high mortality in patients over 65-years-old, induced septic shock by activating invariant natural killer T cells (iNKT) and the hyper-inflammatory responses (66, 110, 163, 164). Tregs reduced the proliferation of iNKT and IL-4 secretion of iNKT induced by glycolipids (including bacterial-derived diacylglycerols). One striking observation was that Tregs significantly increased Foxp3 expression, inhibitory function, and IL-10 secretion after they contacted iNKT, especially in the presence of bacterial diacylglycerols (164). Recent evidence suggests that *Streptococcus pneumoniae* (including its components and live attenuated mutants) and pneumococcal infection may induce Treg proliferation and may be used in the treatment of asthma (165).

Graphene oxide (GO) is a single-atomic layered material composed of carbon with a variety of biomedical applications, such as gene delivery, stem cell differentiation, and cancer therapy (166). In addition, GO has been shown to be able to regulate innate and adaptive immune functions (92, 166, 167). *In vivo*, the administration of GO significantly improved diacylglycerols-induced septic shock and inhibited the capacity of diacylglycerols to induce iNKT-mediated trans-activation and cytokine production of innate and innate-like cells (such as dendritic cells, macrophages, and γδ T cells), which were associated with the ability to increase the amount of Foxp3+ Tregs *via* TGF-β (166). This shows that gut microbiota not only influences the gastrointestinal tract, but also supports immune cells in distal organ sites (168). In another example, dietary supplementation with nonfermentable fiber or high fiber (HF) cellulose altered the gut microbiota and positively impacted metabolic health to confer protection in sepsis models (109, 169). Supplementation with HF amplified the suppressive function of CD4+CD25+Foxp3+ Tregs, inhibited SIRS, and induced anergy in CD4+ T cells as compared to mice on a regular diet (109). These pieces of evidence also suggest that manipulating intestinal microbiota through dietary supplementation with fiber may have broader systemic effects on immune homeostasis by influencing the heterogeneity of CD4+CD25+Foxp3+ Tregs.

Fungi are involved in 20% of sepsis and Candida is the most commonly isolated pathogen (170, 171). Patients with malignancies and immunodeficiencies are more likely to develop *Candida albicans* infection that leads to candidiasis (171). *C. albicans* induces the production of tumor infiltrating and IL-10 producing Tregs through toll-like receptor (TLR) 2, which leads to immune escape (64, 172). Different degrees (such as 1,3-β-D-glucan -positive colonization and invasive candidiasis) of Candida have different effects on patients with abdominal sepsis. Decreased B and NK cell counts, and reduced IL-8 secretion appeared to be associated with a higher risk of subsequent candidiasis, rather than the heterogeneous characteristics of Tregs. In contrast, the risk stratification of candidiasis did not affect the heterogeneous characteristics of Tregs in patients with abdominal sepsis (173).

TIME-DEPENDENT TREG PATTERNS IN SEPSIS

Considering the various failures of clinical trials targeting hyper-inflammatory mediators (especially IL-1β and TNF-α) and the fact that most septic patients who survive the acute stage of hyper-immune and inflammatory responses are burdened by secondary infections, it is necessary to perform basic and translational studies to understand the long-term post-sepsis immune perturbations (26, 27, 45, 46). The heterogeneous characteristics of Tregs are constantly changing over the course of sepsis. In the early stage of sepsis there is no difference in the percentage of Tregs in total CD4+ T cells between future sepsis survivors and non-survivors. However, non-survivors had a lower absolute number of Tregs compared to survivors. At the later stage of sepsis (after 3 days), the absolute number of Tregs increased, while the percentage of Tregs decreased in survivors. Although the absolute number of Tregs increased, the percentage of Tregs progressively increased in non-survivors. Moreover, survivors had a lower percentage of Tregs and a higher absolute number of Tregs (69, 75, 138). During the early stage of sepsis, especially with organs injuries caused by hyper-inflammatory responses (such as ALI, AKI, ALF, etc.), increasing the proportion and absolute number of Tregs is critical to restore

immune-inflammatory homeostasis, and reduce tissue damage and organs injury. Animals depleted of Tregs at this stage are unable to resolve SIRS and die from extensive tissue damage and MODS (20, 21, 70, 81, 98, 104, 108, 174).

Evidence from gene knock-out (KO) mice with sepsis induced by LPS or CLP illustrates that Tregs play a crucial role in inhibiting SIRS and ameliorating acute organs injury in the early stage of sepsis (77–79, 87, 94). Gpr174 deficiency in Tregs promoted the expression of CTLA-4 and the secretion of IL-10 in CD4+CD25+Foxp3+Tregs but the expression and percentage of PD-1 and Foxp3 was not affected. In Gpr174-KO mice induced by LPS or CLP to simulate sepsis, the induction of M2 macrophages in the early stage was Treg dependent and Gpr174-deficient Tregs protected mice from sepsis-induced ALI and improved survival by promoting M2 macrophage polarization (79).

The peritoneal contamination and infection (PCI) mouse model, which is consistent with secondary infections in post-septic patients, induced an increase in Bregs but did not induce a lasting increase in Treg absolute number in the spleens from 1 week to 3.5 months after sepsis induction (97). Since the absolute number of Foxp3+ Tregs in the lung tissues of CLP-induced septic mice increased nearly two-fold on the third day and returned to normal levels on the seventh day, mice were susceptible to intratracheal injection of *Pseudomonas aeruginosa* for 3 days, but not for 7 days (90). This suggests that Tregs have different functions at different stages of sepsis and contribute to secondary *P. aeruginosa* infection. In a study with Xuebijing Injection, which contains 5 Chinese medicine herbal extracts, mice were injected once/day for 5 days after CLP. Septic mice had significantly improved 7-day survival and reduced acute organ injury, which is associated with stimulated IL-10+ Foxp3+ Tregs, inhibited Th17 differentiation, and decreased Th17/Tregs (104). Some TCM, such as rhubarb, have a bidirectional regulatory effect on the heterogeneity of Tregs over time and improve the prognosis of sepsis by increasing the proportion of Tregs in the early stage and decreasing it in the late stage, although the specific molecular mechanism of their effect is not clear (100). Although these results are contradictory, they do imply that Foxp3+ Tregs play an important role in amending early, late, and even long-term immune disturbances after sepsis.

LIMITATIONS OF TREG MODELS IN SEPSIS

While most of the data discussed in this review comes from animal models, their limitations must be acknowledged. Most previous experiments related to sepsis were induced by CLP or LPS, where researchers used inbred mice under a specific pathogen-free (SPF) experimental environment. These methods do not fully conform to clinical heterogeneity and often do not inform the treatment of sepsis in humans (50, 51, 101, 103, 118, 121, 161, 175). In fact, changes in the heterogeneity of Tregs in induced sepsis animal models do not fully reflect clinical sepsis or are even opposite to patients' results (51, 75). Although LPS induction is a frequently used sepsis model, mice and other rodents are much less sensitive to LPS than humans. Thus, a 106 times higher (1-25 mg/kg) dose is required for mice compared to humans, who only need 2-4 ng/kg to induce SIRS (124, 162, 176). Furthermore, in most current experiments using LPS, the regimens and dosages of LPS vary widely among different mouse strains, animal ages, and animal facilities (23, 70, 87, 98, 109, 117, 118). For example, BALB/c mice induced by intraperitoneal injection of LPS (0.2 μg/g of body weight or 5 μg/mouse per day) for 5 consecutive days, showed significant decreases of CD4+, CD8+, CD3z+, and CD19+ cells and an increase of the percentage of CD25+Foxp3+ Tregs, accompanied with increased production of IL-6, TNF-α, and IL-18 in the serum. These results are consistent with the co-existence of SIRS and CARS observed in the early stage of septic patients (4, 15, 26, 45–51, 118). In a cross-design placebo-controlled study of 20 healthy male volunteers who received intravenous LPS (0.8 ng/kg body weight), their circulating neutrophils significantly increased. Additionally, the absolute numbers of CD3+, CD4+, and CD8+ T cells decreased 2 hours after LPS injection. In contrast, the frequency of Tregs and their ability to produce IL-10 did not change (162).

In the CLP model, the cecum of immunocompetent mice is sutured and then punctured to cause spillage of cecal contents into the peritoneum, which creates a life-threatening infection characterized by physical disorders (such as septic shock and acute organ failure) and ultimately death (99, 106, 161). Unfortunately, the precise composition of cecal contents that participates in the infection process is variable and has not been adequately evaluated in the case of acute organ failure (175). To compensate, some investigators tried to adopt intraperitoneal injection of stool suspension or CS, or endotracheal injection of a predetermined pathogen (such as *Klebsiella pneumonia* and *Staphylococcus aureus*, etc.) (59, 67, 97). The "two-hit" model was used to mimic clinical conditions of secondary infection, but different regimens yielded surprisingly different results (57, 70, 83, 90, 97).

Due to their relatively stable genetic uniformity, inbred BALB/c and C57BL/6 mice are most frequently used in sepsis-related studies (47, 59, 65, 70, 83, 86, 98, 118, 177). Nevertheless, researchers are beginning to emphasize the importance of using genetically heterogeneous organisms in experiments since they can better simulate the heterozygosity of humans, especially in multi-dimensional heterogeneous syndromes such as sepsis (19, 23, 67, 85, 100, 135, 136). BALB/c (inbred) and CD-1 (outbred) mice underwent unilateral femoral fracture, splenectomy, and hemorrhagic shock, with increased circulating granulocytes (LY6G+CD11+) in both strains at 24 and 48 hours later. However, CD8+ T cells decreased by 30% within 48h only in BALB/c mice. Circulating CD4+CD25+CD127low Tregs and lymphocytes (CD11B-LY6G-MHC-2+) were always at least 1.5-fold higher in BALB/c mice, while MHC-2 expression in bone marrow decreased in CD-1 mice. In addition, BALB/c mice expressed higher levels of circulatory CD4+CD25+CD127low Tregs and MHC-2+ lymphocytes, compared to CD-1 mice (178).

Based on the high heterogeneity of Tregs observed in clinical sepsis patient samples, we suggest that sepsis animal models should be designed to mimic this heterogeneity. For example, new sepsis models could be designed by guidance from both clinical sepsis patient characteristic and Treg immune checkpoints. Some experimental models of sepsis such as the "memory mouse" (57, 95), "two- or three-hit mouse" (70, 118), and "gene recombination mouse" models (78, 79, 94) have begun to move the field closer to more relevant sepsis models.

THERAPEUTIC INTERVENTIONS TARGETING TREGS

Several lines of evidence from experimental studies suggest that Tregs can be the target for therapeutic interventions. Deletion of Treg Notch4 gene with anti-Notch4 immunization in rodents normalizes dysregulated innate immunity to reduce morbidity and mortality (179). Lymphocyte-deficient recombinase activating gene-1 knockout mice exhibit impairments in lung injury healing. It has been found that administering isolated Tregs in a model of lung injury helps improve recovery (180). Depletion of Foxp3-positive Tregs from proliferating alveolar cells in a rodent model led to a decrease in epithelial proliferation (181). Such observations suggest that there are several pathways to explore regarding the therapeutic role of Tregs in sepsis. Moreover, Th17/Treg ratio alterations in favor of Th17 also have implications for therapeutic utility for lung injury and acute respiratory distress syndrome (182, 183).

DISCUSSION

Sepsis remains the leading cause of death in ICUs due to the progress of aging, numerous chronic comorbidities (diabetes, malignancies, autoimmune diseases, etc.), multi-drug resistant bacterial pathogens caused by excessive use of antibiotics, repeated secondary infections and other factors. The main pathologic mechanism of sepsis-induced immunosuppression is not completely understood. Furthermore, systematic, standardized clinical treatment for sepsis-induced immunosuppression is lacking. Therefore, there is an urgent need for a better understanding of the pathophysiological mechanisms of sepsis. New approaches to identify biological targets and checkpoints for detection, assessment, and management must be developed. Research that is emerging from the study of COVID-19 is likely to further inform scientists about the roles of Tregs in sepsis. In COVID-19 patients, Tregs are reported to behave variably. Whereas some studies have reported decreases in Tregs in COVID-19 patients (184, 185), others have reported increases in Tregs in COVID-19 patients (186, 187). An imbalance in the Treg/Th17 ratio in COVID-19 patients may increase the risk of respiratory failure (74, 188). Overall, to improve sepsis symptoms through the regulation of Tregs, it is necessary to find the optimal balance point for Tregs to play a role in sepsis. Researchers should not only take into account the heterogeneous characteristics of Tregs, but also the characteristics and organ/tissue-specific patterns of the host, the multi-dimensional heterogeneous syndrome of sepsis, the different types of pathogenic organisms, and even different types of laboratory research models and clinical research methods.

AUTHOR CONTRIBUTIONS

Conceptualization, Y-lG, YY, and Y-fC. Writing—original draft preparation, Y-lG, YY, XZ, FC, X-lM, X-sC, C-lW, and Y-cL. Writing—review and editing, Y-lG, Y-fC, and XT. Supervision, S-tS, Y-fC, and Y-lG. Funding acquisition, Y-lG and Y-fC. All authors have read and agreed to the published version of the manuscript.

FUNDING

This work was supported by the National Natural Science Foundation of China (No. 81871593, 81701931), and the National Natural Science Foundation of Tianjin (No. 18JCQNJC10500).

ACKNOWLEDGMENTS

We thank prof. Shu-Zhang Cui of Tianjin Medical University General Hospital for the help with the experimental design.

REFERENCES

1. Rudd KE, Johnson SC, Agesa KM, Shackelford KA, Tsoi D, Kievlan DR, et al. Global, Regional, and National Sepsis Incidence and Mortality, 1990–2017: Analysis for the Global Burden of Disease Study. *Lancet* (2020) 395 (10219):200–11. doi: 10.1016/S0140-6736(19)32989-7
2. Xie J, Wang H, Kang Y, Zhou L, Liu Z, Qin B, et al. The Epidemiology of Sepsis in Chinese ICUs: A National Cross-Sectional Survey. *Crit Care Med* (2020) 48(3):e209–e18. doi: 10.1097/CCM.0000000000004155
3. Weng L, Zeng XY, Yin P, Wang LJ, Wang CY, Jiang W, et al. Sepsis-Related Mortality in China: A Descriptive Analysis. *Intensive Care Med* (2018) 44 (7):1071–80. doi: 10.1007/s00134-018-5203-z
4. Rhodes A, Evans LE, Alhazzani W, Levy MM, Antonelli M, Ferrer R, et al. Surviving Sepsis Campaign: International Guidelines for Management of Sepsis and Septic Shock: 2016. *Intensive Care Med* (2017) 43(3):304–77. doi: 10.1007/s00134-017-4683-6
5. Weiss SL, Peters MJ, Alhazzani W, Agus MSD, Flori HR, Inwald DP, et al. Surviving Sepsis Campaign International Guidelines for the Management of Septic Shock and Sepsis-Associated Organ Dysfunction in Children. *Pediatr Crit Care Med* (2020) 21(2):e52–106. doi: 10.1097/PCC.0000000000002198
6. Karakike E, Kyriazopoulou E, Tsangaris I, Routsi C, Vincent JL, Giamarellos-Bourboulis EJ. The Early Change of SOFA Score as a Prognostic Marker of 28-Day Sepsis Mortality: Analysis Through a Derivation and a Validation Cohort. *Crit Care* (2019) 23(1):387. doi: 10.1186/s13054-019-2665-5
7. De Waele JJ, Akova M, Antonelli M, Canton R, Carlet J, De Backer D, et al. Antimicrobial Resistance and Antibiotic Stewardship Programs in the ICU: Insistence and Persistence in the Fight Against Resistance. A Position Statement From ESICM/ESCMID/WAAAR Round Table on Multi-Drug

Resistance. *Intensive Care Med* (2018) 44(2):189–96. doi: 10.1007/s00134-017-5036-1
8. Klein L, Robey EA, Hsieh C-S. Central CD4+ T Cell Tolerance: Deletion Versus Regulatory T Cell Differentiation. *Nat Rev Immunol* (2018) 19(1):7–18. doi: 10.1038/s41577-018-0083-6
9. von Knethen A, Heinicke U, Weigert A, Zacharowski K, Brune B. Histone Deacetylation Inhibitors as Modulators of Regulatory T Cells. *Int J Mol Sci* (2020) 21(7):2356. doi: 10.3390/ijms21072356
10. Sakaguchi S, Toda M, Asano M, Itoh M, Morse SS, Sakaguchi N. T Cell-Mediated Maintenance of Natural Self-Tolerance: Its Breakdown as a Possible Cause of Various Autoimmune Diseases. *J Autoimmun* (1996) 9 (2):211–20. doi: 10.1006/jaut.1996.0026
11. Ramsdell F, Rudensky AY. Foxp3: A Genetic Foundation for Regulatory T Cell Differentiation and Function. *Nat Immunol* (2020) 21(7):708–9. doi: 10.1038/s41590-020-0694-5
12. Cortez JT, Montauti E, Shifrut E, Gatchalian J, Zhang Y, Shaked O, et al. CRISPR Screen in Regulatory T Cells Reveals Modulators of Foxp3. *Nature* (2020) 582(7812):416–20. doi: 10.1038/s41586-020-2246-4
13. Tatura R, Zeschnigk M, Hansen W, Steinmann J, Vidigal PG, Hutzler M, et al. Relevance of Foxp3(+) Regulatory T Cells for Early and Late Phases of Murine Sepsis. *Immunology* (2015) 146(1):144–56. doi: 10.1111/imm.12490
14. Yao RQ, Ren C, Wang JN, Wu GS, Zhu XM, Xia ZF, et al. Publication Trends of Research on Sepsis and Host Immune Response During 1999-2019: A 20-Year Bibliometric Analysis. *Int J Biol Sci* (2020) 16(1):27–37. doi: 10.7150/ijbs.37496
15. McBride MA, Patil TK, Bohannon JK, Hernandez A, Sherwood ER, Patil NK. Immune Checkpoints: Novel Therapeutic Targets to Attenuate Sepsis-Induced Immunosuppression. *Front Immunol* (2020) 11:624272. doi: 10.3389/fimmu.2020.624272
16. Poujol F, Monneret G, Gallet-Gorius E, Pachot A, Textoris J, Venet F. Ex Vivo Stimulation of Lymphocytes With IL-10 Mimics Sepsis-Induced Intrinsic T-Cell Alterations. *Immunol Invest* (2018) 47(2):154–68. doi: 10.1080/08820139.2017.1407786
17. George JA, Park SO, Choi JY, Uyangaa E, Eo SK. Double-Faced Implication of CD4(+) Foxp3(+) Regulatory T Cells Expanded by Acute Dengue Infection *via* TLR2/MyD88 Pathway. *Eur J Immunol* (2020) 50(7):1000–18. doi: 10.1002/eji.201948420
18. Ono S, Kimura A, Hiraki S, Takahata R, Tsujimoto H, Kinoshita M, et al. Removal of Increased Circulating CD4+CD25+Foxp3+ Regulatory T Cells in Patients With Septic Shock Using Hemoperfusion With Polymyxin B-Immobilized Fibers. *Surgery* (2013) 153(2):262–71. doi: 10.1016/j.surg.2012.06.023
19. Zou Q, Yang M, Yu M, Liu C. Influences of Regulation of miR-126 on Inflammation,Th17/Treg Subpopulation Differentiation, and Lymphocyte Apoptosis Through Caspase Signaling Pathway in Sepsis. *Inflammation* (2020) 43(6):2287–300. doi: 10.1007/s10753-020-01298-7
20. Xia H, Wang F, Wang M, Wang J, Sun S, Chen M, et al. Maresin1 Ameliorates Acute Lung Injury Induced by Sepsis Through Regulating Th17/Treg Balance. *Life Sci* (2020) 254:117773. doi: 10.1016/j.lfs.2020.117773
21. Liu P, Xiao Z, Yan H, Lu X, Zhang X, Luo L, et al. Baicalin Suppresses Th1 and Th17 Responses and Promotes Treg Response to Ameliorate Sepsis-Associated Pancreatic Injury *via* the RhoA-ROCK Pathway. *Int Immunopharmacol* (2020) 86:106685. doi: 10.1016/j.intimp.2020.106685
22. Sun JK, Zhang WH, Chen WX, Wang X, Mu XW. Effects of Early Enteral Nutrition on Th17/Treg Cells and IL-23/IL-17 in Septic Patients. *World J Gastroenterol* (2019) 25(22):2799–808. doi: 10.3748/wjg.v25.i22.2799
23. He W, Xiao K, Xu J, Guan W, Xie S, Wang K, et al. Recurrent Sepsis Exacerbates CD4(+) T Cell Exhaustion and Decreases Antiviral Immune Responses. *Front Immunol* (2021) 12:627435. doi: 10.3389/fimmu.2021.627435
24. Coopersmith CM, De Backer D, Deutschman CS, Ferrer R, Lat I, Machado FR, et al. Surviving Sepsis Campaign: Research Priorities for Sepsis and Septic Shock. *Intensive Care Med* (2018) 44(9):1400–26. doi: 10.1007/s00134-018-5175-z
25. Bone RC, Balk RA, Cerra FB, Dellinger RP, Fein AM, Knaus WA, et al. Definitions for Sepsis and Organ Failure and Guidelines for the Use of Innovative Therapies in Sepsis. The ACCP/SCCM Consensus Conference Committee. American College of Chest Physicians/Society of Critical Care Medicine. *Chest* (1992) 101(6):1644–55. doi: 10.1378/chest.101.6.1644
26. Hotchkiss RS, Monneret G, Payen D. Sepsis-Induced Immunosuppression: From Cellular Dysfunctions to Immunotherapy. *Nat Rev Immunol* (2013) 13 (12):862–74. doi: 10.1038/nri3552
27. Poutsiaka DD, Porto MC, Perry WA, Hudcova J, Tybor DJ, Hadley S, et al. Prospective Observational Study Comparing Sepsis-2 and Sepsis-3 Definitions in Predicting Mortality in Critically Ill Patients. *Open Forum Infect Dis* (2019) 6(7):ofz271. doi: 10.1093/ofid/ofz271
28. Raith EP, Udy AA, Bailey M, McGloughlin S, MacIsaac C, Bellomo R, et al. Prognostic Accuracy of the SOFA Score, SIRS Criteria, and qSOFA Score for In-Hospital Mortality Among Adults With Suspected Infection Admitted to the Intensive Care Unit. *JAMA* (2017) 317(3):290–300. doi: 10.1001/jama.2016.20328
29. Singer M, Deutschman CS, Seymour CW, Shankar-Hari M, Annane D, Bauer M, et al. The Third International Consensus Definitions for Sepsis and Septic Shock (Sepsis-3). *JAMA* (2016) 315(8):801–10. doi: 10.1001/jama.2016.0287
30. Seymour CW, Liu VX, Iwashyna TJ, Brunkhorst FM, Rea TD, Scherag A, et al. Assessment of Clinical Criteria for Sepsis: For the Third International Consensus Definitions for Sepsis and Septic Shock (Sepsis-3). *JAMA* (2016) 315(8):762–74. doi: 10.1001/jama.2016.0288
31. Liu YC, Luo YY, Zhang X, Shou ST, Gao YL, Lu B, et al. Quick Sequential Organ Failure Assessment as a Prognostic Factor for Infected Patients Outside the Intensive Care Unit: A Systematic Review and Meta-Analysis. *Intern Emerg Med* (2019) 14(4):603–15. doi: 10.1007/s11739-019-02036-0
32. Evans L, Rhodes A, Alhazzani W, Antonelli M, Coopersmith CM, French C, et al. Surviving Sepsis Campaign: International Guidelines for Management of Sepsis and Septic Shock 2021. *Crit Care Med* (2021) 49(11):e1063–143. doi: 10.1097/CCM.0000000000005337
33. Kellum JA, Pike F, Yealy DM, Huang DT, Shapiro NI, Angus DC, et al. Relationship Between Alternative Resuscitation Strategies, Host Response and Injury Biomarkers, and Outcome in Septic Shock: Analysis of the Protocol-Based Care for Early Septic Shock Study. *Crit Care Med* (2017) 45(3):438–45. doi: 10.1097/CCM.0000000000002206
34. Ono S, Tsujimoto H, Hiraki S, Aosasa S. Mechanisms of Sepsis-Induced Immunosuppression and Immunological Modification Therapies for Sepsis. *Ann Gastroenterol Surg* (2018) 2(5):351–8. doi: 10.1002/ags3.12194
35. Schmoeckel K, Mrochen DM, Huhn J, Potschke C, Broker BM. Polymicrobial Sepsis and Non-Specific Immunization Induce Adaptive Immunosuppression to a Similar Degree. *PloS One* (2018) 13(2):e0192197. doi: 10.1371/journal.pone.0192197
36. Hotchkiss RS, Karl IE. The Pathophysiology and Treatment of Sepsis. *N Engl J Med* (2003) 348(2):138–50. doi: 10.1056/NEJMra021333
37. Carvelli J, Piperoglou C, Bourenne J, Farnarier C, Banzet N, Demerle C, et al. Imbalance of Circulating Innate Lymphoid Cell Subpopulations in Patients With Septic Shock. *Front Immunol* (2019) 10:2179. doi: 10.3389/fimmu.2019.02179
38. Rhee C, Dantes R, Epstein L, Murphy DJ, Seymour CW, Iwashyna TJ, et al. Incidence and Trends of Sepsis in US Hospitals Using Clinical vs Claims Data, 2009-2014. *JAMA* (2017) 318(13):1241–9. doi: 10.1001/jama.2017.13836
39. Seymour CW, Gesten F, Prescott HC, Friedrich ME, Iwashyna TJ, Phillips GS, et al. Time to Treatment and Mortality During Mandated Emergency Care for Sepsis. *N Engl J Med* (2017) 376(23):2235–44. doi: 10.1056/NEJMoa1703058
40. Lu Y, An L, Liu Q, Li C. Expression and Clinical Correlations of Costimulatory Molecules on Peripheral T Lymphocyte Subsets of Early-Stage Severe Sepsis: A Prospective Observational Study. *Shock* (2018) 49 (6):631–40. doi: 10.1097/SHK.0000000000001017
41. You B, Zhang YL, Luo GX, Dang YM, Jiang B, Huang GT, et al. Early Application of Continuous High-Volume Haemofiltration can Reduce Sepsis and Improve the Prognosis of Patients With Severe Burns. *Crit Care* (2018) 22(1):173. doi: 10.1186/s13054-018-2095-9
42. Liu Y, Zhao W, Chen W, Shen X, Fu R, Zhao Y, et al. Effects of Early Enteral Nutrition on Immune Function and Prognosis of Patients With Sepsis on Mechanical Ventilation. *J Intensive Care Med* (2020) 35(10):1053–61. doi: 10.1177/0885066618809893

43. Yang XY, Song J, Hou SK, Fan HJ, Lv Q, Liu ZQ, et al. Ulinastatin Ameliorates Acute Kidney Injury Induced by Crush Syndrome Inflammation by Modulating Th17/Treg Cells. *Int Immunopharmacol* (2020) 81:106265. doi: 10.1016/j.intimp.2020.106265
44. Antonakos N, Tsaganos T, Oberle V, Tsangaris I, Lada M, Pistiki A, et al. Decreased Cytokine Production by Mononuclear Cells After Severe Gram-Negative Infections: Early Clinical Signs and Association With Final Outcome. *Crit Care* (2017) 21(1):48. doi: 10.1186/s13054-017-1625-1
45. Donnelly JP, Hohmann SF, Wang HE. Unplanned Readmissions After Hospitalization for Severe Sepsis at Academic Medical Center-Affiliated Hospitals. *Crit Care Med* (2015) 43(9):1916–27. doi: 10.1097/CCM.0000000000001147
46. Hotchkiss RS, Colston E, Yende S, Crouser ED, Martin GS, Albertson T, et al. Immune Checkpoint Inhibition in Sepsis: A Phase 1b Randomized Study to Evaluate the Safety, Tolerability, Pharmacokinetics, and Pharmacodynamics of Nivolumab. *Intensive Care Med* (2019) 45 (10):1360–71. doi: 10.1007/s00134-019-05704-z
47. Gao Y, Li L, Liu Y, Li W, Wang Z, Shou S, et al. [Effect of Semaphorin-3A on the Cellular Stability of CD4(+)CD25(+) Regulatory T Cells Induced by Lipopolysaccharide]. *Zhonghua Wei Zhong Bing Ji Jiu Yi Xue* (2020) 32 (12):1454–60. doi: 10.3760/cma.j.cn121430-20200706-00501
48. Gao Y, Wang C, Wang Z, Li W, Liu Y, Shou S, et al. Semaphorin 3A Contributes to Sepsis–Induced Immunosuppression by Impairing CD4+ T Cell Anergy. *Mol Med Rep* (2021) 23(4):302. doi: 10.3892/mmr.2021.11941
49. von Dach E, Albrich WC, Brunel A-S, Prendki V, Cuvelier C, Flury D, et al. Effect of C-Reactive Protein–Guided Antibiotic Treatment Duration, 7-Day Treatment, or 14-Day Treatment on 30-Day Clinical Failure Rate in Patients With Uncomplicated Gram-Negative Bacteremia. *JAMA* (2020) 323 (21):2160–9. doi: 10.1001/jama.2020.6348
50. Gao Y-L, Wang C-X, Wang Z-Y, Li W-J, Liu Y-C, Shou S-T, et al. Targeting Neuropilin-1 Suppresses the Stability of CD4 CD25 Regulatory T Cells via the NF-kb Signaling Pathway in Sepsis. *Infect Immun* (2021) 89(2):e00399–20. doi: 10.1128/IAI.00399-20
51. Martin AN, Alexander-Miller M, Yoza BK, Vachharajani V, McCall CE. Sirtuin1 Targeting Reverses Innate and Adaptive Immune Tolerance in Septic Mice. *J Immunol Res* (2018) 2018:2402593. doi: 10.1155/2018/2402593
52. Daviaud F, Grimaldi D, Dechartres A, Charpentier J, Geri G, Marin N, et al. Timing and Causes of Death in Septic Shock. *Ann Intensive Care* (2015) 5 (1):16. doi: 10.1186/s13613-015-0058-8
53. Olonisakin TF, Suber T, Gonzalez-Ferrer S, Xiong Z, Peñaloza HF, van der Geest R, et al. Stressed Erythrophagocytosis Induces Immunosuppression During Sepsis Through Heme-Mediated STAT1 Dysregulation. *J Clin Invest* (2021) 131(1):e137468. doi: 10.1172/JCI137468
54. Zhang H, Xu CF, Ren C, Wu TT, Dong N, Yao YM. Novel Role of P53 in Septic Immunosuppression: Involvement in Loss and Dysfunction of CD4+ T Lymphocytes. *Cell Physiol Biochem* (2018) 51(1):452–69. doi: 10.1159/000495241
55. Chen CW, Xue M, Zhang W, Xie J, Coopersmith CM, Ford ML. 2B4 But Not PD-1 Blockade Improves Mortality in Septic Animals With Preexisting Malignancy. *JCI Insight* (2019) 4(22):e127867. doi: 10.1172/jci.insight.127867
56. Chen C-W, Mittal R, Klingensmith NJ, Burd EM, Terhorst C, Martin GS, et al. Cutting Edge: 2b4-Mediated Coinhibition of CD4+ T Cells Underlies Mortality in Experimental Sepsis. *J Immunol* (2017) 199(6):1961–6. doi: 10.4049/jimmunol.1700375
57. Sun Y, Anyalebechi JC, Sun H, Yumoto T, Xue M, Liu D, et al. Anti-TIGIT Differentially Affects Sepsis Survival in Immunologically Experienced Versus Previously Naive Hosts. *JCI Insight* (2021) 6(5):e141245. doi: 10.1172/jci.insight.141245
58. Chang KC, Burnham C-A, Compton SM, Rasche DP, Mazuski RJ, McDonough JS, et al. Blockade of the Negative Co-Stimulatory Molecules PD-1 and CTLA-4 Improves Survival in Primary and Secondary Fungal Sepsis. *Crit Care (London England)* (2013) 17(3):R85. doi: 10.1186/cc12711
59. Saito M, Inoue S, Yamashita K, Kakeji Y, Fukumoto T, Kotani J. IL-15 Improves Aging-Induced Persistent T Cell Exhaustion in Mouse Models of Repeated Sepsis. *Shock* (2020) 53(2):228–35. doi: 10.1097/SHK.0000000000001352
60. Xu J, Li J, Xiao K, Zou S, Yan P, Xie X, et al. Dynamic Changes in Human HLA-DRA Gene Expression and Th Cell Subsets in Sepsis: Indications of Immunosuppression and Associated Outcomes. *Scand J Immunol* (2020) 91 (1):e12813. doi: 10.1111/sji.12813
61. Landelle C, Lepape A, Voirin N, Tognet E, Venet F, Bohe J, et al. Low Monocyte Human Leukocyte Antigen-DR is Independently Associated With Nosocomial Infections After Septic Shock. *Intensive Care Med* (2010) 36 (11):1859–66. doi: 10.1007/s00134-010-1962-x
62. Yende S, Kellum JA, Talisa VB, Peck Palmer OM, Chang CH, Filbin MR, et al. Long-Term Host Immune Response Trajectories Among Hospitalized Patients With Sepsis. *JAMA Netw Open* (2019) 2(8):e198686. doi: 10.1001/jamanetworkopen.2019.8686
63. Franekova J, Protus M, Kieslichova E, Brezina A, Komrskova J, Vymetalik J, et al. Changes in Sepsis Biomarkers After Immunosuppressant Administration in Transplant Patients. *Mediators Inflammation* (2021) 2021:8831659. doi: 10.1155/2021/8831659
64. Ahmadi N, Ahmadi A, Kheirali E, Hossein Yadegari M, Bayat M, Shajiei A, et al. Systemic Infection With Candida Albicans in Breast Tumor Bearing Mice: Cytokines Dysregulation and Induction of Regulatory T Cells. *J Mycol Med* (2019) 29(1):49–55. doi: 10.1016/j.mycmed.2018.10.006
65. Drechsler S, Zipperle J, Rademann P, Jafarmadar M, Klotz A, Bahrami S, et al. Splenectomy Modulates Early Immuno-Inflammatory Responses to Trauma-Hemorrhage and Protects Mice Against Secondary Sepsis. *Sci Rep* (2018) 8(1):14890. doi: 10.1038/s41598-018-33232-1
66. Wester AL, Dunlop O, Melby KK, Dahle UR, Wyller TB. Age-Related Differences in Symptoms, Diagnosis and Prognosis of Bacteremia. *BMC Infect Dis* (2013) 13:346. doi: 10.1186/1471-2334-13-346
67. Li L-L, Dai B, Sun Y-H, Zhang T-T. The Activation of IL-17 Signaling Pathway Promotes Pyroptosis in Pneumonia-Induced Sepsis. *Ann Trans Med* (2020) 8(11):674–. doi: 10.21037/atm-19-1739
68. de Roquetaillade C, Mansouri S, Brumpt C, Neuwirth M, Voicu S, Le Dorze M, et al. Comparison of Circulating Immune Cells Profiles and Kinetics Between Coronavirus Disease 2019 and Bacterial Sepsis. *Crit Care Med* (2021) 49(10):1717–25. doi: 10.1097/CCM.0000000000005088
69. Bomans K, Schenz J, Sztwiertnia I, Schaack D, Weigand MA, Uhle F. Sepsis Induces a Long-Lasting State of Trained Immunity in Bone Marrow Monocytes. *Front Immunol* (2018) 9:2685. doi: 10.3389/fimmu.2018.02685
70. Tran DT, Jeong YY, Kim JM, Bae HB, Son SK, Kwak SH. The Anti-Inflammatory Role of Bilirubin on "Two-Hit" Sepsis Animal Model. *Int J Mol Sci* (2020) 21(22):8650. doi: 10.3390/ijms21228650
71. Luo CT, Li MO. Transcriptional Control of Regulatory T Cell Development and Function. *Trends Immunol* (2013) 34(11):531–9. doi: 10.1016/j.it.2013.08.003
72. Zemmour D, Zilionis R, Kiner E, Klein AM, Mathis D, Benoist C. Single-Cell Gene Expression Reveals a Landscape of Regulatory T Cell Phenotypes Shaped by the TCR. *Nat Immunol* (2018) 19(3):291–301. doi: 10.1038/s41590-018-0051-0
73. Wing JB, Tanaka A, Sakaguchi S. Human FOXP3(+) Regulatory T Cell Heterogeneity and Function in Autoimmunity and Cancer. *Immunity* (2019) 50(2):302–16. doi: 10.1016/j.immuni.2019.01.020
74. Yin F, Xi YL, Wang Y, Li BR, Qian J, Ren H, et al. The Clinical Outcomes and Biomarker Features of Severe Sepsis/Septic Shock With Severe Neutropenia: A Retrospective Cohort Study. *Transl Pediatr* (2021) 10(3):464–73. doi: 10.21037/tp-20-230
75. Liu Q, Lu Y, An L, Li CS. B- and T-Lymphocyte Attenuator Expression on Regulatory T-Cells in Patients With Severe Sepsis. *Chin Med J (Engl)* (2018) 131(21):2637–9. doi: 10.4103/0366-6999.244104
76. Jiang W, Li X, Ding H, Wang K, Liu X, Wang Q, et al. PD-1 in Tregs Predicts the Survival in Sepsis Patients Using Sepsis-3 Criteria: A Prospective, Two-Stage Study. *Int Immunopharmacol* (2020) 89(Pt A):107175. doi: 10.1016/j.intimp.2020.107175
77. Lou JS, Wang JF, Fei MM, Zhang Y, Wang J, Guo Y, et al. Targeting Lymphocyte Activation Gene 3 to Reverse T-Lymphocyte Dysfunction and Improve Survival in Murine Polymicrobial Sepsis. *J Infect Dis* (2020) 222 (6):1051–61. doi: 10.1093/infdis/jiaa191
78. Fay KT, Chihade DB, Chen CW, Klingensmith NJ, Lyons JD, Ramonell K, et al. Increased Mortality in CD43-Deficient Mice During Sepsis. *PloS One* (2018) 13(9):e0202656. doi: 10.1371/journal.pone.0202656

79. Qiu D, Chu X, Hua L, Yang Y, Li K, Han Y, et al. Gpr174-Deficient Regulatory T Cells Decrease Cytokine Storm in Septic Mice. *Cell Death Dis* (2019) 10(3):233. doi: 10.1038/s41419-019-1462-z
80. Yu Q, Li Y, Wang H, Xiong H. TSLP Induces a Proinflammatory Phenotype in Circulating Innate Cells and Predicts Prognosis in Sepsis Patients. *FEBS Open Bio* (2019) 9(12):2137–48. doi: 10.1002/2211-5463.12746
81. Zhao J, Liu Y, Hu JN, Peng M, Dong N, Zhu XM, et al. Autocrine Regulation of Interleukin-3 in the Activity of Regulatory T Cells and its Effectiveness in the Pathophysiology of Sepsis. *J Infect Dis* (2021) 223(5):893–904. doi: 10.1093/infdis/jiaa441
82. Xu T, Zhao J, Wang X, Meng Y, Zhao Z, Bao R, et al. CXCL4 Promoted the Production of CD4(+)CD25(+)FOXP3(+)treg Cells in Mouse Sepsis Model Through Regulating STAT5/FOXP3 Pathway. *Autoimmunity* (2020) 53 (5):289–96. doi: 10.1080/08916934.2020.1777283
83. Gaborit BJ, Roquilly A, Louvet C, Sadek A, Tessoulin B, Broquet A, et al. Regulatory T Cells Expressing Tumor Necrosis Factor Receptor Type 2 Play a Major Role in CD4+ T-Cell Impairment During Sepsis. *J Infect Dis* (2020) 222(7):1222–34. doi: 10.1093/infdis/jiaa225
84. Saito M, Fujinami Y, Ono Y, Ohyama S, Fujioka K, Yamashita K, et al. Infiltrated Regulatory T Cells and Th2 Cells in the Brain Contribute to Attenuation of Sepsis-Associated Encephalopathy and Alleviation of Mental Impairments in Mice With Polymicrobial Sepsis. *Brain Behav Immun* (2021) 92:25–38. doi: 10.1016/j.bbi.2020.11.010
85. Baek O, Ren S, Brunse A, Sangild PT, Nguyen DN. Impaired Neonatal Immunity and Infection Resistance Following Fetal Growth Restriction in Preterm Pigs. *Front Immunol* (2020) 11:1808. doi: 10.3389/fimmu.2020.01808
86. Shrestha AK, Bettini ML, Menon RT, Gopal VYN, Huang S, Edwards DP, et al. Consequences of Early Postnatal Lipopolysaccharide Exposure on Developing Lungs in Mice. *Am J Physiol Lung Cell Mol Physiol* (2019) 316 (1):L229–L44. doi: 10.1152/ajplung.00560.2017
87. Zhou M, Fang H, Du M, Li C, Tang R, Liu H, et al. The Modulation of Regulatory T Cells *via* HMGB1/PTEN/beta-Catenin Axis in LPS Induced Acute Lung Injury. *Front Immunol* (2019) 10:1612. doi: 10.3389/fimmu.2019.01612
88. Andrade MMC, Ariga SSK, Barbeiro DF, Barbeiro HV, Pimentel RN, Petroni RC, et al. Endotoxin Tolerance Modulates TREG and TH17 Lymphocytes Protecting Septic Mice. *Oncotarget* (2019) 10(37):3451–61. doi: 10.18632/oncotarget.26919
89. Cao C, Chai Y, Shou S, Wang J, Huang Y, Ma T. Toll-Like Receptor 4 Deficiency Increases Resistance in Sepsis-Induced Immune Dysfunction. *Int Immunopharmacol* (2018) 54:169–76. doi: 10.1016/j.intimp.2017.11.006
90. Hu ZQ, Yao YM, Chen W, Bian JL, Zhao LJ, Chen LW, et al. Partial Depletion of Regulatory T Cells Enhances Host Inflammatory Response Against Acute Pseudomonas Aeruginosa Infection After Sepsis. *Inflammation* (2018) 41(5):1780–90. doi: 10.1007/s10753-018-0821-8
91. Greenberg JA, Hohmann SF, Hall JB, Kress JP, David MZ. Validation of a Method to Identify Immunocompromised Patients With Severe Sepsis in Administrative Databases. *Ann Am Thorac Soc* (2016) 13(2):253–8. doi: 10.1513/AnnalsATS.201507-415BC
92. Shurin MR, Yanamala N, Kisin ER, Tkach AV, Shurin GV, Murray AR, et al. Graphene Oxide Attenuates Th2-Type Immune Responses, But Augments Airway Remodeling and Hyperresponsiveness in a Murine Model of Asthma. *ACS Nano* (2014) 8(6):5585–99. doi: 10.1021/nn406454u
93. Gao DN, Yang ZX, Qi QH. Roles of PD-1, Tim-3 and CTLA-4 in Immunoregulation in Regulatory T Cells Among Patients With Sepsis. *Int J Clin Exp Med* (2015) 8(10):18998–9005.
94. Willers M, Ulas T, Vollger L, Vogl T, Heinemann AS, Pirr S, et al. S100A8 and S100A9 Are Important for Postnatal Development of Gut Microbiota and Immune System in Mice and Infants. *Gastroenterology* (2020) 159 (6):2130–45 e5. doi: 10.1053/j.gastro.2020.08.019
95. Sun Y, Xie J, Anyalebechi JC, Chen CW, Sun H, Xue M, et al. CD28 Agonism Improves Survival in Immunologically Experienced Septic Mice *via* IL-10 Released by Foxp3(+) Regulatory T Cells. *J Immunol* (2020) 205(12):3358–71. doi: 10.4049/jimmunol.2000595
96. Ge Y, Huang M, Wu Y, Dong N, Yao YM. Interleukin-38 Protects Against Sepsis by Augmenting Immunosuppressive Activity of CD4(+) CD25(+) Regulatory T Cells. *J Cell Mol Med* (2020) 24(2):2027–39. doi: 10.1111/jcmm.14902
97. Kulkarni U, Herrmenau C, Win SJ, Bauer M, Kamradt T. IL-7 Treatment Augments and Prolongs Sepsis-Induced Expansion of IL-10-Producing B Lymphocytes and Myeloid-Derived Suppressor Cells. *PloS One* (2018) 13(2): e0192304. doi: 10.1371/journal.pone.0192304
98. Nadeem A, Al-Harbi NO, Ahmad SF, Al-Harbi MM, Alhamed AS, Alfardan AS, et al. Blockade of Interleukin-2-Inducible T-Cell Kinase Signaling Attenuates Acute Lung Injury in Mice Through Adjustment of Pulmonary Th17/Treg Immune Responses and Reduction of Oxidative Stress. *Int Immunopharmacol* (2020) 83:106369. doi: 10.1016/j.intimp.2020.106369
99. Li H, Qiu D, Yang H, Yuan Y, Wu L, Chu L, et al. Therapeutic Efficacy of Excretory-Secretory Products of Trichinella Spiralis Adult Worms on Sepsis-Induced Acute Lung Injury in a Mouse Model. *Front Cell Infect Microbiol* (2021) 11:653843. doi: 10.3389/fcimb.2021.653843
100. Liu J, Li G, Chen YZ, Zhang LD, Wang T, Wen ZL, et al. Effects of Rhubarb on the Expression of Glucocorticoids Receptor and Regulation of Cellular Immunity in Burn-Induced Septic Rats. *Chin Med J (Engl)* (2019) 132 (10):1188–93. doi: 10.1097/CM9.0000000000000201
101. Ge Y, Huang M, Dong N, Yao YM. Effect of Interleukin-36beta on Activating Autophagy of CD4+CD25+ Regulatory T Cells and Its Immune Regulation in Sepsis. *J Infect Dis* (2020) 222(9):1517–30. doi: 10.1093/infdis/jiaa258
102. Brichacek AL, Benkovic SA, Chakraborty S, Nwafor DC, Wang W, Jun S, et al. Systemic Inhibition of Tissue-Nonspecific Alkaline Phosphatase Alters the Brain-Immune Axis in Experimental Sepsis. *Sci Rep* (2019) 9(1):18788. doi: 10.1038/s41598-019-55154-2
103. Gao M, Ou H, Jiang Y, Wang K, Peng Y, Zhang H, et al. Tanshinone IIA Attenuates Sepsis-Induced Immunosuppression and Improves Survival Rate in a Mice Peritonitis Model. *BioMed Pharmacother* (2019) 112:108609. doi: 10.1016/j.biopha.2019.108609
104. Chen X, Feng Y, Shen X, Pan G, Fan G, Gao X, et al. Anti-Sepsis Protection of Xuebijing Injection is Mediated by Differential Regulation of Pro- and Anti-Inflammatory Th17 and T Regulatory Cells in a Murine Model of Polymicrobial Sepsis. *J Ethnopharmacol* (2018) 211:358–65. doi: 10.1016/j.jep.2017.10.001
105. Chen L, Lu Y, Zhao L, Hu L, Qiu Q, Zhang Z, et al. Curcumin Attenuates Sepsis-Induced Acute Organ Dysfunction by Preventing Inflammation and Enhancing the Suppressive Function of Tregs. *Int Immunopharmacol* (2018) 61:1–7. doi: 10.1016/j.intimp.2018.04.041
106. Xie DP, Zhou GB, Chen RL, Qin XL, Du JD, Zhang Y, et al. Effect of Electroacupuncture at Zusanli (ST36) on Sepsis Induced by Cecal Ligation Puncture and Its Relevance to Spleen. *Evid Based Complement Alternat Med* (2020) 2020:1914031. doi: 10.1155/2020/1914031
107. Hou YC, Wu JM, Chen KY, Chen PD, Lei CS, Yeh SL, et al. Effects of Prophylactic Administration of Glutamine on CD4(+) T Cell Polarisation and Kidney Injury in Mice With Polymicrobial Sepsis. *Br J Nutr* (2019) 122 (6):657–65. doi: 10.1017/S0007114519000990
108. Yeh CL, Tanuseputero SA, Wu JM, Tseng YR, Yang PJ, Lee PC, et al. Intravenous Arginine Administration Benefits CD4(+) T-Cell Homeostasis and Attenuates Liver Inflammation in Mice With Polymicrobial Sepsis. *Nutrients* (2020) 12(4):1047. doi: 10.3390/nu12041047
109. Di Caro V, Cummings JL, Alcamo AM, Piganelli JD, Clark RSB, Morowitz MJ, et al. Dietary Cellulose Supplementation Modulates the Immune Response in a Murine Endotoxemia Model. *Shock* (2019) 51(4):526–34. doi: 10.1097/SHK.0000000000001180
110. Yamaguchi M, Hirose Y, Takemura M, Ono M, Sumitomo T, Nakata M, et al. Streptococcus Pneumoniae Evades Host Cell Phagocytosis and Limits Host Mortality Through Its Cell Wall Anchoring Protein PfbA. *Front Cell Infect Microbiol* (2019) 9:301. doi: 10.3389/fcimb.2019.00301
111. Albayati S, Vemulapalli H, Tsygankov AY, Liverani E. P2Y12 Antagonism Results in Altered Interactions Between Platelets and Regulatory T Cells During Sepsis. *J Leukoc Biol* (2020) 110(1):141–53. doi: 10.1002/JLB.3A0220-097R
112. Guo Y, Wu B, Chen Q, Min S. Parecoxib Ameliorates Renal Toxicity and Injury in Sepsis-Induced Mouse Model and LPS-Induced HK-2 Cells. *Drug Dev Res* (2021) 10.1002/ddr.21897. doi: 10.1002/ddr.21897
113. Ahmad A, Vieira JC, de Mello AH, de Lima TM, Ariga SK, Barbeiro DF, et al. The PARP Inhibitor Olaparib Exerts Beneficial Effects in Mice Subjected to Cecal Ligature and Puncture and in Cells Subjected to Oxidative Stress Without Impairing DNA Integrity: A Potential Opportunity for Repurposing

a Clinically Used Oncological Drug for the Experimental Therapy of Sepsis. *Pharmacol Res* (2019) 145:104263. doi: 10.1016/j.phrs.2019.104263
114. Cao C, Yin C, Chai Y, Jin H, Wang L, Shou S. Ulinastatin Mediates Suppression of Regulatory T Cells Through TLR4/NF-kappaB Signaling Pathway in Murine Sepsis. *Int Immunopharmacol* (2018) 64:411–23. doi: 10.1016/j.intimp.2018.09.025
115. Topcu Sarica L, Zibandeh N, Genc D, Gul F, Akkoc T, Kombak EF, et al. Immunomodulatory and Tissue-Preserving Effects of Human Dental Follicle Stem Cells in a Rat Cecal Ligation and Perforation Sepsis Model. *Arch Med Res* (2020) 51(5):397–405. doi: 10.1016/j.arcmed.2020.04.010
116. Chang CL, Chen HH, Chen KH, Chiang JY, Li YC, Lin HS, et al. Adipose-Derived Mesenchymal Stem Cell-Derived Exosomes Markedly Protected the Brain Against Sepsis Syndrome Induced Injury in Rat. *Am J Transl Res* (2019) 11(7):3955–71.
117. Zhang L, Zhang JP, Liu Y, Wang H, Cheng Y, Wang JH, et al. Plasma Transfusion Promoted Reprogramming CD4(+) T Lymphocytes Immune Response in Severe Sepsis Mice Model Through Modulating the Exosome Protein Galectin 9. *Cell Transplant* (2020) 29:963689720947347. doi: 10.1177/0963689720947347
118. Kyvelidou C, Sotiriou D, Zerva I, Athanassakis I. Protection Against Lipopolysaccharide-Induced Immunosuppression by IgG and IgM. *Shock* (2018) 49(4):474–82. doi: 10.1097/SHK.0000000000000937
119. Chihara S, Masuda Y, Tatsumi H, Yamakage M. Evaluation of Pre- and Post-Dilution Continuous Veno-Venous Hemofiltration on Leukocyte and Platelet Function in Patients With Sepsis. *Int J Artif Organs* (2019) 42 (1):9–16. doi: 10.1177/0391398818801292
120. Qi X, Yu Y, Sun R, Huang J, Liu L, Yang Y, et al. Identification and Characterization of Neutrophil Heterogeneity in Sepsis. *Crit Care* (2021) 25 (1):50. doi: 10.1186/s13054-021-03481-0
121. Martin MD, Badovinac VP, Griffith TS. CD4 T Cell Responses and the Sepsis-Induced Immunoparalysis State. *Front Immunol* (2020) 11:1364. doi: 10.3389/fimmu.2020.01364
122. Monneret G, Debard AL, Venet F, Bohe J, Hequet O, Bienvenu J, et al. Marked Elevation of Human Circulating CD4+CD25+ Regulatory T Cells in Sepsis-Induced Immunoparalysis. *Crit Care Med* (2003) 31(7):2068–71. doi: 10.1097/01.CCM.0000069345.78884.0F
123. Venet F, Chung CS, Kherouf H, Geeraert A, Malcus C, Poitevin F, et al. Increased Circulating Regulatory T Cells (CD4(+)CD25 (+)CD127 (-)) Contribute to Lymphocyte Anergy in Septic Shock Patients. *Intensive Care Med* (2009) 35(4):678–86. doi: 10.1007/s00134-008-1337-8
124. Venet F, Pachot A, Debard AL, Bohe J, Bienvenu J, Lepape A, et al. Human CD4+CD25+ Regulatory T Lymphocytes Inhibit Lipopolysaccharide-Induced Monocyte Survival Through a Fas/Fas Ligand-Dependent Mechanism. *J Immunol* (2006) 177(9):6540–7. doi: 10.4049/jimmunol.177.9.6540
125. Huang LF, Yao YM, Dong N, Yu Y, He LX, Sheng ZY. Association Between Regulatory T Cell Activity and Sepsis and Outcome of Severely Burned Patients: A Prospective, Observational Study. *Crit Care* (2010) 14(1):R3. doi: 10.1186/cc8232
126. Tao L, Wang Y, Xu J, Su J, Yang Q, Deng W, et al. IL-10-Producing Regulatory B Cells Exhibit Functional Defects and Play a Protective Role in Severe Endotoxic Shock. *Pharmacol Res* (2019) 148:104457. doi: 10.1016/j.phrs.2019.104457
127. Cagdas D, Halaçlı SO, Tan Ç, Lo B, Çetinkaya PG, Esenboğa S, et al. A Spectrum of Clinical Findings From ALPS to CVID: Several Novel LRBA Defects. *J Clin Immunol* (2019) 39(7):726–38. doi: 10.1007/s10875-019-00677-6
128. Halliday N, Williams C, Kennedy A, Waters E, Pesenacker AM, Soskic B, et al. CD86 Is a Selective CD28 Ligand Supporting FoxP3+ Regulatory T Cell Homeostasis in the Presence of High Levels of CTLA-4. *Front Immunol* (2020) 11:600000. doi: 10.3389/fimmu.2020.600000
129. Mack DG, Lanham AM, Palmer BE, Maier LA, Fontenot AP. CD27 Expression on CD4+ T Cells Differentiates Effector From Regulatory T Cell Subsets in the Lung. *J Immunol* (2009) 182(11):7317–24. doi: 10.4049/jimmunol.0804305
130. Hippen KL, Harker-Murray P, Porter SB, Merkel SC, Londer A, Taylor DK, et al. Umbilical Cord Blood Regulatory T-Cell Expansion and Functional Effects of Tumor Necrosis Factor Receptor Family Members OX40 and 4-1BB Expressed on Artificial Antigen-Presenting Cells. *Blood* (2008) 112 (7):2847–57. doi: 10.1182/blood-2008-01-132951
131. Lucca LE, Dominguez-Villar M. Modulation of Regulatory T Cell Function and Stability by Co-Inhibitory Receptors. *Nat Rev Immunol* (2020) 20 (11):680–93. doi: 10.1038/s41577-020-0296-3
132. Polanczyk MJ, Hopke C, Vandenbark AA, Offner H. Treg Suppressive Activity Involves Estrogen-Dependent Expression of Programmed Death-1 (PD-1). *Int Immunol* (2007) 19(3):337–43. doi: 10.1093/intimm/dxl151
133. Hwang WC, Seo SH, Kang M, Kang RH, Di Paolo G, Choi KY, et al. PLD1 and PLD2 Differentially Regulate the Balance of Macrophage Polarization in Inflammation and Tissue Injury. *J Cell Physiol* (2021) 236(7):5193–211. doi: 10.1002/jcp.30224
134. Yu K, Dong Q, Mao X, Meng K, Zhao X, Ji Q, et al. Disruption of the TSLP-TSLPR-LAP Signaling Between Epithelial and Dendritic Cells Through Hyperlipidemia Contributes to Regulatory T-Cell Defects in Atherosclerotic Mice. *Atherosclerosis* (2015) 238(2):278–88. doi: 10.1016/j.atherosclerosis.2014.12.019
135. Seymour CW, Kennedy JN, Wang S, Chang CH, Elliott CF, Xu Z, et al. Derivation, Validation, and Potential Treatment Implications of Novel Clinical Phenotypes for Sepsis. *JAMA* (2019) 321(20):2003–17. doi: 10.1001/jama.2019.5791
136. Stortz JA, Cox MC, Hawkins RB, Ghita GL, Brumback BA, Mohr AM, et al. Phenotypic Heterogeneity by Site of Infection in Surgical Sepsis: A Prospective Longitudinal Study. *Crit Care* (2020) 24(1):203. doi: 10.1186/s13054-020-02917-3
137. Markwart R, Saito H, Harder T, Tomczyk S, Cassini A, Fleischmann-Struzek C, et al. Epidemiology and Burden of Sepsis Acquired in Hospitals and Intensive Care Units: A Systematic Review and Meta-Analysis. *Intensive Care Med* (2020) 46(8):1536–51. doi: 10.1007/s00134-020-06106-2
138. Greenberg JA, Hrusch CL, Jaffery MR, David MZ, Daum RS, Hall JB, et al. Distinct T-Helper Cell Responses to Staphylococcus Aureus Bacteremia Reflect Immunologic Comorbidities and Correlate With Mortality. *Crit Care* (2018) 22(1):107. doi: 10.1186/s13054-018-2025-x
139. Gea-Banacloche JC, Opal SM, Jorgensen J, Carcillo JA, Sepkowitz KA, Cordonnier C. Sepsis Associated With Immunosuppressive Medications: An Evidence-Based Review. *Crit Care Med* (2004) 32(11 Suppl):S578–90. doi: 10.1097/01.CCM.0000143020.27340.FF
140. Kamboj M, Sepkowitz KA. Nosocomial Infections in Patients With Cancer. *Lancet Oncol* (2009) 10(6):589–97. doi: 10.1016/S1470-2045(09)70069-5
141. Sheth M, Benedum CM, Celi LA, Mark RG, Markuzon N. The Association Between Autoimmune Disease and 30-Day Mortality Among Sepsis ICU Patients: A Cohort Study. *Crit Care* (2019) 23(1):93. doi: 10.1186/s13054-019-2357-1
142. Zhao GJ, Li D, Zhao Q, Song JX, Chen XR, Hong GL, et al. Incidence, Risk Factors and Impact on Outcomes of Secondary Infection in Patients With Septic Shock: An 8-Year Retrospective Study. *Sci Rep* (2016) 6:38361. doi: 10.1038/srep38361
143. Yang XD, Kong FE, Qi L, Lin JX, Yan Q, Loong JHC, et al. PARP Inhibitor Olaparib Overcomes Sorafenib Resistance Through Reshaping the Pluripotent Transcriptome in Hepatocellular Carcinoma. *Mol Cancer* (2021) 20(1):20. doi: 10.1186/s12943-021-01315-9
144. Mukhopadhyay S, Puopolo KM, Hansen NI, Lorch SA, DeMauro SB, Greenberg RG, et al. Impact of Early-Onset Sepsis and Antibiotic Use on Death or Survival With Neurodevelopmental Impairment at 2 Years of Age Among Extremely Preterm Infants. *J Pediatr* (2020) 221:39–46 e5. doi: 10.1016/j.jpeds.2020.02.038
145. Polcwiartek LB, Smith PB, Benjamin DK, Zimmerman K, Love A, Tiu L, et al. Early-Onset Sepsis in Term Infants Admitted to Neonatal Intensive Care Units (2011-2016). *J Perinatol* (2021) 41(1):157–63. doi: 10.1038/s41372-020-00860-3
146. Youssef MAM, Zahran AM, Hussien AM, Elsayh KI, Askar EA, Farghaly HS. In Neonates With Vitamin D Deficiency, Low Lymphocyte Activation Markers are Risk Factors for Infection. *Paediatr Int Child Health* (2019) 39(2):111–8. doi: 10.1080/20469047.2018.1528755
147. Saito K, Wagatsuma T, Toyama H, Ejima Y, Hoshi K, Shibusawa M, et al. Sepsis is Characterized by the Increases in Percentages of Circulating CD4 +CD25+ Regulatory T Cells and Plasma Levels of Soluble CD25. *Tohoku J Exp Med* (2008) 216(1):61–8. doi: 10.1620/tjem.216.61

148. Cho DS, Schmitt RE, Dasgupta A, Ducharme AM, Doles JD. Single-Cell Deconstruction of Post-Sepsis Skeletal Muscle and Adipose Tissue Microenvironments. *J Cachexia Sarcopenia Muscle* (2020) 11(5):1351–63. doi: 10.1002/jcsm.12596
149. Aird WC. Phenotypic Heterogeneity of the Endothelium: I. Structure, Function, and Mechanisms. *Circ Res* (2007) 100(2):158–73. doi: 10.1161/01.RES.0000255691.76142.4a
150. Toledo AG, Golden G, Campos AR, Cuello H, Sorrentino J, Lewis N, et al. Proteomic Atlas of Organ Vasculopathies Triggered by Staphylococcus Aureus Sepsis. *Nat Commun* (2019) 10(1):4656. doi: 10.1038/s41467-019-12672-x
151. Margraf A, Ley K, Zarbock A. Neutrophil Recruitment: From Model Systems to Tissue-Specific Patterns. *Trends Immunol* (2019) 40(7):613–34. doi: 10.1016/j.it.2019.04.010
152. Barrot L, Asfar P, Mauny F, Winiszewski H, Montini F, Badie J, et al. Liberal or Conservative Oxygen Therapy for Acute Respiratory Distress Syndrome. *N Engl J Med* (2020) 382(11):999–1008. doi: 10.1056/NEJMoa1916431
153. Thompson BT, Chambers RC, Liu KD. Acute Respiratory Distress Syndrome. *N Engl J Med* (2017) 377(6):562–72. doi: 10.1056/NEJMra1608077
154. Ranieri VM, Pettila V, Karvonen MK, Jalkanen J, Nightingale P, Brealey D, et al. Effect of Intravenous Interferon Beta-1a on Death and Days Free From Mechanical Ventilation Among Patients With Moderate to Severe Acute Respiratory Distress Syndrome: A Randomized Clinical Trial. *JAMA* (2020) 323(8):725–33. doi: 10.1001/jama.2019.22525
155. D'Alessio FR, Tsushima K, Aggarwal NR, West EE, Willett MH, Britos MF, et al. CD4+CD25+Foxp3+ Tregs Resolve Experimental Lung Injury in Mice and are Present in Humans With Acute Lung Injury. *J Clin Invest* (2009) 119 (10):2898–913. doi: 10.1172/JCI36498
156. Chung HY, Wickel J, Brunkhorst FM, Geis C. Sepsis-Associated Encephalopathy: From Delirium to Dementia? *J Clin Med* (2020) 9(3):703. doi: 10.3390/jcm9030703
157. Sonneville R, de Montmollin E, Poujade J, Garrouste-Orgeas M, Souweine B, Darmon M, et al. Potentially Modifiable Factors Contributing to Sepsis-Associated Encephalopathy. *Intensive Care Med* (2017) 43(8):1075–84. doi: 10.1007/s00134-017-4807-z
158. Ren C, Yao RQ, Zhang H, Feng YW, Yao YM. Sepsis-Associated Encephalopathy: A Vicious Cycle of Immunosuppression. *J Neuroinflamm* (2020) 17(1):14. doi: 10.1186/s12974-020-1701-3
159. Iwashyna TJ, Ely EW, Smith DM, Langa KM. Long-Term Cognitive Impairment and Functional Disability Among Survivors of Severe Sepsis. *JAMA* (2010) 304(16):1787–94. doi: 10.1001/jama.2010.1553
160. Wintermann GB, Brunkhorst FM, Petrowski K, Strauss B, Oehmichen F, Pohl M, et al. Stress Disorders Following Prolonged Critical Illness in Survivors of Severe Sepsis. *Crit Care Med* (2015) 43(6):1213–22. doi: 10.1097/CCM.0000000000000936
161. Dejager L, Pinheiro I, Dejonckheere E, Libert C. Cecal Ligation and Puncture: The Gold Standard Model for Polymicrobial Sepsis? *Trends Microbiol* (2011) 19(4):198–208. doi: 10.1016/j.tim.2011.01.001
162. Brinkhoff A, Siebericchs A, Engler H, Dolff S, Benson S, Korth J, et al. Pro-Inflammatory Th1 and Th17 Cells Are Suppressed During Human Experimental Endotoxemia Whereas Anti-Inflammatory IL-10 Producing T-Cells Are Unaffected. *Front Immunol* (2018) 9:1133. doi: 10.3389/fimmu.2018.01133
163. Kinjo Y, Illarionov P, Vela JL, Pei B, Girardi E, Li X, et al. Invariant Natural Killer T Cells Recognize Glycolipids From Pathogenic Gram-Positive Bacteria. *Nat Immunol* (2011) 12(10):966–74. doi: 10.1038/ni.2096
164. Venken K, Decruy T, Aspeslagh S, Van Calenbergh S, Lambrecht BN, Elewaut D. Bacterial CD1d-Restricted Glycolipids Induce IL-10 Production by Human Regulatory T Cells Upon Cross-Talk With Invariant NKT Cells. *J Immunol* (2013) 191(5):2174–83. doi: 10.4049/jimmunol.1300562
165. Kim BG, Ghosh P, Ahn S, Rhee DK. Pneumococcal Pep27 Mutant Immunization Suppresses Allergic Asthma in Mice. *Biochem Biophys Res Commun* (2019) 514(1):210–6. doi: 10.1016/j.bbrc.2019.04.116
166. Lee SW, Park HJ, Van Kaer L, Hong S, Hong S. Graphene Oxide Polarizes iNKT Cells for Production of TGFbeta and Attenuates Inflammation in an iNKT Cell-Mediated Sepsis Model. *Sci Rep* (2018) 8(1):10081. doi: 10.1038/s41598-018-28396-9
167. Qu G, Liu S, Zhang S, Wang L, Wang X, Sun B, et al. Graphene Oxide Induces Toll-Like Receptor 4 (TLR4)-Dependent Necrosis in Macrophages. *ACS Nano* (2013) 7(7):5732–45. doi: 10.1021/nn402330b
168. Schuijt TJ, Lankelma JM, Scicluna BP, de Sousa e Melo F, Roelofs JJ, de Boer JD, et al. The Gut Microbiota Plays a Protective Role in the Host Defence Against Pneumococcal Pneumonia. *Gut* (2016) 65(4):575–83. doi: 10.1136/gutjnl-2015-309728
169. Morowitz MJ, Di Caro V, Pang D, Cummings J, Firek B, Rogers MB, et al. Dietary Supplementation With Nonfermentable Fiber Alters the Gut Microbiota and Confers Protection in Murine Models of Sepsis. *Crit Care Med* (2017) 45(5):e516–e23. doi: 10.1097/CCM.0000000000002291
170. Boeddha NP, Schlapbach LJ, Driessen GJ, Herberg JA, Rivero-Calle I, Cebey-Lopez M, et al. Mortality and Morbidity in Community-Acquired Sepsis in European Pediatric Intensive Care Units: A Prospective Cohort Study From the European Childhood Life-Threatening Infectious Disease Study (EUCLIDS). *Crit Care* (2018) 22(1):143. doi: 10.1186/s13054-018-2052-7
171. Vincent JL, Sakr Y, Sprung CL, Ranieri VM, Reinhart K, Gerlach H, et al. Sepsis in European Intensive Care Units: Results of the SOAP Study. *Crit Care Med* (2006) 34(2):344–53. doi: 10.1097/01.CCM.0000194725.48928.3A
172. Netea MG, Sutmuller R, Hermann C, van der Graaf CA, van der Meer JW, van Krieken JH, et al. Toll-Like Receptor 2 Suppresses Immunity Against Candida Albicans Through Induction of IL-10 and Regulatory T Cells. *J Immunol* (2004) 172(6):3712–8. doi: 10.4049/jimmunol.172.6.3712
173. Arens C, Kramm T, Decker S, Spannenberger J, Brenner T, Richter DC, et al. Association of Immune Cell Subtypes and Phenotype With Subsequent Invasive Candidiasis in Patients With Abdominal Sepsis. *Shock* (2019) 52 (2):191–7. doi: 10.1097/SHK.0000000000001251
174. Kuhlhorn F, Rath M, Schmoeckel K, Cziupka K, Nguyen HH, Hildebrandt P, et al. Foxp3+ Regulatory T Cells are Required for Recovery From Severe Sepsis. *PloS One* (2013) 8(5):e65109. doi: 10.1371/journal.pone.0065109
175. Alverdy JC, Keskey R, Thewissen R. Can the Cecal Ligation and Puncture Model Be Repurposed To Better Inform Therapy in Human Sepsis? *Infect Immun* (2020) 88(9):e00942–19. doi: 10.1128/IAI.00942-19
176. Barber AE, Coyle SM, Fischer E, Smith C, van der Poll T, Shires GT, et al. Influence of Hypercortisolemia on Soluble Tumor Necrosis Factor Receptor II and Interleukin-1 Receptor Antagonist Responses to Endotoxin in Human Beings. *Surgery* (1995) 118(2):406–10. doi: 10.1016/s0039-6060(05)80352-6
177. Thomas RC, Bath MF, Stover CM, Lambert DG, Thompson JP. Exploring LPS-Induced Sepsis in Rats and Mice as a Model to Study Potential Protective Effects of the Nociceptin/Orphanin FQ System. *Peptides* (2014) 61:56–60. doi: 10.1016/j.peptides.2014.08.009
178. Spenlingwimmer T, Zipperle J, Jafarmadar M, Osuchowski MF, Drechsler S. Comparison of Post-Traumatic Changes in Circulating and Bone Marrow Leukocytes Between BALB/c and CD-1 Mouse Strains. *PloS One* (2019) 14 (9):e0222594. doi: 10.1371/journal.pone.0222594
179. Harb H, Benamar M, Lai PS, Contini P, Griffith JW, Crestani E. Notch4 Signaling Limits Regulatory T-Cell-Mediated Tissue Repair and Promotes Severe Lung Inflammation in Viral Infections. *Immunity* (2021) 54(6):1186–99.e7. doi: 10.1016/j.immuni.2021.04.002
180. D'Alessio FR, Tsushima K, Aggarwal NR, West EE, Willett MH, Britos MF. CD4+CD25+Foxp3+ Tregs Resolve Experimental Lung Injury in Mice and Are Present in Humans With Acute Lung Injury. *J Clin Invest* (2009) 119 (10):2898–913. doi: 10.1172/JCI36498
181. Mock JR, Garibaldi BT, Aggarwal NR, Jenkins J, Limjunyawong N, Singer BD. Foxp3+ Regulatory T Cells Promote Lung Epithelial Proliferation. *Mucosal Immunol* (2014) 7(6):1440–51. doi: 10.1038/mi.2014.33
182. Yu ZX, Ji MS, Yan J, Cai Y, Liu J, Yang HF. The Ratio of Th17/Treg Cells as a Risk Indicator in Early Acute Respiratory Distress Syndrome. *Crit Care* (2015) 19(1):82. doi: 10.1186/s13054-015-0811-2
183. Zhang F, Li MY, Lan YT, Wang CB. Imbalance of Th17/Tregs in Rats With Smoke Inhalation-Induced Acute Lung Injury. *Sci Rep* (2016) 6:21348. doi: 10.1038/srep21348
184. Chen G, Wu MD, Guo W, Cao Y, Huang D, Wang H. Clinical and Immunological Features of Severe and Moderate Coronavirus Disease 2019. *J Clin Invest* (2020) 130(5):2620–9.
185. Wang F, Hou H, Luo Y, Tang G, Wu S, Huang M. The Laboratory Tests and Host Immunity of COVID-19 Patients With Different Severity of Illness. *JCI Insight* (2020) 5(10):e137799.
186. Tan M, Liu Y, Zhou R, Deng X, Li F, Liang K. Immunopathological Characteristics of Coronavirus Disease 2019 Cases in Guangzhou, China. *Immunology* (2020) 160(3):261–8.

187. Neumann J, Prezzemolo T, Vanderbeke L, Roca CP, Gerbaux M, Janssens S. Increased IL-10-Producing Regulatory T Cells Are Characteristic of Severe Cases of COVID-19. *Clin Transl Immunol* (2020) 9(11):e1204.
188. Meckiff BJ, Ramírez-Suástegui C, Fajardo V, Chee SJ, Kusnadi A, Simon H. Imbalance of Regulatory and Cytotoxic SARS-CoV-2-Reactive CD4+ T Cells in COVID-19. *Cell* (2020) 183(5):1340–53.e16. doi: 10.1016/j.cell.2020.10.001

Conflict of Interest: XT was employed by Beijing Qiansong Technology Development Company.

The remaining authors declare that the research was conducted in the absence of any commercial or financial relationships that could be construed as a potential conflict of interest.

Publisher's Note: All claims expressed in this article are solely those of the authors and do not necessarily represent those of their affiliated organizations, or those of the publisher, the editors and the reviewers. Any product that may be evaluated in this article, or claim that may be made by its manufacturer, is not guaranteed or endorsed by the publisher.

frontiers | Frontiers in Immunology

ORIGINAL RESEARCH
published: 04 May 2022
doi: 10.3389/fimmu.2022.857025

Single Cell Dissection of Epithelial-Immune Cellular Interplay in Acute Kidney Injury Microenvironment

Min Zhang[1†], Lingling Wu[1†], Yiyao Deng[2], Fei Peng[1], Tiantian Wang[1], Yinghua Zhao[1], Pu Chen[1], Jiaona Liu[1], Guangyan Cai[1], Liqiang Wang[3], Jie Wu[1*] and Xiangmei Chen[1*]*

[1] Department of Nephrology, First Medical Center of Chinese People's Liberation Army (PLA) of China General Hospital, Nephrology Institute of the Chinese People's Liberation Army, State Key Laboratory of Kidney Diseases, National Clinical Research Center for Kidney Diseases, Beijing Key Laboratory of Kidney Disease Research, Beijing, China, [2] Department of Nephrology, Guizhou Provincial People's Hospital, Guiyang, China, [3] Department of Ophthalmology, Ophthalmology & Visual Science Key Lab of People's Liberation Army (PLA) of China, General Hospital of Chinese People's Liberation Army (PLA) of China, Beijing, China

Background: Understanding the acute kidney injury (AKI) microenvironment changes and the complex cellular interaction is essential to elucidate the mechanisms and develop new targeted therapies for AKI.

Methods: We employed unbiased single-cell RNA sequencing to systematically resolve the cellular atlas of kidney tissue samples from mice at 1, 2 and 3 days after ischemia-reperfusion AKI and healthy control. The single-cell transcriptome findings were validated using multiplex immunostaining, western blotting, and functional experiments.

Results: We constructed a systematic single-cell transcriptome atlas covering different AKI timepoints with immune cell infiltration increasing with AKI progression. Three new proximal tubule cells (PTCs) subtypes (PTC-S1-new/PTC-S2-new/PTC-S3-new) were identified, with upregulation of injury and repair-regulated signatures such as Sox9, Vcam1, Egr1, and Klf6 while with downregulation of metabolism. PTC-S1-new exhibited pro-inflammatory and pro-fibrotic signature compared to normal PTC, and trajectory analysis revealed that proliferating PTCs were the precursor cell of PTC-S1-new, and part of PTC-S1-new cells may turn into PTC-injured and then become fibrotic. Cellular interaction analysis revealed that PTC-S1-new and PTC-injured interacted closely with infiltrating immune cells through CXCL and TNF signaling pathways. Immunostaining validated that injured PTCs expressed a high level of TNFRSF1A and Kim-1, and functional experiments revealed that the exogenous addition of TNF-α promoted kidney inflammation, dramatic injury, and specific depletion of TNFRSF1A would abrogate the injury.

OPEN ACCESS

Edited by:
Alessandra Stasi,
University of Bari Aldo Moro, Italy

Reviewed by:
Fabio Sallustio,
University of Bari Aldo Moro, Italy
Sharon Natasha Cox,
University of Bari Aldo Moro, Italy
Sian Piret,
Stony Brook University,
United States

***Correspondence:**
Liqiang Wang
liqiangw301@163.com
Jie Wu
wujie301@126.com
Xiangmei Chen
xmchen301@126.com

[†]These authors have contributed equally to this work

Specialty section:
This article was submitted to Inflammation, a section of the journal Frontiers in Immunology

Received: *18 January 2022*
Accepted: *04 April 2022*
Published: *04 May 2022*

Citation:
Zhang M, Wu L, Deng Y, Peng F, Wang T, Zhao Y, Chen P, Liu J, Cai G, Wang L, Wu J and Chen X (2022) Single Cell Dissection of Epithelial-Immune Cellular Interplay in Acute Kidney Injury Microenvironment. Front. Immunol. 13:857025. doi: 10.3389/fimmu.2022.857025

Conclusions: The single-cell profiling of AKI microenvironment provides new insight for the deep understanding of molecular changes of AKI, and elucidates the mechanisms and developing new targeted therapies for AKI.

Keywords: acute kidney injury, renal tubular epithelial cells, microenvironment, intercellular crosstalk, trajectory analysis

INTRODUCTION

Acute kidney injury (1–3) (AKI) is a serious health risk, characterized by an abrupt loss of renal function, which is also a leading cause of chronic kidney disease (CKD) and end-stage renal failure. AKI commonly caused by ischemia, sepsis, or nephrotoxic insult, which result from a variety of conditions, including major surgery, sepsis, trauma, dehydration, and toxic drug damage. The incidence of AKI has gradually increased in recent years, with a relatively high incidence of 3%-5% among the general population in hospitals which can be as high as 30%-60% in the intensive care unit (ICU). The mortality rate can be as high as 60-70% when combined with multi-organ failure which has caused a great economic and mental burden for patients and society (4).

AKI is usually characterized by pathological alterations (5–7) such as proximal tubule cells (PTCs) dysfunction or death, triggering a poorly understood autologous cellular repair program. Also, infiltrating immune cells (8–13) undergo phenotypic and functional changes in response to AKI injury and repair processes. Studies (14–17) using bulk transcriptional profiling have characterized molecular characteristics associated with kidney injury and recovery. The transcriptional average across cell populations was revealed, which may hide or skew signals of interest with specific cellular identities and biologically-relevant mechanisms. Dissecting the molecular basis associated with AKI microenvironment changes and the complex cellular interaction is essential to elucidate the mechanisms and develop new targeted therapies for AKI.

Single-cell RNA-sequencing (scRNA-seq) (18–24) is a powerful technology capable of revealing the heterogeneous cellular and molecular characteristics along with the disease initiation and progression. Recent studies for AKI, using scRNA-seq, identified novel cell-subtypes with diverse transcription phenotype response to AKI (9, 12, 24). Additionally, infiltrating immune cells such as Treg (12) and myeloid cells (9) associated with AKI injury and repair were identified. What remains unknown is how infiltrating immune cells influence the process of AKI damage and repair.

Here, we report findings from scRNA-seq analysis of 52,162 cells from mouse kidney tissue samples at 1, 2 and 3 days after ischemia-reperfused AKI and healthy control. We uncovered three PTC-new subtypes and found that PTC-S1-new exhibited pro-inflammatory and pro-fibrotic signature. Proliferating PTCs were the precursor cells of PTC-S1-new, and part of PTC-S1-new cells may turn into PTC-injured and then become fibrotic in the case of sustained damage. Also, the PTC-injured highly expressed Tnfrsf1a and Kim-1 and interacted closely with macrophage and monocyte through Tnfrsf1a/Tnf signaling axis. Functional experiments revealed that the exogenous addition of TNF-α dramatically promoted kidney inflammation and injury and specific depletion of TNFRSF1A would abrogate the injury.

RESULTS

Dynamic Changes of Cellular Proportion and Phenotype During the IRI AKI

To obtain a comprehensive cellular atlas alongside AKI progression, the kidney sample of mice at 1, 2 and 3 days after ischemia-reperfused AKI and healthy control were subjected for scRNA-seq and each group contained 6 samples (**Figure 1A**). The renal tubules show obvious damage at 24 hours after IRI, mainly manifested by vacuolar degeneration of renal tubular epithelial cells, partial detachment of brush border and disordered cell arrangement. At 48 hours, histopathology images show severe detachment of renal tubular epithelial cells, the appearance of cellular tubular pattern and protein tubular pattern, and at 72 hours, some renal tubular epithelial cells appear to regenerate and rearrange. Compared with the control group, the acute tubular necrosis score and serum concentrations of serum creatine (Scr) and blood urea nitrogen (BUN) increase significantly at 24 hours and 48 hours after IRI, and decrease with the initiation of tubular epithelial cell regeneration and repair at 72 hours after IRI (**Figure 1B** and **Supplementary Figure 1**). In parallel with the acute tubular necrosis score, the serum concentrations of Scr and BUN recover to baseline level at 72 hours after IRI (**Figure 1B** and **Supplementary Figure 1**). The single-cell suspensions of six mice were pooled together in each single cell experiment and then loaded onto one microfluidic chip to generate the complementary deoxyribonucleic acid (cDNA) library following the method in Conway BR., et al (9). A total of 52,162 high quality cells passed quality control (methods, **Supplementary Figure 2**) and these cells could be defined as 21 cell subtypes including epithelial cells such as PTCs, distal tubular cells, podocytes, principal cells, endothelial cells, fibroblast, and immune cells such as T cells, myeloid cells (**Figure 1C**). Most sequenced cells were PTCs, three new PTC subtypes (PTC-S1-new/PTC-S2-new/PTC-S3-new), and mixed cell types (expressing markers of different renal cell types) are identified (**Figure 1D**). We found that the portion of normal PTCs (PTC-S1, PTC-S2, PTC-S3) change dramatically along with AKI progression (**Figure 1E**), indicating that AKI results in PTCs dysfunction or death, and also AKI triggered the PTC to repair itself on the other, therefore, novel PTC subtypes would generate. Additionally, the portion of immune cells expanded in

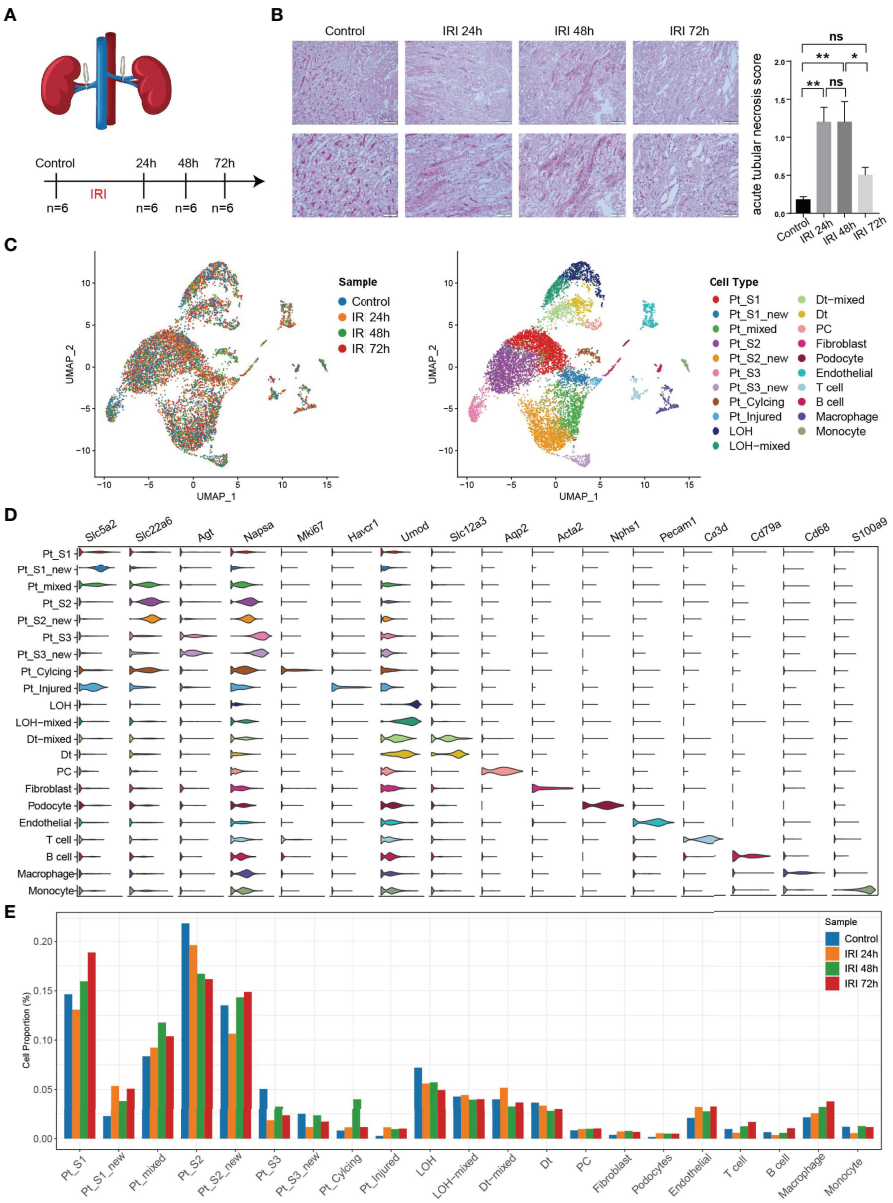

FIGURE 1 | An overview of single cell transcriptomic atlas of mouse IRI kidney. **(A)** Summary of experimental strategy. n = 6 mice per group. **(B)** The histopathology images and acute tubular necrosis score in control, IRI 24h, IRI 48h and 72h, One-way ANOVA followed by Turkey's multiple comparisons was used for three or more groups comparisons. *p<0.05, **p<0.01. **(C)** The distribution of 52,162 high-quality kidney cells in distinct sample timepoints (left) and cell types (right). **(D)** Cell type annotation and representative marker genes expression in 21 cell types. **(E)** Relative contribution of each cell type in distinct sample timepoints. ns, Not Statistically Significant.

the kidney along with AKI (**Figure 1E**) indicate the important role of immune cells in AKI (9).

Pro-Inflammatory and Pro-Fibrotic PTCs Subtypes Expanded in AKI

After annotation of cell subtypes, we then compared the molecular characteristics and the transcription correlation of PTC subtypes. As reported previously, the PTC-injured cells exhibited a high expression level of injury associated signature such as Havcr1 (Kim-1), Krt8, Spp1, Spp2, Vcam1(**Figures 2A, B**). In this study, we also found that the PTC-injured and part of PTC-new cells expressed a high level of pro-inflammatory and pro-fibrotic signatures such as Cxcl10, Cxlc1, Nfkbia, Nfkbib, Nfkb1, Nfkb2, and Col18a1 (**Figure 2B**) Also, the portion of PTC-injured and PTC-S1-new cells elevated in the kidney along with AKI, indicated that pro-inflammatory and pro-fibrotic PTCs subtypes expanded in AKI. Additionally, the injured PTCs had a higher expression level of antigen-presentation genes such as H2-Aa and H2-Eb1

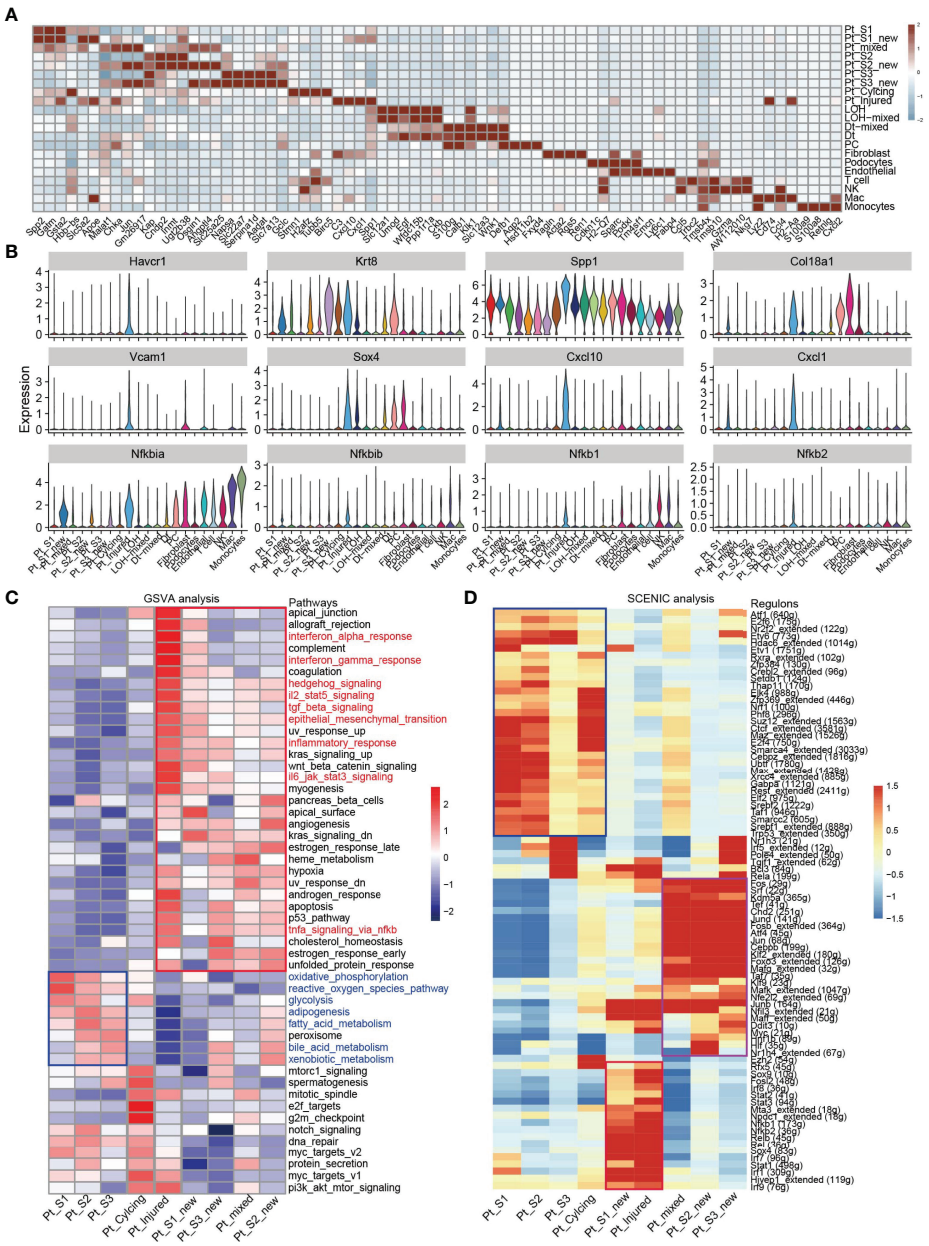

FIGURE 2 | Transcriptomic features of distinct cell types. **(A)** Top 4 differentially expressed genes in 21 cell types. **(B)** The expression level of representative kidney injury and inflammatory signatures in 21 cell types. **(C)** Enriched signaling pathways in PTC-new, injured PTC and normal PTC, estimated by GSVA. **(D)** Enriched regulons in PTC-new, injured PTC and normal PTC, estimated by SCENIC.

(**Figure 2A** and **Supplementary Figure 3**), indicating that PTCs would exhibit part time immunization features under injured condition. We also compared the functional difference and enriched signaling pathways among PTC subtypes and we found that pro-inflammatory signaling pathways such as Interferon alpha and gamma, IL2 stat5 signaling, TGF beta signaling, IL6 jak stat3, and TNF were mainly enriched in PTC-new and PTC-injured, with highest expression level in PTC-injured (**Figure 2C**). PTC-new and PTC-injured showed impairment of metabolism signaling pathways such as oxidative phosphorylation, glycolysis, fatty acid metabolism, and xenobiotic metabolism (**Figure 2C** and **Supplementary Figure 4**). Additionally, the single-cell regulatory network inference and clustering (SCENIC) analysis revealed that TNF (25) signaling pathway associated regulons such as Nfkb1, Nfkb2 and Interferon alpha and gamma signaling pathway associated regulons such as Irf1, Irf7, and Irf8, were enriched in PTC-S1-new and PTC-injured (**Figure 2D**). We then analyzed the transcription characteristic between PTC-new and normal PTCs,

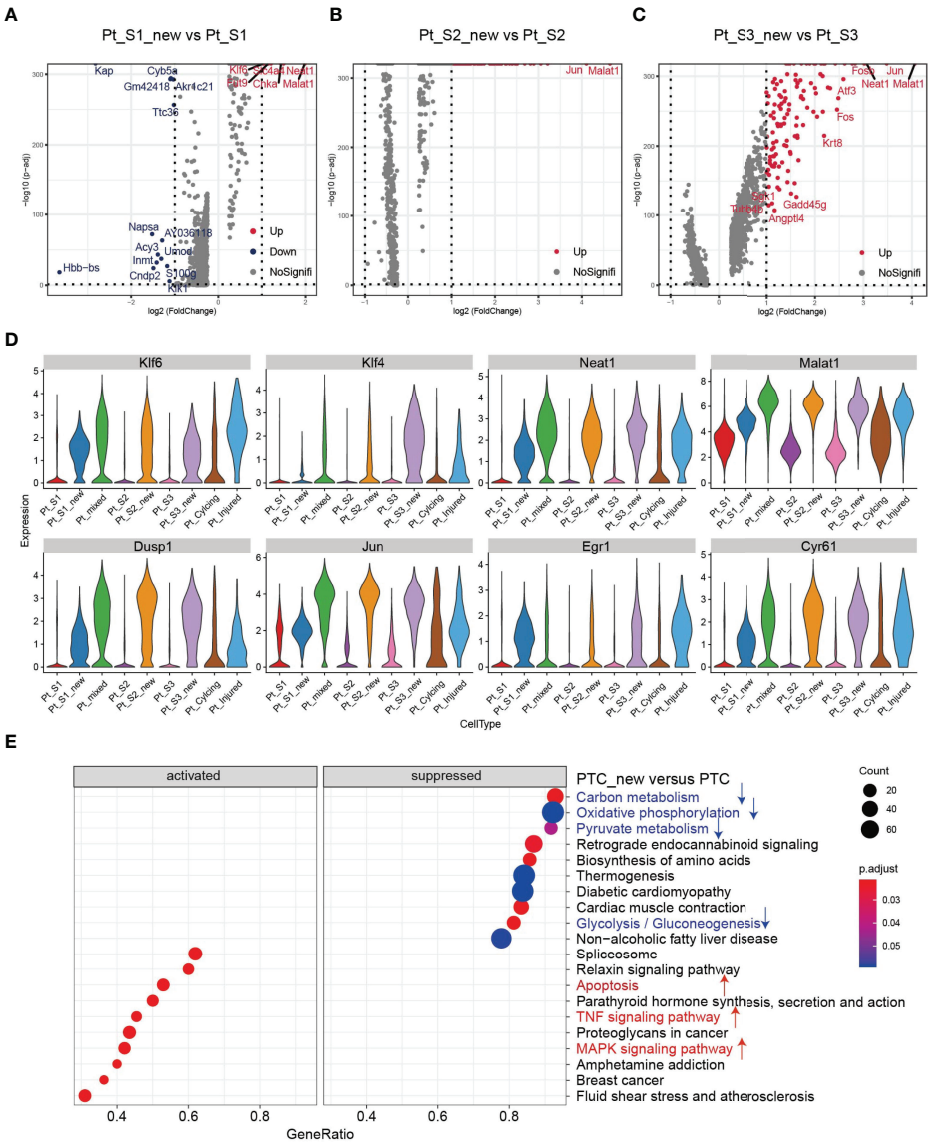

FIGURE 3 | Transcriptomic features of PTC-new subtypes. **(A–C)** Volcano plot showing the differentially expressed genes in PTC-S1-new versus PTC-S1 **(A)**, PTC-S2-new versus PTC-S2 **(B)**, PTC-S3-new versus PTC-S3 **(C)**. **(D)** The expression level of representative kidney injury or repair regulated signatures in PTC subtypes. **(E)** Enriched gene ontogeny (GO) among PTC-new subtypes versus normal PTC.

and explored the difference between the PTC-new and normal PTCs (**Figures 3A–D**). Interestingly, most up-regulated genes or transcription factors in PTC-new were kidney injury or repair regulated genes such as Klf4 (25), Klf6 (26), Neat1 (27), Malat1 (28), and Egr1 (29) (**Figures 3A–D**). Compared to normal PTCs, the PTC-new exhibited a high level of MAPK, TNF signaling pathway and associated genes Dusp1 and Jun (**Figure 3E**), which also supported the findings that PTC-new were pro-inflammatory.

Trajectory Analysis of PTCs Subtypes

Tissue repair and regeneration are very complex biological events, where successful attainment requires far more than mere cell division because the proliferative cells may replace the injured cells and promote repair (7, 30). We observed that the portion of PTC-cycling cells elevated along with the AKI (**Figure 1E**) and highlighted the important role of proliferative PTC-cycling cells in AKI repair. We employed the pseudo-time trajectory analysis (31) based on gene expression simulation to infer the cellular differentiation routines or potential transition between PTC-S1-new, PTC-injured, PTC-cycling, and fibroblast (**Figures 4A–C**). The pseudo-time trajectory axis indicated that PTC-cycling cells could differentiate into PTC-S1-new and part of PTC-S1-new cells may then turned into PTC-injured and fibroblast (**Figures 4B, C**). Pseudo-temporal expression dynamics of specific representative genes (**Figure 4D** and **Supplementary Figure 5**) and transcriptome factors

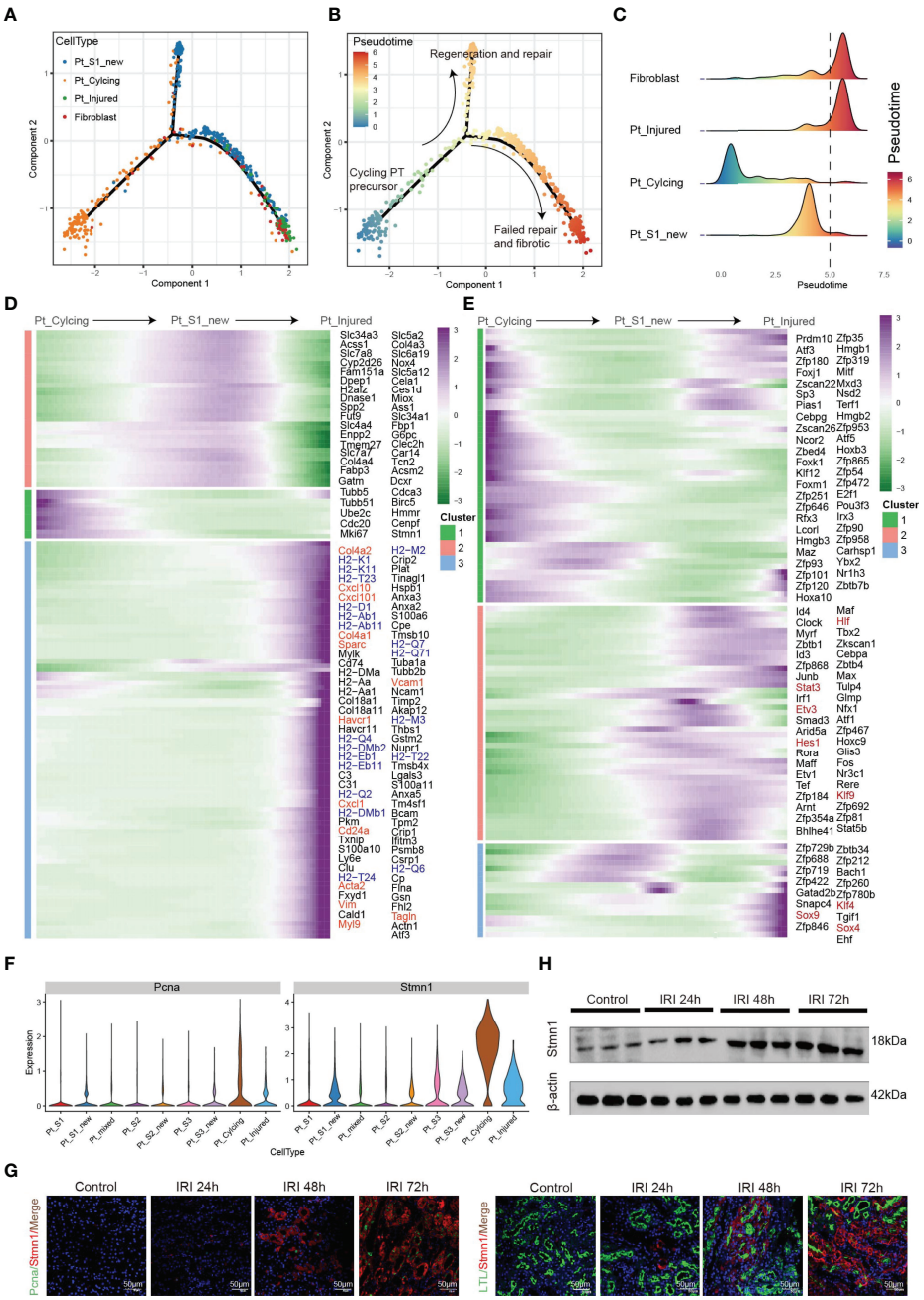

FIGURE 4 | Pseudo-time trajectory analysis among PTC. **(A–C)** Potential differentiation routines among PTC-S1-new, PTC-cycling, PTC-injured, and fibroblast. **(D, E)** Pseudo-temporal expression dynamics of specific representative genes **(D)** and transcriptome factors **(E)** alongside AKI progression. **(F)** The expression of cycling marker Stmn1 and Pcna in PTC subtypes. **(G)** Immunostaining showing the distribution of cycling PTC alongside the AKI progression. **(H)** Western blot showed the expression of Stmn1 with the time-dependent effect of IRI in the mouse kidney.

(**Figure 4E**) also marked the progression of PTC-cycling cells into PTC-S1-new, PTC-injured, and finally acquired fibrotic phenotype. The results presented here delineate the potential translation paths of PTC subtypes and PTC-S1-new may be an important node that determines fibrotic and normal repair. We also revealed injured and repair associated genes and transcription factors such as Hif (32), Irf1 (33), Klf4 (25), Hes1 (34), and Klf6 (26) (**Figures 4D, E**) involved in AKI progression, which may be important biomarkers for screening AKI progression. We also found PTC-cycling and part of PTC-new expressed proliferative markers such as Stmn1 and Pcna (**Figure 4F**). The immunostaining and Western Blot results

showed that the expression of cycling markers Stmn1 and Pcna increased along with the AKI progression (**Figures 4G, H**), which validated the important role of cycling PTCs in AKI progression and renal regeneration.

Interplay Between PTCs Subtypes and Infiltrating Immune Cells

Immune response-mediated kidney injury is an important factor in the progression of AKI but the detail molecular mechanism requires further investigation. As described above, our single cell transcriptomic analysis revealed the PTC-injured, part of PTC-new exhibited inflammatory, fibrotic features, and the portion of immune cells elevated along with with AKI progression, indicating the important role of the immune cell in AKI. We therefore employed the CellChat (35) package to infer the cellular interplay mechanism between PTC-new, PTC-injured, and infiltrating immune cells. Interestingly, the interaction node numbers in PTC-S1-new and PTC-injured were the highest among PTCs (**Figure 5A**) and these two subtypes interacted closely with infiltrating immune cells such as T cells, macrophage, and monocytes (**Figure 5A**). Intercellular crosstalk analysis revealed that the inflammatory signaling pathways such as CXCL, TNF, VCAM, and Complement were more enriched between PTC-injured,

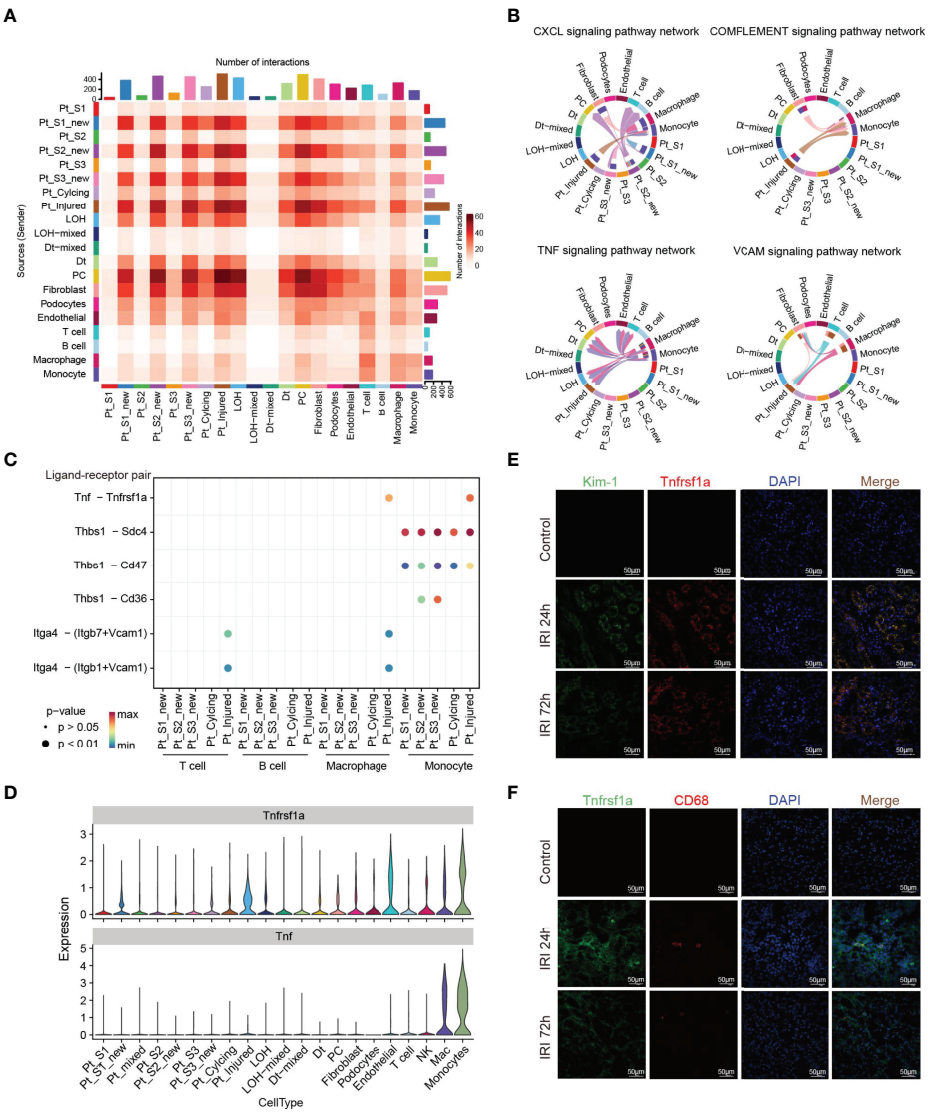

FIGURE 5 | Intercellular crosstalk analysis in AKI microenvironment. **(A)** Number of inferred interactions in 21 cell types. **(B, C)** Enriched immune signaling pathway networks **(B–D)** and significant ligand-receptor Tnf-Tnfrsf1a pair **(C, D)** in injured PTC, PTC-new and immune cells. **(E)** Immunostaining showing the spatial distribution of injured PTC marker Kim-1 and Tnfrsf1a alongside AKI timepoints. **(F)** Immunostaining showing the spatial distribution of CD68 expressing myeloid cells and Tnfrsf1a expressing PTCs alongside AKI timepoints.

macrophage, and monocytes (**Figures 5B–D** and **Supplementary Figure 6**). Further ligand-receptor analysis revealed that immune signal axis such as Tnf–Tnfrsf1a, Itga4-Vcam1, Thbs1–Sdc4, Cxcl1–Cxcr2 might participate in the intercellular crosstalk between injured PTCs, macrophage, and monocytes (**Figures 5B–D** and **Supplementary Figure 6**). Additionally, immunostaining confirmed that the injured PTCs expressed a high level of TNFRSF1A, with co-expression of injured PTC marker Kim-1 (**Figure 5E**). We also found that CD68 positive myeloid cells interplayed closely with Tnfrsf1a positive PTC-injured cells (**Figure 5F**), highlighting the important role of infiltrating immune cell in AKI progression.

Role of TNFRSF1A-TNF Signaling Axis in Kidney Injury

The intercellular crosstalk analysis and the immunostaining validation experiment provided evidence that the infiltrating macrophage and monocyte interacted closely with PTC-injured through the Tnf–Tnfrsf1a axis (**Figures 5B–F**). To investigate the role of the Tnf–Tnfrsf1a axis in kidney injury, we constructed TNFRSF1A silencing (**Supplementary Figure 7**). Quantitative

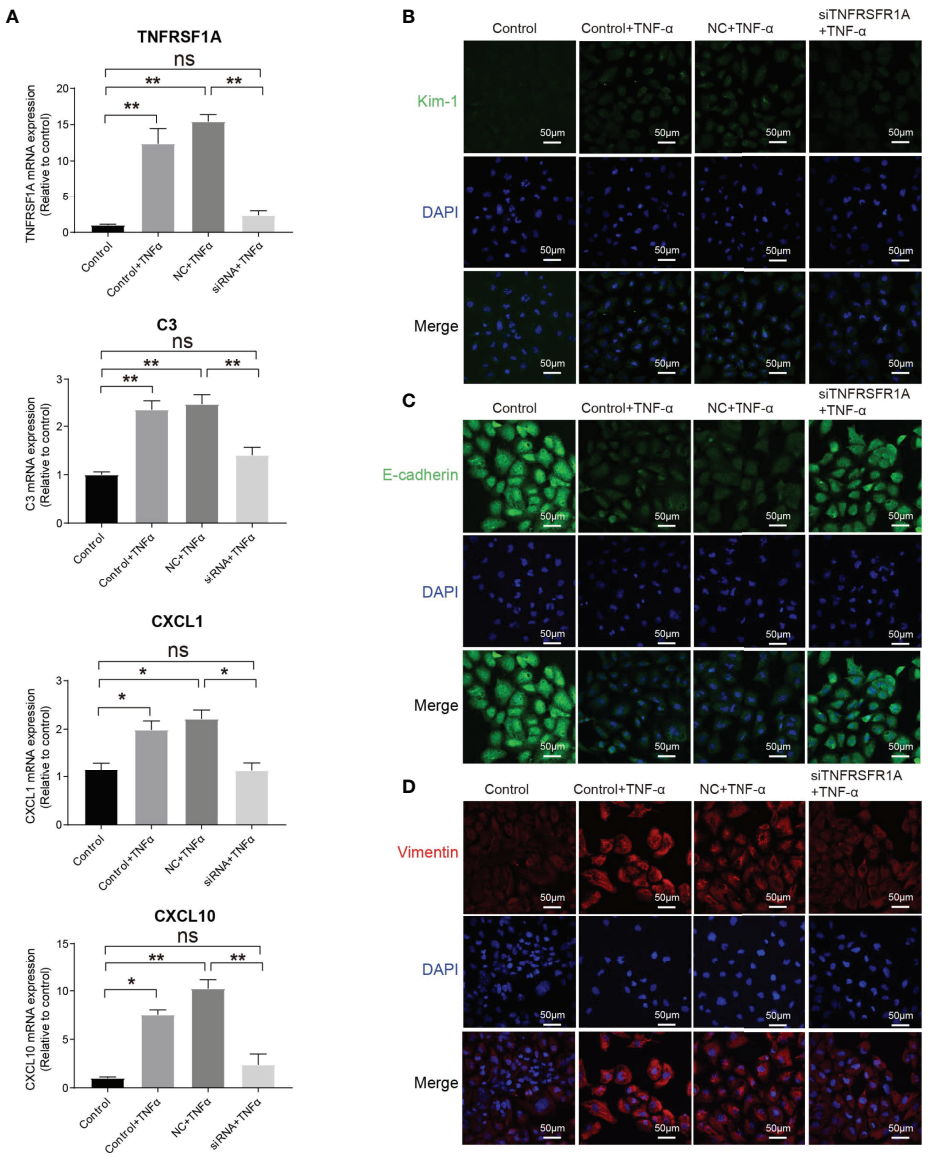

FIGURE 6 | Role of TNF/TNFRSF1A in AKI. **(A)** Expression level of TNFRSF1A and inflammatory signatures C3, CXCL1 and CXCL10 when receiving TNF-α stimulation or not. **(B–D)** Immunostaining showing the expression of injury marker Kim-1 **(B)**, PTC marker (E-cadherin, C) and trans-differentiation marker (Vimentin, D) when receiving TNF-α stimulation or not. Data are performed as means ± SD for three independent experiments. One-way ANOVA with Turkey *post hoc* tests was used for three or more group comparisons. *p<0.05, **p<0.01. ns, Not Statistically Significant.

PCR revealed that exogenous TNFα recombinant protein stimulation significantly promoted PTCs TNFRSF1A mRNA expression, while no significant changes were observed in the siTNFRSF1A + TNFα group (**Figure 6A**). We further examined other inflammation-related indicators and found that TNF-α stimulation significantly increased the expression of inflammatory signatures such as C3, CXCL1, and CXCL10 in PTCs, while no significant expression changes in the siTNFRSF1A + TNFα group compared to the control group (**Figure 6A**). We also found that TNF-α stimulation significantly promoted the expression of the PTC injury marker (Kim-1, **Figure 6B**) and the renal epithelium trans-differentiation marker (Vimentin, **Figure 6C**), while it downregulated the expression of renal tubular epithelial cells marker (E-cadherin, **Figure 6D**). These results suggest that the TNF-α dramatically promoted kidney inflammation and injury and specific depletion of TNFRSF1A would abrogate the injury (36–39).

DISCUSSION

AKI is a potentially fatal disease which can trigger or exacerbate CKD, and is associated with high mortality and morbidity. The progression of AKI to CKD usually undergoes immune cell infiltration, renal cells phenotypic alterations, and then ECM deposition which leads to pathological fibrosis. Immune response-mediated kidney injury is an important factor in the progression of AKI, which determines normal repair or pathological repair when it progresses to CKD. Comprehensively dissecting the key cellular player and intercellular crosstalk target associated with AKI pathobiology is critical for underlying mechanisms to determine the transition from acute to chronic injury, precision diagnosis, and develop novel therapy strategies for AKI.

Several studies have characterized diverse immune cell subtypes and associated features along with the AKI progression, identified renal repair, and injury associated myeloid and T cell subtypes (9, 12, 24). Conway BR et al., utilized scRNA-seq to uncover the myeloid cell diversity and found that monocyte acquired proinflammatory, profibrotic phenotype that expressed Arg1 and the $Mmp2^{+}$ macrophages expanded during repair (9). Fernanda et al., reported that expansion of tissue-resident IL-$33R^{+}$ and IL-$2Ra^{+}$ regulatory T cells (Tregs), before injury, protected the kidney from injury and fibrosis (12). Some studies focused on the diversity of PTC phenotype, the mixed-identity PTCs, injured PTCs, and the identity of failed-repair PTCs (24, 40–42), as well as novel genes and potential pathologic intercellular crosstalk targets such as Ahnak, Sh3bgrl3, Col18a1, Krt20, Vcam1, and Ccl2 (42). These studies have broadened our knowledge of understanding AKI onset and progression. However, the cellular origin of PTC-injured, the molecular characteristics of injured PTCs, the dynamic molecular change along with AKI progression, and how infiltrating immune cells influence the process of AKI and repair, remains poorly investigated.

In this study, we employed unbiased scRNA-seq to systematically resolve the cellular atlas and microenvironment associated with AKI progression. We identified three PTC-new subtypes, and the mixed PTCs indicated that renal epithelial cells may exhibit diverse transcriptome phenotypes in response to injury. Interestingly, the PTC-new cells exhibited impairment of metabolic features and upregulation of proinflammatory and pro-fibrotic features compared to the normal PTCs. Additionally, the kidney injury associated genes, (TFs, pathways, and regulons) were enriched in PTC-new and mixed PTCs, with the highest expression level in the PTC-injured subpopulation. Further cellular differentiation and trajectory analysis indicated that PTC-cycling cells may turn into PTC-S1-new, and then to PTC-injured, and lastly became fibrotic. Importantly, we found that infiltrating immune cells (mainly as monocyte and macrophage) interact closely with PTC-injured and influence the process of AKI progression mainly through inflammatory signaling pathways such as CXCL, complement, VCAM, and TNF. Immunostaining also validated that injured PTCs expressed a high level of TNFRSF1A and injury marker Kim-1, and functional experiments revealed that the exogenous addition of TNF-α dramatically promoted kidney inflammation and injury and specific depletion of TNFRSF1A would abrogate the injury.

Taken together, our study provides a comprehensive cellular atlas for depicting the AKI microenvironment and key molecular pathways that are perturbed in AKI. The results presented here highlighted Tnf–Tnfrsf1a (36–39) and Cxcl1–Cxcr2 pathways (43, 44) and were potential targets of kidney injury, which may be a benefit for AKI repair.

MATERIALS AND METHODS

Ethics Statement

This study was conducted according to the principles expressed in the declaration of Helsinki. Ethical approval was obtained from the Ethics Committee of the Chinese People's Liberation Army General Hospital with number 2019-X5-65.

Mice, Surgical Procedures, and Serum Analysis

C57BL/6 mice (20–25 g) were purchased from the Animal Center of Chinese PLA General Hospital. All animal procedures were approved by the Institutional Animal Care and Use Committee at the Chinese PLA General Hospital and Military Medical College. The 24 male mice were randomly assigned to two groups: 18 mice underwent bilateral renal ischemia and reperfusion surgery (the AKI group), and the remaining 6 mice underwent sham surgery (the control group). Renal ischemia (28 min) and reperfusion and renal sham surgery were performed as described previously. At 24h, 48h, and 72h after reperfusion, blood and kidney samples were harvested for further processing. Kidney injury was assessed by measuring the levels of serum creatinine and blood urea nitrogen

by a quantitative colorimertic assay and calculating the changes in the levels. Blood samples were collected from the vena cava at the indicated time points and the serum was separated by centrifugation at 3,000 rpm for 15 min at 4°C; and then serum Cr and BUN examinations were performed. Serum Scr were measured with the DuantiChromTM Creatinine Assy Kit (Bioassy system, US, DICT-500) by the improved Jaffe method, while the BUN concentration levels were detected with the DuantiChromTM Urea Assy Kit (Bioassy system, US, DIUR-500) by the improved Jung method. For the measurements of serum creatinine and BUN, six animals were analyzed per group and three technical repeats were analyzed from each example.

Histopathological Examination

A quarter of the kidney was fixed in 4% formaldehyde, dehydrated, and embedded in paraffin. Tissue sections (4 μm) were stained with periodic acid–Schiff (PAS). Histological examinations were performed in a blinded manner for acute tubular necrosis (ATN) scores regarding the grading of tubularnecrosis, cast formation, tubular dilation, and loss of brush border as described previously. Fifteen non-overlapping fields (400×) were randomly selected and scored as follows: 0, none; 1, 1–10%; 2, 11–25%; 3, 26–45%; 4, 46–75%; and 5,>76%.

Western Blot

Mouse renal tissue or cells were lysed with RIPA lysis buffer containing protease inhibitors (1 μg/mL leupeptin, 1 μg/mL aprotinin and 100 μmol/L PMSF). After a 30 minute incubation, the samples were centrifuged at 13800 g at 4°C for 30 minutes. The protein concentration was determined by a BCA protein assay kit (Thermo Fisher Scientific, USA). Approximately 40 μg of protein from each sample was separated by 8%- 15% SDS- PAGE. The samples were transferred from the SDS- PAGE gels to membranes. The membranes were blocked and incubated in antibodies against Stmn1 (1:1000, abcam, ab52630), GAPDH (1:10000, proteintech, 60004-1-Ig) and β-actin (1:10000, proteintech, 66009-1-Ig) overnight at 4°C. Finally, the membranes were incubated with secondary antibody at room temperature for 2 hours. ImageJ was used for blot analysis. All experiments were repeated three times.

Cell Culture

HK-2 cells were purchased from ATCC (CRL-2190). Cells were inoculated into 24-well plates lined with coverslips and cultured in DMEM/F12 medium containing 10% FBS at 37°C in a 5% CO2 incubator. Small interfering RNA (siRNA) was produced by Gene Pharma (Gene Pharma Co.,Ltd., China). The target sequence of siRNA for human TNFRSF1A was as follows: Sense: 5'-GGUGGAAGUCCAAGCUCUATT-3', Antisense: 5'-UAGAGCUUGGACUUCCACCTT and NC was used as negative control. The cells were divided into 4 groups: Control group, Control+TNFα group (human-derived TNFα recombinant protein treated group), NC+TNFα group (no significant RNA transfection + human derived TNFα recombinant protein treated group), and siRNA+TNFα group (siRNA transfected with TNFRSF1A + human derived TNFα recombinant protein treated group). At approximately 70% cell fusion, the corresponding si-TNFRSF1A and nonsense RNAs were transfected using Lipofectamine_RNAiMAX for the siRNA +TNFα and NC+TNFα groups, and 15 ng/ml of human-derived TNFα recombinant protein (Biolegend, Cat717904) was given 24 h post-transfection to stimulate For the Control+TNFα group, only 15ng/ml of human TNFα recombinant protein was administered for 24 h. The Control group was left untreated.

qRT-PCR Analysis

Total RNA was extracted from cells using TRIzol and reversely transcribed to cDNA using ProtoScript® II First Strand cDNA Synthesis Kit (E6560S, NEB) according to the manufacturer's instructions. qRT-PCR was conducted using PowerUp SYBR Green Master Mix (Applied Biosystems, Foster City, CA, USA) and performed using the CFX-96 (Bio-Rad, USA). The cycling parameters were as follows: 10 min at 95°C, 45 cycles of 10 s at 95°C, and 30 cycles at 58°C following the manufacturer's instructions. Data were performed as fold induction relative to the control group and the relative mRNA level of target gene was analyzed by the formula $2-\Delta Ct$ ($\Delta Ct = Ct^{target} - Ct^{18S}$). The primer sequences are shown in **Supplementary Table S1**.

Immunofluorescence Staining

For mouse samples, tissue specimens were fixed in 4% paraformaldehyde and embedded in paraffin. Tissue samples were then cut at 4 μm thickness and sequentially treated with 1% SDS and normal goat serum before being incubated with Anit-PCNA (abcam, ab29, 1:100), Anti-Stathmin 1 (abcam, ab52630, 1:100), Anti-Kim-1 (R&D, AF1817, 1:400), Anti-CD68(abcam, ab125212, 1:200), and TNFR1(proteintech, 60192-1-Ig, 1:100) overnight at 4°C. The sections were washed and probed with Cy3-conjugated secondary antibody (red) and FITC- conjugated secondary antibody (green) or LTL (Vector Laboratories, FL-1321, 1:400) at room temperature for 1 hour. DAPI was added to stain the nuclei. The tissue sections were imaged by confocal fluorescence microscopy. Each experiment was repeated three times. For cell samples, cells were washed with PBS and fixed with 4% paraformaldehyde for 15 min. The cells were then permeabilized with 0.2% Triton X-100 for 15min and blocked with 5% BSA in PBS for 1h at room temperature. Cells were then incubated overnight at 4° with Anti-E-Cadherin (R&D, AF748, 1:400), Anti-Kim-1 (R&D, AF1817, 1:400), and Anti-Vimentin (abcam, ab92547, 1:200). After cells were washed with PBS three times and incubated with secondary antibodies (Cy3 conjugated anti-rabbit antibody and FITC conjugated anti-Goat antibody) for 1h at room temperature, they were washed again and mounted onto glass slides with Flouroshield Mounting Medium with DAPI (abcam, ab104139). The cells were imaged by confocal fluorescence microscopy.

Sample Processing and Cell Sorting

Surgical resected fresh kidney samples were minced and enzymatically digested to obtain single-cell suspensions. Briefly, the samples were minced into <1 mm3 pieces and digested with 5 mL digestion buffer containing DNase I (1 mg/mL, Sigma) and collagenase IV (2 mg/mL, Sigma) for 30 min at 37°C. Next, the

resulting suspension was mixed with 5 mL 2% FBS/PBS, filtered with a 70-μm pore size cell strainer (Corning, USA), and centrifuged at 300 g for 5 min at 4°C. After removal of the supernatant, the cell pellet was resuspended in 2 mL red blood cell lysis buffer (BD) for 3 min at room temperature and centrifuged at 300 g for 5 min at 4°C. Then, the supernatant was removed, the cell pellet was resuspended in 100 μL 1% BSA/PBS, and the cells were incubated with 7-AAD (BioLegend) before cell sorting. For the following single-cell library preparation and sequencing, we sorted and collected 7-AAD negative live cells using a BD FACSAria II (BD).

Single-Cell mRNA Library Preparation and Sequencing

The single-cell suspensions were prepared from pools of six animals from each group and then loaded onto a microfluidic chip to generate the complementary deoxyribonucleic acid (cDNA) library using a commercial 10x Genomics platform (10x Genomics, Pleasanton, CA, USA). Single-cell transcriptome amplification and library preparation were performed using the Single-Cell 3' Library Kit v3 (10x Genomics) by Capitalbio Technology Corporation according to manufacturer's instructions. Then, the libraries were pooled and sequenced across six lanes on an Illumina NovaSeq 6000 system (Illumina, Inc., San Diego, CA, USA).

Pre-Processing of scRNA-Seq Data

The raw sequencing FASTQ files were aligned to the mm10 reference genome using the cellranger count function of CellRanger (10X Genomics, v5) to produce a gene expression matrix *via* the STAR algorithm. Then, the raw gene expression matrices were processed by the Seurat (45) R package (version 4.0.0). As the kidney is a highly metabonomic organ, the renal cells serve important roles in energy metabolism, and these cells featured a high ratio of mitochondrial genome transcripts (22). Therefore, low-quality cells were removed according to the following criteria: cells that had fewer than 2,001 unique molecular identifiers (UMIs), more than 6,000 or less than 501 expressed genes, or over 50% of UMIs derived from the mitochondrial genome as described previously. Included genes were expressed in at least ten cells in a sample. We removed potential cell doublets using the DoubletFinder (46) R package. The single cell transcriptome expression matrices of the remaining high-quality cells were integrated with the "RunFastMNN" function of SeuratWrappers package, normalized to the total cellular UMI count, and scaled (scale.factor = 1e4) by regressing out the total cellular UMI counts and percentage of mitochondrial genes. Then, we selected highly variable genes (HVGs) for principal component analysis (PCA), and the top 30 significant principal components (PCs) were selected for Uniform Manifold Approximation and Projection (UMAP) dimension reduction and visualization of gene expression.

Determination of Cell Type

We calculated the differentially expressed genes (DEGs) of each cell subcluster by the "FindAllMarker" function with default parameters provided by Seurat. The cell types and subtypes were annotated according to their expression of the known canonical marker genes of the respective cell types. Cell subclusters with similar gene expression patterns were annotated as the same cell type.

Trajectory Analysis

To illustrate the potential cellular differentiation routines (31) and dissect the origin of PTC-injured subpopulation, the PTC-injured, PTC-cycling, PTC-S1-new were selected and the top 150 signature genes were calculated by differentialGeneTest function provided by Monocle algorithm. The cell differentiation trajectory was inferred with the default parameters of Monocle after dimension reduction and cell ordering. Then, the 'DDRTree' function was used for dimensionality reduction, and the 'plot_cell_trajectory' function was used for visualization.

Single-Cell Regulatory Network Analysis

To explore the single-cell gene regulatory network among different PTC cell subclusters, we analyzed the differentially expressed transcriptome factors with a standard pipeline implemented in R using the SCENIC (47) R package (https://github.com/aertslab/SCENIC). Briefly, the gene expression matrices of the cell subclusters were estimated using GENIE3 to build the initial co-expression gene regulatory networks (GRN). Then, regulon data were analyzed using the RcisTarget package to create TF motifs. The regulon activity scores of each cell were calculated from the AUC by the AUCell package. We filtered the regulons with a correlation coefficient >0.3 with at least one other regulon and the regulons that were activated in at least 30% of the cell subclusters were selected for the subsequent visualization.

Pathway Analysis

DEGs with $|logFC| > 0.5$ and $adj.p.val < 0.05$ were adopted for GO enrichment analysis. The compareCluster function in the clusterProfiler R package was used to find different enriched GO terms between distinct PTC subclusters. To assess the different pathways between distinct PTC subsets, GSVA (48) analysis was performed using the hallmark gene sets provided by the Molecular Signatures Database (MSigDB) and calculated with a linear model offered by the limma package.

Intercellular Crosstalk Analysis

To explore potential intercellular crosstalk between infiltrating immune cells and PTC-injured subpopulation, we implied the ligand-receptor distribution and expression of infiltrating immune cells and PTC-injured subpopulation with a standard pipeline implemented in R using CellChat (35) R package, as previously reported. We chose the receptors and ligands expressed in more than 10% of the cells in the specific cluster for subsequent analysis. The interaction pairs whose ligands belonged to the VCAM, TNF, Complement, and CXCL families were selected for the evaluation of intercellular crosstalk between the distinct PTC subpopulations and infiltrating immune cells.

Data Availability

The accession number for the raw data reported in this paper have been deposited in the Genome Sequence Archive (GSA) under

accession number CRA006298 and the processed data can be accessed in https://ngdc.cncb.ac.cn/omix/view/OMIX001004.

Statistical Analysis

Data were analyzed using the non-parametric Mann-Whitney U test of two group and one-way ANOVA with Tukey's multiple comparisons test for three or more group. $P < 0.05$ was statistically significant. Statistical analyses were performed using GraphPad Prism 5.0 and data are expressed as mean ± SD.

DATA AVAILABILITY STATEMENT

The datasets presented in this study can be found in online repositories. The names of the repository/repositories and accession number(s) can be found below: GSA, https://ngdc.cncb.ac.cn/gsa/browse/CRA006298; OMIX, https://ngdc.cncb.ac.cn/omix/release/OMIX001004.

ETHICS STATEMENT

The animal study was reviewed and approved by the Ethics Committee of the Chinese People's Liberation Army General Hospital with number 2019-X5-65.

AUTHOR CONTRIBUTIONS

MZ was responsible for the single cell analysis, and the writing of the manuscript. LLW collected the samples and performed functional experiment with the help of YD, TW, YZ, JL, and PC. LQW, JW, and XC were responsible for the study concept, design, and interpretation. All authors participated in the discussion. All authors contributed to the article and approved the submitted version.

FUNDING

This work was supported by National Key R&D Program of China (2017YFA0103203, 2017YFA0103200), National Natural Science Foundation of China (82030025), Military Medical Key Projects (BLB19J009), and the National Key R&D Program of China (2018YFA0108803).

SUPPLEMENTARY MATERIAL

The Supplementary Material for this article can be found online at: https://www.frontiersin.org/articles/10.3389/fimmu.2022.857025/full#supplementary-material

REFERENCES

1. Peerapornratana S, Manrique-Caballero CL, Gómez H, Kellum JA. Acute Kidney Injury From Sepsis: Current Concepts, Epidemiology, Pathophysiology, Prevention and Treatment. *Kidney Int* (2019) 96:1083–99. doi: 10.1016/j.kint.2019.05.026
2. Fähling M, Seeliger E, Patzak A, Persson PB. Understanding and Preventing Contrast-Induced Acute Kidney Injury. *Nat Rev Nephrol* (2017) 13:169–80. doi: 10.1038/nrneph.2016.196
3. Bellomo R, Kellum JA, Ronco C. Acute Kidney Injury. *Lancet* (2012) 380:756–66. doi: 10.1016/S0140-6736(11)61454-2
4. Rossaint J, Zarbock A. Acute Kidney Injury: Definition, Diagnosis and Epidemiology. *Minerva Urol Nefrol* (2016) 68:49–57.
5. Chang-Panesso M, Humphreys BD. Cellular Plasticity in Kidney Injury and Repair. *Nat Rev Nephrol* (2017) 13:39–46. doi: 10.1038/nrneph.2016.169
6. Kusaba T, Lalli M, Kramann R, Kobayashi A, Humphreys BD. Differentiated Kidney Epithelial Cells Repair Injured Proximal Tubule. *Proc Natl Acad Sci USA* (2014) 111:1527–32. doi: 10.1073/pnas.1310653110
7. Yang L, Besschetnova TY, Brooks CR, Shah JV, Bonventre JV. Epithelial Cell Cycle Arrest in G2/M Mediates Kidney Fibrosis After Injury. *Nat Med* (2010) 16:535–43, 1p following 143. doi: 10.1038/nm.2144
8. Brandt S, Ballhause TM, Bernhardt A, Becker A, Salaru D, Le-Deffge HM, et al. Fibrosis and Immune Cell Infiltration Are Separate Events Regulated by Cell-Specific Receptor Notch3 Expression. *J Am Soc Nephrol* (2020) 31:2589–608. doi: 10.1681/ASN.2019121289
9. Conway BR, O'Sullivan ED, Cairns C, O'Sullivan J, Simpson DJ, Salzano A, et al. Kidney Single-Cell Atlas Reveals Myeloid Heterogeneity in Progression and Regression of Kidney Disease. *J Am Soc Nephrol* (2020) 31:2833–54. doi: 10.1681/ASN.2020060806
10. Bolisetty S, Zarjou A, Hull TD, Traylor AM, Perianayagam A, Joseph R, et al. Macrophage and Epithelial Cell H-Ferritin Expression Regulates Renal Inflammation. *Kidney Int* (2015) 88:95–108. doi: 10.1038/ki.2015.102
11. Wen Y, Yan HR, Wang B, Liu BC. Macrophage Heterogeneity in Kidney Injury and Fibrosis. *Front Immunol* (2021) 12:681748. doi: 10.3389/fimmu.2021.681748
12. do Valle Duraes F, Lafont A, Beibel M, Martin K, Darribat K, Cuttat R, et al. Immune Cell Landscaping Reveals a Protective Role for Regulatory T Cells During Kidney Injury and Fibrosis. *JCI Insight* (2020) 5(3):e130651. doi: 10.1172/jci.insight.130651
13. Lee S, Huen S, Nishio H, Nishio S, Lee HK, Choi BS, et al. Distinct Macrophage Phenotypes Contribute to Kidney Injury and Repair. *J Am Soc Nephrol* (2011) 22:317–26. doi: 10.1681/ASN.2009060615
14. Liu J, Kumar S, Dolzhenko E, Alvarado GF, Guo J, Lu C, et al. Molecular Characterization of the Transition From Acute to Chronic Kidney Injury Following Ischemia/Reperfusion. *JCI Insight* (2017) 2(18):e94716. doi: 10.1172/jci.insight.94716
15. Kumar S, Liu J, McMahon AP. Defining the Acute Kidney Injury and Repair Transcriptome. *Semin Nephrol* (2014) 34:404–17. doi: 10.1016/j.semnephrol.2014.06.007
16. Supavekin S, Zhang W, Kucherlapati R, Kaskel FJ, Moore LC, Devarajan P. Differential Gene Expression Following Early Renal Ischemia/Reperfusion. *Kidney Int* (2003) 63:1714–24. doi: 10.1046/j.1523-1755.2003.00928.x
17. Kieran NE, Doran PP, Connolly SB, Greenan MC, Higgins DF, Leonard M, et al. Modification of the Transcriptomic Response to Renal Ischemia/Reperfusion Injury by Lipoxin Analog. *Kidney Int* (2003) 64:480–92. doi: 10.1046/j.1523-1755.2003.00106.x
18. Wu H, Kirita Y, Donnelly EL, Humphreys BD. Advantages of Single-Nucleus Over Single-Cell RNA Sequencing of Adult Kidney: Rare Cell Types and Novel Cell States Revealed in Fibrosis. *J Am Soc Nephrol* (2019) 30:23–32. doi: 10.1681/ASN.2018090912
19. Liao J, Yu Z, Chen Y, Bao M, Zou C, Zhang H, et al. Single-Cell RNA Sequencing of Human Kidney. *Sci Data* (2020) 7:4. doi: 10.1038/s41597-019-0351-8
20. Rao DA, Arazi A, Wofsy D, Diamond B. Design and Application of Single-Cell RNA Sequencing to Study Kidney Immune Cells in Lupus Nephritis. *Nat Rev Nephrol* (2020) 16:238–50. doi: 10.1038/s41581-019-0232-6
21. Potter SS. Single-Cell RNA Sequencing for the Study of Development, Physiology and Disease. *Nat Rev Nephrol* (2018) 14:479–92. doi: 10.1038/s41581-018-0021-7

22. Park J, Shrestha R, Qiu C, Kondo A., Huang S, Werth M, et al. Single-Cell Transcriptomics of the Mouse Kidney Reveals Potential Cellular Targets of Kidney Disease. *Science* (2018) 360:758–63. doi: 10.1126/science.aar2131
23. Fu J, Akat KM, Sun Z, Zhang W, Schlondorff D, Liu Z, et al. Single-Cell RNA Profiling of Glomerular Cells Shows Dynamic Changes in Experimental Diabetic Kidney Disease. *J Am Soc Nephrol* (2019) 30:533–45. doi: 10.1681/ASN.2018090896
24. Rudman-Melnick V, Adam M, Potter A, Chokshi SM, Ma Q, Drake KA, et al. Single-Cell Profiling of AKI in a Murine Model Reveals Novel Transcriptional Signatures, Profibrotic Phenotype, and Epithelial-To-Stromal Crosstalk. *J Am Soc Nephrol* (2020) 31:2793–814. doi: 10.1681/ASN.2020010052
25. Wen Y, Lu X, Ren J, Privratsky JR, Yang B, Rudemiller NP, et al. KLF4 in Macrophages Attenuates Tnfα-Mediated Kidney Injury and Fibrosis. *J Am Soc Nephrol* (2019) 30:1925–38. doi: 10.1681/ASN.2019020111
26. Piret SE, Guo Y, Attallah AA, Horne SJ, Zollman A, Owusu D, et al. Krüppel-Like Factor 6-Mediated Loss of BCAA Catabolism Contributes to Kidney Injury in Mice and Humans. *Proc Natl Acad Sci USA* (2021) 118(23): e2024414118. doi: 10.1073/pnas.2024414118
27. Jiang X, Li D, Shen W, Shen X, Liu Y. LncRNA NEAT1 Promotes Hypoxia-Induced Renal Tubular Epithelial Apoptosis Through Downregulating miR-27a-3p. *J Cell Biochem* (2019) 120:16273–82. doi: 10.1002/jcb.28909
28. Xu L, Hu G, Xing P, Zhou M, Wang D. Paclitaxel Alleviates the Sepsis-Induced Acute Kidney Injury *via* lnc-MALAT1/miR-370-3p/HMGB1 Axis. *Life Sci* (2020) 262:118505. doi: 10.1016/j.lfs.2020.118505
29. Chen J, Chen Y, Olivero A, Chen X. Identification and Validation of Potential Biomarkers and Their Functions in Acute Kidney Injury. *Front Genet* (2020) 11:411. doi: 10.3389/fgene.2020.00411
30. Nguan CY, Guan Q, Gleave ME, Du C. Promotion of Cell Proliferation by Clusterin in the Renal Tissue Repair Phase After Ischemia-Reperfusion Injury. *Am J Physiol Renal Physiol* (2014) 306:F724–33. doi: 10.1152/ajprenal.00410.2013
31. Trapnell C, Cacchiarelli D, Grimsby J, Pokharel P, Li S, Morse M, et al. The Dynamics and Regulators of Cell Fate Decisions Are Revealed by Pseudotemporal Ordering of Single Cells. *Nat Biotechnol* (2014) 32:381–6. doi: 10.1038/nbt.2859
32. Fu ZJ, Wang ZY, Xu L, Chen XH, Li XX, Liao WT, et al. HIF-1α-BNIP3-Mediated Mitophagy in Tubular Cells Protects Against Renal Ischemia/Reperfusion Injury. *Redox Biol* (2020) 36:101671. doi: 10.1016/j.redox.2020.101671
33. Huang Y, Zhou J, Wang S, Xiong J, Chen Y, Liu Y, et al. Indoxyl Sulfate Induces Intestinal Barrier Injury Through IRF1-DRP1 Axis-Mediated Mitophagy Impairment. *Theranostics* (2020) 10:7384–400. doi: 10.7150/thno.45455
34. Inoue T, Abe C, Kohro T, Tanaka S, Huang L, Yao J, et al. Non-Canonical Cholinergic Anti-Inflammatory Pathway-Mediated Activation of Peritoneal Macrophages Induces Hes1 and Blocks Ischemia/Reperfusion Injury in the Kidney. *Kidney Int* (2019) 95:563–76. doi: 10.1016/j.kint.2018.09.020
35. Jin S, Guerrero-Juarez CF, Zhang L, Chang I., Ramos R, Kuan CH, et al. Inference and Analysis of Cell-Cell Communication Using CellChat. *Nat Commun* (2021) 12:1088. doi: 10.1038/s41467-021-21246-9
36. Jin HY, Chen LJ, Zhang ZZ, Xu YL, Song B, Xu R, et al. Deletion of Angiotensin-Converting Enzyme 2 Exacerbates Renal Inflammation and Injury in Apolipoprotein E-Deficient Mice Through Modulation of the Nephrin and TNF-Alpha-TNFRSF1A Signaling. *J Transl Med* (2015) 13:255. doi: 10.1186/s12967-015-0616-8
37. Huang L, Zhang R, Wu J, Chen J, Grosjean F, Satlin LH, et al. Increased Susceptibility to Acute Kidney Injury Due to Endoplasmic Reticulum Stress in Mice Lacking Tumor Necrosis Factor-α and its Receptor 1. *Kidney Int* (2011) 79:613–23. doi: 10.1038/ki.2010.469
38. Speeckaert MM, Speeckaert R, Laute M, Vanholder R, Delanghe JR, et al. Tumor Necrosis Factor Receptors: Biology and Therapeutic Potential in Kidney Diseases. *Am J Nephrol* (2012) 36:261–70. doi: 10.1159/000342333
39. Xu C, Chang A, Hack BK, Eadon MT, Alper SL, Cunningham P. N, et al. TNF-Mediated Damage to Glomerular Endothelium Is an Important Determinant of Acute Kidney Injury in Sepsis. *Kidney Int* (2014) 85:72–81. doi: 10.1038/ki.2013.286
40. Kirita Y, Wu H, Uchimura K, Wilson PC, Humphreys BD. Cell Profiling of Mouse Acute Kidney Injury Reveals Conserved Cellular Responses to Injury. *Proc Natl Acad Sci USA* (2020) 117:15874–83. doi: doi:10.1073/pnas.2005477117
41. Melo Ferreira R, Sabo AR, Winfree S, Collins KS, Janosevic D, Gulbronson CJ, et al. Integration of Spatial and Single-Cell Transcriptomics Localizes Epithelial Cell-Immune Cross-Talk in Kidney Injury. *JCI Insight* (2021) 6 (12):e147703. doi: 10.1172/jci.insight.147703
42. Gerhardt LMS, Liu J, Koppitch K, Cippà PE., McMahon AP. Single-Nuclear Transcriptomics Reveals Diversity of Proximal Tubule Cell States in a Dynamic Response to Acute Kidney Injury. *Proc Natl Acad Sci USA* (2021) 118(27):e2026684118. doi: 10.1073/pnas.2026684118
43. Liu P, Li X, Lv W, Xu Z. Inhibition of CXCL1-CXCR2 Axis Ameliorates Cisplatin-Induced Acute Kidney Injury by Mediating Inflammatory Response. *BioMed Pharmacother* (2020) 122:109693. doi: 10.1016/j.biopha.2019.109693
44. Zhou X, Xiao F, Sugimoto H, Li B, McAndrews KM, Kalluri R. Acute Kidney Injury Instigates Malignant Renal Cell Carcinoma *via* CXCR2 in Mice With Inactivated Trp53 and Pten in Proximal Tubular Kidney Epithelial Cells. *Cancer Res* (2021) 81:2690–702. doi: 10.1158/0008-5472.CAN-20-2930
45. Stuart T, Butler A, Hoffman P, Hafemeister C, Papalexi E, Mauck WM 3rd, et al. Comprehensive Integration of Single-Cell Data. *Cell* (2019) 177:1888–902.e21. doi: 10.1016/j.cell.2019.05.031
46. McGinnis CS, Murrow LM, Gartner ZJ. DoubletFinder: Doublet Detection in Single-Cell RNA Sequencing Data Using Artificial Nearest Neighbors. *Cell Syst* (2019) 8:329–37.e4. doi: 10.1016/j.cels.2019.03.003
47. Aibar S, González-Blas CB, Moerman T, Huynh-Thu VA, Imrichova H, Hulselmans G, et al. SCENIC: Single-Cell Regulatory Network Inference and Clustering. *Nat Methods* (2017) 14:1083–6. doi: 10.1038/nmeth.4463
48. Hänzelmann S, Castelo R, Guinney J. GSVA: Gene Set Variation Analysis for Microarray and RNA-Seq Data. *BMC Bioinf* (2013) 14:7. doi: 10.1186/1471-2105-14-7

Conflict of Interest: The authors declare that the research was conducted in the absence of any commercial or financial relationships that could be construed as a potential conflict of interest.

frontiers | Frontiers in Medicine

ORIGINAL RESEARCH
published: 06 June 2022
doi: 10.3389/fmed.2022.890782

ACE2 Promoted by STAT3 Activation Has a Protective Role in Early-Stage Acute Kidney Injury of Murine Sepsis

*Tianxin Chen[1], Zhendong Fang[2], Jianfen Zhu[3], Yinqiu Lv[1], Duo Li[1] and Jingye Pan[2,4]**

[1] Department of Nephrology, The First Affiliated Hospital of Wenzhou Medical University, Wenzhou, China, [2] Department of Key Laboratory of Intelligent Critical Care and Life Support Research of Zhejiang Province, The First Affiliated Hospital of Wenzhou Medical University, Wenzhou, China, [3] Department of Endoscopy Center, The First Affiliated Hospital of Wenzhou Medical University, Wenzhou, China, [4] Department of ICU, The First Affiliated Hospital of Wenzhou Medical University, Wenzhou, China

Sepsis-induced AKI (SIAKI) is the most common complication with unacceptable mortality in hospitalized and critically ill patients. The pathophysiology of the development of SIAKI is still poorly understood. Our recent work has demonstrated the role of signal transducer and activator of transcription 3 (STAT3) pathways in regulating inflammation and coagulation in sepsis. We hypothesized that STAT3 activation has a critical role in early-stage SIAKI. The early-stage SIAKI model was established in cecal ligation and puncture (CLP) mice, which recapitulates the clinical and renal pathological features of early-stage AKI patients. Brush border loss (BBL) was the specific pathological feature of acute tubular injury in early-stage AKI. The role of STAT3 signaling and angiotension system in early-stage SIAKI was evaluated. The STAT3 activation (increased pSTAT3) and increased angiotensin-converting enzyme 2 (ACE2) expressions were observed in CLP mice. The low responsive expressions of pSTAT3 and ACE2 to septic inflammation in CLP AKI mice were associated with BBL. Correlation analysis of proteins' expressions showed pSTAT3 expression was significantly positively related to ACE2 expression in CLP mice. Reduced pSTAT3 after S3I201 intervention, which blocked STAT3 phosphorylation, decreased ACE2 expression, and exacerbated tubular injury in early-stage SIAKI. Our data indicate that endogenous increase of ACE2 expression upregulated by STAT3 activation in early-stage SIAKI play protective role against acute tubular injury.

Keywords: sepsis, acute kidney injury, acute tubular injury, STAT3, angiotensin-converting enzyme

OPEN ACCESS

Edited by:
Alessandra Stasi,
University of Bari Aldo Moro, Italy

Reviewed by:
Al-Shaimaa Faissal Ahmed,
Minia University, Egypt
Huijing Xia,
Louisiana Stete University Health Sciences Center, United States
Davide Medica,
University of Eastern Piedmont, Italy

***Correspondence:**
Jingye Pan
icupjy330@163.com

Specialty section:
This article was submitted to Nephrology, a section of the journal Frontiers in Medicine

Received: *06 March 2022*
Accepted: *25 April 2022*
Published: *06 June 2022*

Citation:
Chen T, Fang Z, Zhu J, Lv Y, Li D and Pan J (2022) ACE2 Promoted by STAT3 Activation Has a Protective Role in Early-Stage Acute Kidney Injury of Murine Sepsis. Front. Med. 9:890782. doi: 10.3389/fmed.2022.890782

INTRODUCTION

Sepsis is the clinical condition for blood poisoning by microorganism and a systemic inflammatory response to infection, which is the most common cause of acute kidney injury (AKI) in critically ill patients (1, 2). Sepsis-induced AKI (SIAKI) is associated with unacceptable morbidity and mortality (2). SIAKI is thought to reflect pathophysiology distinct from other AKI and the mechanisms of SIAKI are not well understood (3–5). Therefore, identifying the exact onset of AKI in sepsis is nearly impossible, leading to difficulty in timely intervention for prevention of SIAKI.

The signal transducer and activator of transcription (STAT) family of proteins regulate a wide variety of cellular processes and diseased conditions. Of the members of the STAT family, STAT3 is essential for normal cell and organ development and adaptive response to stress (6). STAT3 has only recently been investigated for its role in kidney diseases and demonstrated protective responses in animal models of ischemic AKI (7–10). The regulatory function of STAT3 in sepsis has recently attracted great attention and the critical role of STAT3 in the sepsis pathophysiology has been reported in many studies. Some studies have shown that STAT3 activation contributes to organ protection in sepsis (11–15). However, other studies have demonstrated that the suppression of STAT3 activity may ameliorate the organ inflammatory responses and display remarkable protective effects in sepsis (16–20). While the above studies confuse our understanding of STAT3 function in sepsis, essentially little is known about the exact role of STAT3 activation in early-stage AKI. Our recent work has demonstrated that STAT3 is a therapeutic target for sepsis through regulating inflammation and coagulation (21). Therefore, we hypothesized that STAT3 activation has a critical role in early-stage SIAKI. Early-stage AKI, based on Kidney Diseases Improving Global Outcomes (KDIGO) AKI criteria (22), was established and used to examine the role of STAT3 signaling in cecal ligation and puncture (CLP) sepsis model.

METHODS

Experimental Animal Model

All animal studies were approved by the Wenzhou Medical University Institutional Animal Care Committee and adhered to National Institutes of Health guidelines for the care and use of laboratory animals. Male C57BL/6 mice (8-week age) were acclimated and maintained in a conventional, light-cycled facility. C57BL/6 mice were purchased from Shanghai SLAC Laboratory Animal Co (Shanghai, China). Mice were a priori randomized to an exposure (CLP vs. sham operation).

Cecal ligation and puncture sepsis models were performed as previously described with some modifications (21). Mice were anesthetized with 1% sodium pentobarbital (0.1 ml/10 g body weight; Bio-Techne, China) before the operation. After laparotomy, the cecum was identified, then a 5-0 silk ligature was placed 5 mm from the cecal tip. The cecum was punctured twice with a 21-gauge needle (Kindly, Shanghai, China) and gently squeezed to express a 1 mm column of fecal material Sham-operated animals were established similarly without ligation or puncture. All animals were closely assessed every 6 h for the following 2 days. Plasma and urine samples were collected. At the terminal time point (24, and 48 h post-surgery), blood was collected from heart for biochemical measurements. The kidneys were harvested for histopathological examinations.

Early-Stage AKI Definitions and Pilot Protocols

In order to mimic the human AKI as closely as possible, diagnosis of early-stage AKI was decided according to KDIGO-derived AKI criteria: Increase in Scr to X1.5∼2 times baseline within 48 h. The mean Scr value of 24 C57 mice was used as the baseline value. Mice were subjected to the following protocols: (1) normal control C57 mice (NC mice); (2) sham operation (SO mice); (3) CLP without AKI (CLPnoAKI mice); (4) AKI after CLP 24 h (CLP24hAKI mice); (5) AKI after CLP 48 h (CLP48hAKI mice).

S3I-201 Intervention Experiment

To examine the role of STAT3 signaling in SIAKI, S3I-201 (a STAT3 phosphorylation inhibitor) were purchased from Sigma Aldrich China-Mainland (Shanghai, China). S3I-201 was dissolved in 100% dimethyl sulfoxide (DMSO) and then diluted with corn oil to 1%. Briefly, 2.5 mg of S3I-201 was dissolved in 50 μl DMSO to give a master liquid concentration of 50 mg/ml. Then, 50 μl of this DMSO master liquid was mixed with 4,950 μl corn oil to give a working solution of 0.5 mg/ml. The vehicle for this part was prepared by dissolving 50 μl of 100% DMSO in 4,950 μl corn oil (1% DMSO). S3I201 (10 mg/kg) or vehicle was intraperitoneally administered to mice immediately after CLP. Mice were subjected to the following protocols: (1) CLP plus vehicle; (2) CLP plus S3I201.

Matched Case-Control Study in AKI-1 Stage Patients

Between January 1st, 2018 and December 31st, 2020, 45 patients with AKI-1 stage and 95 age and primary disease matched control patients without AKI were collected retrospectively at the Department of Nephrology in the First Affiliated Hospital of Wenzhou Medical University. These patients had complete data of clinical medical history, biochemical tests and renal pathological diagnosis. This retrospective observational study was approved by Institutional Ethics Committee.

Histopathological Examination

Periodic Acid-Schiff (PAS) and Hematoxylin and eosin (H&E) staining of kidney tissues were performed at the First Affiliated Hospital of Wenzhou Medical University Histopathology Lab utilizing standard procedures. Histologic changes of renal tissue were evaluated by assessment of the extent of tubular vacuolation, brush border loss (BBL), tubular dilation and cast formation in the cortex, outer medulla, and inner medulla scored according to the following criteria as follow: zero point, normal; 1 point, below 30% of the pertinent area; 2 points, 30%−70% of the pertinent area; 3 points, over 70% of the pertinent area. Apoptotic cells in sections of mouse kidneys were detected by TdT-mediated dUTP Nick-End Labeling (TUNEL) kit (Abcam china, Moganshan Rd. Hangzhou) detection. Neutrophils were detected by stained with anti-MPO. The total numbers of apoptotic bodies and neutrophils per field were counted.

Plasma Assay

Scr were quantified by sarcosine oxidase enzymatic (SOE) assays and urea levels were determined by urease-UV fixed rate (enzymatic method) in the department of Clinical Laboratory, the First Affiliated Hospital of Wenzhou Medical University, Wenzhou, China. Laboratory technician blinded to the intervention of serum samples. Serum IL-10 and TNF-a levels

were determined using specific sandwich enzyme immunometric assay kits (Abcam China, Moganshan Rd. Hangzhou).

Immunoblotting

Renal tissues were lysed in Radio Immunoprecipitation Assay (RIPA) buffer using a tissue homogenizer. Protein extracts were separated on 4%−12% SDS-polyacrylamide gels and transferred to nitrocellulose membranes. Detection was performed using antibodies: STAT3, pSTAT3, B-cell lymphoma-2 (Bcl-2) and b-actin from Cell Signaling Technology (CST-US subsidiary in China. Shengxia Road. Pudong Shanghai). AGT1R and ACE2 antibodies for immunoblotting were form Abcam China (Moganshan Rd. Hangzhou).

Quantitative Real-Time PCR

RNA was extracted from snap-frozen kidneys using TRIzol (Invitrogen. Thermo Fisher Scientific-CN, Pudong Shanghai, China). Reverse transcription was performed using the cDNA Reverse Transcription Kit (Invitrogen. Thermo Fisher Scientific-CN, Pudong Shanghai, China) according to the manufacturer's protocols. The Light Cycler and SYBR Green PCR Master Mix (Roche Life Science, China) were applied to detect mRNA expression with primer pair sequences. Beta actin was used as an internal control. The $2^{-\Delta\Delta ct}$ method was used to analyze the relative changes in mRNA expression. The sequences of primers used for qRT-PCR are listed as follows: Beta actin, forward 5′-AGGAGTACGATGAGTCCGGC-3′, reverse 5′-AGGGTGTAAAACGCAGCTCAG-3′; ACE2, forward 5′-CTCTGGGAATGAGGACACGG-3′, reverse 5′-CCATAGGCATGGGATCGTGG-3′; AGT1R, forward 5′-GTCTACCACATGCACCGTGA-3′, reverse 5′-CTCCTGAGAGGGTCCGAAGA-3′.

Statistical Analyses

Data were reported as means with SD. Unpaired *t*-test was used for analysis of 2 groups and one-way ANOVA was used for analysis for three or more groups followed by Tukey's test. For the correlation analysis, R^2 was obtained and analyzed with Pearson correlation test for continuous variables and Spearman rank correlation test for categorical data. Significance was set at $p < 0.05$. *p*-value is indicated as $^{*}p < 0.05$; $^{**}p < 0.01$; $^{***}p < 0.001$; $^{****}p < 0.0001$; $p > 0.05$, not significant (ns).

RESULT

Establishment of KDIGO-Derived AKI Diagnosis in CLP Model

The mean value of Scr in 24 8-week-old C57 mice was 0.09 ± 0.02 mg/dl (**Supplementary Figure 1**), which was identified as baseline Scr of C57 mice. Increase in Scr to 0.09X (1.5–2.0) mg/dl within 48 h was defined as AKI-1 stage by KDIGO AKI criteria. 4 of 5 CLP mice at 24 h and 3 of 5 CLP mice at 48 h had early-stage AKI (AKI-1 stage). 3 NC, 3 SO and 3 CLP mice did not develop AKI.

Biochemical and Renal Histopathological Features of Early-Stage SIAKI

CLP24hAKI and CLP48hAKI mice exhibited a significant increase in Scr compared with NC, SO and CLPnoAKI mice (**Figure 1A**). There were no differences of blood BUN level among CLP24hAKI, CLP48hAKI, NC and SO mice (**Figure 1B**). To evaluate inflammatory reaction of CLP model, serum TNF-α and IL-10 levels by ELISA were evaluated in NC, SO and CLP mice. The results indicated that the CLP induced hyperinflammatory response. Both serum TNF-α and IL-10 levels increased obviously in CLP mice, but did not reach statistical significance among CLPnoAKI, CLP24hAKI, and CLP48hAKI mice (**Supplementary Figure 2**).

Renal morphologic evaluation based on HE-staining showed mild tubular damage with vacuolization but no tubular necrosis, thrombosis, infiltrating inflammatory cells or cast formation both in cortex and the outer stripe of outer medulla (OSOM) of SO and CLP mice (**Figure 2**). There was no significant difference in tubular injury scores between SO and CLP mice. TUNEL staining did not find apoptotic bodies in both SO and CLP mice. However, PAS-staining revealed focal tubular BBL in one CLP24hAKI and two CLP48hAKI mice. Representative images of no BBL showed in **Figure 3A** and BBL in CLP AKI mice in **Figures 3B,C**.

Slight increase in Scr and focal BBL in proximal tubules were the specific features of early-stage AKI in CLP mice.

Early-Stage AKI in CLP Mice Recapitulates the Clinical and Renal Pathological Features of Early-Stage AKI Patients

To assess whether or not the early-stage AKI in CLP model adequately mimic AKI patients, 45 patients diagnosed as AKI-1 stage using KDIGO definition and 95 patients without AKI were analyzed. AKI patients had a slight increase in Scr compared with no AKI patients (1.38 ± 0.14 vs. 1.02 ± 0.14 mg/dl, $p < 0.001$). There was no significant difference in BUN between patients with and without AKI (18.6 ± 10.0 vs. 20.0 ± 5.9 mg/dl, $p = 0.15$).

Renal biopsies from AKI-1 stage patients were compared with biopsies from no AKI patients. Many tubular injury morphologic changes were present in the biopsies of patients, but only the BBL was significantly related to AKI (**Figure 3D**). In 45 AKI patients, BBL was present in 39 patients and absent in six patients. BBL was also present in 10 of 95 no AKI patients (**Supplementary Figure 3**). Slight increases in Scr and BBL in proximal tubules were important features of early-stage AKI patients.

Early-stage AKI in CLP mice based on KDIGO-derived AKI diagnosis criteria had the similar biochemical and renal histopathological features to early-stage AKI patients.

STAT3 Activation and ACE2 Expression Play Protective Role on Acute Tubular Injury in CLP AKI Mice

Increased level of activated STAT3 (pSTAT3) was detected in renal tissues from CLP mice (**Figures 4A,B**), furthermore, pSTAT3 level in renal tissues from CLP AKI mice was significantly higher than that from CLPnoAKI mice (**Figure 4B**).

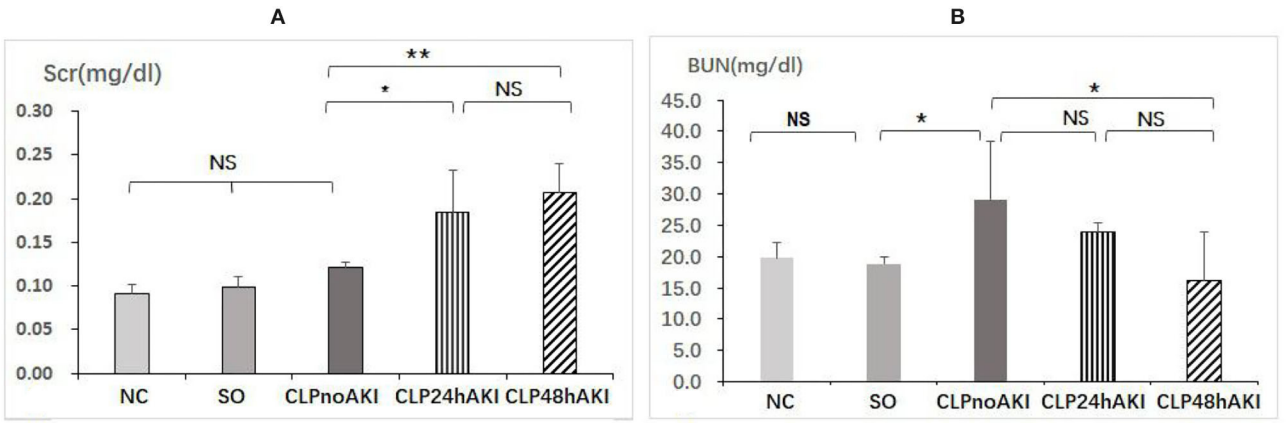

FIGURE 1 | CLP sepsis induces early acute kidney injury. **(A)** Scr had significant increases in CLP24hAKI ($n = 4$) and CLP48hAKI ($n = 3$) mice compared with CLPnoAKI($n = 3$) mice (CLP24hAKI vs. SO, 0.19 ± 0.05 vs. 0.12 ± 0.06, $p = 0.011$; CLP48hAKI vs. SO, 0.21 ± 0.05 vs. 0.12 ± 0.06, $p = 0.003$). **(B)** Serum BUN had significant increases in CLPnoAKI compared with SO ($n = 3$) and CLP48hAKI mice(CLPnoAKI vs. SO, 29.1 ± 9.3 vs. 18.9 ± 1.2, $p = 0.039$; CLPnoAKI vs. CLP48hAKI,29.1 ± 9.3 vs. 16.2 ± 7.8, $p = 0.013$); there are no differences among NC ($n = 3$), SO, CLP24hAKI and CLP48hAKImice. NC, Normal control C57 mice; SO, Sham Operation; CLPnoAKI, CLP without AKI; CLP24hAKI, AKI after CLP 24 h; CLP48hAKIAKI after CLP 48 h. *, $p<0.05$; **, $p<0.01$; NS, $p > 0.05$.

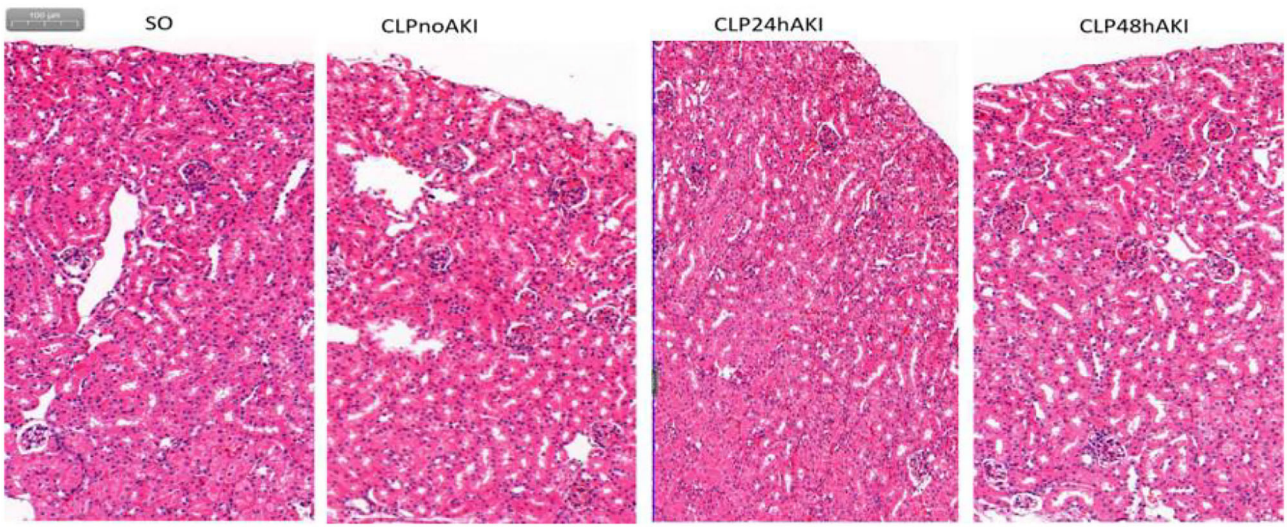

FIGURE 2 | Representative HE staining images (original magnification, ×100) of the cortex and the outer stripe of the outer medulla (OSOM) in each group were shown. There was no significant difference in tubular change scores between each group. SO, Sham Operation; CLPnoAKI, CLP without AKI; CLP24hAKI, AKI after CLP 24 h; CLP48hAKI, AKI after CLP 48 h.

In agreement with TUNEL staining that did not find apoptotic bodies in both SO and CLP mice, apoptosis associated proteins (Caspase 3, cleaved-caspase 3, Bcl-2) were no differences between SO and CLP mice (**Figure 4A**).

To evaluate the role of AGT1R and ACE2 on the early-stage AKI, the expressions of AGT1R and ACE2 in mice renal cortex and medulla were checked. Decreased expression of AGT1R and increased expression of ACE2 determined by Western blot were detected in renal cortex tissues from CLP mice (**Figure 4**C). Weak expressions of AGT1R (**Figure 4D**) and relative strong expressions of ACE2 (**Figure 4E**) in CLP were observed in our study. Correlation analysis of protein relative expression in CLP mice showed pSTAT3 level positively correlated with ACE2 expression (**Figure 4F**). Real-time PCR analyses indicated that AGT1R mRNA expression was reduced, but ACE2 mRNA expression was increased in renal cortex tissues from CLP mice (**Supplementary Figures 4A,B**). Focal BBL in renal cortex was observed in three of seven CLP AKI mice. In order to evaluate the role of STAT3 signaling and angiotensin system on the acute tubular injury, renal cortical tissues from three CLP AKI with BBL mice were compared with cortical tissues from four CLP AKI without BBL mice. The different expressions of ACE2, AGT1R, STAT3, pSTAT3, Caspase 3, cleaved-caspase 3, Bcl-2, and b-actin protein in renal cortex tissues between CLP AKI with

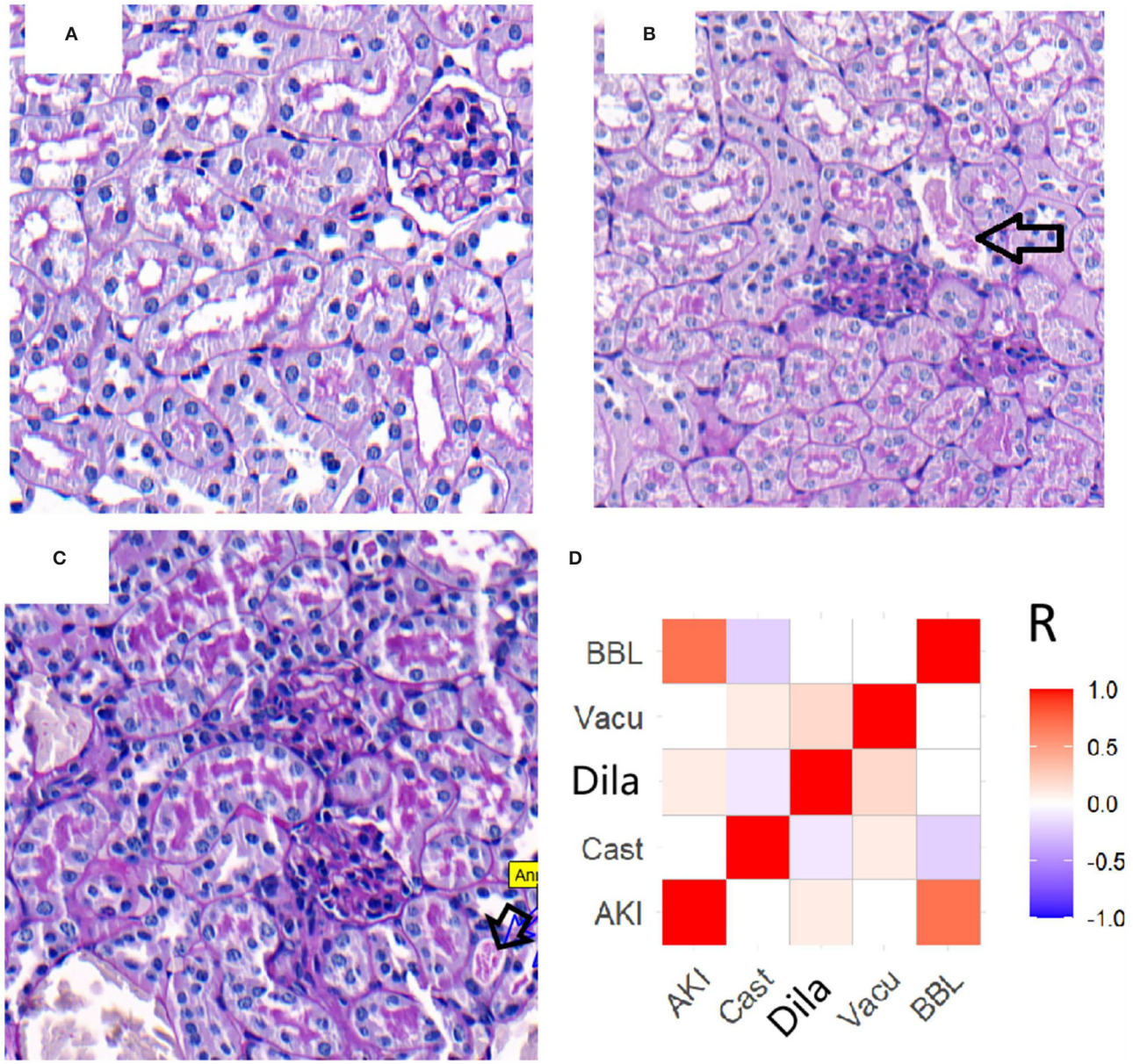

FIGURE 3 | Representative images (original magnification, ×200) of brush border loss in CLP AKI mice. **(A)** CLP48hAKI mice without BBL. **(B)** Focal BBL in renal cortical fields of CLP24hAKI mice. **(C)** Local BBL in renal cortical fields of CLP28hAKI mice. **(D)** Correlations between AKI and acute tubular lesions in patients. AKI correlated with BBL score significantly ($R = 0.752$, $p < 0.001$). The completely loss of brush border (arrows). CLP24hAKI, AKI after CLP 24 h; CLP48hAKI, AKI after CLP 48h.AKI, acute kidney injury; Cast, tubular cast formation; Dila, tubular dilation; Vacu, tubular vacuolation; BBL, brush border loss.

BBL and without BBL mice were analyzed (**Figures 5A,B**). The expressions of pSTAT3, Bcl-2 and ACE2 in CLP AKI without BBL mice were higher than that in CLP AKI with BBL mice (**Figure 5C**). Real-time PCR analyses indicated that AGT1R mRNA expression was reduced (**Figure 5D**), but ACE2 mRNA expression was increased in renal cortex tissues from CLP AKI without BBL mice (**Figure 5E**).

To examine the role of STAT3 signaling in SIAKI, S3I201 intervention experiment was conducted. Ten mice were intraperitoneally administered with S3I201 after CLP (CLP with S3I201 mice), five of 10 CLP with S3I201 mice had early-stage SIAKI. Another 10 mice were intraperitoneally administered with vehicle (CLP with vehicle mice), three of 10 CLP with vehicle mice had early-stage SIAKI. There was no significant difference in SIAKI incidence between CLP with S3I201 and with vehicle mice during 24 h (50 vs. 30%, $p > 0.05$). There was no significant difference in Scr level between CLP with S3I201 and with vehicle AKI mice (**Figure 6A**). The

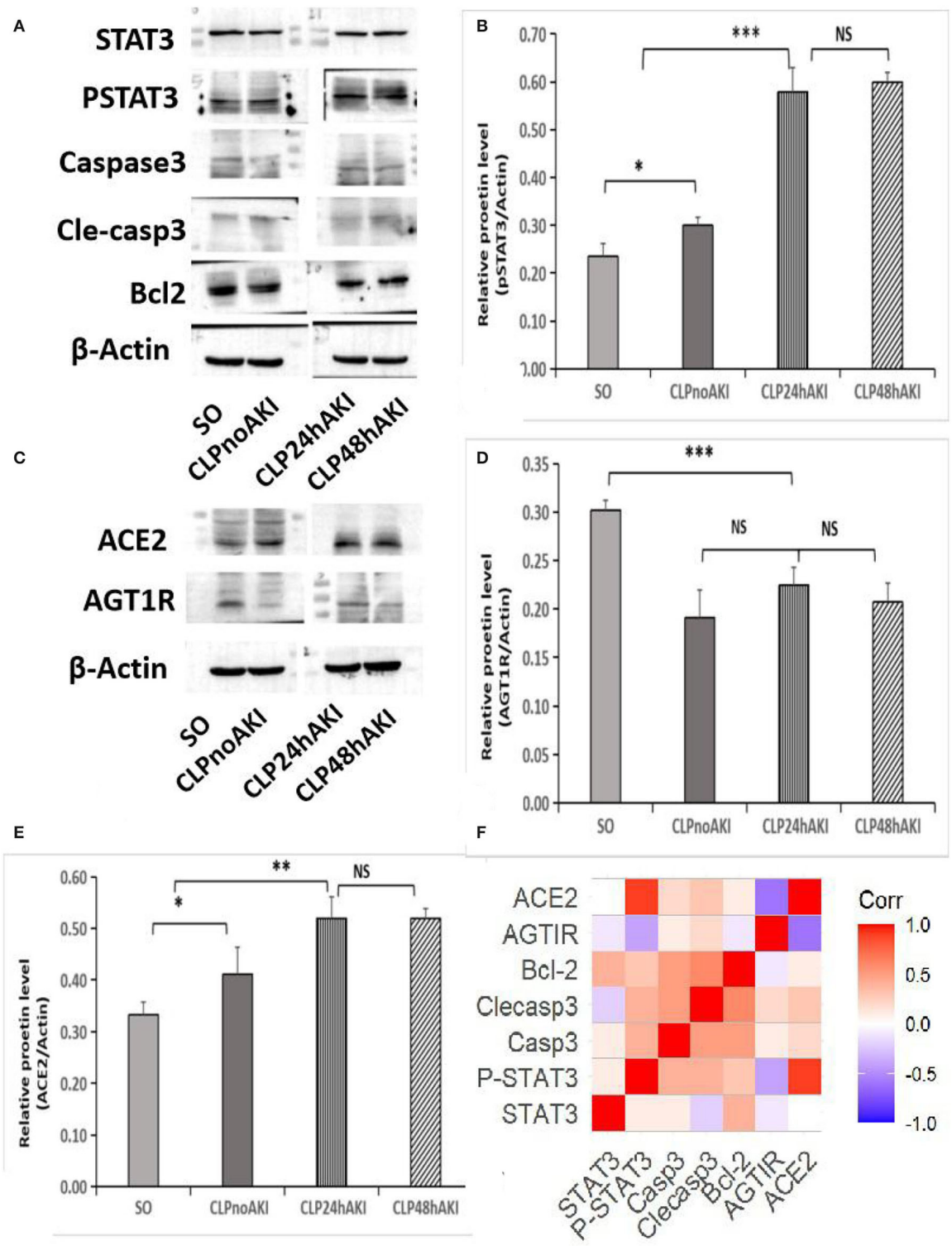

FIGURE 4 | Increased expressions of pSTAT3 and ACE2 were associated with SIAKI. **(A)** Western blot analyses of STAT3, pSTAT3, Caspase 3, cleaved-caspase 3, Bcl-2 and b-actin levels in renal cortex tissues of SO and CLP mice. **(B)** Relative pSTAT3 levels in each group. **(C)** Western blot analyses of ACE2 and AGT1R expression. **(D)** Relative AGT1R levels in each group. **(E)** Relative ACE2 levels in each group; **(F)** Correlations of proteins expression in CLP mice. pSTAT3 level positively correlated with ACE2 expression ($R = 0.874$, $p < 0.001$). Significant relations between 2 factors are highlighted. STAT3,signal transducer and activator of transcription 3; pSTAT3, phosphorylated STAT3; Casp3, caspase3; Clecasp3, cleaved-caspase3;Bcl-2,B-cell lymphoma-2; AGT1R, Angiotensin II Type 1 Receptor; ACE2, angiotensin converting enzyme 2. *, $p<0.05$; **, $p<0.01$; ***, $p<0.001$.

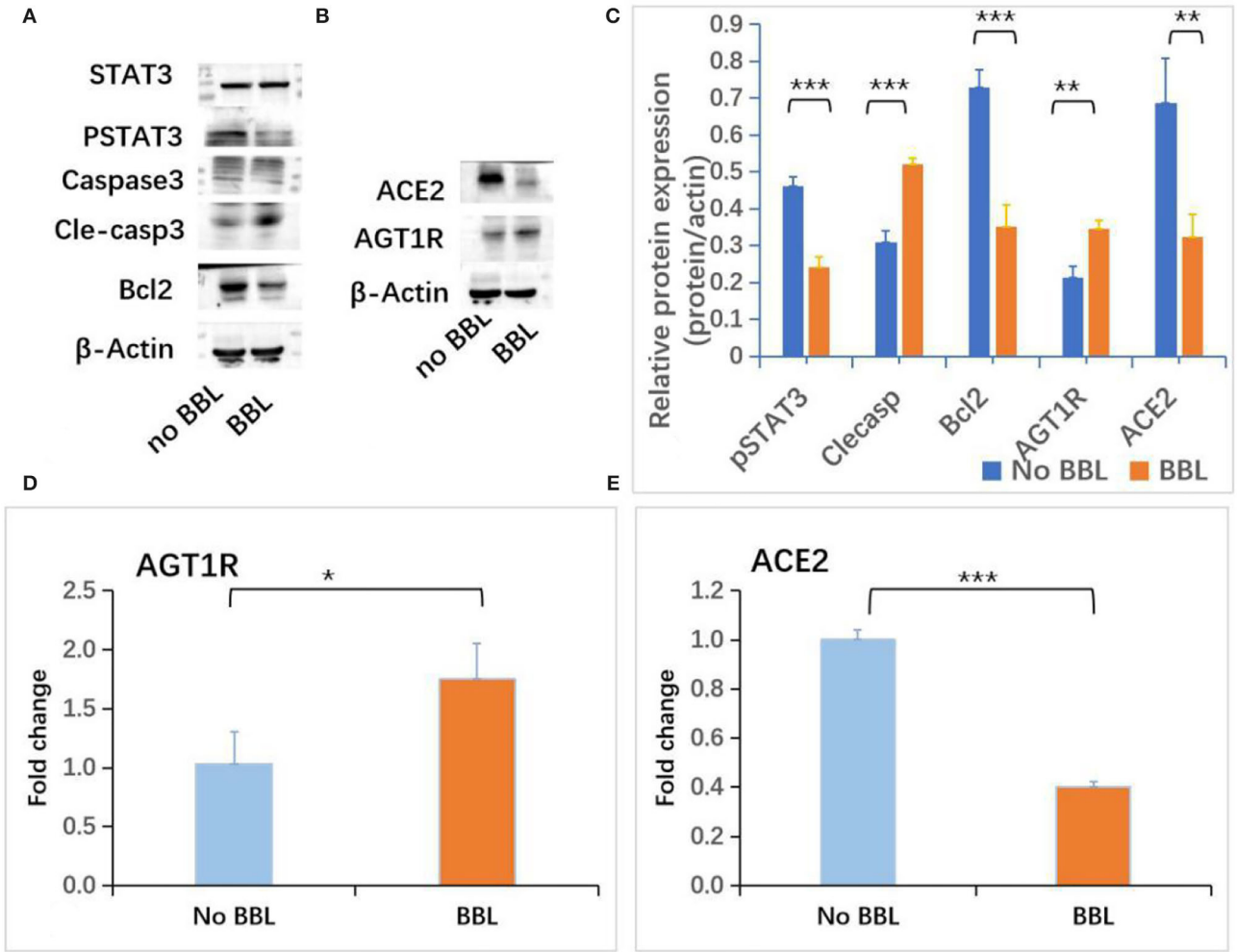

FIGURE 5 | Increased expressions of pSTAT3 and ACE2 were associated with BBL SIAKI. **(A)** Western blot analyses of STAT3, pSTAT3, caspase 3, cleaved-caspase 3 and Bcl-2 levels in renal cortex tissues of CLP AKI mice. **(B)** Western blot analyses of ACE2 and AGT1R levels in renal cortex tissues of CLP AKI mice. **(C)** The differences of pSTAT3, Cleaved-caspase 3, Bcl2, AGT1R and ACE2 expressions between No BBL and BBL mice. **(D)** The difference of AGT1R mRNA expression determined by RT-PCT between No BBL and BBL mice. **(E)** The difference of ACE2 mRNA expression determined by RT-PCT between No BBL and BBL mice. *, $p<0.05$; **, $p<0.01$; ***, $p<0.001$.

levels of pSTAT3 and ACE2 in renal cortex were analyzed by Western blot in AKI mice (**Figure 6B**). Decreased level of pSTAT3 and ACE2 were detected in CLP with S3I201 AKI mice (**Figures 6C,D**). Real-time PCR analyses indicated that ACE2 mRNA expression was reduced significantly in CLP with S3I201 AKI mice (**Figure 6E**). Compared with CLP with vehicle AKI mice, CLP with S3I201 AKI mice had higher acute tubular injury scores (**Figure 6F**).

DISCUSSION

In this study, we were successful in establishing KDIGO-derived AKI diagnosis in CLP mice model. Comparing the data from early-stage SIAKI mice and AKI patients, we found that early-stage SIAKI in CLP mice had similar biochemical and renal histopathological features to AKI patients. Many previous studies have used acute renal failure animal models for preventing the progression of AKI to chronic kidney disease (10, 17, 18, 23–26), but few have used early-stage AKI model for inhibiting the occurrence and development of AKI. Current management of AKI, a potentially fatal disorder in sepsis patients, is merely supportive. No promising new treatment strategies have demonstrated efficacy in early-stage patients with SIAKI by now. Although many reasons could account for this dilemma, the use of animal models that do not adequately mimic patient early-stage AKI may be the contributing factor. Therefore, this KDIGO-derived AKI diagnosis model can be a powerful research model for clarification of molecular pathogenesis and the discovery of drugs to preventing AKI.

To the best of our knowledge, this is the first study to explore the molecular mechanism of early-stage SIAKI by

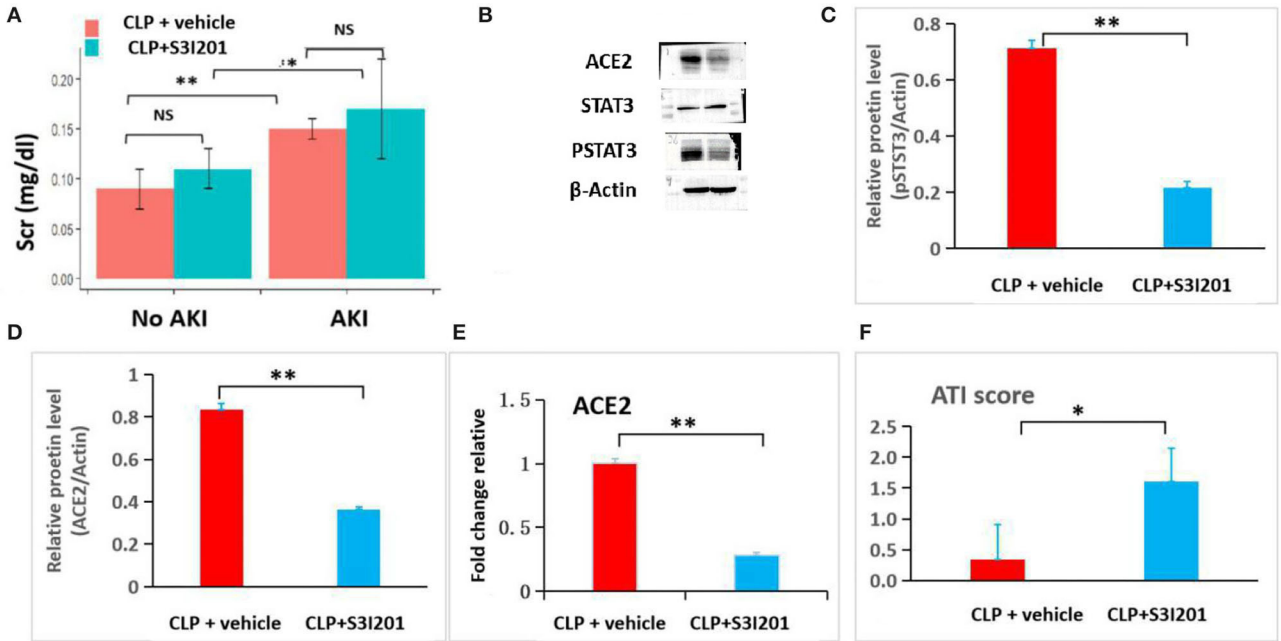

FIGURE 6 | S3I201 intervention experiment in CLP mice. **(A)** Scr had significant increases in CLP with vehicle ($n = 7$) and S3I201 ($n = 5$) AKI mice compared with CLP with vehicle ($n = 7$) and S3I201 ($n = 5$) noAKI mice. **(B)** Western blot analyses of ACE2, STAT3 and pSTAT3 levels in renal cortex tissues of CLP with vehicle and S3I201 AKI mice. **(C)** Relative pSTAT3 levels in CLP with vehicle and S3I201 AKI mice. **(D)** Relative ACE2 levels in CLP with vehicle and S3I201 AKI mice. **(E)** ACE2 mRNA expression in CLP with vehicle and S3I201 AKI mice determined by RT-PCT. **(F)** Acute tubular injury scores in CLP with vehicle and S3I201 AKI mice. ATI, acute tubular injury. *, $p<0.05$; **, $p<0.01$.

comparing CLP no AKI and CLP AKI mice. Previous CLP animal experiments didn't distinguish CLP no AKI from CLP AKI. For example, in a recent published experiment showed CLP mice had AKI at 12 h after surgery, but in fact three of eight CLP AKI mice at 12 h didn't develop into AKI (27). Seven of 10 CLP mice in our pilot experiment and three of 10 CLP with vehicle mice in S3I201 intervention experiment had early-stage AKI, which was similar to the incidence of AKI in sepsis patients reported by clinical studies (2, 28–30).

Our study observed some new phenomena. First, focal BBL in proximal tubules was the specific renal pathological feature of early-stage AKI. The morphologic changes of tubular injury include vacuolation, BBL, dilation and cast formation in AKI-1 stage patients, but only the BBL was significantly related to AKI. Second, acute renal function decrease may parallel acute tubular injury and occur simultaneously. Acute renal function decrease also can occur prior or posterior to acute tubular injury. A recent study of early-stage AKI in sepsis also found that renal dysfunction occurs prior to tubular cell injury and histopathological findings of postmortem sepsis patients did not draw a direct line between severity of renal parenchymal damage and functional decline (31). These findings suggested that different mechanisms may be involved in the development of acute tubular injury and acute renal function decline in early-stage AKI. The relationship between tubular injury and acute renal function decrease in sepsis remains unclear. Previous report showed that acute renal function decrease caused by acute tubular injury and tubuloglomerular feedback may be the main mechanism of tubular injury making functional decline (32). Therefore, the relation between renal function decline and acute tubular injury is more complex than previously thought in early-stage SIAKI.

Our pilot CLP experiment showed that AKI mice had increased pSTAT3 and ACE2 expressions compared to SO. However, CLPAKI mice with acute tubular injury were associated with decreased PSTAT3 and ACE2 expressions. These findings suggest that STAT3 activation and increased ACE2 expression may be the compensatory response to inflammation after infection. CLPAKI mice with low response will be vulnerable to inflammatory reaction and likely to have tubular injury. S3I201 intervention experiment found that deceased pSTAT3 and ACE2 expressions due to the inhibition of STAT3 activation were not associated with SIAKI incidence, but aggravated tubular injury, which indicated that the responsive increase of pSTAT3 and ACE2 may not participate the development of SIAKI initially but play a protective role for renal tubular. The expressions of apoptosis associated proteins were no differences among SO, CLP AKI and CLP no AKI mice, which was similar to the results of a recent SIAKI study (31). However, increased cleaved-caspase 3 and decreased Bcl-2 expressions were detected in CLPAKI mice with BBL. Previous study also found cleaved-caspase 3 was increased in CLP rat with tubular injury (17).

Angiotensin II (Ang II) exerts its biologic effects of vasoconstriction through binding to the angiotensin type 1 receptor (AGT1R). Ang II responsiveness is determined by the expression of AGT1R. Angiotensin-converting enzyme

2 (ACE2) catalyzes Ang II conversion to angiotensin-(1–7), and ACE2/Ang 1–7 axis counteracts the Ang II/AGT1R axis. Clinical trials have demonstrated Ang II effectively increased blood pressure and may have benefits to AKI patients with renal replacement in vasodilatory shock, but no benefits for preventing early-stage SIAKI deterioration (33–35). ACE2/Ang 1–7 and Ang II/AGT1R axis may play critical role in SIAKI, which was investigated in our study. Increased AGT1R and decreased ACE2 expressions were associated with BBL, which may result from focal microvascular hypoperfusion due to efferent arteriolar constriction mediated by increased AGT1R and decreased ACE2 expression. Correlation analysis of protein relative expressions in CLP mice showed pSTAT3 level was only related to ACE2 expression, suggesting ACE2 may be regulated by STAT3 activation. The inhibition of STAT3 activation resulted in the decrease of ACE2 expression and deterioration of tubular injury in CLP mice. Previous published studies also found that ACE2 activator had protective role for renal tubular and ACE2 insufficiency was associated with increased severity of lung injury in sepsis (36, 37).

There are limitations in our study. First, CLP model with young mice has well-documented deficiencies as a model of clinical sepsis and SIAKI (38, 39). However, CLP has important advantages over many other rodent sepsis models, such as endotoxemia (40–42). Further, early-stage AKI in CLP mice reliably recapitulates the biochemical and renal pathological features of AKI-1 stage patients in our study. Second, sepsis is a heterogeneous disease with respect to pathogens and response to infection, limiting the applicability of standardized model. Third, Scr is not the most perfect biomarker of acute renal function decrease. Although there are multiple promising serum and urinary biomarkers (such as Kidney injury molecule 1), Scr is still the major biomarkers of kidney function recommended by KDIGO guideline and remains the most commonly used biomarker in the worldwide. Furthermore, Scr determined by SOE assays in our study was similar to the level of high-performance liquid chromatography (HPLC) Scr reported in previous study (43, 44). Scr quantified by SOE assays in our study, which are more precise and less susceptible to interfere with non-creatinine chromogens than compensated Jaffe methods, provide more reliable estimations of renal function decrease. Fourth, blood pressure and angiotensin 2 levels have not been evaluated in this study. All mice survived after 24 or 48 h in our experiments, which suggested CLP mice may not have severe hypotension.

In conclusion, STAT3 activation due to septic inflammation may promote ACE2 expression, and then attenuate acute tubular injury in early-stage SIAKI. The KDIGO-derived AKI diagnosis model can be a powerful research model for the discovery of drugs to preventing AKI deterioration.

DATA AVAILABILITY STATEMENT

The raw data supporting the conclusions of this article will be made available by the authors, without undue reservation.

ETHICS STATEMENT

The studies involving human participants were reviewed and approved by the Ethical Committee of First Affiliated Hospital of Wenzhou Medical University. The Ethics Committee waived the requirement of written informed consent for participation. All animal studies were approved by the Wenzhou Medical University Institutional Animal Care Committee.

AUTHOR CONTRIBUTIONS

TC and JP conceived study. ZF conducted animal experiments. JZ collected patients' data. TC analyzed experimental data, analyzed and interpreted results, and wrote the manuscript. YL and DL reviewed pathological image. JP commented on the manuscript. All authors contributed to the article and approved the submitted version.

FUNDING

This research was supported by Zhejiang Provincial Natural Science Foundation of China under Grant No. LY21H050004, National Natural Science Foundation of China under Grant No. 81873949.

ACKNOWLEDGMENTS

We thank Zhouqing Huang, Tingting Wang, Fanfan Li, Mo Shen, Xinxin Zhou, Keqing Shi and Jinrong Tian for technical assistance.

SUPPLEMENTARY MATERIAL

The Supplementary Material for this article can be found online at: https://www.frontiersin.org/articles/10.3389/fmed.2022.890782/full#supplementary-material

Supplementary Figure 1 | Baseline mice Scr value. The mean value of Scr in 24 8-week-old C57 mice was 0.09 ± 0.02 mg/dl.

Supplementary Figure 2 | CLP sepsis induces an inflammatory state: **(A)** Serum TNF-a had significant increases in CLP mice than SO and NC mice. **(B)** Serum IL-10 had significant increases in CLP mice than SO and NC mice. NC, Normal control C57 mice; SO, Sham Operation; CLPnoAKI, CLP without AKI; CLP24hAKI, AKI after CLP 24 h; CLP48hAKIAKI after CLP 48 h. *$p < 0.05$; **$p < 0.01$; ***$p < 0.001$; NS, $p > 0.05$.

Supplementary Figure 3 | Representative images (original magnification, x400) and renal function changes in patients. **(A)** A AKI patient with BBL (AKIandBBL); **(B)** A patient had BBL, but no AKI (BBLnoAKI); **(C)** A AKI patient without BBL(AKInoBBL); **(D)** Changes of Scr values in three patients. Scr, serum creatinine; Prebiopsy, 2–7 days before the day of biopsy; Postbiopsy, 2–7 days after the day of biopsy.

Supplementary Figure 4 | AGT1R and ACE2 mRNA expression in CLP mice. **(A)** AGT1R mRNA expression determined by RT-PCT; **(B)** ACE2 mRNA expression determined by RT-PCT. ACE2, angiotensin converting enzyme 2; AGT1R:Angiotensin II Type 1 Receptor.

REFERENCES

1. Singer M, Deutschman CS, Seymour CW, Shankar-Hari M, Annane D, Bauer M, et al. The Third International Consensus definitions for sepsis and septic shock (Sepsis-3). *JAMA*. (2016) 315:801–10. doi: 10.1001/jama.2016.0287
2. Peerapornratana S, Manrique-Caballero CL, Gómez H, Kellum JA. Acute kidney injury from sepsis: current concepts, epidemiology, pathophysiology, prevention and treatment. *Kidney Int*. (2019) 96:1083–99. doi: 10.1016/j.kint.2019.05.026
3. Kellum JA, Prowle JR. Paradigms of acute kidney injury in the intensive care setting. *Nat Rev Nephrol.* (2018) 14:217–30. doi: 10.1038/nrneph.2017.184
4. Gómez H, Kellum JA. Sepsis-induced acute kidney injury. *Curr Opin Crit Care.* (2016) 22:546–53. doi: 10.1097/MCC.0000000000000356
5. Bellomo R, Kellum JA, Ronco C, Wald R, Martensson J, Maiden M, et al. Acute kidney injury in sepsis. *Intensive Care Med.* (2017) 43:816–28. doi: 10.1007/s00134-017-4755-7
6. Bharadwaj U, Kasembeli MM, Robinson P, Tweardy DJ. Targeting Janus kinases and signal transducer and activator of transcription 3 to treat inflammation, fibrosis, and cancer: rationale, progress, and caution [published correction appears in Pharmacol Rev. 2020;72:605]. *Pharmacol Rev*. (2020) 72:486–526. doi: 10.1124/pr.119.018440
7. Pang M, Ma L, Gong R, Tolbert E, Mao H, Ponnusamy M, et al. A novel STAT3 inhibitor, S3I-201, attenuates renal interstitial fibroblast activation and interstitial fibrosis in obstructive nephropathy. *Kidney Int.* (2010) 78:257–68. doi: 10.1038/ki.2010.154
8. Kulkarni OP, Hartter I, Mulay SR, Hagemann J, Darisipudi MN, Kumar Vr S, et al. Toll-like receptor 4-induced IL-22 accelerates kidney regeneration. *J Am Soc Nephrol.* (2014) 25:978–89. doi: 10.1681/ASN.2013050528
9. Xu MJ, Feng D, Wang H, Guan Y, Yan X, Gao B. IL-22 ameliorates renal ischemia-reperfusion injury by targeting proximal tubule epithelium. *J Am Soc Nephrol.* (2014) 25:967–77. doi: 10.1681/ASN.2013060611
10. Dube S, Matam T, Yen J, Mang HE, Dagher PC, Hato T, et al. Endothelial STAT3 modulates protective mechanisms in a mouse ischemia-reperfusion model of acute kidney injury. *J Immunol Res*. (2017) 2017:4609502. doi: 10.1155/2017/4609502
11. Hilliard KL, Allen E, Traber KE, Kim Y, Wasserman GA, Jones MR, et al. Activation of hepatic STAT3 maintains pulmonary defense during endotoxemia. *Infect Immun.* (2015) 83:4015–27. doi: 10.1128/IAI.00464-15
12. Wang L, Zhao YL, Liu NN, Zhu XS, Liu QQ, Mei HY, et al. Epithelial HO-1/STAT3 affords the protection of subanesthetic isoflurane against zymosan-induced lung injury in mice. *Oncotarget.* (2017) 8:54889–903. doi: 10.18632/oncotarget.18605
13. Kano A, Wolfgang MJ, Gao Q, Jacoby J, Chai GX, Hansen W, et al. Endothelial cells require STAT3 for protection against endotoxin-induced inflammation. *J Exp Med*. (2003) 198:1517–25. doi: 10.1084/jem.20030077
14. Matsukawa A, Takeda K, Kudo S, Maeda T, Kagayama M, Akira S. Aberrant inflammation and lethality to septic peritonitis in mice lacking STAT3 in macrophages and neutrophils. *J Immunol.* (2003) 171:6198–205. doi: 10.4049/jimmunol.171.11.6198
15. Yoo JY, Huso DL, Nathans D, Desiderio S. Specific ablation of Stat3 beta distorts the pattern of Stat3-responsive gene expression and impairs recovery from endotoxic shock. *Cell*. (2002) 108:331–44. doi: 10.1016/S0092-8674(02)00636-0
16. Lee JE, Lee AS, Kim DH, Jung YJ, Lee S, Park BH, et al. Janex-1, a JAK3 inhibitor, ameliorates tumor necrosis factorαinduced expression of cell adhesion molecules and improves myocardial vascular permeability in endotoxemic mice. *Int J Mol Med*. (2012) 29:864–70. doi: 10.3892/ijmm.2012.920
17. Zhang B, Guo Z, Lai S, Chen H. Interference with miR-210 Alleviated renal injury in septic rats by inhibiting JAK-STAT pathway. *Inflammation*. (2020) 43:2156–65. doi: 10.1007/s10753-020-01283-0
18. Zhu H, Wang X, Wang X, Liu B, Yuan Y, Zuo X. Curcumin attenuates inflammation and cell apoptosis through regulating NF-κB and JAK2/STAT3 signaling pathway against acute kidney injury. *Cell Cycle.* (2020) 19:1941–51. doi: 10.1080/15384101.2020.1784599
19. Yun Y, Chen J, Wang X, Li Y, Hu Z, Yang P, et al. Tofacitinib ameliorates lipopolysaccharide-induced acute kidney injury by blocking the JAK-STAT1/STAT3 signaling pathway. *Biomed Res Int*. (2021) 2021:8877056. doi: 10.1155/2021/8877056
20. Zhang H, Sha J, Feng X, Hu X, Chen Y, Li B, et al. Dexmedetomidine ameliorates LPS induced acute lung injury *via* GSK-3β/STAT3-NF-κB signaling pathway in rats. *Int Immunopharmacol.* (2019) 74:105717. doi: 10.1016/j.intimp.2019.105717
21. Xu S, Pan X, Mao L, Pan H, Xu W, Hu Y, et al. Phospho-Tyr705 of STAT3 is a therapeutic target for sepsis through regulating inflammation and coagulation. *Cell Commun Signal.* (2020) 18:104. doi: 10.1186/s12964-020-00603-z
22. Kellum JA, Lameire N, Group KAGW. Diagnosis, evaluation, and management of acute kidney injury: a KDIGO summary (Part 1). *Crit Care.* (2013) 17:204. doi: 10.1186/cc11454
23. Lin HY, Chen Y, Chen YH, Ta AP, Lee HC, MacGregor GR, et al. Tubular mitochondrial AKT1 is activated during ischemia reperfusion injury and has a critical role in predisposition to chronic kidney disease. *Kidney Int.* (2021) 99:870–84. doi: 10.1016/j.kint.2020.10.038
24. Wu CK, Wu CL, Lee TS, Kou YR, Tarng DC. Renal tubular epithelial TRPA1 acts as an oxidative stress sensor to mediate ischemia-reperfusion-induced kidney injury through MAPKs/NF-κB signaling. *Int J Mol Sci*. (2021) 22:2309. doi: 10.3390/ijms22052309
25. Ferrè S, Deng Y, Huen SC, Lu CY, Scherer PE, Igarashi P, et al. Renal tubular cell spliced X-box binding protein 1 (Xbp1s) has a unique role in sepsis-induced acute kidney injury and inflammation. *Kidney Int*. (2019) 96:1359–73. doi: 10.1016/j.kint.2019.06.023
26. Perše M, Večerić-Haler Ž. Cisplatin-induced rodent model of kidney injury: characteristics and challenges. *Biomed Res Int*. (2018) 2018:1462802. doi: 10.1155/2018/1462802
27. Liu Z, Yang D, Gao J, Xiang X, Hu X, Li S, et al. Discovery and validation of miR-452 as an effective biomarker for acute kidney injury in sepsis. *Theranostics*. (2020) 10:11963–75. doi: 10.7150/thno.50093
28. Bagshaw SM. Uchino S,Bellomo R, Morimatsu H, Morgera S, Schetz M, et al. Septic acute kidney injury in critically ill patients: clinical characteristics and outcomes. *Clin J Am Soc Nephrol.* (2007) 2:431–9. doi: 10.2215/CJN.03681106
29. Bagshaw SM, George Bellomo R, Morimatsu H, Morgera S, Schetz M, et al. Early acute kidney injury and sepsis: a multicentre evaluation. *Crit Care*. (2008) 12:R47. doi: 10.1186/cc6863
30. Bagshaw SM, Lapinsky S, Dial S, Arabi Y, Dodek P, Wood G, et al. Acute kidney injury in septic shock: clinical outcomes and impact of duration of hypotension prior to initiation of antimicrobial therapy. *Intensive Care Med.* (2009) 35:871–81. doi: 10.1007/s00134-008-1367-2
31. Leisman DE, Fernandes TD, Bijol V, Abraham MN, Lehman JR, Taylor MD, et al. Impaired angiotensin II type 1 receptor signaling contributes to sepsis-induced acute kidney injury. *Kidney Int.* (2021) 99:148–60. doi: 10.1016/j.kint.2020.07.047
32. Khanna A, English SW, Wang XS, Ham K, Tumlin J, Szerlip H„ et al. Angiotensin II for the treatment of vasodilatory shock. *N Engl J Med.* (2017) 377:419–30.
33. Tumlin JA, Murugan R, Deane AM, Ostermann M, Busse LW, Ham KR, et al. Outcomes in patients with vasodilatory shock and renal replacement therapy treated with intravenous angiotensin II. *Crit Care Med.* (2018) 46:949–57. doi: 10.1097/CCM.0000000000003092
34. Bellomo R, Forni LG, Busse LW, McCurdy MT, Ham KR, Boldt DW, et al. Renin and survival in patients given angiotensin II for catecholamine-resistant vasodilatory shock. A clinical trial. *Am J Respir Crit Care Med*. (2020) 202:1253–61. doi: 10.1164/rccm.201911-2172OC
35. Gomez H, Ince C, De Backer D, Pickkers P, Payen D, Hotchkiss J, et al. A unified theory of sepsis-induced acute kidney injury: inflammation, microcirculatory dysfunction, bioenergetics, and the tubular cell adaptation to injury. *Shock*. (2014) 41:3–11. doi: 10.1097/SHK.0000000000000052
36. Abdel-Fattah MM, Elgendy ANAM, Mohamed WR. Xanthenone, ACE2 activator, counteracted gentamicin-induced nephrotoxicity in rats: Impact on oxidative stress and ACE2/Ang-(1-7) signaling. *Life Sci.* (2021) 275:119387. doi: 10.1016/j.lfs.2021.119387
37. Chawla LS, Chen S, Bellomo R, Tidmarsh GF. Angiotensin converting enzyme defects in shock: implications for future therapy. *Crit Care.* (2018) 22:274. doi: 10.1186/s13054-018-2202-y

38. Iskander KN, Craciun FL, Stepien DM, Duffy ER, Kim J, Moitra R, et al. Cecal ligation and puncture-induced murine sepsis does not cause lung injury. *Crit Care Med.* (2013) 41:159–70. doi: 10.1097/CCM.0b013e3182676322
39. Zingarelli B, Coopersmith CM, Drechsler S, Efron P, Marshall JC, Moldawer L, et al. Part I: Minimum Quality Threshold in Preclinical Sepsis Studies (MQTiPSS) for study design and humane modeling endpoints. *Shock.* (2019) 51:10–22. doi: 10.1097/SHK.0000000000001243
40. Dejager L, Pinheiro I, Dejonckheere E, Libert C. Cecal ligation and puncture: the gold standard model for polymicrobial sepsis? *Trends Microbiol.* (2011) 19:198–208. doi: 10.1016/j.tim.2011.01.001
41. Libert C, Ayala A, Bauer M, Cavaillon JM, Deutschman C, Frostell C, et al. Part II: Minimum Quality Threshold in Preclinical Sepsis Studies (MQTiPSS) for types of infections and organ dysfunction endpoints. *Shock.* (2019) 51:23–32. doi: 10.1097/SHK.0000000000001242
42. Remick DG, Newcomb DE, Bolgos GL, Call DR. Comparison of the mortality and inflammatory response of two models of sepsis: lipopolysaccharide vs. cecal ligation and puncture. *Shock.* (2000) 13:110–6. doi: 10.1097/00024382-200013020-00004
43. Miyaji T, Hu X, Yuen PS, Muramatsu Y, Iyer S, Hewitt SM. at al. Ethyl pyruvate decreases sepsis-induced acute renal failure and multiple organ damage in aged mice. *Kidney Int.* (2003) 64:1620–31. doi: 10.1046/j.1523-1755.2003.00268.x
44. Leisman DE, Fernandes TD, Bijol V, Leelahavanichkul A, Yasuda H, Kim SM, et al. AP214, an analogue of alpha-melanocyte-stimulating hormone, ameliorates sepsis-induced acute kidney injury and mortality. *Kidney Int.* (2008) 73:1266–74. doi: 10.1038/ki.2008.97

Conflict of Interest: The authors declare that the research was conducted in the absence of any commercial or financial relationships that could be construed as a potential conflict of interest.

Publisher's Note: All claims expressed in this article are solely those of the authors and do not necessarily represent those of their affiliated organizations, or those of the publisher, the editors and the reviewers. Any product that may be evaluated in this article, or claim that may be made by its manufacturer, is not guaranteed or endorsed by the publisher.

frontiers | Frontiers in Medicine

ORIGINAL RESEARCH
published: 23 June 2022
doi: 10.3389/fmed.2022.904286

The Severity of Acute Kidney and Lung Injuries Induced by Cecal Ligation and Puncture Is Attenuated by Menthol: Role of Proliferating Cell Nuclear Antigen and Apoptotic Markers

Aliaa Anter[1†], Al-Shaimaa F. Ahmed[1†], Asmaa S. A. Hammad[1], Waleed Hassan Almalki[2], Sara Mohamed Naguib Abdel Hafez[3], AlShaimaa W. Kasem[4], Mohamed A. El-Moselhy[1,5], Mohammad W. Alrabia[6], Ahmed R. N. Ibrahim[7,8] and Mahmoud El-Daly[1]*

[1] Department of Pharmacology and Toxicology, Faculty of Pharmacy, Minia University, Minya, Egypt, [2] Department of Pharmacology and Toxicology, Umm Al-Qura University, Makkah, Saudi Arabia, [3] Department of Histology and Cell Biology, Faculty of Medicine, Minia University, Minya, Egypt, [4] Department of Pathology, Faculty of Medicine, Minia University, Minya, Egypt, [5] Department of Clinical Pharmacy and Pharmacology, Ibn Sina National College for Medical Studies, Jeddah, Saudi Arabia, [6] Department of Microbiology and Medical Parasitology, Faculty of Medicine, King Abdulaziz University, Jeddah, Saudi Arabia, [7] Department of Clinical Pharmacy, College of Pharmacy, King Khalid University, Abha, Saudi Arabia, [8] Department of Biochemistry, Faculty of Pharmacy, Minia University, Minya, Egypt

OPEN ACCESS

Edited by:
Alessandra Stasi, University of Bari Aldo Moro, Italy

Reviewed by:
Davide Medica, University of Eastern Piedmont, Italy
Gianvito Caggiano, University of Bari Aldo Moro, Italy
Maria Teresa Cimmarusti, University of Bari Aldo Moro, Italy

***Correspondence:**
Al-Shaimaa F. Ahmed
Shaimaa_faissal@minia.edu.eg

† These authors have contributed equally to this work

Specialty section:
This article was submitted to Nephrology, a section of the journal Frontiers in Medicine

Received: *25 March 2022*
Accepted: *16 May 2022*
Published: *23 June 2022*

Citation:
Anter A, Ahmed AF, Hammad ASA, Almalki WH, Abdel Hafez SMN, Kasem AW, El-Moselhy MA, Alrabia MW, Ibrahim ARN and El-Daly M (2022) The Severity of Acute Kidney and Lung Injuries Induced by Cecal Ligation and Puncture Is Attenuated by Menthol: Role of Proliferating Cell Nuclear Antigen and Apoptotic Markers. Front. Med. 9:904286. doi: 10.3389/fmed.2022.904286

Objective: Sepsis-induced acute lung injury (ALI) and acute kidney injury (AKI) are major causes of mortality. Menthol is a natural compound that has anti-inflammatory and antioxidative actions. Since exaggerated inflammatory and oxidative stress are characteristics of sepsis, the aim of this study was to evaluate the effect of menthol against sepsis-induced mortality, ALI, and AKI.

Methods: The cecal ligation and puncture (CLP) procedure was employed as a model of sepsis. Rats were grouped into sham, sham-Menthol, CLP, and CLP-Menthol (100 mg/kg, p.o).

Key Findings: A survival study showed that menthol enhanced the survival after sepsis from 0% in septic group to 30%. Septic rats developed histological evidence of ALI and AKI. Menthol markedly suppressed sepsis induced elevation of tissue TNF-a, ameliorated sepsis-induced cleavage of caspase-3 and restored the antiapoptotic marker Bcl2.

Significance: We introduced a role of the proliferating cell nuclear antigen (PCNA) in these tissues with a possible link to the damage induced by sepsis. PCNA level was markedly reduced in septic animals and menthol ameliorated this effect. Our data provide novel evidence that menthol protects against organ damage and decreases mortality in experimental sepsis.

Keywords: menthol, cecal ligation and puncture, AKI, ALI, PCNA

INTRODUCTION

Sepsis is a complex and serious complication in postoperative critical care patients, mainly because of infection. It is a major cause of ICU patient morbidity as well as mortality (1, 2). The condition is characterized by multiple organ damage, with the kidneys and the lungs being the most vulnerable organs (3). About 50% of patients with sepsis may experience acute kidney (AKI) and lung injuries (ALI). Despite all improved and labored treatment strategies to medicate sepsis patients, the mortality rate for patients with AKI and ALI is at alarming levels (up to 70%) (4, 5). Thus, the research aiming to identify novel therapies and prevention approaches, which should be both effective and safe, is a pressing need for sepsis management.

The underlying mechanisms of sepsis and its complications are not completely identified. During the acute phase of sepsis, microbial components trigger the immune and inflammatory cascades. However, the exaggerated release of cytokines during the acute stage of sepsis leads to multiple tissue damage. Sepsis-associated hemodynamic changes serve an initial function in counteracting foreign organisms tissue infiltration through inhibition of vascular tone and boosting the coagulation cascade (6, 7). This increased endothelial permeability during sepsis enhances infiltration of immune cells to the site of injury. This leads to intensive vascular leakage which insults the host tissues through excessive loss of intracellular plasma volume, subsequent hypotension, and decreased perfusion to vital organs. Thus, the host response becomes pathoadaptive and imposes a considerable threat to the host (8). Increased tissue infiltration by activated immune cells provokes tissue inflammation and excessive generation of reactive oxygen species (ROS), which are hallmarks of sepsis, and the associated multiple organ damage (7, 9). ROS-induced damage of the mitochondrial membrane and its altered permeability activates the mitochondria apoptotic cascade (10, 11). In sepsis, increased levels of TNF-α activate the external apoptotic pathways, which involves the activation of death receptors (12). Activated apical caspase-9 and -8, from either pathway, activate the effector caspases (caspases-3, -6, and -7). Intriguingly, activated caspase-3 mediates a feedback activation of caspase-8 and -9. Thus, besides its function as an effector caspase, caspase-3 maximizes the activation of apical caspases and the interaction between the two major apoptotic pathways (13). On the other hand, Bcl2 is an antiapoptotic protein, which maintains the permeability of the mitochondrial membrane and modulates cytochrome c release (14). Previous studies showed that the protein level of the proliferating cell nuclear antigen (PCNA) positively correlates with the regenerative capacity of tissues (15). PCNA interferes with apoptosis by binding procaspases, which prevents their activation and inhibits apoptosis (16).

Phytochemicals are promising therapeutic candidates for many disease conditions because of their antioxidant, anti-inflammatory, and immune system modulatory effects. Menthol, the main volatile ingredient of peppermint oil, has long been used in traditional medicine for its antispasmodic and carminative properties. Previous research highlighted the analgesic (17), antitussive (18), immune-modulatory (19), and the anti-apoptotic actions (20) of menthol. The anti-inflammatory and antioxidative (19–23) effects are of special importance to the current study. Besides, menthol is an ingredient of many pharmaceutical preparations effective in the management of respiratory diseases such as sinusitis, allergic rhinitis, and bronchitis (24). A recent study illustrated that menthol alleviated cigarette smoke-induced lung injury *via* suppression of oxidative stress and inflammation (25). Similarly, other studies reported menthol-induced liver and kidney protection against acute injury induced by various chemical insults (26, 27). Like the work by Liu et al. (25), the results of these studies showed that antioxidative and anti-inflammatory mechanisms are involved in menthol-induced protection (26, 27). In addition, menthol activates transient receptor potential (TRP) melastatin 8 (TRPM8) (28), which mediates its analgesic effects (29). On the other hand, pharmacological activation of TRPM8 was anti-inflammatory in a mouse model of colitis (30). The safety of menthol is well established, in an early study, oral administration of menthol up 667 mg/kg/day was not associated with any observed adverse effects (31). In another study, the plasma concentration of menthol was reported to reach 20 μM within 1 h in rats that have been administered 400 mg of menthol/kg body weight i.p (32). All menthol isomers are well absorbed after oral and are excreted as glucuronides. In rats, an extensive enterohepatic circulation is reported. For all isomers of menthol, a very low acute oral toxicity with LD_{50} values normally greater than 2,000 mg/kg bw has been reported (33).

Since exaggerated inflammatory and deregulated immune responses and increased oxidative stress are hallmarks of sepsis, we hypothesized that menthol would improve sepsis outcomes *via* its inflammatory and antioxidant properties. Thus, this study aimed to test the effect of menthol on the survival and acute organ injury in the kidney and lungs of experimentally induced septic animals. We evaluated the underlying mechanisms of such protective effects of menthol.

MATERIALS AND METHODS

Animals and Experimental Design

Female Wistar rats, weighing between 250–300 g, were obtained from the animal care center of Nahda University at Beni Suef (NUB), Beni-Suef, Egypt. The rats were left for 1 week for acclimatization and kept at constant temperature and under a 12 h light-dark cycle with free access to food and water until the day of the experiment. This study was approved in January 2020 by The Commission on the Ethics of Scientific Research, Faculty of Pharmacy, Minia University (Approval Number: ES02/2020).

Sepsis was induced by cecal ligation and puncture procedure (CLP) as described previously (34). Briefly, animals were anesthetized by a mixture of ketamine (50 mg/kg) and xylazine (10 mg/kg), and a 2-cm ventral midline abdominal incision in the lower left quadrant of the body was performed. The cecum was exposed, ligated just below the ileocecal valve with a surgical 0.3-mm silk thread, and punctured twice with an 18-gauge needle. The punctured cecum was massaged gently to squeeze a small amount of the bowel content and placed back

in the abdominal cavity, and the wounded abdominal wall was then sutured. Immediately after the operation, normal saline (3 mL/100 g) was injected subcutaneously. Sham-operated rats were subjected to all the previous steps except for the cecum ligation and puncture. The study groups were: Sham (vehicle-treated), Sham-treated with menthol (100 mg/kg, p.o) (35), CLP (vehicle-treated) and CLP-treated with menthol (100 mg/kg, p.o). Animals received either vehicle (distilled water) or menthol (as a suspension in distilled water) treatments 2 h after the CLP procedure. Menthol was obtained from Sigma-Aldrich Inc. (Cat. No. 63670). Since our study was the first to examine the effect of menthol on an animal model of sepsis, the dose, route and timing of administration were all based on several pilot studies on the effect of menthol on the survival of animals after CLP. The oral route of 100 mg/kg given to rats 2 h after CLP gave the best results in terms of survival. As previously stated in the introduction section, menthol administered by the oral route exhibits high bioavailability and safety (36).

For the survival study, separate groups were applied ($n = 10$/group) from the other study where the rats were observed for 10 days to report mortality. For the mechanistic study, a total of 28 rats were used, sham ($n = 6$), sham-menthol ($n = 6$), CLP ($n = 10$) and CLP-menthol ($n = 6$). Twenty-four hours after sepsis induction, all rats were sacrificed by exsanguination after an i.p injection of thiopental sodium (50 mg/kg).

Assessment of Total Leukocytic Cell Counts and Total Protein in the Bronchoalveolar Lavage Fluid

The bronchoalveolar lavage fluid (BALF) was obtained by washing the airways three times with 0.5 ml of saline using a tracheal cannula (37). The BALF was used for the determination of total protein and WBC count. Briefly, after centrifugation (1,000 rpm, 10 min at 4°C) of the BALF, the cell pellet was resuspended in 0.5 ml PBS and the total cells were counted using a hemocytometer. Total protein was measured in the supernatant of the BALF based on its reaction with copper ions that produces a blue-violet color proportional to the concentration of the protein in the sample using a commercial kit (BioMed, Egypt).

Assessment of Serum Creatinine

Blood was collected by exsanguination from thiopental-sedated animals and centrifuged after 10 min to obtain serum samples. Creatinine was determined according to the method described by **Schirmeister** (38) using a commercial kit from Biodiagnostic, Egypt.

Histopathological Examination

Specimens from the left lung and kidney tissues were immediately cut into small pieces, fixed in 10% formol saline, and processed to get 5 μm thick paraffin sections for Hematoxylin and Eosin (H & E) study (39). Slides stained with H & E were microscopically analyzed by light microscopy (Olympus CX 23L). Blind pathological assessment was carried out on lung and kidney tissues from each group ($n = 6$). The lung injury was graded on a scale of 0–4 (0, absent; 1, light; 2, moderate; 3, strong; 4, intense) for alveolar wall thickness, intra-alveolar edema and congestion, and damaged membranes. The lung injury score was calculated as the mean of the scores for the separate parameters. Kidney injury was assessed for the percentages of glomerular damage, mesangial cells proliferation, tubular damage, tubular edema, and congestion that were scored as follows: 0 = none, 1 = 0–20%, 2 = 20–50%, 3 = 50–70%, 4 = more than 70%. For each animal, at least 10 fields from the lung or kidney sections were examined, and the average scores were recorded (40).

Determination of Oxidative Stress Parameters in Lung and Kidney Tissue Homogenates

Tissue samples of the right lung and kidney were homogenized to assess the different biochemical markers. The content of the marker of lipid peroxidation malondialdehyde (MDA) was determined colorimetrically in lung and kidney tissue homogenates according to the method of Buege and Aust (41). The concentration of total nitrates was colorimetrically measured after reducing nitrates in the samples to nitrites by a cadmium reagent, and the ability of nitrite ions to form a colored azo-dye in the presence of the Griess reagents as previously described (42).

GSH concentration was measured colorimetrically according to the method described by Rifai (43). The activity of SOD was determined according to a previously described method (44) using a commercially available kit (Biodiagnostic, Egypt).

Immunohistochemical Assessment of Lung and Kidney Caspase-3, Bcl-2, Proliferating Cell Nuclear Antigen, and TNF-α

Paraffin-embedded sections of the lung and kidney specimens were processed for the immunohistochemical study (45). Immunohistochemical staining was carried out for cleaved caspase-3, B-cell lymphoma 2 (Bcl-2) protein, proliferating cell nuclear antigen (PCNA), and TNF-α using rabbit monoclonal anti-caspase-3 (catalog number ab32042, Abcam, Cambridge, United Kingdom), rabbit polyclonal anti-Bcl-2 (catalog number ab194583, Abcam, Cambridge, United Kingdom), mouse monoclonal anti-PCNA (catalog number ab29, Abcam, Cambridge, United Kingdom), and rabbit monoclonal anti-TNF-α (catalog number EPR21753-109, Abcam, Cambridge, United Kingdom), respectively. To ensure the specificity of the antibody reaction, a control experiment was performed following the same steps, but without the addition of the primary antibody. Positive controls samples were human vascular endothelial cells for caspase-3, human lung cancer for Bcl-2, liver tissue for PCNA, and rat splenocytes for TNF-α .

Image Capture

The photography was performed in the Histology and Cell Biology Department, Faculty of Medicine, Minia University. An Olympus (U.TV0.5XC-3) light microscope with a digital camera was used in this experiment. Photomicrographs were assessed by Adobe Photoshop.

Morphometric Study

Ten random non-overlapping fields for each slide from each group from lung and kidney tissues were selected and imaged using power X400 (46, 47). The mean surface area fraction of anti-cleaved caspase-3, PCNA, Bcl2, and TNF-α immuno-positive cells were measured using ImageJ software (version 1.51k, Wayne Rasband, National Institutes of Health, United States) for image analysis.

Statistical Analysis

The GraphPad Prism 6 (version 6.0; San Diego, CA, United States) software was used for statistical analyses. Data are expressed as mean ± SEM. The difference between means of different groups was analyzed using one-way analysis of variance (ANOVA), followed by the Tukey-Kramer post-ANOVA test for multiple comparisons. Animal survival data were analyzed using the Log-rank Mantel-Cox test. The results were considered statistically significant if the p-values were < 0.05. The correlation between parameters related to kidney injury or lung injury was determined by calculation of the Pearson correlation coefficient, r. The correlation is weak when $r < |0.3|$, moderate when $|0.3| \leq r \leq |0.7|$. The correlation is considered strong when $r > |0.7|$.

RESULTS

Effect of Menthol on Sepsis-Induced Mortality

Rats in different groups (sham, sham-Menthol, CLP, or CLP-Menthol) were monitored every 24 h for 10 days after induction of sepsis. **Figure 1** shows the survival rate of different groups. All rats in the CLP group died within 7 days after the surgical induction of sepsis. In contrast, Menthol (100 mg/kg) treatment reduced the overall mortality by 40% ($p < 0.05$). In addition, all septic animals in the menthol-treated group survived the first 24 h after surgery, while the vehicle-treated CLP rats showed 30% mortality. After 2 days of sepsis induction, the vehicle-treated CLP group showed higher mortality (70%) than the menthol-treated septic rats (40%). Three days after surgery, the menthol-treated group showed no more mortality (40% survival). Both the sham-operated or the sham-operated menthol-treated groups did not show any mortality. These results show the protective role of menthol treatment against mortality in septic rats.

Protective Effect of Menthol on Sepsis-Induced Acute Lung Injury

We assessed the protective effect of menthol on lung tissues after induction of sepsis by histopathological examination of paraffin-fixed sections, and by determination of the total protein concentration and WBC count in BALF. H&E-stained lung sections from the sham groups showed normal alveolar spaces **(arrow)** separated by non-congested vascular spaces **(arrowhead)** as shown in **Figure 2A**. The histological examination of vehicle-treated CLP lung tissues revealed thickened alveolar spaces with alveolar wall damage **(arrow)** separated by dilated and congested vascular spaces (**arrowhead).** Sections obtained from the menthol-treated CLP group showed normal alveolar spaces with intact alveolar walls **(arrow)** separated by mild congested vascular spaces (**arrowhead).** The lung injury scores increased markedly in the CLP group in comparison with the menthol-treated CLP rats, which showed significantly decreased lung injury scores (**Figure 2B**).

Moreover, the total protein content and the total number of WBCs were significantly higher in the BALF collected from septic rats if compared with sham groups, while the treatment of CLP animals with menthol resulted a significant ($p < 0.05$) reduction of both total protein and the count of blood cells in collected BALF (**Figures 2C,D**).

Protective Effect of Menthol on Sepsis-Induced Acute Kidney Injury

The kidney tissues from sham or sham-menthol-treated groups showed normal histological appearance, normal interstitial tissue, and lack of congestion or inflammatory infiltration upon histological examination (**Figure 3A**). The CLP group showed moderately damaged renal glomeruli,

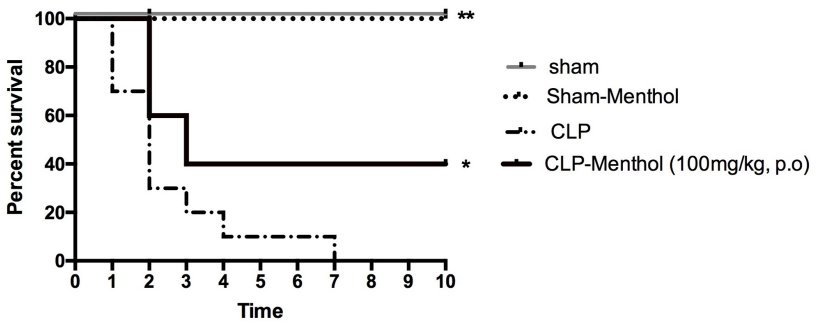

FIGURE 1 | Effect of Menthol treatment on sepsis-induced mortality. Surgical induction of sepsis by the cecal ligation and puncture (CLP) procedure resulted in 100% mortality within 7 days ($n = 10$). Menthol treatment (100 mg/kg, p.o), 2 h after CLP, significantly improved the survival of septic rats ($n = 10$). Sham or sham menthol-treated rats ($n = 10$) showed no mortality. Survival analysis was carried out using the Log-rank Mantel-Cox test. * and ** Significantly different from the vehicle-treated CLP group at $p < 0.05$ and $p < 0.01$, respectively.

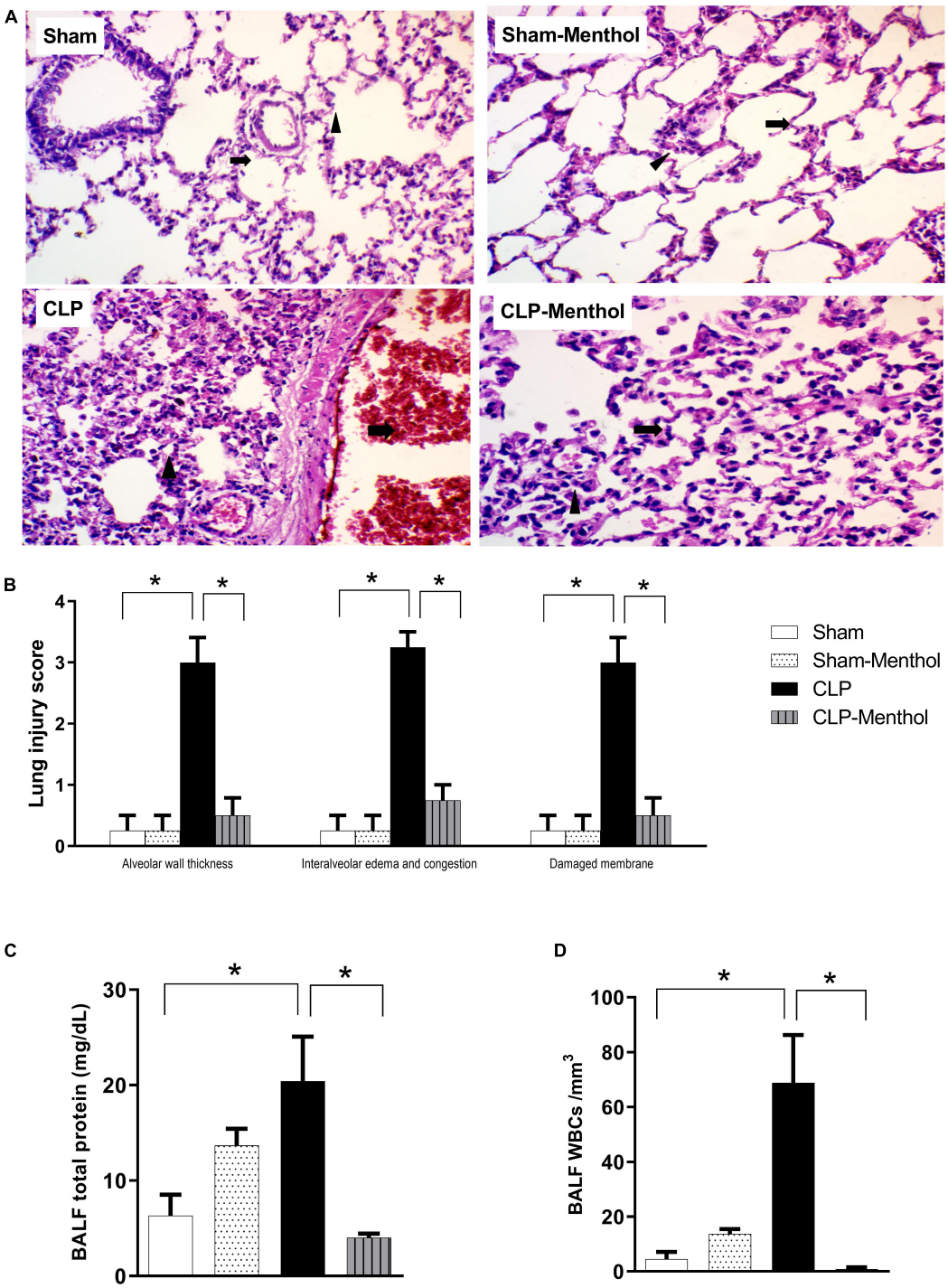

FIGURE 2 | Effect of menthol on sepsis-induced acute lung injury. Sepsis was induced by CLP under general anesthesia as described under the "Materials and Methods" section. Animals were killed after 24 h of CLP and the lung injury was assessed by histological examination of H&E-stained (200×) sections **(A,B)** and by determination of the protein and total WBCs in the bronchoalveolar lavage (BALF; **C,D**) in all groups (n = 6 per group). **(A)** Representative photomicrographs showing that menthol treatment attenuated the histopathological changes induced by sepsis in the lung tissue. The sham groups (Sham and Sham-Menthol) showed normal lung alveolar spaces (arrow) separated by non-congested vascular spaces (arrowhead). The lung tissue of the vehicle-treated CLP group (CLP) showed thickened alveolar spaces with alveolar wall damage (arrow) separated by dilated and congested vascular spaces (arrowhead). Lung tissues from the menthol-treated septic rats (CLP-Menthol) showed normal alveolar spaces with intact alveolar wall (arrow) separated by mild congested vascular spaces (arrowhead). Summary of the mean values of the combined lung injury scores (at least 10 fields per section from 6 animals) of different groups is shown **(B)**. The total protein content **(C)** and the total leucocyte count **(D)** in BALF of different groups (n = 6) are also shown. Data represent the mean ± SEM of 6 independent observations. Data were analyzed by one-way ANOVA followed by the Tukey-Kramer post- test for multiple comparisons. *Significantly different at $p < 0.05$ compared to the CLP group.

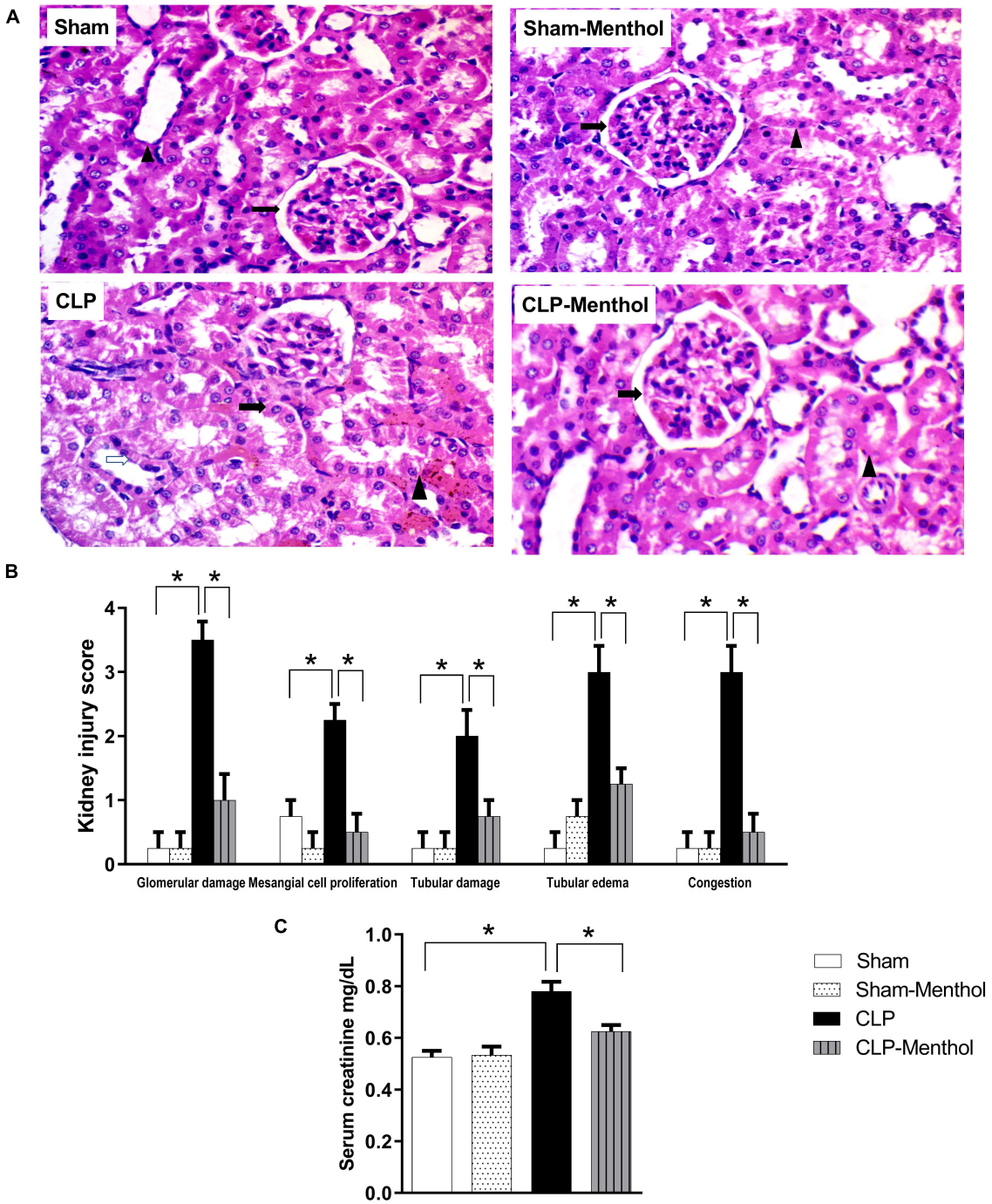

FIGURE 3 | Effect of menthol treatment on sepsis-induced acute kidney injury. Sepsis was induced by CLP under general anesthesia as described under the "Materials and Methods" section. Animals were killed after 24 h of CLP and the kidney injury was assessed by histological examination of H&E-stained (200X) 5 μm sections **(A,B)** and by determination of serum creatinine concentration **(C)** in all groups (n = 6 per group). **(A)** Representative photomicrographs showing that menthol treatment attenuated the histopathological changes induced by sepsis in kidney tissues (H&E stain, 200X). The sham groups (Sham and Sham-Menthol) showed normal histological appearance with normal interstitial tissue without congestion or inflammatory cell infiltration. The glomeruli of the vehicle-treated CLP group (CLP) showed moderate damage and obliterated Bowman's spaces. These sections showed proliferated mesangial cells (arrow) surrounded by tubules with focal areas of tubular damage (white arrow), tubular edema, compressed intratubular vascular spaces (arrowhead) and congested interstitial tissue. Menthol treated group showed renal glomerulus with normal histological appearance (arrow) surrounded by tubules (arrowhead) with normal interstitial tissue without congestion or inflammatory infiltrates. **(B)** Bar charts showing analysis of the mean values of combined kidney injury scores (at least 10 fields per section from 6 animals per group). **(C)** Bar graph showing the serum creatinine data from the different groups. All data represent the mean ± SEM of 6 independent observations. Data were analyzed by one-way ANOVA followed by the Tukey-Kramer post- test for multiple comparisons. *Significantly different at $p < 0.05$ compared to the CLP group.

obliterated Bowman's spaces, proliferated mesangial cells (**arrow**) surrounded by tubules with focal areas of tubular damage **(white arrow),** tubular edema with compressed intratubular vascular spaces (**arrowhead**), and congested interstitial tissues. On the other hand, sections from the menthol-treated CLP group showed normal renal glomeruli (**arrow**) surrounded by tubules (**arrowhead**) with normal interstitial tissue, without congestion or inflammatory infiltrates (**Figure 3A**). Kidney injury scores were obviously increased in the vehicle-treated CLP group, while administration of menthol in CLP rats markedly reduced these scores (**Figure 3B**).

To evaluate kidney function, the serum creatinine level was measured in all groups. Induction of sepsis by the CLP procedure significantly ($p < 0.05$) increased the serum creatinine level compared with the sham group, while menthol treatment after CLP surgery significantly ($p < 0.05$) abolished this increase (**Figure 3C**).

Menthol Reduces Oxidative and Improves Antioxidant Activity in Lung and Kidney Tissues of Septic Animals

To evaluate the role of menthol on sepsis-induced increased oxidative stress in the lung and renal tissues, we measured the levels of lipid peroxidation, total nitrate/nitrite, SOD, and GSH (**Figures 4**, **5**). The results revealed that induction of sepsis in the CLP model elevated MDA and total nitrate/nitrite levels in both lung and kidney homogenates. Sepsis induction significantly decreased the levels of the measured antioxidant markers; SOD and GSH. Administration of menthol 2 h after CLP induction improved the antioxidant

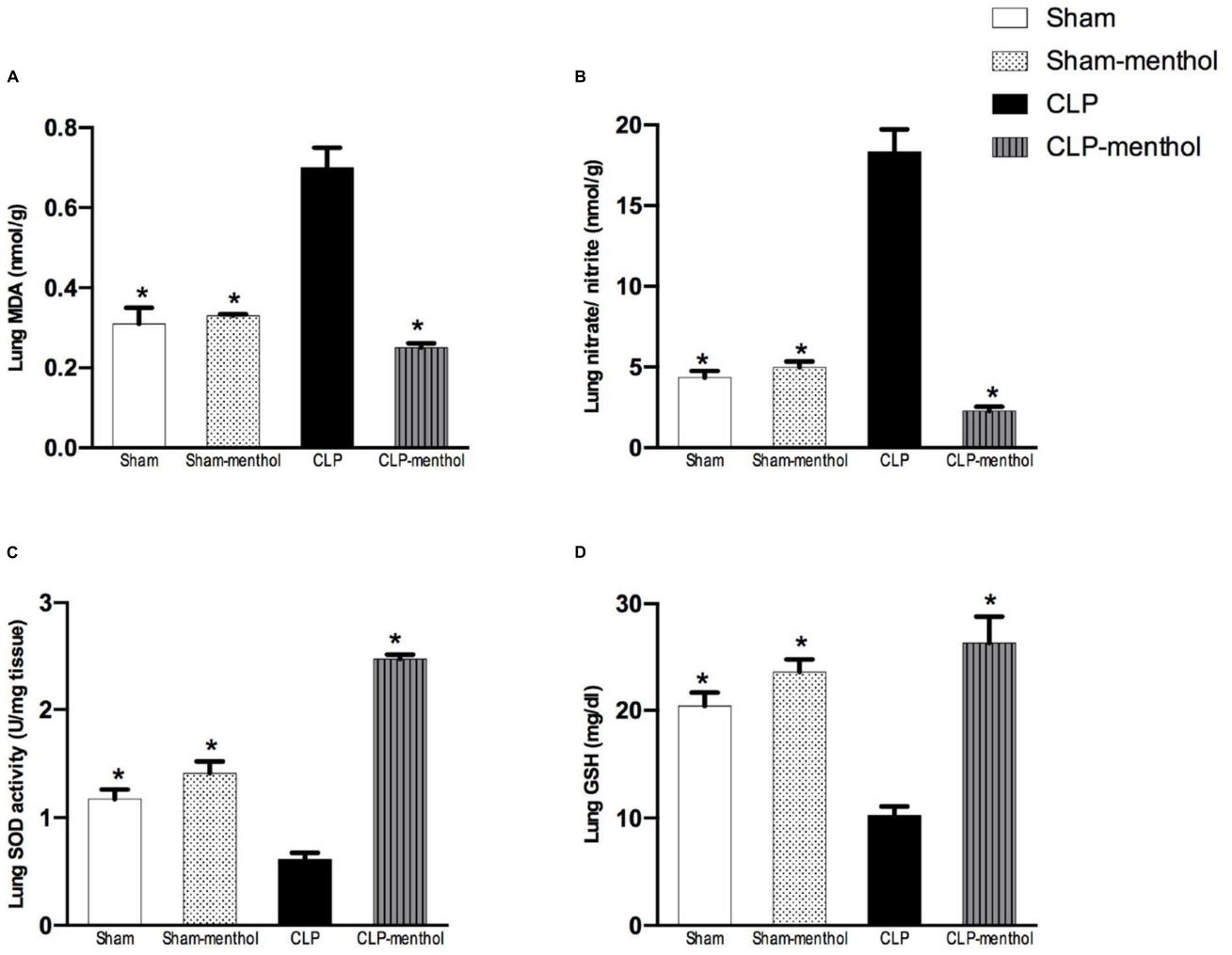

FIGURE 4 | Menthol treatment improves pulmonary oxidative stress status and inhibits the sepsis-induced reduction of the antioxidant capacity of lung tissue. Menthol treatment of CLP rats ameliorated CLP-induced oxidative imbalance in lung tissues as shown with the results of **(A)**, malondialdehyde (MDA), **(B)** nitrate/nitrite, **(C)** activity of superoxide dismutase (SOD) and **(D)**, reduced glutathione (GSH). Menthol (100 mg/kg, p.o), 2 h after surgery. $n = 6$ per group. Data were analyzed by one-way ANOVA followed by Tukey's post-test for multiple comparison. Data represent the mean ± SEM of 6 independent observations. *Significantly different from the CLP group at $p < 0.05$.

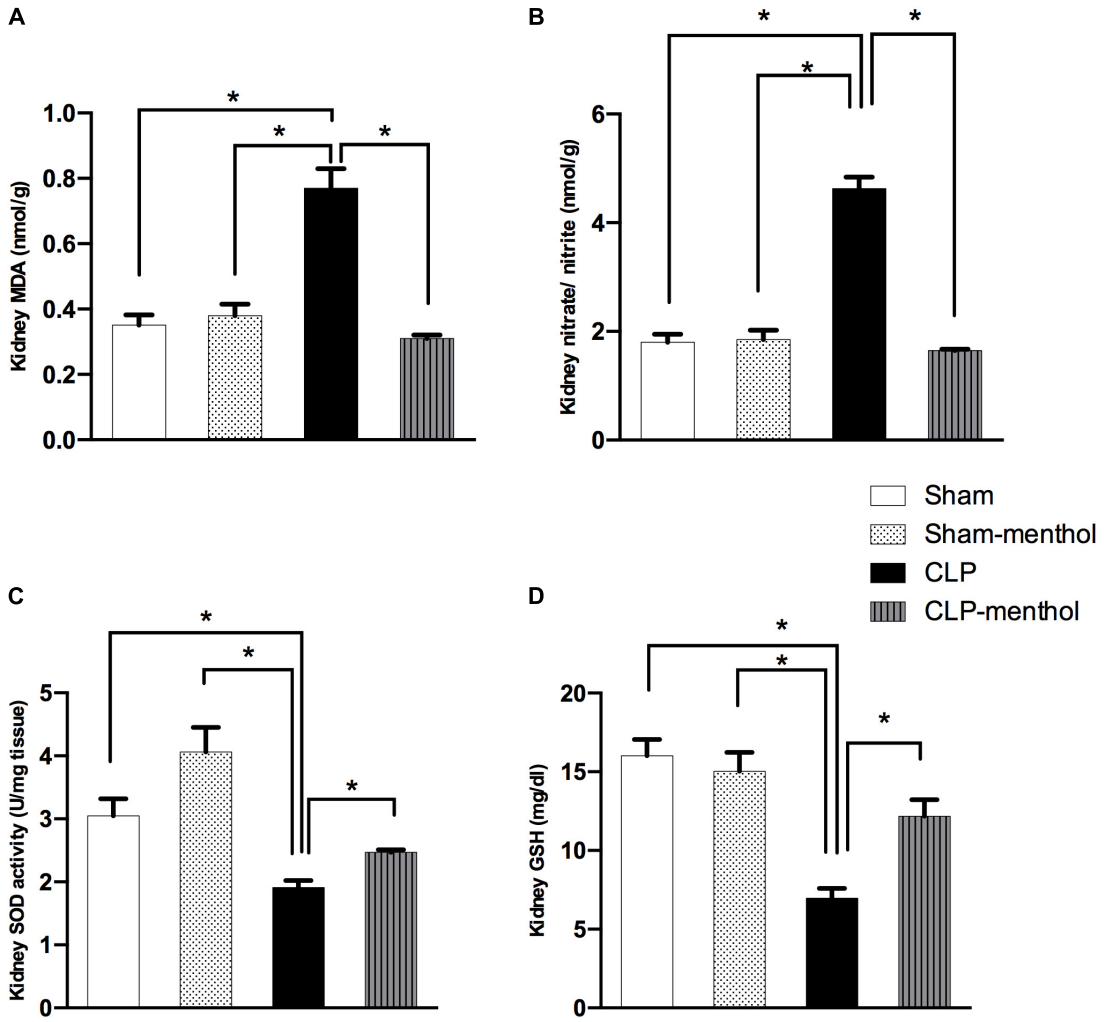

FIGURE 5 | Menthol treatment attenuates renal oxidative stress and restores the antioxidant capacity of renal tissue. Cecal ligation and puncture enhanced oxidative stress which is normalized by menthol (100 mg/kg, p.o), 2 h after surgery as shown with the results of **(A)**, malondialdehyde (MDA), **(B)** nitrate/nitrite, **(C)** activity of superoxide dismutase (SOD) and **(D)**, reduced glutathione (GSH). $n = 6$ per group. Data were analyzed by one-way ANOVA followed by Tukey-Kramer post-test for multiple comparison. Data represent the mean ± SEM of 6 independent observations. *Significantly different from the CLP group at $p < 0.05$.

capacity in comparison with the vehicle-treated CLP group. The tissues from the CLP-menthol group manifested significant reductions in MDA and total nitrate/nitrite levels in the lung and kidney homogenates, besides the restoration of sepsis-induced impairment of the tissue antioxidant capacity.

Menthol Reduces Sepsis-Induced TNF-α Expression in Lung and Kidney Tissues

Both lung and renal tissues in the sham groups (**Figures 6A,C**) showed weak TNF-α immunostaining within the alveoli of the lung tissue, the renal glomeruli, or tubules. The vehicle-treated CLP group exhibited a significant ($p < 0.05$) increase in both the number and immune intensity of immunoreactive cells within the lining cells of the alveoli or glomerular or tubular cells if compared with the sham groups. Additionally, as shown in **Figures 6B,D**, menthol treatment after CLP significantly attenuated the increase in the number of TNF-α immunoreactive cells in the previously mentioned areas compared to the CLP group.

Menthol Attenuates Sepsis-Induced Apoptosis in Lung and Kidney Tissues

This study determined the immunoreactivity of the lung and kidney tissues to caspase-3 as a marker of cellular apoptosis. Data in **Figures 7A,C** show that both lung and renal tissues in the sham groups (Sham and Sham-Menthol) showed faint caspase-3 immunostaining; either cytoplasmic and/or nuclear, within the cells lining the alveoli of lung tissue, in renal glomerular, or tubular cells. Samples from septic rats exhibited a clear increase in the number

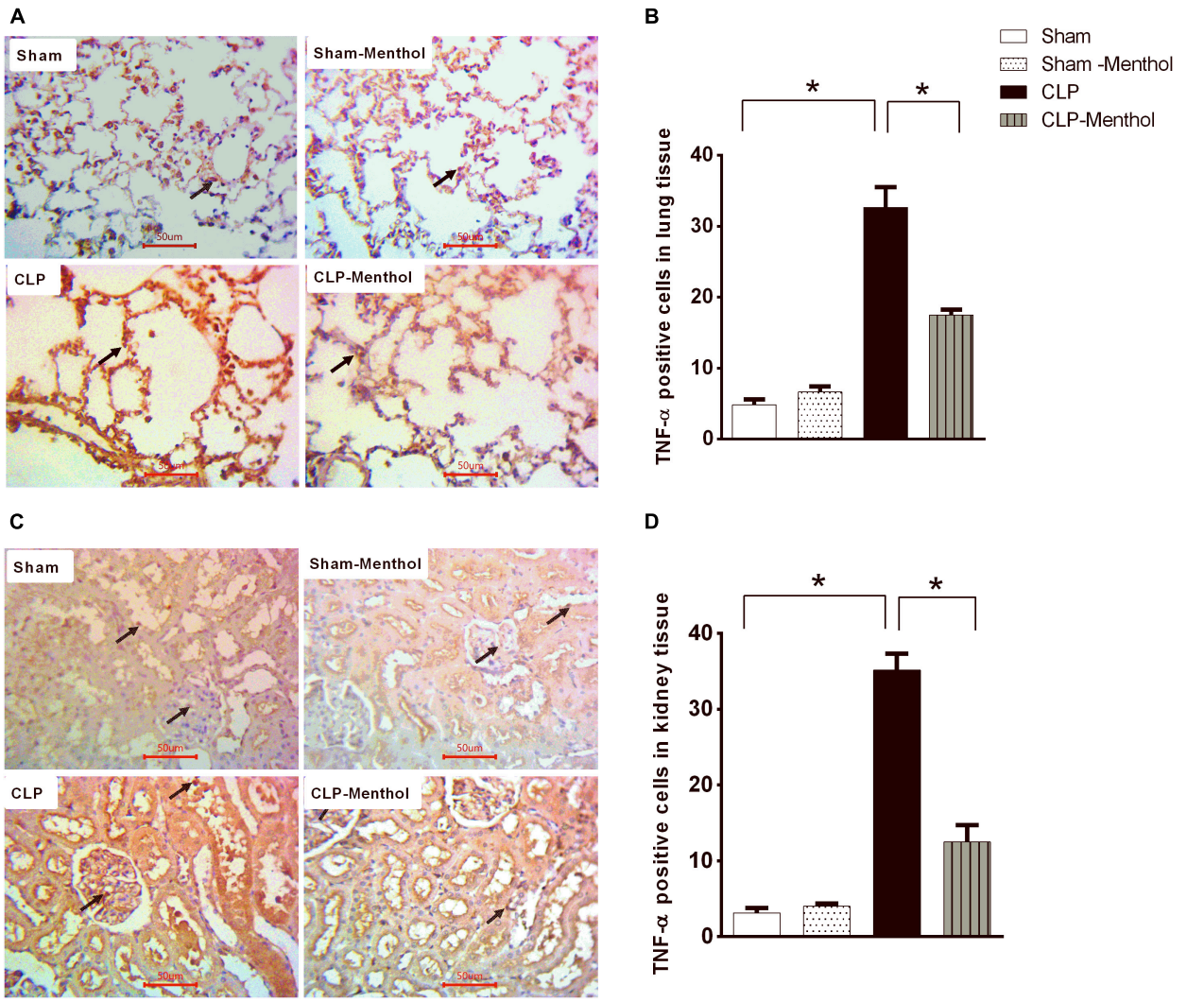

FIGURE 6 | Effect of Menthol on TNF-α expression in the lung and kidney tissue of septic rats. Immunohistochemical staining of TNF-α in paraffin-embedded lung **(A)** and kidney **(C)** sections was carried out as described under the "Materials and Methods" section. Rabbit monoclonal anti-TNF-α (cat. # EPR21753-109, Abcam, Cambridge, United Kingdom) was used to probe tissue TNF-α. Ten random fields per slide from each group ($n = 6$) were selected and imaged (400X). The mean surface area fraction of TNF-α immuno-positive cells was measured using ImageJ software. Representative photomicrographs **(A)** showing TNF-α immunoreactivity in lung tissues. Bar charts **(B)** show semi-quantitative analysis of data in A from sections of the sham, sham-Menthol, CLP, and CLP-Menthol groups. TNF-α immunoreactivity in kidney sections **(C)** from all groups are semi-quantitatively analyzed in **(D)**. Data represent the mean ± SEM of 6 independent observations. Data were analyzed by one-way ANOVA followed by the Tukey-Kramer post-test for multiple comparisons. *Significantly different at $p < 0.05$ compared to the CLP group.

and intensity of immunoreactive cells within these cells; either cytoplasmic and/or nuclear, if compared to the sham group. The sections of the menthol-treated CLP group revealed a significant ($p < 0.05$) decrease in the number of immunoreactive cells compared to the vehicle-treated CLP group (**Figures 7B,D**).

We also examined the expression level of the Bcl2 protein, which negatively regulates cellular apoptosis, by immunohistochemistry. In contrast with caspase-3 results, the sham groups showed strong Bcl2 nuclear immunostaining within the lining cells of the alveoli of lung tissue, in renal glomeruli, or tubules (**Figures 8A,C**). In the CLP model, lung and kidney tissues exhibited a significant ($p < 0.05$) decrease in Bcl2-immunoreactive cells within the lining cells of the alveoli, the glomeruli, or tubular cells, if compared with the sham groups. Treatment of septic rats with menthol led to a significant ($p < 0.05$) increase in Bcl2-immunoreactivity compared with the CLP group (**Figures 8B,D**).

Menthol Restores Proliferating Cell Nuclear Antigen Expression in the Lung and Kidney Tissues of Septic Rats

The proliferating cell nuclear antigen (PCNA) has an important role in nucleic acid metabolism during

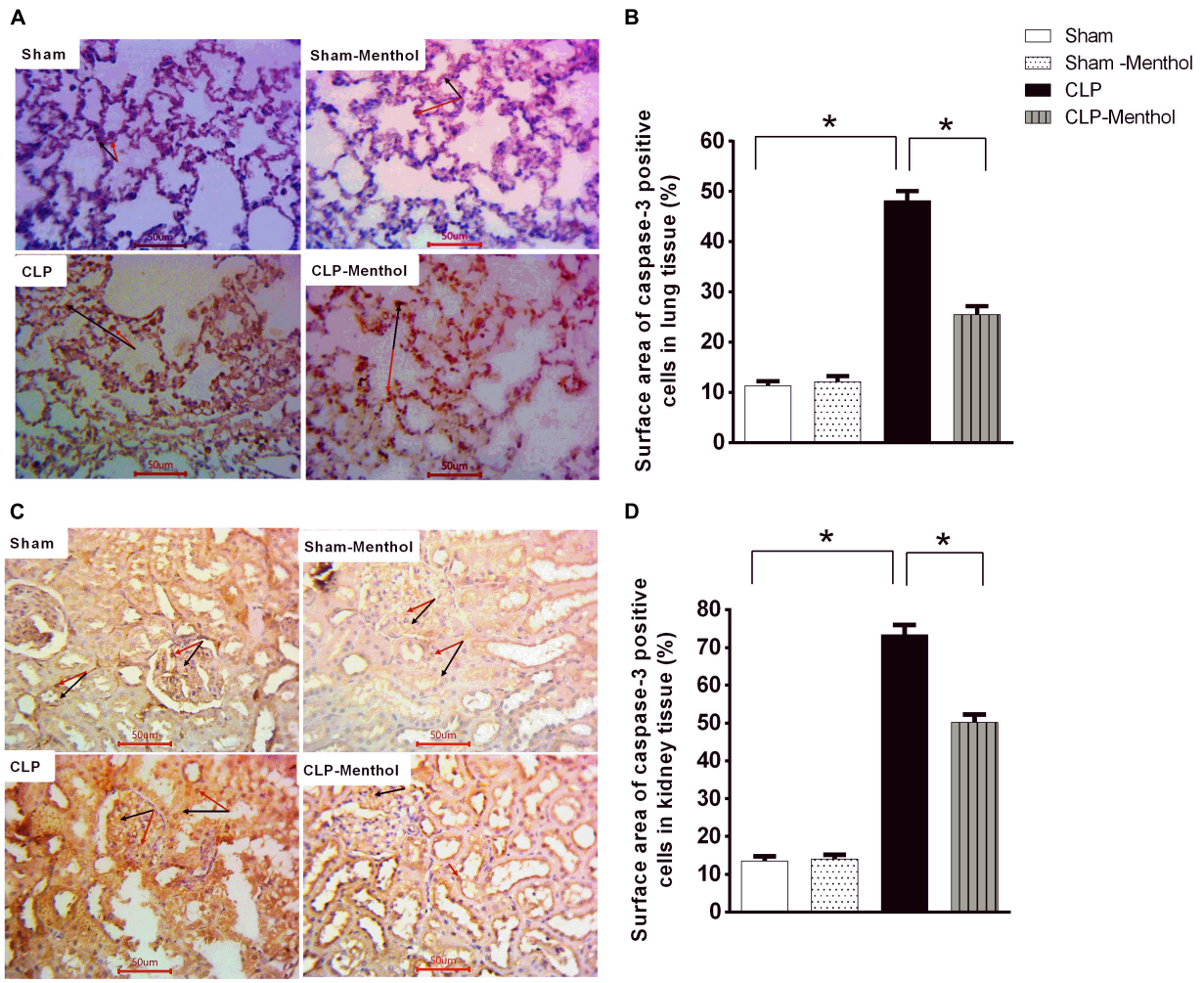

FIGURE 7 | Caspase-3 expression in the lung and kidney tissues of septic rats. Tissue levels of cleaved caspase-3 were determined semi-quantitatively by immunohistochemical staining of paraffin-embedded lung **(A)** and kidney **(C)** sections (see "Materials and Methods" section). Rabbit monoclonal anti-caspase-3 (cat. # ab32042, Abcam, Cambridge, United Kingdom) was used. Ten random fields per slide from each group ($n = 6$) were selected and imaged (400×). The mean surface area fraction of caspase-3 immuno-positive cells was measured using ImageJ software. Representative photomicrographs **(A)** showing caspase-3 immunoreactivity in lung tissues. Summary data in the Bar charts **(B)** show semi-quantitative analysis of data in **(A)** from tissue sections of the sham, sham-Menthol, CLP, and CLP-Menthol groups. Data of caspase-3 immunoreactivity in kidney sections **(C)** from sham, sham-Menthol, CLP, and CLP-Menthol groups are semi-quantitatively analyzed in **(D)**. Data in the bar charts represent the mean ± SEM of 6 independent observations. Data were analyzed by one-way ANOVA followed by the Tukey-Kramer post- test for multiple comparisons. *Significantly different at $p < 0.05$ compared to the CLP group.

replication and repair processes. It is also involved in cell proliferation after injury and is an endogenous inhibitor of cell apoptosis. The results of this study showed that lung and kidney tissues from the sham groups (sham and sham-menthol) showed strong nuclear PCNA signal within the lining cells of the alveoli, the renal glomeruli, and tubules (**Figures 9A,C**). Lung and kidney tissues from the vehicle-treated septic rats showed an obvious decrease in nuclear PCNA immune-intensity within these cells, when compared to the sham groups. Interestingly, lung and kidney sections from the CLP-menthol group showed significantly elevated nuclear PCNA immunoreactivity compared with the CLP group (**Figures 9B,D**).

Correlation Analysis Between the Measured Parameters and Kidney or Lung Injury

Correlation analysis shows that lung injury score possesses a strong correlation with the levels of MDA, nitrate/nitrite, caspase and TNF-α and a strong negative correlation with level of Bcl2, PCNA and GSH. However, only moderate negative correlation was detected between lung injury score and SOD as shown in **Figure 10**. Data also reveal that kidney injury score has a strong positive correlation with the level of serum creatinine, TNF-α and caspase. In addition to a strong negative correlation with GSH, Bcl2 and PCNA (**Figure 11**). However, Kidney injury is moderately correlated with total

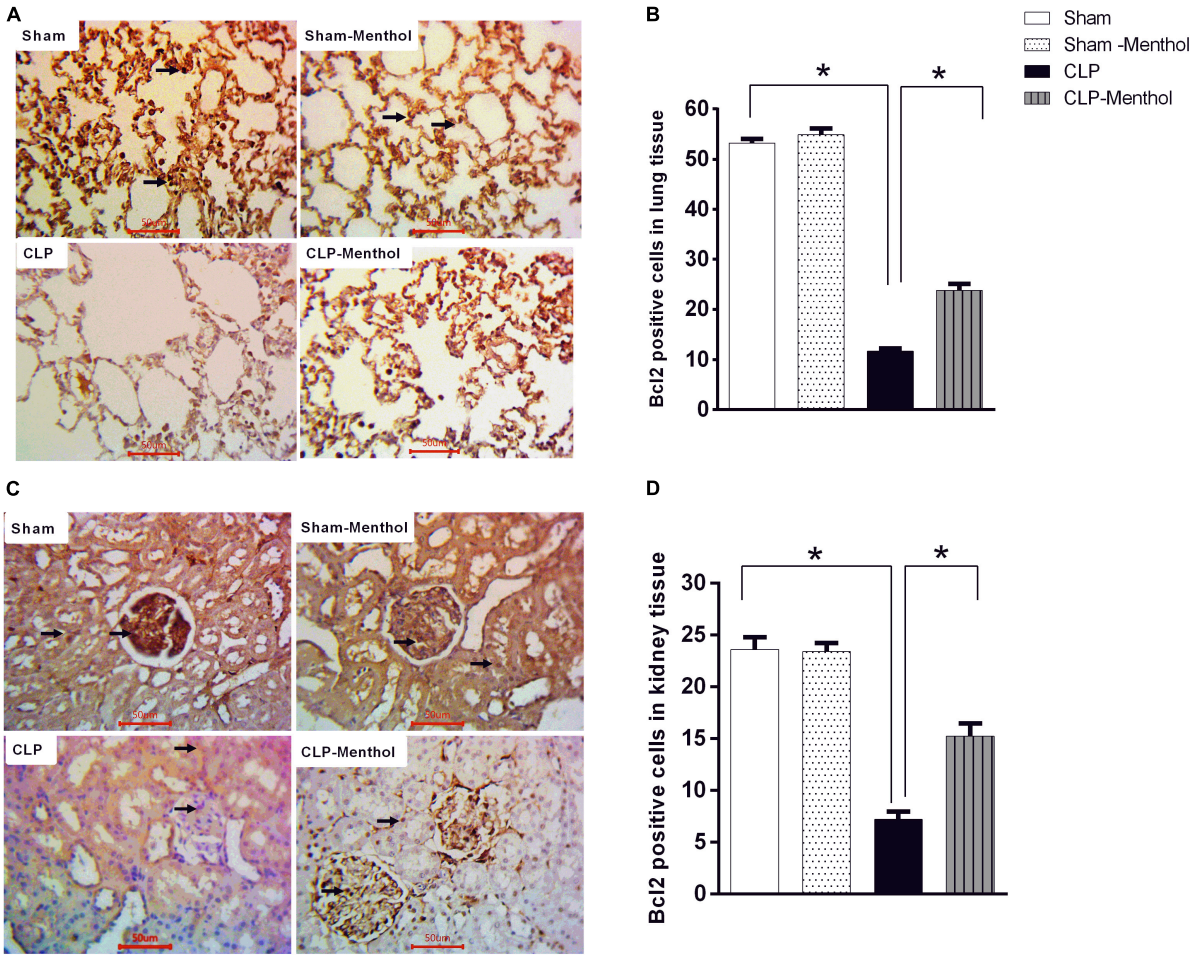

FIGURE 8 | Bcl-2 expression in the lung and kidney tissues in different groups. Protein expression of Bcl-2 was achieved by immunohistochemical staining of paraffin-embedded lung **(A)** and kidney **(C)** sections was carried out after probing the sections with rabbit polyclonal anti- Bcl-2 (cat. # ab194583, Abcam, Cambridge, United Kingdom). The mean surface area fraction of Bcl-2 immuno-positive cells form images (400X) was measured using ImageJ software. Representative photomicrographs **(A)** showing the effect of menthol treatment on Bcl-2 immunoreactivity in lung tissues. A semi-quantitative analysis of the immunostaining data from ten random fields per slide from each group ($n = 6$) is depicted in **(B)**. Data of Bcl-2 immunoreactivity in the kidney sections from different groups are semi-quantitatively analyzed in **(D)**. Data represent the mean ± SEM of 6 independent observations. Data were analyzed by one-way ANOVA followed by the Tukey-Kramer post- test for multiple comparisons. *Significantly different at $p < 0.05$ compared to the CLP group.

nitrate/nitrite and MDA. Data are presented as correlation matrix of the Pearson's correlation coefficient between the measured parameters.

DISCUSSION

Multiple organ damage during the pathogenesis of sepsis results from the aggressive activation of the inflammatory and oxidative stress cascades and contributes to the high mortality rate characteristic of sepsis (9). In the current study, induction of experimental sepsis in rats induced acute lung and kidney injury and significant mortality. Our results show, for the first time, that menthol administration, 2-h after induction of sepsis, effectively enhanced the survival of septic rats and alleviated sepsis-induced lung and kidney tissue damage.

In this study, we observed a decline of function in the lung and kidneys of septic rats. Higher serum creatinine of septic compared with non-septic animals and infiltration of protein and leukocytes in the BALF are indicators of kidney and lung injury, respectively, which correlates with the high mortality rate observed in the septic rats. The kidney and lungs of septic rats exhibited high levels of tissue damage upon histological examination, which further highlights the detrimental effects of sepsis on different organs. Interestingly, oral treatment with menthol (100 mg/Kg), 2 h after surgery, ameliorated the impaired kidney function and restored the level of proteins and leukocytes in the BALF of septic rats. Histopathological findings of the lung and kidney tissues supported the beneficial effects of menthol. Thus, menthol effectively domesticated the state of sepsis and successfully preserved organ functions. These ameliorative effects of menthol treatment improved the survival

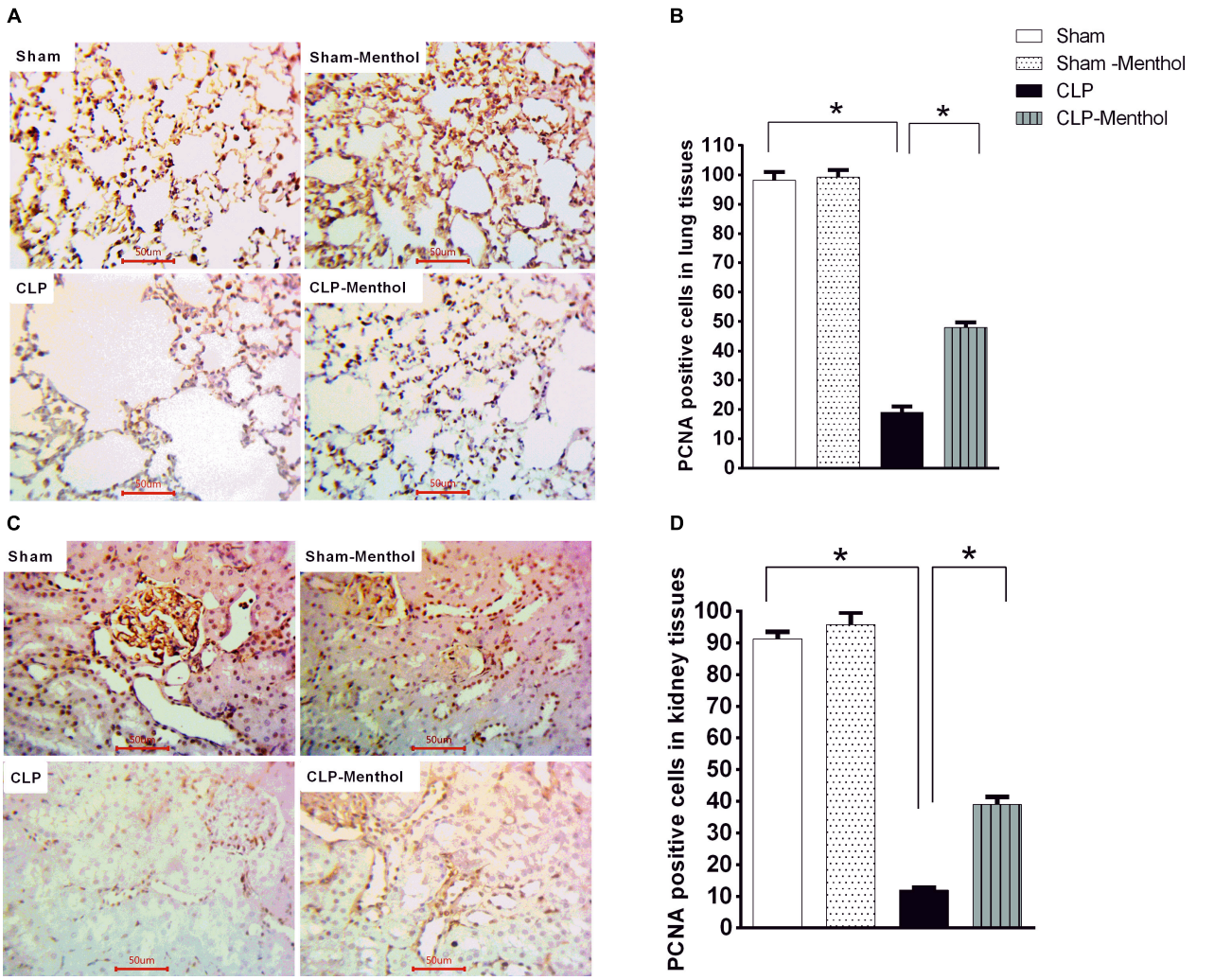

FIGURE 9 | Menthol attenuates sepsis-induced reduction of PCNA expression in lung and kidney tissues. Determination of the tissue levels of PCNA was carried out by immunohistochemical staining of paraffin-embedded lung **(A)** and kidney **(C)** sections, as described in the "Materials and Methods" section. Mouse monoclonal anti-PCNA (cat. # ab29, Abcam, Cambridge, United Kingdom) was used in this experiment. Images of 10 random fields per slide from each group ($n = 6$) were selected and the mean surface area fraction of PCNA immuno-positive cells was measured using ImageJ software. Representative photomicrographs **(A)** showing PCNA immunoreactivity in lung tissues, and the Bar charts **(B)** show a semi-quantitative analysis of the data from all groups. Photomicrographs showing PCNA immunoreactivity in the kidney sections are shown **(C)**, which are semi-quantitatively analyzed in **(D)**. Data in the bar charts represent the mean ± SEM of 6 independent observations. Data were analyzed by one-way ANOVA followed by the Tukey-Kramer post- test for multiple comparisons. *Significantly different at $p < 0.05$ compared to the CLP group.

of the menthol-treated CLP group (40%) compared with the septic rats (0%) by the end of the 10-days observation period. Recent studies showed that menthol-containing herbal extracts protect the kidneys in chemotherapy- (48) and gentamicin-induced (49) nephrotoxicity. Others have shown that menthol inhibited pulmonary inflammation and epithelial remodeling when inhaled by asthmatic animals (50).

The exaggerated inflammatory response during sepsis triggers the massive formation of reactive oxygen species (ROS). The mitochondria act both as a significant source and as a target for ROS. Sepsis provokes a cellular energy crisis, with systemic activation of the mitochondrial tricarboxylic acid cycle, and gluconeogenesis (51, 52). Such metabolic changes augment the production of reactive oxygen species (ROS)—key contributors to the pathology of sepsis. Increased ROS generation alters the chemistry of cellular proteins through nitrosylation, oxidation, and acetylation, not to mention the deterioration of mitochondrial membrane function because of increased lipid peroxidation (53). The enzymes of the electron transport chain are highly sensitive to oxidative stress, which contributes to the uncoupling of oxidative phosphorylation, and increased ROS production (51, 54). Thus, ROS-induced alteration of mitochondrial membrane permeability and respiratory enzymes switches on a ROS circuit, where increased ROS levels induce further ROS release from the mitochondria (54, 55). As shown by our data, induction

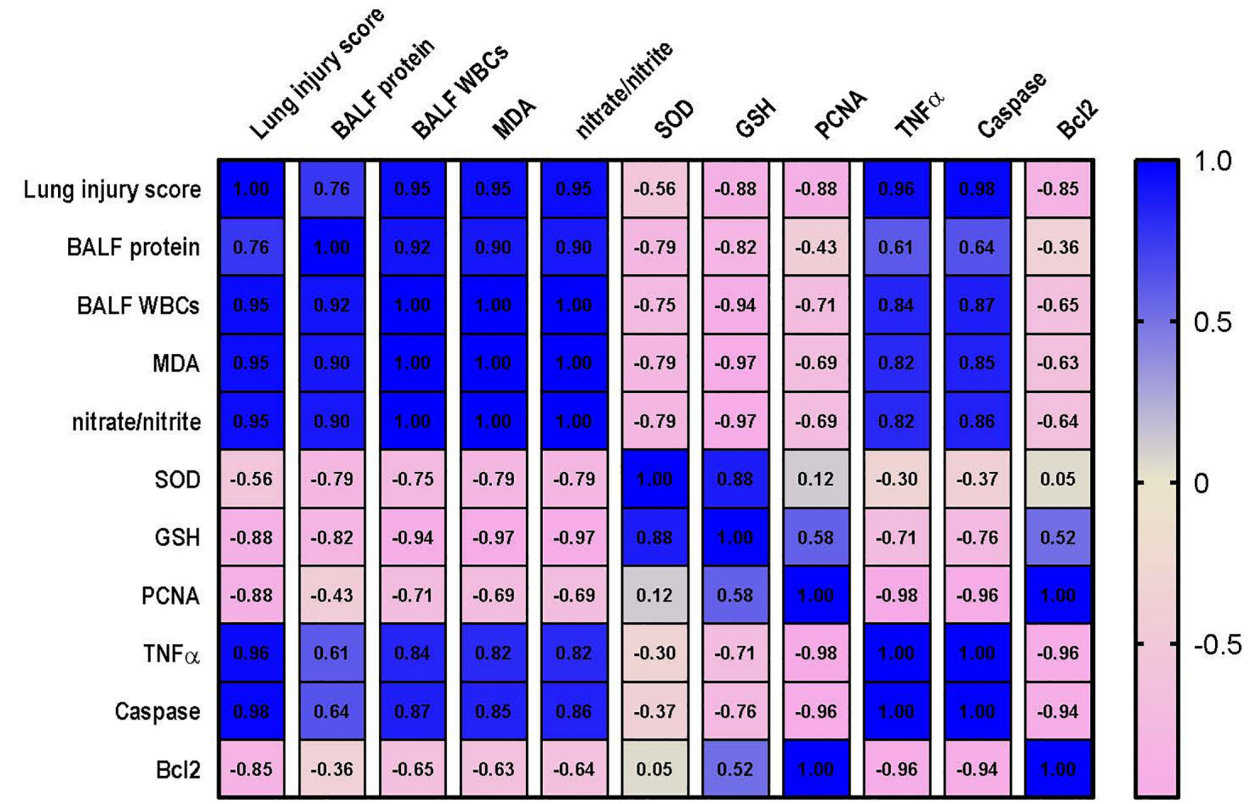

FIGURE 10 | Correlation analysis of lung injury and measured parameters. Correlation matrix between lung injury score and related parameters. Data from different experiments were analyzed for correlation using the Pearson correlation coefficient (r). Positive values indicate a positive correlation while negative values indicate a negative one. When r is in the range of | 0.3| –| 0.7|, this indicates a moderate correlation, and when $r >$ | 0.7|, this means a strong correlation. BALF, bronchoalveolar lavage fluid; MDA, malondialdehyde; SOD, superoxide dismutase; GSH, reduced glutathione; PCNA, proliferating cell nuclear antigen; TNF–α, tumor necrosis factor α; Bcl2, B cell lymphoma 2.

of sepsis by CLP markedly increased oxidative stress-related parameters and decreased the activity of the endogenous antioxidant system. Menthol treatment, however, restored the antioxidant activity in the lung and kidneys of septic rats, which conforms with its well-documented antioxidant effects (56–59). Sepsis reduces the activity of heat shock protein-70 (60), which is involved in a variety of biological activities, including the reduction of oxidative stress. Interestingly, the results of a previous study showed that menthol-treated rats exhibited higher HSP70 expression, which correlated to its mucosal protection (20), and may also explain its antioxidant effect reported in our study.

TNF-α-mediated signaling augments mitochondrial ROS generation (11). Septic conditions manifest high levels of TNF-α in clinical (61) and experimental (62) settings. Since our data showed that menthol reduced the expression of lung and kidney TNF-α, this finding provides another explanation for the observed reduction in ROS levels within these tissues. The inhibitory effect of menthol on tissue TNF-α expression might depend on its potential activation of TRPM8 channels, which may serve an anti-inflammatory function to balance the pro-inflammatory responses of other TRP channels, such as TRPV1 and TRPA1 (63). Since activation of TRPM8 by menthol occurs with a low EC_{50} 4–80 μM (64) compared to other targets [refer to a comprehensive review on menthol targets (33)], we can argue that the effects were are observing can be largely attributed to activation or TRMP8 channels.

Activation of TRPM8 by menthol significantly abolished the Angiotensin-II-evoked oxidative stress and hydrogen peroxide release in vascular smooth muscles cells (65). The antioxidant mechanism of menthol involved TRPM8-dependent antagonism of the angiotensin-triggered induction of NADPH oxidases NOX1 and NOX4 (65). When TRPM8 channels are activated, the macrophages express and release the anti-inflammatory cytokine interleukin 10 (IL-10), while the release of TNF-α decreases (66). The well-known cooling effect of menthol might explain its inhibition of TNF-α expression. The study by Wang et al. (67) demonstrated that both menthol and cold stress inhibit the release of TNF-α through interaction with NF-κB; the nuclear transcription factor controlling the production of TNF-α and other pro-inflammatory mediators (68).

In our study, rats subjected to CLP showed a significant elevation of both ROS and TNF-α, which justifies the increased expression of active caspase-3 within lung and kidney tissues and explains the observed functional deterioration. Meanwhile,

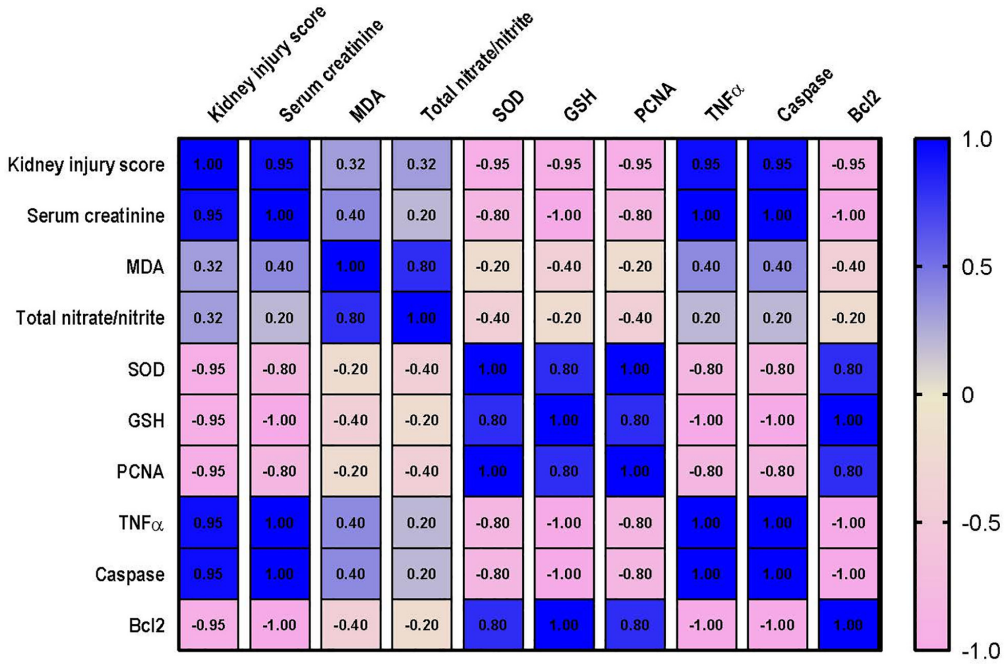

FIGURE 11 | Correlation analysis of Kidney injury and measured parameters. Correlation matrix between kidney injury score and related parameters. Data from different experiments were analyzed for correlation using the Pearson correlation coefficient (r). Positive values indicate a positive correlation while negative values indicate a negative one. When r is in the range of | 0.3| –| 0.7|, this indicates a moderate correlation, and when $r >$ | 0.7|, this means a strong correlation. MDA, malondialdehyde; SOD, superoxide dismutase; GSH, reduced glutathione; PCNA, proliferating cell nuclear antigen; TNF–α, tumor necrosis factor α; Bcl2, B cell lymphoma 2.

menthol effectively mitigated apoptosis, which is clear from our data showing the reduction in the lung and kidney expression of caspase-3. In our study, menthol inhibited the sepsis-induced reduction of tissue Bcl2 levels, parallel to menthol-induced tissue protection and improved survival. The protective effects of Bcl2 against acute lung injury might explain the protective effects of menthol in the current work. A recent study showed that besides the antiapoptotic function of Bcl2, its overexpression inhibits mitophagy *via* modulating the PINK1/Parkin pathway in a model of acute lung injury (69). Moreover, the enhanced expression of Bcl2 induced by menthol in septic rats may explain its ability to improve the pulmonary epithelial barrier. Although further elucidation of this effect is required, the recent findings of Otani et al. (70) support it. Their results suggested that the upregulation of Bcl2 counteracts the dysregulated permeability of intestinal cells in a mouse CLP model. Further, other researchers (71) recently proposed a relation between blood Bcl2 levels and survival in septic patients. Thus, the modulatory effect of menthol, and possibly other TRPM8 agonists, on Bcl2 expression and function, and its effect on the prognosis of sepsis is intriguing and needs further investigation.

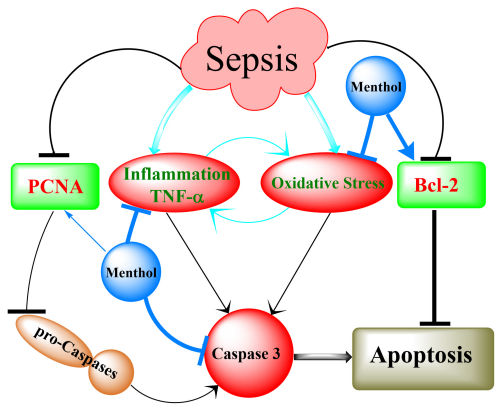

FIGURE 12 | Summary of the mechanisms involved in menthol-induced protection against sepsis. Induction of sepsis by CLP upregulates inflammation (TNF-α) and oxidative stress, which in turn activates caspases to execute cellular apoptosis. This effect is augmented by destabilization of the antiapoptotic factor Bcl-2. Downregulation of proliferating cell nuclear antigen (PCNA) contributes to the conversion of procaspases into active caspases (Caspase 3). Menthol *via* inhibition of oxidative stress and inflammation on one hand, and preservation of PCNA and Bcl-2 of the other, abrogates sepsis-induced organ damage.

Consistent with our findings, experimental induction of sepsis reduced the expression of PCNA in hepatocytes (72), and cardiomyocytes (73). In the current work, menthol preserved PCNA levels in the lung and kidneys of septic rats, which is in harmony with the observed reduction of activated caspase-3 expression. Experimental induction of severe sepsis reduced the expression of PCNA, which correlated with diminished

hepatic tissue regenerative capacity (74). These findings (74), and ours, are further supported by the results of Abcejo et al. (72). Their results showed that PCNA expression inversely correlates with disease severity and mortality. Animals with severe sepsis displayed lower PCNA levels and higher mortality compared with those having a moderate phenotype (72). The CLP procedure adopted in our study represents a severe sepsis phenotype and shows a mortality profile comparable to the severe sepsis presented in the study by Abcejo et al. (72), which explains the decreased expression of PCNA observed in our untreated septic rats. Thus, the ability of menthol to preserve renal and pulmonary levels of PCNA, although partial, might provide further explanation for the enhanced survival of menthol-treated septic rats. However, whether this preservation of PCNA level is a consequence of the menthol-induced reduction of sepsis severity *via* reducing oxidative stress and inflammation or is a direct effect of menthol is yet to be answered. Nonetheless, preservation of PCNA levels in the lung and kidney of menthol-treated rats apparently contributes to lower organ damage and improves survival after CLP.

There are several limitations in our study, including the inclusion of a standard drug, which is actually hard to find in sepsis research as there are no definite treatment of sepsis or its associated organ dysfunction. Also, our study would be strengthened by the measurement of plasma menthol concentration as well as its concentration in the kidneys or lungs. In addition, because menthol appears to be a molecule with multiple cellular targets, future studies using specific antagonists would help in identifying the actual mechanism of menthol action in sepsis.

CONCLUSION

In conclusion, the results of our study showed for the first time the protective effects of oral menthol treatment against sepsis-induced mortality and damage in the lung and kidneys of septic rats. The protective mechanisms triggered by menthol include anti-oxidative, anti-inflammatory, and anti-apoptotic pathways (**Figure 12**). These findings open new horizons to discover novel targets for the management of sepsis.

DATA AVAILABILITY STATEMENT

The raw data supporting the conclusions of this article will be made available by the authors, without undue reservation.

ETHICS STATEMENT

The animal study was reviewed and approved by the Commission on the Ethics of Scientific Research, Faculty of Pharmacy, Minia University (Approval Number: ES02/2020).

AUTHOR CONTRIBUTIONS

AAn, AAh, ME-D, and AH: execution of experiments, sample collection, and data handling and manuscript writing and revision. WA: design of the experiment, manuscript writing and revision, and funding source. WA and SA: histopathology and the immunohistochemistry studies and revision and approval of manuscript. ME-M and MA: critical manuscript revision, data analysis, and approval of final manuscript. AI: critical manuscript revision, data analysis, approval of final manuscript and funding. All authors listed have made a substantial, direct, and intellectual contribution to the work, and approved it for publication.

FUNDING

The authors extend their appreciation to the Deanship of Scientific Research at King Khalid University for funding this work through Small Groups Project under grant number (RGP.1/271/43) as well as Deanship of Scientific Research at Umm Al-Qura University (grant code 22UQU4310387DSR08) for financial support. The authors would also like to thank Dr. Heba Adel Habib and Amr A. Kamel (Faculty of Pharmacy, Minia University) for technical assistance.

ACKNOWLEDGMENTS

This work was funded by the Deanship of Scientific Research at King Khalid University through Small Groups Project under grant number (RGP.1/271/43) and the Deanship of Scientific Research at Umm Al-Qura University (grant code 22UQU4310387DSR08).

REFERENCES

1. Martin GS, Mannino DM, Eaton S, Moss M. The epidemiology of sepsis in the United States from 1979 through 2000. *N Engl J Med.* (2003) 348:1546–54. doi: 10.1056/NEJMoa022139
2. Singer M, Deutschman CS, Seymour CW, Shankar-Hari M, Annane D, Bauer M, et al. The third international consensus definitions for sepsis and septic shock (sepsis-3). *JAMA.* (2016) 315:801–10.
3. Ranieri VM, Thompson BT, Barie PS, Dhainaut JF, Douglas IS, Finfer S, et al. Drotrecogin alfa (activated) in adults with septic shock. *N Engl J Med.* (2012) 366:2055–64. doi: 10.1056/NEJMoa1202290
4. Cawcutt KA, Peters SG. Severe sepsis and septic shock: clinical overview and update on management. *Mayo Clin Pro.* (2014) 89:1572–8. doi: 10.1016/j.mayocp.2014.07.009
5. Genga KR, Russell JA. Update of sepsis in the intensive care unit. *J Innate Immun.* (2017) 9:441–55. doi: 10.1159/000477419
6. De Backer D, Orbegozo Cortes D, Donadello K, Vincent JL. Pathophysiology of microcirculatory dysfunction and the pathogenesis of septic shock. *Virulence.* (2014) 5:73–9. doi: 10.4161/viru.26482
7. Russell JA, Rush B, Boyd J. Pathophysiology of septic shock. *Crit Care Clin.* (2018) 34:43–61. doi: 10.7759/cureus.24376

8. Goldenberg NM, Steinberg BE, Slutsky AS, Lee WL. Broken barriers: a new take on sepsis pathogenesis. *Sci Transl Med.* (2011) 3:88ps25. doi: 10.1126/scitranslmed.3002011
9. Gustot T. Multiple organ failure in sepsis: prognosis and role of systemic inflammatory response. *Curr Opin Crit Care.* (2011) 17:153–9. doi: 10.1097/MCC.0b013e328344b446
10. Sinha K, Das J, Pal PB, Sil PC. Oxidative stress: the mitochondria-dependent and mitochondria-independent pathways of apoptosis. *Arch Toxicol.* (2013) 87:1157–80. doi: 10.1007/s00204-013-1034-4
11. Schulze-Osthoff K, Bakker A, Vanhaesebroeck B, Beyaert R, Jacob WA, Fiers W. Cytotoxic activity of tumor necrosis factor is mediated by early damage of mitochondrial functions. Evidence for the involvement of mitochondrial radical generation. *J Biol Chem.* (1992) 267:5317–23.
12. Barber RC, Aragaki C, Rivera-Chavez F, Purdue G, Hunt J, Horton J. TLR4 and TNF-α polymorphisms are associated with an increased risk for severe sepsis following burn injury. *J Med Genet.* (2004) 41:808–13. doi: 10.1136/jmg.2004.021600
13. Yang S, Thor AD, Edgerton S, Yang X. Caspase-3 mediated feedback activation of apical caspases in doxorubicin and TNF-α induced apoptosis. *Apoptosis.* (2006) 11:1987–97. doi: 10.1007/s10495-006-0084-y
14. Kluck RM, Bossy-Wetzel E, Green DR, Newmeyer DD. The release of cytochrome c from mitochondria: a primary site for Bcl-2 regulation of apoptosis. *Science.* (1997) 275:1132–6. doi: 10.1126/science.275.5303.1132
15. Choe KN, Moldovan GL. Forging ahead through darkness: PCNA, still the principal conductor at the replication fork. *Mol Cell.* (2017) 65:380–92. doi: 10.1016/j.molcel.2016.12.020
16. Witko-Sarsat V, Mocek J, Bouayad D, Tamassia N, Ribeil JA, Candalh C, et al. Proliferating cell nuclear antigen acts as a cytoplasmic platform controlling human neutrophil survival. *J Exp Med.* (2010) 207:2631–45. doi: 10.1084/jem.20092241
17. Nesterkina M, Kravchenko I. Analgesic activity of novel GABA esters after transdermal delivery. *Nat Prod Commun.* (2016) 11:1419–20.
18. Plevkova J, Kollarik M, Poliacek I, Brozmanova M, Surdenikova L, Tatar M, et al. The role of trigeminal nasal TRPM8-expressing afferent neurons in the antitussive effects of menthol. *J Appl Physiol.* (2013) 115:268–74. doi: 10.1152/japplphysiol.01144.2012
19. Zaia MG, Cagnazzo T, Feitosa KA, Soares EG, Faccioli LH, Allegretti SM, et al. Anti-inflammatory properties of menthol and menthone in *Schistosoma mansoni* infection. *Front Pharmacol.* (2016) 7:170. doi: 10.3389/fphar.2016.00170
20. Rozza AL, Meira de Faria F, Souza Brito AR, Pellizzon CH. The gastroprotective effect of menthol: involvement of anti-apoptotic, antioxidant and anti-inflammatory activities. *PLoS One.* (2014) 9:e86686. doi: 10.1371/journal.pone.0086686
21. Juergens UR, Stober M, Vetter H. The anti-inflammatory activity of L-menthol compared to mint oil in human monocytes in vitro: a novel perspective for its therapeutic use in inflammatory diseases. *Eur J Med Res.* (1998) 3:539–45.
22. Mogosan C, Vostinaru O, Oprean R, Heghes C, Filip L, Balica G, et al. A comparative analysis of the chemical composition, anti-inflammatory, and antinociceptive effects of the essential oils from three species of *Mentha* cultivated in Romania. *Molecules.* (2017) 22:263. doi: 10.3390/molecules22020263
23. Mimica-Dukic N, Bozin B, Sokovic M, Mihajlovic B, Matavulj M. Antimicrobial and antioxidant activities of three *Mentha* species essential oils. *Planta Med.* (2003) 69:413–9. doi: 10.1055/s-2003-39704
24. Nishino T, Tagaito Y, Sakurai Y. Nasal inhalation of l-menthol reduces respiratory discomfort associated with loaded breathing. *Am J Respir Crit Care Med.* (1997) 156:309–13. doi: 10.1164/ajrccm.156.1.9609059
25. Liu Y, Li A, Feng X, Jiang X, Sun X, Huang W, et al. alleviates cigarette smoke extract induced lung injury in rats by inhibiting oxidative stress and inflammation: via nuclear factor kappa B, p38 MAPK and Nrf2 signalling pathways. *RSC Adv.* (2018) 8:9353–63. doi: 10.1039/c8ra00160j
26. Hajian S, Rafieian-Kopaei M, Nasri H. Renoprotective effects of antioxidants against Cisplatin nephrotoxicity. *J Nephropharmacol.* (2014) 3:39–42.
27. Bellassoued K, Ben Hsouna A, Athmouni K, van Pelt J, Makni Ayadi F, Rebai T, et al. Protective effects of *Mentha piperita* L. leaf essential oil against CCl4 induced hepatic oxidative damage and renal failure in rats. *Lipids Health Dis.* (2018) 17:9. doi: 10.1186/s12944-017-0645-9
28. Bautista DM, Siemens J, Glazer JM, Tsuruda PR, Basbaum AI, Stucky CL, et al. The menthol receptor TRPM8 is the principal detector of environmental cold. *Nature.* (2007) 448:204–8. doi: 10.1038/nature05910
29. Liu B, Fan L, Balakrishna S, Sui A, Morris JB, Jordt SE. TRPM8 is the principal mediator of menthol-induced analgesia of acute and inflammatory pain. *Pain.* (2013) 154:2169–77. doi: 10.1016/j.pain.2013.06.043
30. Ramachandran R, Hyun E, Zhao L, Lapointe TK, Chapman K, Hirota CL, et al. TRPM8 activation attenuates inflammatory responses in mouse models of colitis. *Proc Natl Acad Sci USA.* (2013) 110:7476–81. doi: 10.1073/pnas.1217431110
31. National Toxicology P. Bioassay of dl-menthol for possible carcinogenicity. *Natl Cancer Inst Carcinog Tech Rep Ser.* (1979) 98:1–131.
32. Tani M, Onimaru H, Ikeda K, Kawakami K, Homma I. Menthol inhibits the respiratory rhythm in brainstem preparations of the newborn rats. *Neuroreport.* (2010) 21:1095–9. doi: 10.1097/WNR.0b013e3283405bad
33. Oz M, El Nebrisi EG, Yang KS, Howarth FC, Al Kury LT. Cellular and molecular targets of menthol actions. *Front Pharmacol.* (2017) 8:472. doi: 10.3389/fphar.2017.00472.I
34. Deitch EA. Animal models of sepsis and shock: a review and lessons learned. *Shock.* (1998) 9:1–11.
35. Alsharari SD, King JR, Nordman JC, Muldoon PP, Jackson A, Zhu AZ, et al. Effects of menthol on nicotine pharmacokinetic, pharmacology and dependence in mice. *PLoS One.* (2015) 10:e0137070. doi: 10.1371/journal.pone.0137070
36. Wang T, Wang B, Chen H. Menthol facilitates the intravenous self-administration of nicotine in rats. *Front Behav Neurosci.* (2014) 8:437. doi: 10.3389/fnbeh.2014.00437
37. Wang S, Zhou J, Kang W, Dong Z, Wang H. Tocilizumab inhibits neuronal cell apoptosis and activates STAT3 in cerebral infarction rat model. *Bosn J Basic Med Sci.* (2016) 16:145. doi: 10.17305/bjbms.2016.853
38. Schirmeister J. Determination of creatinine in serum. *Dtsch Med Wschr.* (1964) 89:1940.
39. Bancroft JD, Gamble M. *Theory and Practice of Histological Techniques*. Amsterdam, NL: Elsevier Health Sciences (2008).
40. Ashcroft T, Simpson JM, Timbrell V. Simple method of estimating severity of pulmonary fibrosis on a numerical scale. *J Clin Pathol.* (1988) 41:467–70. doi: 10.1136/jcp.41.4.467
41. Buege JA, Aust SD. Microsomal lipid peroxidation. *Methods Enzymol.* (1978) 30:302–10.
42. Sastry KV, Moudgal RP, Mohan J, Tyagi JS, Rao GS. Spectrophotometric determination of serum nitrite and nitrate by copper-cadmium alloy. *Anal Biochem.* (2002) 306:79–82. doi: 10.1006/abio.2002.5676
43. Rifai N. *Tietz Textbook of Clinical Chemistry and Molecular Diagnostics – E-Book*. Amsterdam, NL: Elsevier Health Sciences (2017).
44. Marklund S, Marklund G. Involvement of the superoxide anion radical in the autoxidation of pyrogallol and a convenient assay for superoxide dismutase. *Eur J Biochem.* (1974) 47:469–74. doi: 10.1111/j.1432-1033.1974.tb03714.x
45. Côté S. Current protocol for light microscopy immunocytochemistry. *Immunohistochemistry.* (1993) 148–67.
46. Ahmed ASF, Bayoumi A, Eltahir HM, Abdel Hafez S, Abouzied MM. Amelioration of sepsis-induced liver and lung injury by a superoxide dismutase mimetic; role of TNF-α and caspase-3. *J Adv Biomed Pharmaceutical Sci.* (2020) 3, 31–39. doi: 10.21608/JABPS.2019.19876.1061
47. Hafez SMNA, Zenhom NM, Abdel-Hamid HA. Effects of platelet rich plasma on experimentally induced diabetic heart injury. *Int Immunopharmacol.* (2021) 96:107814. doi: 10.1016/j.intimp.2021.107814
48. Abdel-Daim MM, Mahmoud OM, Al Badawi MH, Alghamdi J, Alkahtani S, Salem NA. Protective effects of *Citrus limonia* oil against cisplatin-induced nephrotoxicity. *Environ Sci Pollut Res Int.* (2020) 27:41540–50. doi: 10.1007/s11356-020-10066-x
49. Dhanarasu S, Selvam MS, Alkhalaf AA, Aloraifi AKK, Al-Shammari NKA. Ameliorative and erythrocytes membrane stabilizing effects of *Mentha piperita* on experimentally induced nephrotoxicity by gentamicin. *Egypt Acad J Biolog Sci.* (2018) 10:23–37.
50. Kim MH, Park SJ, Yang WM. Inhalation of essential oil from *Mentha piperita* ameliorates PM10-exposed asthma by targeting IL-6/JAK2/STAT3 pathway

based on a network pharmacological analysis. *Pharmaceuticals (Basel).* (2020) 14:2. doi: 10.3390/ph14010002
51. Zhang H, Feng YW, Yao YM. Potential therapy strategy: targeting mitochondrial dysfunction in sepsis. *Mil Med Res.* (2018) 5:41. doi: 10.1186/s40779-018-0187-0
52. Lee I, Hüttemann M. Energy crisis: the role of oxidative phosphorylation in acute inflammation and sepsis. *Biochim Biophys Acta.* (2014) 1842:1579–86. doi: 10.1016/j.bbadis.2014.05.031
53. Suliman HB, Welty—Wolf KE, Carraway MS, Schwartz DA, Hollingsworth JW, Piantadosi CA. Toll—like receptor 4 mediates mitochondrial DNA damage and biogenic responses after heat—inactivated E. coli. *FASEB J.* (2005) 19:1531–3. doi: 10.1096/fj.04-3500fje
54. Sharma NK, Tashima AK, Brunialti MKC, Ferreira ER, Torquato RJS, Mortara RA, et al. Proteomic study revealed cellular assembly and lipid metabolism dysregulation in sepsis secondary to community-acquired pneumonia. *Sci Rep.* (2017) 7:1–13. doi: 10.1038/s41598-017-15755-1
55. Arulkumaran N, Deutschman CS, Pinsky MR, Zuckerbraun B, Schumacker PT, Gomez H, et al. Mitochondrial function in sepsis. *Shock.* (2016) 45:271–81.
56. Liu Z, Shen C, Tao Y, Wang S, Wei Z, Cao Y, et al. Chemopreventive efficacy of menthol on carcinogen-induced cutaneous carcinoma through inhibition of inflammation and oxidative stress in mice. *Food Chem Toxicol.* (2015) 82:12–8. doi: 10.1016/j.fct.2015.04.025
57. Borowiec AS, Sion B, Chalmel F, Rolland AD, Lemonnier L, De Clerck T, et al. Cold/menthol TRPM8 receptors initiate the cold—shock response and protect germ cells from cold—shock–induced oxidation. *FASEB J.* (2016) 30:3155–70. doi: 10.1096/fj.201600257R
58. Yang SA, Jeon SK, Lee EJ, Shim CH, Lee IS. Comparative study of the chemical composition and antioxidant activity of six essential oils and their components. *Nat Prod Res.* (2010) 24:140–51. doi: 10.1080/14786410802496598
59. Mimica-Dukič N, Bozin B, Sokovič M, Mihajlovič B, Matavulj M. Antimicrobial and antioxidant activities of three *Mentha* species essential oils. *Planta Med.* (2003) 69:413–9. doi: 10.1055/s-2003-39704
60. Bruemmer-Smith S, Stüber F, Schroeder S. Protective functions of intracellular heat-shock protein (HSP) 70-expression in patients with severe sepsis. *Intensive Care Med.* (2001) 27:1835–41. doi: 10.1007/s00134-001-1131-3
61. Lv S, Han M, Yi R, Kwon S, Dai C, Wang R. Anti—TNF—α therapy for patients with sepsis: a systematic meta—analysis. *Int J Clin Pract.* (2014) 68:520–8. doi: 10.1111/ijcp.12382
62. Zamora ZB, Borrego A, López OY, Delgado R, González R, Menéndez S, et al. Effects of ozone oxidative preconditioning on TNF-α release and antioxidant-prooxidant intracellular balance in mice during endotoxic shock. *Mediators Inflamm.* (2005) 2005:16–22. doi: 10.1155/MI.2005.16
63. Silverman HA, Chen A, Kravatz NL, Chavan SS, Chang EH. Involvement of neural transient receptor potential channels in peripheral inflammation. *Front Immunol.* (2020) 11:590261. doi: 10.3389/fimmu.2020.590261
64. Behrendt HJ, Germann T, Gillen C, Hatt H, Jostock R. , Characterization of the mouse cold-menthol receptor TRPM8 and vanilloid receptor type-1 VR1 using a fluorometric imaging plate reader (FLIPR) assay. *Br J Pharmacol.* (2004) 141:737–45. doi: 10.1038/sj.bjp.0705652
65. Huang F, Ni M, Zhang JM, Li DJ, Shen FM. TRPM8 downregulation by angiotensin II in vascular smooth muscle cells is involved in hypertension. *Mol Med Rep.* (2017) 15:1900–8. doi: 10.3892/mmr.2017.6158
66. Khalil M, Alliger K, Weidinger C, Yerinde C, Wirtz S, Becker C, et al. Functional role of transient receptor potential channels in immune cells and epithelia. *Front Immunol.* (2018) 9:174. doi: 10.3389/fimmu.2018.00174
67. Wang XP, Yu X, Yan XJ, Lei F, Chai YS, Jiang JF, et al. TRPM8 in the negative regulation of TNFα expression during cold stress. *Sci Rep.* (2017) 7:1–11.
68. Serasanambati M, Chilakapati SR. Function of nuclear factor kappa B (NF-kB) in human diseases-a review. *South Indian J Biol Sci.* (2016) 2: 368–87.
69. Zhang Z, Chen Z, Liu R, Liang Q, Peng Z, Yin S, et al. Bcl-2 proteins regulate mitophagy in lipopolysaccharide-induced acute lung injury via PINK1/Parkin signaling pathway. *Oxid Med Cell Longev.* (2020) 2020:6579696.
70. Otani S, Oami T, Yoseph BP, Klingensmith NJ, Chen CW, Liang Z, et al. Overexpression of BCL-2 in the intestinal epithelium prevents sepsis-induced gut barrier dysfunction via altering tight junction protein expression. *Shock.* (2020) 54:330–6. doi: 10.1097/SHK.0000000000001463
71. Lorente L, Martín MM, Ortiz-López R, González-Rivero AF, érez-Cejas AP, Martín M, et al. Circulating Bcl-2 concentrations and septic patient mortality. *Enferm Infecc Microbiol Clin.* (2020) 39:330–4. doi: 10.1016/j.eimce.2020.06.017
72. Abcejo A, Andrejko KM, Ochroch EA, Raj NR, Deutschman CS. Impaired hepatocellular regeneration in murine sepsis is dependent on regulatory protein levels. *Shock.* (2011) 36:471–7. doi: 10.1097/SHK.0b013e31822d60ff
73. Qian Y, Qian F, Zhang W, Zhao L, Shen M, Ding C, et al. Shengjiang Powder ameliorates myocardial injury in septic rats by downregulating the phosphorylation of P38-MAPK. *J Biosci.* (2019) 44:40.
74. Weiss YG, Bellin L, Kim PK, Andrejko KM, Haaxma CA, Raj N, et al. Compensatory hepatic regeneration after mild, but not fulminant, intraperitoneal sepsis in rats. *Am J Physiol Gastrointest Liver Physiol.* (2001) 280:G968–73. doi: 10.1152/ajpgi.2001.280.5.G968

Conflict of Interest: The authors declare that the research was conducted in the absence of any commercial or financial relationships that could be construed as a potential conflict of interest.

Publisher's Note: All claims expressed in this article are solely those of the authors and do not necessarily represent those of their affiliated organizations, or those of the publisher, the editors and the reviewers. Any product that may be evaluated in this article, or claim that may be made by its manufacturer, is not guaranteed or endorsed by the publisher.

frontiers | Frontiers in Immunology

REVIEW
published: 07 July 2022
doi: 10.3389/fimmu.2022.905601

Multi-Omics Techniques Make it Possible to Analyze Sepsis-Associated Acute Kidney Injury Comprehensively

Jiao Qiao [1,2,3] *and Liyan Cui* [1,2*]

[1] Department of Laboratory Medicine, Peking University Third Hospital, Beijing, China, [2] Core Unit of National Clinical Research Center for Laboratory Medicine, Peking University Third Hospital, Beijing, China, [3] Institute of Medical Technology, Peking University Health Science Center, Beijing, China

Sepsis-associated acute kidney injury (SA-AKI) is a common complication in critically ill patients with high morbidity and mortality. SA-AKI varies considerably in disease presentation, progression, and response to treatment, highlighting the heterogeneity of the underlying biological mechanisms. In this review, we briefly describe the pathophysiology of SA-AKI, biomarkers, reference databases, and available omics techniques. Advances in omics technology allow for comprehensive analysis of SA-AKI, and the integration of multiple omics provides an opportunity to understand the information flow behind the disease. These approaches will drive a shift in current paradigms for the prevention, diagnosis, and staging and provide the renal community with significant advances in precision medicine in SA-AKI analysis.

Keywords: sepsis-associated acute kidney injury, pathophysiology, biomarkers, omics database, multi-omics integration

OPEN ACCESS

Edited by:
Alessandra Stasi, University of Bari Aldo Moro, Italy

Reviewed by:
Gianvito Caggiano, University of Bari Aldo Moro, Italy
Vincenzo Cantaluppi, Università del Piemonte Orientale, Italy

***Correspondence:**
Liyan Cui
cliyan@163.com

Specialty section:
This article was submitted to Inflammation, a section of the journal Frontiers in Immunology

Received: *27 March 2022*
Accepted: *10 June 2022*
Published: *07 July 2022*

Citation:
Qiao J and Cui L (2022) Multi-Omics Techniques Make it Possible to Analyze Sepsis-Associated Acute Kidney Injury Comprehensively. Front. Immunol. 13:905601. doi: 10.3389/fimmu.2022.905601

INTRODUCTION

The development of SA-AKI has been widely concerned but poorly understood in recent years, and its definition covers a heterogeneous group of diseases (1). In 2016, The Third International Consensus Definitions for Sepsis and Septic Shock (Sepsis-3) was proposed (2). Since then, SA-AKI has generally been defined as sepsis or septic shock involving the kidney, resulting in a progressive decline in renal function while meeting the Global Organization for Prognosis of Kidney Disease (KDIGO) CRITERIA for AKI and excluding other possible causes of renal impairment (3, 4). AKI and sepsis are defined using clinical symptoms (5). AKI is defined as loss of renal function, increased serum creatinine (SCr) levels, and/or decreased urine production (6); Sepsis is defined as a life-threatening organ dysfunction caused by uncontrolled infection and host reactions (7). Septic shock, a subset of sepsis, is strongly associated with a higher risk of death in circulatory, molecular, and metabolic abnormalities than sepsis alone. Patients with septic shock, characterized by hypotension, can be clinically identified by the need for antihypertensive agents to maintain mean artery≥65mmHg and serum lactic acid > 2mmol/L (>18mg/dL), excluding hypovolemia (8).

Currently, little is known about the epidemiology of SA-AKI. Adhikari et al. (9) extrapolated from incidence rates in the United States to estimate that there are as many as 19 million cases of

sepsis per year worldwide. The annual incidence of SA-AKI may be about 6 million cases, or close to 1 case per 1,000 people, but the actual incidence is likely to be much higher. Although sepsis has long been recognized as the most common cause of AKI in critically ill patients, sepsis and its treatment may damage the kidneys. For example, a multinational, multi-center, prospective epidemiological survey showed that sepsis accounted for 45% - 70% of all AKI cases in intensive care units (10); However, AKI from any source was associated with a higher risk of sepsis, and Mehta et al. (11) found that 40% of severely ill patients developed sepsis after AKI, suggesting that AKI may increase the risk of sepsis. As individual syndromes, sepsis and AKI predispose hosts to each other, and it is often difficult to determine the exact timing of the onset of these two syndromes clinically.

Observational studies have shown that damage during SA-AKI occurs early in the critical course of illness and after admission to ICU. In a recent large cohort study, 68% of 5443 patients with septic shock developed evidence of AKI within 6 hours of the visit (12). However, AKI in late sepsis was associated with poorer clinical outcomes and increased mortality (76.5% compared with 61.5% in early AKI) (13). The high-risk group for SA-AKI is elderly patients, more common in women, and the combination of chronic kidney disease, diabetes, heart failure, malignant tumor, and liver disease will increase the susceptibility of patients to SA-AKI (14, 15). SA-AKI was strongly associated with adverse clinical outcomes compared with non-septic AKI. Firstly, Compared with non-septic AKI, SA-AKI was associated with higher severity scores, increased need for RRT, increased risk of death, and prolonged LOS (16). Secondly, SA-AKI was associated with a longer hospital stay (37 days vs. 21 days) and a gradual increase in hospital stay depending on the severity of AKI (17). Thirdly, long-term outcomes of SA-AKI patients depend on the severity of AKI and recovery status at discharge and have a similar prognosis to non-septic AKI (18). Finally, patients with recovered AKI are still at risk for chronic kidney disease (CKD), end-stage renal disease, and death, depending on the severity of AKI, RRT requirements, and recovery status during hospitalization. One study observed CKD at 1 year in 21%, 30%, and 79% of 105 survivors of AKI reversal, recovery, and non-recovery, respectively (19).

This review focused on integrating multiple types of omics data into SA-AKI studies. This review was divided into three parts. First, we outlined the pathophysiology and biomarkers of SA-AKI; Secondly, we discussed the application of multi-omics techniques in THE study of SA-AKI. Finally, we outline the new techniques and prospects of multi-omics approaches.

PATHOPHYSIOLOGICAL MECHANISMS OF SA-AKI

Our understanding of the pathogenesis of SA-AKI is limited. Much of the current understanding of SA-AKI has been extrapolated from animal models of sepsis, *in vitro* cell studies, and postmortem observations in humans with sepsis. Postmortem kidney biopsy samples from patients provide invaluable information about proper clinical conditions. The National Institutes of Health has launched programs such as the Kidney Precision Medicine Program to expand our understanding of AKI by obtaining kidney biopsies from patients with AKI to address AKI research's technical and ethical limitations. SA-AKI animal models provide a wealth of observational data for complex and invasive measures not available in humans, such as monitoring renal blood flow (RBF), microvascular flow, cortical and medullary perfusion, oxygenation, and renal tubule health.

SA-AKI Models

In mammals represented by mice and rats, there are three main SA-AKI modeling methods (20): (1) Direct endotoxin administration, in which lipopolysaccharide (LPS) is directly injected into the peritoneum or intravenously. LPS is a cell wall component of Gram-negative bacteria; (2) Cecum ligation puncture (CLP) or intraperitoneal implants of excrement and urine, similar model USES the ascending colon bracket, it allows the feces from the intestinal leakage to the peritoneum, CLP model induced sepsis is relatively easy, but with the severity of the sepsis, the amount and type of bacteria release is different also, does not necessarily lead to AKI. (3) The bacterial implant model is where bacterial impregnation is placed at the desired location (within the peritoneum or blood vessels), most commonly with fibrin clots. The most widely used animal models are the first two, in which inflammation occurs, microvascular permeability increases, and white blood cells are recruited; Hemodynamic parameters changed, GFR decreased, and renal function deteriorated. In all mammals (but most commonly used in large mammals (pigs and sheep) and zebrafish), direct bacterial delivery of live bacteria from Gram-negative and Gram-positive bacteria directly to the host (vein, peritoneal, subcutaneous, or directly into organs) is commonly used (20). In a recent prospective controlled study, the septic shock sheep model was widely used to study SA-AKI *in vivo* using Gram-negative bacteria and to assess renal function, histology, and glomerular ultrastructure in patients with septic shock (21). It overcomes the shortcomings of the endotoxin model and supports the view that early SA-AKI represents renal insufficiency.

The ideal animal model of sepsis should consistently translate relevant information from animal studies into the human condition. Rodents are small and relatively inexpensive, but the correlation between the mouse endotoxemia model and human gene change was very low and almost random ($R^2 = 0.01$) (22). Compared with small animals, large animals such as pigs have similar cytokine and immune cell profiles and exhibit the characteristic symptoms of human infection (23). In addition, pigs are anatomically and physiologically similar to human kidneys and have obvious advantages in modeling operations. Pigs have a more macroscopic anatomical structure, the renal artery, renal vein and ureter can be easily separated during surgery, and instruments used in laparoscopic surgery for adults or children can also be used in miniature pigs. Therefore, pigs appear to be an appropriate animal model for SA-AKI.

A conference on What are the Microbial components involved in the pathogenesis of Sepsis held at Rockefeller University in May 1998 discussed the relative merits of the 2-hit hypothesis to explain the process of fatal septic shock and the "multi-hit" collaborative threshold hypothesis (24). The development of the 2-hit models allowed the researchers to determine the role of inflammatory mediators in susceptibility to post-injury infection and to create 2-hit models that replicate the clinical situation to generate different injury-specific inflammation patterns, from which to account for the complex interrelationships occurring in sepsis. 2-hit models of CLP and P. aeruginosa inoculation have been reported as clinically relevant sepsis models, J.m. Walker et al. (25)studied the possible beneficial effect of Specialized Pro-considerations Mediators (SPMs) given in the postsepsis stage to reduce infection/injury in a second blow. Results show that RvD2 Resolvin D2 (RvD2) promotes host defense by increasing TLR-2 signaling and macrophage/monocyte phagocytosis in less lethal and less inflammatory bacterial sepsis 48 h after the onset of sepsis. Jacqueline Unsinger et al. (26) examined IL-7, currently in several clinical trials (including hepatitis and human immunodeficiency virus), for improved survival in a 2-hit fungal sepsis model. Clinically relevant 2-hit models can provide a clearer understanding of the *in vivo* mechanisms of host defense in sepsis. While there are similarities in temporal inflammation and genomic host response patterns between humans and mice, the mouse immune system is more resistant. Human sepsis complications usually occur within a few days of trauma, and mice must be artificially created (27). In addition, it may vary depending on the type of injury and other variables such as outbreeding/inbreeding lines, rodent age, etc. Therefore, the similarity of the immune inflammatory blueprint in the 2-hit models between the animal and the patient should determine the timing of the impact (28).

The ideal animal model of sepsis should consistently translate relevant information from animal studies into the human condition. Currently, most animal studies use young, healthy models with no comorbidities. After searching for keywords (SA-AKI, models, comorbidities), there are very few literature studies on SA-AKI models associated with comorbidities such as advanced age, cardiovascular events, etc. One study used trauma/hemorrhage two-strike model (TH, first strike) and caecal ligation puncture model (CLP, second strike) in female (♀) and male (♂)CD-1 mice aged 3, 15, and 20 months. The study showed that age/sex differences in survival, while undeniably influential, were not reflected in the response patterns delineated between the corresponding groups. The exact role of gender/age in sepsis outcomes requires further experimental and clinical review. Another study was Kent Doi et al. (29)constructed 2-hit models of FA-CLP mice to replicate the clinical findings of high sepsis mortality in CKD patients. By introducing preexisting co-existence to mimic the common observation that human sepsis is more common in patients with underlying chronic diseases.

Pathophysiological Mechanisms

Since SA-AKI can occur in the absence of clinical symptoms of renal hypoperfusion and hemodynamic instability and the presence of normal or increased global renal blood flow, it is gradually recognized that ischemia-reperfusion injury is not the only mechanism of SA-AKI, and the "unified theory" theory is widely accepted (**Figure 1**). The pathophysiology of SA-AKI involves injury and dysfunction of many cell types, including macrophages, vascular endothelial cells (ECs), and renal tubular epithelial cells (TECs), as well as their crosstalk and association (30). There is increasing evidence that the pathogenesis of SA-AKI is multifactorial and complex, involving the interaction between inflammation, microcirculation dysfunction, and metabolic reprogramming.

Inflammatory and Immune Response

Dysregulated inflammation is the primary cause of many downstream complications, including kidney injury (31). In fact, the more significant the inflammatory response is more likely to lead to direct kidney damage. Macrophages play a central role in innate immunity (32). The first stage of the host response involves pathogen-associated molecular patterns (PAMP) binding to pattern recognition receptors (PRR) of innate immune cells, such as toll-like receptors, triggering downstream cascades of signals involved in early innate immune responses, leading to the synthesis and release of pro-inflammatory cell molecules and chemokines. Renal Tubular epithelial cells (RTECs) also express Toll-like receptors, especially TLR2 and TLR4 (33). A variety of cell-derived mediators release damage-related molecular patterns (DAMP) after tissue injury, promoting the pro-inflammatory phenotype (M1) of macrophages, activating the same sequence of events as PAMP amplifies the initial host response and affects local and distal cellular function, including proteolytic enzymes, reactive oxygen species (ROS), and neutrophil extracellular traps (NETs) (34, 35). During the progression of SA-AKI to CKD, resident cells with a specific phenotype undergo dedifferentiation, followed by proliferation and redifferentiation. Macrophages play an important role in this process. In addition to the proinflammatory phenotype described above, macrophages also have a profibrotic phenotype, stimulating fibroblasts and myofibroblasts, accompanied by the deposition of type I and III collagen and fibronectin. RTECs during repair may be involved in higher regenerative potential and anti-apoptotic ability (36).

Endothelial Injury and Microcirculation Dysfunction

The second cell type that is vulnerable is the EC. Sepsis stimulates endothelial cells to produce nitric oxide, leading to vascular dilation, loss of self-regulation, and endothelial dysfunction. Changes in cell-to-cell contact between endothelial cells are mediated by interactions between VEGF, VEGFR2, Ang, VE-cadherin, and ligand adhesion molecules, as well as complex interactions between endothelial cells and leukocytes that allow leukocytes to pass through (37). Many molecules simultaneously

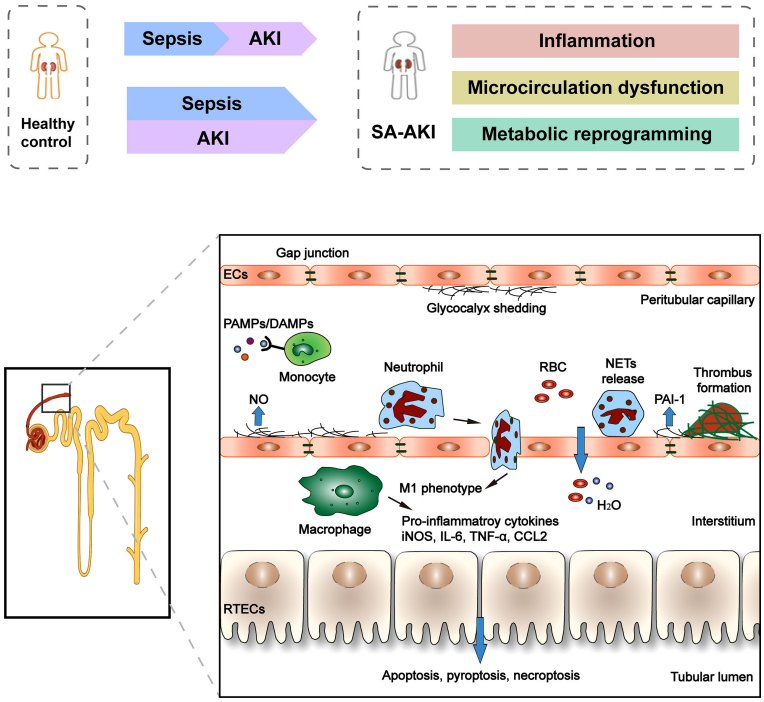

FIGURE 1 | Clinical course and pathophysiology of SA-AKI. Sepsis is the most common cause of AKI in critically ill patients. However, sepsis and AKI predispose hosts to each other, and it is often difficult to determine the exact timing of the onset of these two syndromes clinically. There is increasing evidence that the pathogenesis of SA-AKI is the "unified theory" theory involving the interaction between inflammation, microcirculation dysfunction, and metabolic reprogramming. The pathophysiology of SA-AKI involves injury and dysfunction of many cell types, including macrophages, ECs, and RTECs. PAMP and/or DAMP released from damaged tissues activate and promote the pro-inflammatory phenotype (M1) of macrophages, resulting in the release of pro-inflammatory cytokines and chemokines, which can cause damage to kidney tissues. The second cell type that is vulnerable is the EC. Sepsis stimulates endothelial cells to produce nitric oxide, which causes blood vessels to dilate. Many molecules simultaneously control microvascular permeability, resulting in insufficient blood volume relative to the vessel when tight cellular connections loosen. In addition, during the period of sepsis, confirmed microvascular thrombosis related to inflammation. In RTECs, infiltration of inflammatory cells and a large number of inflammatory factors lead to deterioration of renal function, apoptotic cell death, and sublethal injury.

control microvascular permeability, resulting in insufficient blood volume relative to the vessel when tight cellular connections loosen. In addition, during the period of sepsis, confirmed microvascular thrombosis related to inflammation, bacterial pathogen associated molecular patterns were found in endothelial cells, platelets, and leukocytes on the surface of the PRR, bacterial endotoxin can also stimulate tissue factor expression and original activation increase fibrinolytic enzyme inhibitor 1 (PAI-1) levels, blocking fibrinolysis and subsequent initiation of the coagulation process promotes microvascular thrombosis (38, 39).

RETCs Apoptotic Cell Death and Sublethal Injury

In RTECs, infiltration of inflammatory cells and a large number of inflammatory factors lead to deterioration of renal function, apoptotic cell death, and sublethal injury. Sublethal changes in RTECs include loss of cell polarity, reduced tight junction protein expression, and biological energy disturbance (40). During the progression of SA-AKI to CKD, like immune cells, early metabolic reprogramming of TECs into aerobic glycolysis improves resistance and tolerance. In addition, epigenetic changes may occur, with cell cycle stagnation in the G2/M phase and a significant increase in connective tissue growth factor and TGF-β production (41).

Metabolic Reprogramming

Among the various cell types of the kidney, RTECs are the most metabolically active cells in the kidney and are very sensitive to septic-related injury. Under normal physiological conditions, oxidative phosphorylation (OXPHOS) produces more than 95% of the cellular energy of ATP (42), and aerobic respiration is the main mechanism of ATP production. However, during SA-AKI, RTECs may first convert to glycolysis, converting pyruvate to lactic acid, an inefficient mechanism for producing ATP. For example, CLP animal models and human SA-AKI lead to decreased ATP levels in the kidney (43). Inhibition of aerobic glycolysis and induction of OXPHOS can reduce susceptibility to AKI and significantly improve survival rate (44). As ATP levels decrease, adenosine monophosphate activated protein kinase (AMPK) activates, on the one hand leading to increased glycolysis, FA oxidation, and glucose transport capacity. On the other hand, it induces the production of key antioxidant enzymes and induces mitochondrial biogenesis through the peroxisome proliferator activated receptor (PPAR) γ CoActivator -1 α (PGC-1 α). Late activation of AMPK may

eventually stabilize the energy balance through cell survival and mitochondrial biogenesis. The availability of functional mitochondria is an important component of cell metabolism and metabolic reprogramming. Sepsis results in significant mitochondrial damage and activation of mitochondrial quality control processes, such as mitochondrial autophagy (damaged mitochondria are swallowed into cells for recycling), biogenesis (new functional mitochondrial synthesis), or interference with cellular signaling pathways, such as the Akt/mTORC1/HIF-1 α pathway (45). Metabolic reprogramming may lead to optimization of RTECs energy consumption, reprogramming of substrate utilization, and enhanced cell resistance to oxidative damage (45). Therefore, the effect of OXPHOS induction or OXPHOS modulator promotion on mitochondrial function is closely related to renal function and survival rate during sepsis.

THE DIAGNOSTIC OR THERAPUEITIC INTERVENTIONS OF SA-AKI

The prevention of SA-AKI is complex, and most patients have already shown apparent renal insufficiency when seeking treatment. Therapeutically, SA-AKI remains largely supportive and nonspecific. Therefore, SA-AKI urgently needs to find more effective prevention and intervention methods. The past decade has seen an explosion in the use of high-throughput technologies and computational integration of multidimensional data. Integrating multi-omics studies offers a deeper understanding of the mechanisms of SA-AKI and the possibility of individualized treatment on an individual basis. Next, the existing prevention and treatment interventions for SA-AKI were discussed.

Antibiotics and Source Control

Early and appropriate sepsis source control were associated with a reduced risk of AKI and a greater likelihood of renal recovery within 24 hours (15). Improved monitoring of host responses through the use of transcriptomic and/or metabolomic analysis describes several novel interventions targeting immunotherapy. An example of a promising but failed attempt is a drug targeting toll-like receptor (TLR). In addition, a new type of epigenetic therapy that regulates interference in the epigenetic process of gene transcription in immune cells during sepsis could be used to restore the possibility of immune function. Induction of immunity and reversal of immune paralysis by β -glucan, and direct pharmacological manipulation of epigenetic enzymes (46). SIRT1 inhibitor EX-527, a small molecule-SIRT1 binding site that shuts down NAD +, increases leukocyte accumulation in the peritoneum and improves peritoneal bacterial clearance, showing significant protective effects during abdominal sepsis in mice (47).

Fluid Resuscitation

Fluid resuscitation is the cornerstone of septic shock management. An initial moderate infusion of resuscitation solution (30 mL/kg within the first 3 hours) was followed by dynamic measurements of fluid reactivity to determine the need for fluid or vasoactive agents. There is clear evidence that excessive resuscitation is also harmful in the case of AKI (48). However, complimentary analysis analysis of the ProCESS trial focused on renal outcomes up to 1 year and found that the use of early goal-directed therapy, alternative resuscitation, or conventional care did not affect the development of new AKI, AKI severity, fluid overload, RRT requirements, or renal function recovery (18).

Vasoactive Agent

In the case of SA-AKI, several large multicenter trials have looked at traditional drugs such as norepinephrine (norepinephrine), epinephrine, vasopressin, and dopamine, as well as more novel drugs such as angiotensin II and levosimendan (49). Norepinephrine is recommended as the first-line agent for septic shock treatment, and vasopressin is the consensus first-line agent for septic shock treatment (50). A small subgroup analysis of patients treated with RRT showed that patients receiving angiotensin II required less RRT than placebo and were more likely to survive to day 28 (53% versus 30%; P=0.012), the results need to be validated in a larger SA-AKI cohort (51).

Drug Therapy

Another treatment for sepsis is to protect individual organs. In preclinical and small clinical studies, recombinant human alkaline phosphatase (AP) has shown a protective effect against SA-AKI through direct dephosphorylation of endotoxin leading to reduced inflammation and organ dysfunction and improved survival (52). In a recent international, randomized, double-blind, placebo-controlled, dose-discovery adaptive Phase IIa/IIb study of 301 PATIENTS with SA-AKI, 1.6 mg/kg was found to be the optimal dose with no significant improvement in short-term renal function compared with placebo. However, the use of AP was associated with a reduction in day 28 mortality (17.4% versus 29.5% in the placebo group) (52).

Thiamine deficiency is associated with anaerobic metabolism and increased lactic acid. Adding thiamine improves mitochondrial function in sepsis. In a secondary analysis of a single-center, randomized, double-blind, placebo-controlled trial, patients randomized to intravenous thiamine (200 mg twice daily for 7 days) had lower AKI severity and fewer patients received RRT (53). Targeted therapies, such as targeting apoptotic pathways with caspase inhibitors and inhibiting inflammatory cascades, have shown some promising results in experimental models (54).

As of June 2022, a search at www.clinicaltrials.gov listed 2,772 sepsis studies, of which 94 SA-AKI studies and 49 involved intervention (clinical trials). Many other compounds are being actively investigated for sepsis, such as remtimod, pirfenidone sustained release, l-carnitine, and probiotics.

Renal Replacement Therapy

Guidelines suggest using continuous or intermittent renal replacement therapy (weak recommendation, low-quality evidence) for patients with adult sepsis/septic shock who

develop AKI and require RRT (2). Widely accepted indications for initiation of RRT include refractory fluid overload, severe hyperkalemia, and metabolic acidosis in which drug therapy fails, uremic signs (pericarditis and encephalopathy), dialyzable drug or toxicosis (55). There is little data on the effect of RRT initiation timing (early and delayed strategies) on SA-AKI. Early initiation of RRT may improve prognosis by limiting systemic inflammation, fluid overload, and organ damage, but there are currently no specific RCTs to determine the optimal time to initiate RRT in SA-AKI. In the RENAL and ATN studies, there was no significant difference in the odds ratio (OR) of mortality in patients with sepsis who received higher and lower intensities of RRT (56). In addition, SA-AKI has associated with lower SCr and more pronounced oliguria, so the less severe KDIGO stage defining these criteria may underestimate the severity of AKI and create a bias in the time to define RRT. New potential biomarkers that can predict AKI severity, such as TIMP-2 x IGFBP-7, may help determine when to start RRT in this setting (57).

THE OMICS ERA AND ITS IMPACT ON THE STUDY OF SA-AKI

SA-AKI is currently defined in terms of clinical symptoms, and there is considerable variation in disease presentation, progression, and response to treatment, highlighting the heterogeneity of the underlying biological mechanisms. As a result, clinicians encounter much uncertainty when considering the best treatment and risk prediction.

Omics refers to the comprehensive study of the roles, relationships, and effects of various molecules in biological cells. Today, omics technologies are advancing rapidly, and large datasets can be obtained from individuals and patient populations of the SA-AKI genotype-phenotypic continuum (**Figure 2**). Starting with genomics, new sequencing technologies have been used rapidly elucidate entire genomes and simultaneously analyze all genes (58). There are also transcriptomics (the study of the expression of all genes in a cell or organism), proteomics (the analysis of all proteins), metabolomics (the comprehensive analysis of all metabolic small molecules), epigenomics, metagenomics, glycomics, lipidomics, connectomics, and so on (59). A fundamental shift in integrative biology from focusing on the function of individual molecules or pathways to analyzing biological systems as a unified whole is the direction in which omics technology is developing. Combined with these high-dimensional data sets, computational methods such as machine learning provide the opportunity to reclassify patients into molecularly defined subgroups that better reflect underlying disease mechanisms, with the ultimate goal of improving diagnostic classification, risk stratification, and allocation of molecular, disease-specific therapies for patients with SA-AKI. Therefore, we will first discuss the application of individual omics techniques to the study of SA-AKI (**Table 1**) and then provide a comprehensive use of multi-omics.

Introduction of Omics Techniques and the Application in SA-AKI

Genomics

Genomics is used to identify individual genetic variation and disease susceptibility and studies relatively few individual heritable traits at specific loci. The completion of the Human Genome Project led to the initial sequencing of > 20,000-30,000 genes in the human genome, while current genomic studies have whole-genome sequencing, including regulatory regions and other untranslated regions, to identify potentially pathogenic variations anywhere in the genetic code; Whole exome sequencing, involving the sequencing of protein-coding regions of the genome, is a widely used next-generation sequencing (NGS) method. The human exome makes up no more than 2% of the genome, but it contains about 85% of the variants known to be associated with disease, making this approach a cost-effective alternative to whole genome sequencing; DNA microarrays rely on nucleic acid hybridization to detect the presence of SNPs and CNVs (83).

Studies have used large-scale genomic approaches to identify SNPs using microarrays of known variations in specific diseases to identify genetic variants associated with SA-AKI. Angela J. Frank et al. (60) included 1264 patients with septic shock, of whom 887 white patients were randomly assigned to the discovery and validation cohort, and found that 5 SNPs were associated with SA-AKI, such as BCL2, SERPINA, and SIK3 genes. Subsequently, Vilander (61) and colleagues included genetic samples from 2567 patients without chronic kidney

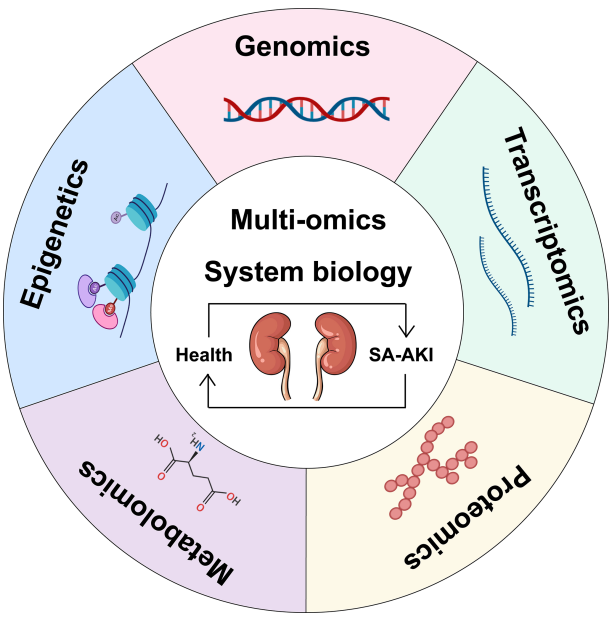

FIGURE 2 | Schematic representation of a multi-omics approach to SA-AKI. Single omics data can be integrated into multiple-omics and combined with systems biology to understand the pathophysiological mechanisms of SA-AKI better and facilitate the discovery and development of emerging biomarkers for treatment.

TABLE 1 | Summary of omics studies of SA-AKI.

Study	Omic technology	Methods/models	Major findings
Frank, 2013 (60)	Genomics-DNA microarray	1,264 patients with septic shock, of these, 887 white patients were randomly assigned to the discovery and validation cohort	5 SNPs were associated with SA-AKI: BCL2, SERPINA, SIK3 genes.
Vilander, 2017 (61)	Genomics-SNP genotyping	2567 patients without chronic kidney disease and with a genetic sample, 837 had sepsis and 627 had septic shock	SERPINA4 and SERPINA5, but not BCL2 and SIK3 are associated with acute kidney injury in critically ill patients with septic shock.
Genga, 2018 (62)	Genomics-DNA polymorphisms	Two cohorts were retrospectively analyzed: Derivation Cohort (202 patients with sepsis enrolled at the Emergency Department from 2011 to 2014 in Vancouver, Canada); Validation Cohort (604 septic shock patients enrolled into the Vasopressin in Septic Shock Trial (VASST)).	CETP modulates HDL-C levels in sepsis. CETP genotype may identify patients at high-risk of sepsis-associated AKI.
Vilander, 2019 (63)	Genomics-Genotyping polymorphism	653 patients with sepsis, 300 had KDIGO stage 2 or 3 AKI and 353 did not (KDIGO Stage 0)	Association between short repeats of HMOX1 and AKI risk in sepsis patients.
Sun, 2020 (64)	Genomics-SNP genotyping	235 patients with AKI and 235 patients without AKI (No AKI)	SNPS in NFKB1 loci rs41275743 and RS4648143 are associated with the risk of AKI in sepsis patients.
Tran, 2011 (65)	Transcriptomics-gene expression microarray	Mice after intraperitoneal injection of LPS (Global knockouts and mice with the floxed PGC-1α allele have been previously described)	Restored expression of the mitochondrial biogenesis factor PGC-1α appears to be necessary for recovery from endotoxemic AKI.
Basu, 2011 (66)	Transcriptomics-gene expression microarray	179 children with septic shock and 53 age-matched normal controls	There were 21 unique gene probes upregulated in patients with SSAKI compared to patients without SSAKI.
Ge, 2017 (67)	Transcriptomics-gene expression microarray	Patients with sepsis induced AKI (n = 6), patients without sepsis AKI (n = 6), and healthy volunteers (n = 3)	miR-4321; miR-4270 were significantly upregulated in the sepsis-induced AKI compared with sepsis-non AKI, while only miR-4321 significantly overexpressed in the sepsis groups compared with control groups.
Hultström, 2018 (68)	Transcriptomics-gene expression microarray	Six high-quality microarray studies of renal gene expression after AKI	5,254 differentially expressed genes in at least one of the AKI models; MYC may be a central regulator of renal gene expression in tissue injury during AKI.
Tod, 2020 (69)	Transcriptomics-gene expression microarray	Mice after intraperitoneal injection of LPS	MiR-762 expression was significantly increased in the early stages of septic AKI, and clusters of miR-144/451 were upregulated at 24 h.
Holly, 2006 (70)	Urine proteomics-DIGE, MS	Rat CLP sepsis	A potential biomarker and drug target, Meprin-1-alpha, was identified in a septicaemic induced ARF rat model.
Maddens, 2012 (71)	Urine, plasma, tissue proteomics gel-free technique	Mice uterus ligation and E. coli inoculation	Urinary chitinase 3-like protein 1 and -3 and acidic mammalian chitinase discriminated sepsis from sepsis-induced AKI in mice.
Wu, 2015 (72)	Tissue proteomics-DIGE, MALDI-TOF/TOF MS	Mouse CLP sepsis	Phosphorylated MYL12B can be used as a potential plasma biomarker for early diagnosis of SA-AKI.
Hinkelbein, 2017 (73)	Tissue proteomics-DIGE, MS	Rat CLP sepsis	MUP5 decreased in SA-AKI. Mitochondrial energy production and electron transport were found to be significantly correlated with proteins.
Hashida, 2017 (74)	Proteomics from hemofilter adsorbates- SDS PAGE, MS	20 patients with AKI on ICU admission and who received continuous renal replacement therapy (CRRT) as usual care between June 2012 and March 2014 were studied.	Three proteins, including carbonic anhydrase 1 (CA1) and leucine-rich α -2-glycoprotein (LRG1), were identified in all samples from patients with sepsis compared with those without sepsis.
Li, 2020 (75)	Urinary proteomics-MS	Rat CLP sepsis; Sepsis was validated in human patients	PARK7 and CDH16 have been identified as novel biomarkers for the early diagnosis of septic AKI.
Lin, 2020 (76)	Tissue global Proteomic and Phosphoproteomic-SDS PAGE, MS	Mouse CLP moderately severe sepsis	2,119 protein and 2950 phosphorus sites were identified; Several new and/or less studied S-AKI labeled proteins Hmgcs2 Serpin S100a8 and Chil3 were validated.
Waltz, 2016 (77)	Tissue (whole kidney) metabolomics-LC/MS	Mice CLP sepsis	CLP induced renal injury as evidenced by elevated serum creatinine, blood urea nitrogen, and cystatin C. Global energetic profile in sepsis showed an increase in glycolytic intermediates with decreased flux through the tricarboxylic acid (TCA) cycle. Multiple inflammatory markers were elevated in response to CLP. Levels of osmotic regulators varied, with an overall increase in pinitol, urea, and taurine in response to CLP.
Li, 2017 (78)	Tissue and serum metabolomics-1H NMR	Mice after intraperitoneal injection of LPS	Obvious decreases in betaine, taurine, lactate, glucose, and significant increases in 3-CP, acetoacetate, pyruvate, NADPH, creatine, creatinine, TMAO in LPS mice.

(Continued)

TABLE 1 | Continued

Study	Omic technology	Methods/models	Major findings
Rodrigues, 2018 (79)	Urine metabolomics-NMR	Rat CLP sepsis	1H nuclear magnetic resonance analysis detected important increases in urinary creatine, allantoin, and dimethylglycine levels in septic rats. However, dimethylamine and methylsulfonylmethane metabolites were more frequently detected in septic animals treated with 6G or 10G, and were associated with increased survival of septic animals.
Garcia, 2019 (80)	Tissue, plasma, and urine metabolomics-NMR	Pigs infused with E. coli	Metabolic differences between control animals and septicemic animals: In renal tissue, lactic acid and niacin increased, while valine, aspartate, glucose and threonine decreased; Iso-glutamate n-acetyl glutamine n-acetyl aspartic acid and ascorbic acid increased, while inositol and phenylacetyl glycine decreased in urine; And In serum, lactate alanine pyruvate and glutamine increased, while valine glucose and betaine concentrations decreased.
Ping, 2019 (81)	Tissue metabolomics-GC-TOFMS	Rat after intraperitoneal injection of LPS	Metabolic disorders of taurine, pantothenic acid, and phenylalanine and phenylalanine in the renal cortex are associated with the development of SA-AKI.
Lin, 2020 (82)	Plasma metabolomics-GC/MS	Plasma samples from 31 patients with sepsis and 23 healthy individuals.	The downregulated energy, amino acid, and lipid metabolism found in our study may serve as a novel clinical marker for the dysregulated internal environment, particularly involving energy metabolism, which results in sepsis.

disease, including 837 cases of sepsis and 627 cases of septic shock, and found that SERPINA4 and SERPINA5, but not BCL2 and SIK3 are associated with acute kidney injury in critically ill patients with septic shock. In addition to focusing on variants that influence survival after SA-AKI, the second goal is to find variants that influence SA-AKI risk. Laura M. Vilander et al. (64) found that SNPs in NFKB1 loci rs41275743 and RS4648143 are associated with the risk of AKI in sepsis patients.

Epigenomics

Epigenomics regulates gene transcription through epigenetic changes such as DNA methylation, histone modification, and changes in non-coding RNA expression. Binnie (84) and colleagues performed epigenome-wide DNA methylation analysis on whole blood samples from 68 sepsis and 66 non-sepsis severely ill adults and found 668 differential methylation regions (DMR), of which the majority (61%) were hypermethylated. SA-AKI research is currently focused on animal studies. Selective IIa class HDAC inhibitor TMP195 may have renal protective effects in LPS-induced SA-AKI mouse models (85). In LPS-induced AKI, down-regulation of miR-29B-3p exacerbates podocyte damage by targeting HDAC4. miR-29b-3p may be an important target for AKI therapy (86). Future research into the mechanisms of sepsis may aim to integrate epigenomics and transcriptome to determine how much variation in transcriptome is influenced by methylation, histone modifications, and non-coding transcripts.

Transcriptomics

Transcriptomics is the study of complete gene transcripts or RNA types that are transcribed by specific cells, tissues, or individuals at specific times and states (87). It includes both coding RNAs that are translated into proteins and non-coding RNAs that are involved in post-transcriptional control, which further affect gene expression. Unlike genomics, which focuses on static DNA sequences, transcriptomics can identify genes and gene networks that are activated or suppressed under specific conditions to assess dynamic gene expression patterns. At the quantitative level, with reference, genes could be quantitatively analyzed, while without reference, only Unigene (optimized transcript) could be quantitatively analyzed, and downstream differential gene analysis and functional annotation could be performed. At the structural level, parameters can be used for variable clipping, SNP analysis, gene structure optimization, and new gene prediction. At present, it has been widely used in basic research, clinical diagnosis, drug development, and other fields.

Mei Tran et al. (65) performed microarray sequencing after intraperitoneal injection of LPS in mice and found that restoring the expression of mitochondrial biogenic factor PGC-1α was necessary for the recovery of endotoxin AKI, indicating that changes in gene expression pathways related to cell metabolism and mitochondrial function were most abundant in septic LPS mice. In a study of 179 children with septic shock and 53 age-matched normal controls, Rajit K Basu et al. (66) found that 21 unique gene probes were upregulated in SA-AKI patients compared with non-SA-AKI patients. In other microarray experiments using miRNAs (non-translational RNA molecules with transcriptional regulatory functions), Qin-min Ge et al. (67) found that miR-4321 and miR-4270 were significantly upregulated in septic induced AKI compared with non-septic AKI, while only miR-4321 was significantly overexpressed in the septic group compared with the control group. Pal Tod et al. (69) observed that miR-762 expression was significantly increased in early septic AKI and the miR-144/451 cluster was upregulated at 24 h after intraperitoneal injection of LPS in mice.

Proteomics

With the development of omics technology, research has shifted to the analysis of translation "products" of cellular proteins and RNA transcripts. By mRNA transcription and protein modification after translation (add or remove phosphate or methyl specific molecular etc.) make the proteome is highly dynamic, can not necessarily infer from the level of gene expression in specific protein level, greatly increased the complexity of protein and peptide, has brought the huge challenge for proteomics analysis (88). The introduction of a

variety of techniques, such as two-dimensional gel electrophoresis, liquid chromatography, and mass spectrometry, with high sensitivity and resolution mass spectrometry, has enabled the identification and quantification of proteins and peptides in tissues and biological fluids and has provided new insights into disease-related processes at the molecular level (89).

High-throughput proteomic analysis of urine, plasma, and tissue samples has identified emerging biomarkers and drug targets. To construct a new rat model of acute renal failure induced by sepsis with heterogenous response similar to that in humans. DIGE was used to detect changes in urinary protein and identify potential biomarkers and drug targets for Meprin-1-alpha (70); MUP5 decreased in SA-AKI, and mitochondrial energy production and electron transport were significantly correlated with protein (73). PARK7 and CDH16 are considered novel biomarkers for early diagnosis of septic AKI and validated in human patients (75). In the Mouse CLP Sepsis model, the Tissue Proteomics-Dige and MALDI-Tof/TOF MS techniques were used to identify the phosphorylated MYL12B as a potential plasma biomarker for the early diagnosis of SA-AKI (72). Tomoaki Hashida et al. studied 20 AKI patients hospitalized in ICU from June 2012 to March 2014 by Proteomics from Hemofilter Bates SDS PAGE, MS. Three proteins, including carbonic anhydrase 1 (CA1) and leucine-rich α-2-glycoprotein (LRG1), were detected in samples from all sepsis patients who received continuous renal replacement therapy (CRRT) under conventional care, compared with those who were not infected with sepsis (74).

Several recent studies have identified several promising candidate marker proteins for disease onset and progression, and further identified pathways specific to SA-AKI and its transition to CKD. The moderate and severe mouse CLP sepsis models were established, and the time changes of kidney proteomics and phosphorylated proteomics were examined on days 2 and 7 after surgery, and 2119 protein sites and 2950 phosphorus sites were identified. Several new and/or less studied SA-AKI labeled proteins Hmgcs2, Serpin S100A8, and Chil3 were validated (76). In the migration and E. coli inoculation model, Using proteomics Gel-free technique, urine chitinase 3-like proteins 1, 3 and acidic mammalian chitinase were found to distinguish between sepsis and mouse septicaemic induced AKI, NGAL, and thioredoxins, and increased with the severity of AKI (71).

Metabonomics

Metabolomics refers to the comprehensive and systematic identification and quantitative analysis of molecular metabolites of less than 1000 daltons in biological samples such as blood and tissues under physiological or pathological conditions, which may more accurately describe the cellular processes active under any conditions (90). Metabolomics studies use two main methods to detect metabolites: nuclear magnetic resonance (NMR) and liquid chromatography/mass spectrometry (LC/MS). NMR is quantitative, non-destructive, reproducible, and can accurately quantify the abundance and molecular structure of metabolites (91). The sample preparation is simple and the measurement time is relatively short, which is suitable for high-throughput, untargeted metabolite fingerprint study. But the disadvantage is relatively low sensitivity. LC/MS is also widely used in metabolomics, with higher sensitivity and quantification of more metabolites, but with poor accuracy and reproducibility. Sample preparation and solvent selection are even more critical in MS-based experiments because metabolite extraction requires the removal of proteins and salts that adversely affect the quality of the measurement as well as the instrument itself. MS mass analyzers in metabolomics commonly use quadrupole time of flight, Orbitrap, and Fourier transform, which are suitable for distinguishing the chemical complexity of metabolomics (92).

Metabolites are the final products of biological activities and are the most direct and comprehensive biomarkers reflecting physiological phenotypes. More and more studies have shown that changes in energy metabolic pathways, also known as metabolic reprogramming, are an important factor in the pathophysiology of SA-AKI. Therefore, it is of great significance to study the metabolic changes of SI-AKI and identify its early biomarkers for early clinical diagnosis and treatment. Firstly, inflammatory metabolites and products of kidney damage increase. Paul Waltz et al. (77) used metabolomics-LC/MS technology in the MICE CLP Sepsis model and found that the evidence of CLP-induced kidney injury is increased serum creatinine, blood urea nitrogen, and cystatin C. CLP raises multiple inflammatory markers. Levels of osmotic regulators varied, with an overall increase in pinitol, urea, and taurine in response to CLP. Francisco Adelvane de Paulo Rodrigues (79) and colleagues detected significant increases in creatine, allantoin, and dimethylglycine levels in septic rats by 1-hour NMR analysis. However, dimethylamine and methanosulfonyl metabolites were detected more frequently in septic animals treated with 6-gingerol (6G) and 10-gingerol (10G) and were associated with increased survival in septic animals. Gingerol alleviates septic AKI by reducing renal dysfunction, oxidative stress, and inflammatory response, and the mechanism may be related to the increased production of dimethylamine and methanosulfonyl methane.

Secondly, the overall energy spectrum of sepsis showed an increase in glycolysis intermediates and a decrease in flux through the tricarboxylic acid (TCA) cycle. Similar changes in metabolites were also observed through tissue and serum metabolomics-1H NMR after LPS injection in mice. The contents of betaine, taurine, lactic acid, and glucose in LPS mice were significantly decreased. The contents of 3-CP, acetoacetic acid, pyruvate, NADPH, creatine, creatinine, and trimethylamine oxide were significantly increased (78). In large animal models of pigs infused with E. coli, metabolic differences were found between control and sepsis animals: lactic acid and niacin increased in renal tissues, while valine, aspartic acid, glucose, and threonine decreased; The contents of isoglutamate-acetylglutamate-acetylaspartic acid and ascorbic acid in the urine increased, while the contents of inositol and phenylacetyl glycine decreased. Serum concentrations of lactic

acid, alanine, pyruvate, and glutamine increased, while those of valine, glucose and betaine decreased (80).

In addition, in plasma samples from 31 patients with sepsis and 23 healthy individuals, metabolomics-GC/MS suggest that down-regulation of energy, amino acid, and lipid metabolism may serve as a new clinical marker for identifying internal environmental disorders, especially involving energy metabolism, leading to sepsis (82).

Omics Techniques in SA-AKI Outcome Events

Through literature review, SA-AKI is important to the two topics cited above and is considered a major public health problem associated with increased mortality and progression to CKD. However, relevant studies are mainly focused on prospective and observational cohort studies of patients in the real world, and there are still few studies on omics technology. Omics, especially multi-omics, may have more in-depth exploration and analysis of the two topics, which is the direction of further research of omics technology in SA-AKI.

While maintaining homeostasis, the kidney, as an endocrine and immune organ, may regulate distant multi-organ dysfunction. Several recent experimental studies have shown that AKI is associated with extensive damage to distant organs such as the lungs, heart, liver, and intestines (93, 94). The function of remote organs can be affected by a variety of biologically related pathways, such as transcriptome changes, apoptosis, upregulation of various damage promoting molecules, oxidative stress, inflammation, and loss of vascular function (95). In addition, the severity of organ dysfunction is independently associated with mortality, which can rise to as high as 45%-60% when AKI is associated with other organ dysfunction, such as acute respiratory distress syndrome [ARDS], heart failure, or sepsis. In a prospective observational cohort of 1753 patients with critically ill AKI, SA-AKI (n = 833) was associated with an increased risk of in-hospital death. In a systematic review of long-term renal outcomes after septic AKI and long-term renal outcomes, studies using keywords associated with septic AKI were identified from PubMed and CINAHL databases within 5 years, with a time range of 28 days to 3 years for long-term renal outcomes, Most take one year. Renal outcomes range from recovery to renal replacement therapy to death. All of these studies excluded patients with CKD (96).

The molecular mechanisms underlying AKI's transformation into CKD are complex, and most literature has focused on the complex balance between adaptation and maladaptive repair processes (97). Maladaptive repair leads to chronic damage and loss of kidney function, setting the stage for CKD, which eventually progresses to ESRD. This process is accompanied by permanent changes in undesirable structures, persistent low-grade inflammation, activation of perivascular and interstitial fibroblasts, vascular sparseness, and parenchymal ischemia (98). The integration of multiple omics techniques opens up new possibilities for improving our understanding of AKI and the driving forces behind the transition from AKI to CKD. Yi-han Lin et al. (76) analyzed the changes in the global proteome and phosphorylated proteome levels in renal tissues on day 2 and day 7 after CLP by constructing a mouse model of moderate severity CLP and using filter-based sample processing method combined with an unlabeled quantitative method, corresponding to SA-AKI and transition to CKD, respectively. It provides a view that renal tissue dynamically regulates the oxidative stress induced by sepsis, and provides enlightenment for the exploration of potential diagnosis and treatment methods in the future. In this study, a total of 2119 proteins and 2950 phosphates were identified to identify specific response pathways to SA-Aki-CKD transformation, including regulation of cellular metabolism, oxidative stress, and energy expenditure in the affected kidney. Of these, the majority (56%) are associated with small molecular metabolic processes (FDR = 3.35E-48), such as lipids, nucleotides, alcohol, and other fatty acids. Network analysis also revealed that several protein clusters, such as REDOX enzyme complex, peroxisome, and cytochrome P450 (CYP) family proteins, may play important roles in the AKI-CKD transition.

Novel Biomarkers for SA-AKI

The role of emerging biomarkers in different renal syndromes, including SA-AKI, is a rapidly growing area of research. In patients with sepsis, early detection of AKI is critical to provide optimal treatment and avoid further kidney damage. Because specific biomarkers can detect renal stress or damage before significant changes in function (preclinical AKI) or even before the absence of functional changes (subclinical AKI), studying SA-AKI biomarkers could provide additional insights into the pathophysiology of SA-AKI (99). In order to provide prevention and early diagnosis of treatment when it is most effective. **Table 2** summarizes some of the biomarkers studied in SA-AKI from the aspects of inflammatory, endothelial injury, tubule injury, and AKI risk markers, to provide prevention and early diagnosis when treatment is most effective.

Renal tubular cell damage contributes to the spread of AKI during sepsis. Among the newer biomarkers, neutrophil gelatinase-associated lipid carrier protein (NGAL), kidney injury molecule-1 (KIM-1), liver-type fatty acid binding protein (L-FABP), and cystatin C(Cys C) accelerated the diagnosis of SA-AKI. NGAL is the most widely studied renal biomarker which is a member of the human lipid carrier protein family and consists of 178 amino acid residues (114). The level of NGAL increased sharply after kidney injury, which can be used as an early sensitive biomarker of kidney injury. NGAL expression is inconsistent in SA-AKI. Studies have shown that urinary NGAL has higher specificity for S-AKI than plasma NGAL (80.0% vs 57.0%) (115). Sollip Kim et al. found in A systematic review and meta-analysis that plasma NGAL had A high sensitivity and A high negative predictive value for AKI in adult sepsis patients. However, this study did not reveal the usefulness of urine NGAL (116). KIM-1 is a type I transmembrane glycoprotein encoded by the TIM-1 gene and is a member of the T cell immunoglobulin mucin (TIM) gene family. Kim-1 was first used as a biomarker for acute kidney injury (AKI) in 2002, but there is little evidence to support its

TABLE 2 | Summary of biomarkers used to detect SA-AKI.

Types of biomarker	Biomarker	Source	Potential use in SA-AKI
Inflammation biomarkers	IL-6	Mononuclear macrophages, Th2 cells, vascular endothelial cells and fibroblasts	Baseline IL-6 at admission predicted AKI in patients with severe sepsis, and IL-6 also predicts the development of AKI and need for RRT in patients with severe sepsis (100).
	IL-18	Monocytes, dendritic cells, macrophages and epithelial cells	In a prospective, multicenter cohort, UIL-18 independently predicted the progression of septic AKI (AUC 0.619; 95% CI, 0.525 to 0.731) (101).
	sTREM-1	Activated receptors selectively expressed on the surfaces of neutrophils, macrophages, and mature monocytes	In patients with sepsis, The AUC values of plasma STREM-1 in the diagnosis and prediction of AKI (24h before diagnosis) were 0.794 and 0.746, respectively. The AUC values of urine STREM-1 were 0.707 and 0.778. ACU 0.922 was predicted 48 hours before diagnosis, and urine STREM-1 was a fairly good predictor (102).
Endothelial injury biomarkers	Ang	Ang1 is mainly synthesized by paravascular sertoli cells, vascular smooth muscle cells and tumor cells; Ang2 is mainly synthesized by vascular smooth muscle cells	Ang1 has a protective effect against endotoxemia, increasing vasoconstriction and reducing pulmonary microvascular leakage associated with inflammation (103). Circulating Ang1 levels were suppressed in critically ill patients with septic shock (104). Circulating Ang-2 is a strong independent predictor of mortality in ICU dialysis-dependent AKI patients (105).
	VE-cadherin	Vascular endothelial cell	Plasma sVE-cadherin was independently associated with AKI-RRT, suggesting that disruption of endothelial adhesion and connectivity may contribute to the pathogenesis of organ dysfunction in sepsis (106).
	sTM	Vascular endothelial cell	Compared with sepsis non-AKI group, sTM in SA-AKI group was significantly different (P<0.0001); Multivariate logistic regression analysis showed that sTM was an independent predictor of AKI, and AUROC was 0.758(P<0.0001) (107).
Tubular injury biomarkers	NGAL	Leukocytes, loops of medullary and collecting ducts	SA-AKI patients have higher detectable plasma and urine NGAL compared with non-septic AKI patients. These differences in NGAL values in SA-AKI may have diagnostic and clinical relevance as well as pathogenetic implications (108).
	KIM-1	RTECs	UKIM-1 and sKIM-1 levels were significantly higher in SA-AKI than in patients without AKI. ROC of uKIM-1 and sKIM-1 for AKI prediction was 0.607 and 0.754, respectively (109).
	L-FABP	Liver cells; RTECs	Urinary L-FABP level may be a predictive marker of sepsis severity and mortality, and can serve as a useful biomarker for patients with sepsis complicated with AKI (109).
	Cys C	All nucleated cells	Urine and plasma are of value in the diagnosis and prediction of AKI occurrence (24 hours before diagnosis) in patients with SA-AKI (21). Aydogdu et al. confirmed that plasma and urine Cys-C were good markers for early diagnosis of septic associated AKI (AUCs 0.82 and 0.86, respectively) (110). However, some studies in adults and newborns have shown that sepsis has no effect on plasma or urine levels of Cys-C (111, 112).
AKI risk biomarkers	[TIMP-2] • [IGFBP7]	TIMP-2 is synthesized by RTECs; IGFBP7 is expressed in almost all epithelial cells	[TIMP-2] • [IGFBP7] predicted the development of stage 2 and 3 AKI in high-risk and critically ill patients with sepsis with an AUC of 0.84. The biomarker performed similarly regardless of disease severity (SOFA score), with a sensitivity of 77.5% and specificity of 75% for severe AKI at a cut-off value of 1.0 (113).
	Electronic alerts, electronic risk algorithms	\	Several alarms have shown the ability to predict sepsis and AKI separately, and the combination of biochemical biomarkers may help enrich the detection and risk stratification of SA-AKI (20).

IL-6, Interleukin-6; IL-18, Interleukin-18; sTREM-1, Soluble triggering receptor expressed myeloidcells 1; Ang, Angiopoietins; sTM, Soluble thrombomodulin; NGAL, Neutrophil gelatinase-associated lipocalin; KIM-1, Kidney Injury Molecule-1; L-FABP, Liver-type fatty acid binding protein; Cys C, Cystatin C; TIMP-2, Tissue Inhibitors Of Metalloproteinase 2; IGFBP7, Insulin-like growth factor binding protein-7.

role in S-AKI. Similar to uKIM-1, sKIM-1 can also predict the occurrence of septic AKI at an early stage, but it has no predictive value to judge the severity of AKI and the prognosis of sepsis (109). However, these biomarkers lack the ability to further the stratification of SA-AKI risk or inform us of primary and secondary sites of injury.

Tissue Inhibitors Of metalloproteinase 2 (TIMP-2) stimulate P27 expression (117). Insulin-like growth factor binding protein-7 (IGFBP7) increases the expression of p53 and P21 (118). [TIMP-2]• [IGFBP7] (a biomarker of cell cycle arrest) accurately predict stage 2-3 AKI as defined by KDIGO within 12 hours; Induced stagnation of the renal tubule cell G_1 cycle occurs simultaneously with early cell damage caused by ischemia or inflammatory processes. Changes in urine [TIMP-2]•[IGFBP7] after initial fluid resuscitation identified different risks of AKI progression in sepsis patients in the ProCESS trial of 688 septic shock patients at [TIMP-2]•[IGFBP7] before and after 6-hour resuscitation. According to the APACHE II score, clinical response to resuscitation was weak in predicting endpoint (AUC 0.68, 95%CI 0.62-0.73), It was improved by the addition of [TIMP-2]•[IGFBP7] (0.72, 95%CI 0.66-0.77 P =0.03) (119).

There are no widely accepted risk scores for SA-AKI, and only the HELENICC score currently predicts mortality in patients requiring renal replacement therapy (RRT) (120). Comparing 30 patients before electronic alert activation with 30 patients after electronic alert activation, the time to receive any sepsis-related intervention was shorter after an alert, with a median difference of 3.5 hours (P = 0.02) (121). Using electronic health records to create electronic alert systems has the potential to identify high-risk patients and initiate interventions more quickly. Using real-time data from electronic health records to identify patients with

SA-AKI, automatic alarms are combined with biochemical biomarker testing to improve case detection and risk stratification for SA-AKI (122).

Omics Databases on Kidney Disease

Omics database provides the latest information about the molecular function orientation and expression, to store information about has conducted a similar experiment, is helpful to study design, the study of kidney disease is a valuable tool. For clinical practice, systems biology methods and high throughput technology to promote medical revolution from passive to active and prevention, through the powerful calculation method, find new biomarkers. The development of diagnostic tools to elucidate the pathogenesis and create models for possible therapies for patient screening, diagnosis, prevention and treatment. Omics is ongoing and is expected to be gradually introduced into clinical practice within the next decade (123). In this review, referring to Theofilos Papadopoulos et al. (124), we describe universal omics databases covering a wide range of molecular and pathological information as well as specific databases for kidney disease (**Table 3**).

MULTI-OMICS INTEGRATION

Numerous studies have shown that the integration of multi-omics data sets has been applied to a wide range of biological problems, helping to unravel the underlying mechanisms at the multi-omics level. Yehudit Hasin et al. (125) proposed a comprehensive analysis method of multiple sets of data, which is divided into three categories: genomic priority that attempts to determine the mechanism of GWAS loci leading to disease, the phenotypic priority that seeks to understand the pathway leading to disease, and the environmental priority that uses environment as the primary variable to study its interfering pathway or interaction with genetic variation. Although current omics research on SA-AKI has focused on a single omics study, only a few studies have integrated multiple omics techniques to address the three critical issues of SA-AKI.

① Subtypes and classification of SA-AKI based on multiple omics features.

There has not been a multi-omics integrated study involved.

② Prognostic biomarkers for SA-AKI, including disease diagnosis and driver genes.

A good example is Raymond J. Langley et al. (126) and his colleagues examined clinical characteristics and plasma metabolomics and proteomics of patients with community-acquired sepsis upon arrival at the hospital emergency department and 24 h later. Different characteristics of proteins and metabolomics are concentrated in fatty acid transport and β -oxidation, gluconeogenesis, and citric acid cycles and vary more as death approaches. However, the metabolomics and proteomics of survivors of mild sepsis were not different from those of survivors of severe sepsis or septic shock. An algorithm derived from clinical features and measurements of seven metabolites predicted patient survival.

③Gain insight into the pathophysiology of SA-AKI.

Takashi Hato and his colleagues conducted two experiments specifically targeting SA-AKI. A combination of transcriptomics, proteomics, and metabolomics, showed that endotoxin preconditioning reprogrammed macrophages and tubules to create a protective environment to prevent severe AKI in septic mouse models, upregulating the antibacterial molecule itaconic acid and its activase Irg1. Many genes activated by endotoxin were located near heterochromatin, suggesting that epigenetic regulation may be involved in the preconditioning response (127). In the second study, they used gram-negative sepsis model for the translation group, transcriptome, and proteome of the joint inspection new; translation will be closed as a vital characteristic of the late sepsis, further found that 5 'cap dependency translation close the reversal of the improved degree of kidney damage caused by sepsis.

Mariam P. Alexander et al. (128) compared COVID-19 AKI with SA-AKI, and analyzed the morphological, transcriptome, and proteomic characteristics of postmortem kidneys. Transcriptomics found that COVID-19 AKI and SA-AKI have a rich transcriptional pathway associated with inflammation (apoptosis, autophagy, major histocompatibility complex I and II, and Type 1 T-assisted cell differentiation) compared to non-infectious AKI; Proteomic pathway analysis showed that both of them were enriched to a lesser extent in necrotic apoptosis and Sirtuin signaling pathways, both of which are involved in the regulatory response of inflammation.

NEW TECHNIQUES AND FUTURE PERSPECTIVES

Our understanding of disease processes will likely to evolve rapidly and revolutionarily as new technologies and methods development. For example, techniques such as scRNA-seq and mononuclear RNA-seq (snRNA-seq) provide insights into the molecular processes of SA-AKI at the cellular level, with artificial intelligence aimed at accurately predicting the onset of SA-AKI in advance. In future applications, tissue samples or whole organs can be sequentially analyzed through a combination of these techniques to generate spatial multi-omics datasets, which are expected to provide unprecedented insights into the deep molecular biology of the system under study.

Integrating Microarray-Based Spatial Transcriptomics and Single-Cell RNA-Seq

ScRNA-seq provides detailed information on single-cell transcriptional expression, allowing cell-to-cell analysis of RNA expression differences (129). It uses a variety of methods for cell isolation and transcription amplification, such as microfluidics devices that capture cells in hydrogel droplets or methods that rely on physical isolation of a cell (such as fluorescent-activated cell sorting into a 96-well plate and microfluidics chip used by Fluidigm C1) from another well (130). Due to the heterogeneous cell types (such as epithelial cells, endothelial cells, fibroblasts, vascular smooth muscle, and immune cells) in different renal

TABLE 3 | General omics and Kidney-specific databases.

Tool	Data types	Purpose
Genomics		
GeneCards (http://www.genecards.org/)	Contains >152 000 GeneCards genes; Gene-centric data from approximately 150 network sources; Detailed information on all annotated and predicted human genes	Search for human genetic information; The first key to the study of gene function
Online Mendelian Inheritance in Man (http://www.omim.org/)	>15 000 genes; Contains a central database of information and literature on human genetic diseases and genetic loci	Looks for the latest clinical testing standards and trends;Provides detailed information about this class of annotations from gene sequences, maps, literature and other databases
NephQTL (http://www.nephqtl.org)*	Compartment-specific (glomeruli and tubulointerstitium) gene expression profiles from biopsy samples of 187 participants in the NEPTUNE cohort; Genotype frequency of SNPs in the NEPTUNE cohort	Compartment-specific (glomerular and tubule) eQTL discovery
Human Kidney eQTL Atlas (http://www.susztaklab.com/eqtl)*	Compartment-specific (glomeruli and tubulointerstitium) gene expression profiles from biopsy samples of 151 participants linked to SNP data	Compartment-specific (glomerular and tubule), as well as whole kidney eQTL discovery
Transcriptomics		
Gene Expression Omnibus (GEO) (http://www.ncbi.nlm.nih.gov/gds)	3848 data sets based on arrays and sequences; Storage of chips, second-generation sequencing and other high-throughput sequencing data	Gene expression data repository, data analysis and visualization
ArrayExpress (https://www.ebi.ac.uk/arrayexpress/)	60,054 high-throughput experiments; Storage of chips and high-throughput sequencing data	Arrayexpress database for EBI, similar to GEO database; Archives of Functional Genomics
Expression Atlas (https://www.ebi.ac.uk/gxa/)	1572 data sets; Provides information on gene expression patterns under different biological conditions	More focus on baseline trials
miRBase (http://www.mirbase.org)	28 645 miRNA entries from 223 species; Details of all published and annotated miRNAs	Databases used to study miRNA
Nephroseq (https://www.nephroseq.org/)*	26 data sets (1989 samples); Transcriptome analysis of biopsy samples from patients with renal disease; Clinical metadata from patients	Identifying disease-related signatures; Correlation of gene expression with clinical features
Renal Gene Expression Database (RGED) (http://rged.wall-eva.net/)*	88 research papers analysed; Contains comprehensive gene expression data sets from kidney disease studies	Contains comprehensive gene expression data sets from kidney disease studies; Provides a user-friendly utility for the nephropathy research community
Rebuilding a Kidney Consortium (http://www.rebuildingakidney.org)*	scRNA-seq visualizations from kidney biopsy samples, model systems and organoids; Shared resources with GUDMAP Lab protocols; Antibody validation; Cataloguing of iPSC lines	Coordinate studies and data relevant to nephron regeneration; Primary data access
Nephrocell (http://nephrocell.miktmc.org/)*	scRNA-seq data from kidney biopsy samples and organoids	Cell-selective gene marker identification
Proteomics		
PRoteomics IDEntifications (PRIDE) (https://www.ebi.ac.uk/pride/archive/)	Store 3342 items for protein/peptide identification, post-translational modifications, and supporting spectral evidence; One of the most prominent data repositories for proteomic data based on mass spectrometry (MS); Allows viewing of 2d gels and query scores	To enable the proteomics community to share publicly or in private partnerships the vast amounts of data generated by proteomics laboratories around the world.
Human Protein Atlas (http://www.proteinatlas.org/)	213 tissue and cell line samples; Proteomic analysis based on 24,028 antibodies against 16,975 unique proteins	To understand the expression of human protein in tissues, cell localization and pathological expression.
Human Kidney and Urine Proteome Project (HKUPP) (http://www.hkupp.org/)*	Look for proteins in renal structures (glomerulus, human medulla) and urine; Allows viewing of 2d gels and query scores	To promote proteomics research in the field of nephrology to better understand kidney function and the pathogenesis of kidney disease, and to define new biomarkers and therapeutic targets.
Urinary Protein Biomarker Database (http://122.70.220.102/biomarker)*	> 400 reports on humans and animals; 819 human biomarkers and 33 animal biomarkers were collected from the published literature	To obtain urinary protein specific biomarker candidates
Metabolomics		
Human Metabolome Database(HMDB) (http://www.hmdb.ca/)	Contains experimental MS/MS data for more than 5,700 compounds, experimental 1 H and 13 C NMR data (and allocation) for more than 1,300 compounds, and GC/MS spectral and retention index data for more than 780 compounds;	Obtain detailed information about metabolites and their associations with pathways, proteins, and reactions

(Continued)

TABLE 3 | Continued

Tool	Data types	Purpose
Kyoto Encyclopedia of Genes and Genomes (KEGG) (https://www.kegg.jp)	One of the most complete and widely used databases containing metabolic pathways (495 reference pathways) from a variety of organisms (>4,700)	Understand a repository of advanced features and utilities for biological systems;
	>17,000 compounds, 10,000 drugs and nearly 11,000 glycan structures	With powerful graphics function, more intuitive and comprehensive understanding of metabolic pathways
Metabolite Link (Metlin) (https://metlin.scripps.edu)	>240,000 metabolites and 72,000 high resolution MS/MS spectrograms; A repository of mass spectrometry metabolite data	Emphasis should be placed on the identification of non-targeted Metabolomics metabolites in liquid
The Small Molecule Pathway Database (SMPDB) (http://smpdb.ca/)	910 hand-painted small molecule metabolic pathways, including 468 drug pathways, 232 disease pathways, 105 metabolic pathways and more than 100 other pathways; A database of interactive, visual small molecular pathways	Cleverly detailed hyperlinked diagrams of human metabolic pathways, metabolic disease pathways, metabolite signaling pathways, and drug activity pathways
Multi-omics		
Multi-Omics Profiling Expression Database (MOPED) (http://moped.proteinspire.org)	Absolute and relative protein expression data from more than 250 large-scale experiments; >500,000 proteomic absolute and relative expression records; >500,000 proteomic absolute and relative expression records; Relative gene expression data	Used to query different types of omics expression data and data visualization; View expression data, pathway mapping, and direct connections between proteins and genes; Provides a background for the exploration of multiple omics expressive data
Kidney Systems Biology Project (https://hpcwebapps.cit.nih.gov/ESBL/Database/)*	Transcriptomic, protein, Chip-seq data from model systems and renal epithelial cells	Gene- and protein-centred queries in kidney tissues, cells and segments
Kidney and Urinary Pathway Knowledge Base (KUPKB) (http://www.kupkb.org/)*	> 220 experiments; Contains data from renal and urinary high-throughput experiments, with rich links to other biological data, forming a single integrated repository	Collect open omics data related to kidney disease

microenvironments and interactions, SA-AKI has different effects on various cells in the kidney. scRNA-seq enables researchers to detect highly variable genes (HVGS) between cells that contribute to mixed populations, which cannot be achieved by bulk RNA-seq (131). One of the significant challenges of the scRNA-seq data is matching the RNA profile with its location (spatial information) in the tissue (132). Spatial transcriptome sequencing provides complete tissue spatial location information, enabling spatial localization of different single-cell subpopulations by adding spatial information to scRNA-seq data, increasing understanding of specific cell subpopulations and their interactions in development, homeostasis, and disease (133).

Currently, there are few studies on single-cell RNA sequencing technology for SA-AKI. Ricardo Melo Ferreira et al. (134) used single-cell sequencing to deconvolution the signature of each spatial transcriptome point in the mouse CLP model to determine the co-localization mode between immune cells and epithelial cells. Spatial transcriptomics revealed that infiltrating macrophages dominate the exocortical features, and Mdk was identified as the corresponding chemokine, revealing the mechanisms driving immune cell infiltration and detecting associated cell subsets to complement single-cell sequencing. Danielle Janosevic et al. (135) provided a detailed and accurate view of the evolution of renal endotoxemia at the cellular and molecular levels by sequencing single-cell RENAL RNA in a mouse endotoxemia model, providing the first description of spatio-temporal endotoxin-induced transcriptome changes in the kidney. It reveals that the involvement of various cell populations is organized and highly coordinated in time, promoting the further investigation of human sepsis.

Artificial Intelligence

Artificial intelligence (AI) technology has emerged as doctors face the challenge of being overwhelmed by the amount of data generated in healthcare today (136). Artificial intelligence is a scientific discipline that aims to understand and design computer systems that display intellectual processes (137). Machine learning (ML), a subset of artificial intelligence, may detect disease onset before clinical symptoms appear, allowing for a more proactive approach (138). In machine learning, supervised learning and reinforcement learning are widely used (139).

In the narrative review of the clinical application of artificial intelligence in sepsis, 15 articles about the use of AI model to diagnose sepsis, the model with the best performance reached 0.97 AUROC; 7 prognostic articles, predicting mortality over time with an AUROC of up to 0.895; 3 articles on helping to treat sepsis, in which AI use was associated with the lowest mortality (140). Kumardeep Chaudhary et al. (141) used deep learning to identify the septicemic AKI subtype unknowingly and inexplicably from routinely collected data from electronic health records is the first study to use routinely collected electronic health record data to identify the clinical subtype of SA-AKI syndrome in the ICU. When combined with other biomarkers and omics data, this approach could further accelerate research into the discovering of new biomarkers and dysregulation pathways for SA-AKI.

At present, the comprehensive performance evaluation of machine learning models is limited by research heterogeneity. In addition, because clinical implementation of models is rare, there is an urgent need to determine the clinical impact on different patient populations to ensure universality (142).

CONCLUSIONS

Despite significant advances in our understanding of the pathophysiology and detection markers of SA-AKI, it remains a common and highly hazardous complication of the critically ill disease. The development of multiple omics studies, which have increased the availability of kidney tissue, blood and urine samples, and patient data, has provided a tremendous opportunity to increase our understanding of SA-AKI. As the cost of omics analysis continues to decrease, the emergence of more types of omics techniques and studies integrating multiple omics techniques can be integrated into the clinic and guide the personalized treatment of SA-AKI. Such advances, however, will require a more careful selection of models and research techniques to study the effects of this molecular involvement on SA-AKI in greater detail, addressing the common challenges of omics in distinguishing causal and reactive changes in the context of disease.

AUTHOR CONTRIBUTIONS

JQ designed and wrote the review, drew the figures and tables. LC revised this manuscript and reviewed the figures and tables. All authors contributed to the article and approved the submitted version.

FUNDING

National Natural Science Foundation of China (61771022), Key Clinical Specialty Funding Project of Beijing.

REFERENCES

1. Stanski NL, Wong HR. Prognostic and Predictive Enrichment in Sepsis. *Nat Rev Nephrol* (2020) 16(1):20–31. doi: 10.1038/s41581-019-0199-3
2. Singer M, Deutschman CS, Seymour CW, Shankar-Hari M, Annane D, Bauer M, et al. The Third International Consensus Definitions for Sepsis and Septic Shock (Sepsis-3). *JAMA* (2016) 315(8):801–10. doi: 10.1001/jama.2016.0287
3. Bellomo R, Kellum JA, Ronco C, Wald R, Martensson J, Maiden M, et al. Acute Kidney Injury in Sepsis. *Intensive Care Med* (2017) 43(6):816–28. doi: 10.1007/s00134-017-4755-7
4. Godin M, Murray P, Mehta RL. Clinical Approach to the Patient With AKI and Sepsis. *Semin Nephrol* (2015) 35(1):12–22. doi: 10.1016/j.semnephrol.2015.01.003
5. Ronco C, Bellomo R, Kellum JA. Acute Kidney Injury. *Lancet* (2019) 394 (10212):1949–64. doi: 10.1016/S0140-6736(19)32563-2
6. Thomas ME, Blaine C, Dawnay A, Devonald MA, Ftouh S, Laing C, et al. The Definition of Acute Kidney Injury and its Use in Practice. *Kidney Int* (2015) 87(1):62–73. doi: 10.1038/ki.2014.328
7. Hollenberg SM, Singer M. Pathophysiology of Sepsis-Induced Cardiomyopathy. *Nat Rev Cardiol* (2021) 18(6):424–34. doi: 10.1038/s41569-020-00492-2
8. Font MD, Thyagarajan B, Khanna AK. Sepsis and Septic Shock - Basics of Diagnosis, Pathophysiology and Clinical Decision Making. *Med Clin North Am* (2020) 104(4):573–85. doi: 10.1016/j.mcna.2020.02.011
9. Adhikari NK, Fowler RA, Bhagwanjee S, Rubenfeld GD. Critical Care and the Global Burden of Critical Illness in Adults. *Lancet* (2010) 376 (9749):1339–46. doi: 10.1016/S0140-6736(10)60446-1
10. Uchino S, Kellum JA, Bellomo R, Doig GS, Morimatsu H, Morgera S, et al. Acute Renal Failure in Critically Ill Patients: A Multinational, Multicenter Study. *JAMA* (2005) 294(7):813–8. doi: 10.1001/jama.294.7.813
11. Mehta RL, Bouchard J, Soroko SB, Ikizler TA, Paganini EP, Chertow GM, et al. Sepsis as a Cause and Consequence of Acute Kidney Injury: Program to Improve Care in Acute Renal Disease. *Intensive Care Med* (2011) 37(2):241–8. doi: 10.1007/s00134-010-2089-9
12. Sood MM, Shafer LA, Ho J, Reslerova M, Martinka G, Keenan S, et al. Early Reversible Acute Kidney Injury is Associated With Improved Survival in Septic Shock. *J Crit Care* (2014) 29(5):711–7. doi: 10.1016/j.jcrc.2014.04.003
13. Lima RS, Marques CN, Silva Júnior GB, Barbosa AS, Barbosa ES, Mota RM, et al. Comparison Between Early and Delayed Acute Kidney Injury Secondary to Infectious Disease in the Intensive Care Unit. *Int Urol Nephrol* (2008) 40(3):731–9. doi: 10.1007/s11255-008-9352-9
14. Bagshaw SM, George C, Bellomo R. ANZICS Database Management Committee. Early Acute Kidney Injury and Sepsis: A Multicentre Evaluation. *Crit Care* (2008) 12(2):R47. doi: 10.1186/cc6863
15. Bagshaw SM, Lapinsky S, Dial S, Arabi Y, Dodek P, Wood G, et al. Acute Kidney Injury in Septic Shock: Clinical Outcomes and Impact of Duration of Hypotension Prior to Initiation of Antimicrobial Therapy. *Intensive Care Med* (2009) 35(5):871–81. doi: 10.1007/s00134-008-1367-2
16. Cruz MG, Dantas JG, Levi TM, Rocha Mde S, de Souza SP, Boa-Sorte N, et al. Septic Versus non-Septic Acute Kidney Injury in Critically Ill Patients: Characteristics and Clinical Outcomes. *Rev Bras Ter Intensiva* (2014) 26 (4):384–91. doi: 10.5935/0103-507X.20140059
17. Bagshaw SM, Uchino S, Bellomo R, Morimatsu H, Morgera S, Schetz M, et al. Septic Acute Kidney Injury in Critically Ill Patients: Clinical Characteristics and Outcomes. *Clin J Am Soc Nephrol* (2007) 2(3):431–9. doi: 10.2215/CJN.03681106
18. Kellum JA, Chawla LS, Keener C, Singbartl K, Palevsky PM, Pike FL, et al. The Effects of Alternative Resuscitation Strategies on Acute Kidney Injury in Patients With Septic Shock. *Am J Respir Crit Care Med* (2016) 193(3):281–7. doi: 10.1164/rccm.201505-0995OC
19. Chua HR, Wong WK, Ong VH, Agrawal D, Vathsala A, Tay HM, et al. Extended Mortality and Chronic Kidney Disease After Septic Acute Kidney Injury. *J Intensive Care Med* (2020) 35(6):527–35. doi: 10.1177/0885066618764617
20. Poston JT, Koyner JL. Sepsis Associated Acute Kidney Injury. *BMJ* (2019) 364:k4891. doi: 10.1136/bmj.k4891
21. Coquerel D, Lamoureux J, Chagnon F, Trân K, Sage M, Fortin-Pellerin E, et al. Apelin-13 in Septic Shock: Effective in Supporting Hemodynamics in Sheep But Compromised by Enzymatic Breakdown in Patients. *Sci Rep* (2021) 11(1):22770. doi: 10.1038/s41598-021-02087-4
22. Seok J, Warren HS, Cuenca AG, Mindrinos MN, Baker HV, Xu W, et al. Genomic Responses in Mouse Models Poorly Mimic Human Inflammatory Diseases. *Proc Natl Acad Sci USA* (2013) 110(9):3507–12. doi: 10.1073/pnas.1222878110
23. Huang J, Bayliss G, Zhuang S. Porcine Models of Acute Kidney Injury. *Am J Physiol Renal Physiol* (2021) 320(6):F1030–44. doi: 10.1152/ajprenal.00022.2021
24. Horn DL, Morrison DC, Opal SM, Silverstein R, Visvanathan K, Zabriskie JB. What are the Microbial Components Implicated in the Pathogenesis of Sepsis? Report on a Symposium. *Clin Infect Dis* (2000) 31(4):851–8. doi: 10.1086/318127
25. Walker JM, Sundarasivarao PYK, Thornton JM, Sochacki K, Rodriguez A, Spur BW, et al. Resolvin D2 Promotes Host Defense in a 2 - Hit Model of

Sepsis With Secondary Lung Infection. *Prostaglandins Other Lipid Mediat* (2022) 159:106617. doi: 10.1016/j.prostaglandins.2022.106617
26. Unsinger J, Burnham CA, McDonough J, Morre M, Prakash PS, Caldwell CC, et al. Interleukin-7 Ameliorates Immune Dysfunction and Improves Survival in a 2-Hit Model of Fungal Sepsis. *J Infect Dis* (2012) 206(4):606–16. doi: 10.1093/infdis/jis383
27. Gentile LF, Nacionales DC, Cuenca AG, Armbruster M, Ungaro RF, Abouhamze AS, et al. Identification and Description of a Novel Murine Model for Polytrauma and Shock. *Crit Care Med* (2013) 41(4):1075–85. doi: 10.1097/CCM.0b013e318275d1f9
28. Drechsler S, Zipperle J, Rademann P, Jafarmadar M, Klotz A, Bahrami S, et al. Splenectomy Modulates Early Immuno-Inflammatory Responses to Trauma-Hemorrhage and Protects Mice Against Secondary Sepsis. *Sci Rep* (2018) 8(1):14890. doi: 10.1038/s41598-018-33232-1
29. Doi K, Leelahavanichkul A, Hu X, Sidransky KL, Zhou H, Qin Y, et al. Pre-Existing Renal Disease Promotes Sepsis-Induced Acute Kidney Injury and Worsens Outcome. *Kidney Int* (2008) 74(8):1017–25. doi: 10.1038/ki.2008.346
30. Li C, Wang W, Xie SS, Ma WX, Fan QW, Chen Y, et al. The Programmed Cell Death of Macrophages, Endothelial Cells, and Tubular Epithelial Cells in Sepsis-AKI. *Front Med (Lausanne)* (2021) 8:796724. doi: 10.3389/fmed.2021.796724
31. Alobaidi R, Basu RK, Goldstein SL, Bagshaw SM. Sepsis-Associated Acute Kidney Injury. *Semin Nephrol* (2015) 35(1):2–11. doi: 10.1016/j.semnephrol.2015.01.002
32. Crayne CB, Albeituni S, Nichols KE, Cron RQ. The Immunology of Macrophage Activation Syndrome. *Front Immunol* (2019) 10:119. doi: 10.3389/fimmu.2019.00119
33. Kalakeche R, Hato T, Rhodes G, Dunn KW, El-Achkar TM, Plotkin Z, et al. Endotoxin Uptake by S1 Proximal Tubular Segment Causes Oxidative Stress in the Downstream S2 Segment. *J Am Soc Nephrol* (2011) 22(8):1505–16. doi: 10.1681/ASN.2011020203
34. Timmermans K, Kox M, Scheffer GJ, Pickkers P. Danger in the Intensive Care Unit: Damps in Critically Ill Patients. *Shock* (2016) 45(2):108–16. doi: 10.1097/SHK.0000000000000506
35. Ma KC, Schenck EJ, Pabon MA, Choi AMK. The Role of Danger Signals in the Pathogenesis and Perpetuation of Critical Illness. *Am J Respir Crit Care Med* (2018) 197(3):300–9. doi: 10.1164/rccm.201612-2460PP
36. Ferenbach DA, Bonventre JV. Mechanisms of Maladaptive Repair After AKI Leading to Accelerated Kidney Ageing and CKD. *Nat Rev Nephrol* (2015) 11(5):264–76. doi: 10.1038/nrneph.2015.3
37. Simons M, Gordon E, Claesson-Welsh L. Mechanisms and Regulation of Endothelial VEGF Receptor Signalling. *Nat Rev Mol Cell Biol* (2016) 17(10):611–25. doi: 10.1038/nrm.2016.87
38. Ince C, Mayeux PR, Nguyen T, Gomez H, Kellum JA, Ospina-Tascón GA, et al. The Endothelium in Sepsis. *Shock* (2016) 45(3):259–70. doi: 10.1097/SHK.0000000000000473
39. Raymond SL, Holden DC, miRa JC, Stortz JA, Loftus TJ, Mohr AM, et al. Microbial Recognition and Danger Signals in Sepsis and Trauma. *Biochim Biophys Acta Mol Basis Dis* (2017) 1863(10 Pt B):2564–73. doi: 10.1016/j.bbadis.2017.01.013
40. Gomez H, Ince C, De Backer D, Pickkers P, Payen D, Hotchkiss J, et al. A Unified Theory of Sepsis-Induced Acute Kidney Injury: Inflammation, Microcirculatory Dysfunction, Bioenergetics, and the Tubular Cell Adaptation to Injury. *Shock* (2014) 41(1):3–11. doi: 10.1097/SHK.0000000000000052
41. Cianciolo Cosentino C, Skrypnyk NI, Brilli LL, Chiba T, Novitskaya T, Woods C, et al. Histone Deacetylase Inhibitor Enhances Recovery After AKI. *J Am Soc Nephrol* (2013) 24(6):943–53. doi: 10.1681/ASN.2012111055
42. Houten SM, Violante S, Ventura FV, Wanders RJ. The Biochemistry and Physiology of Mitochondrial Fatty Acid β-Oxidation and Its Genetic Disorders. *Annu Rev Physiol* (2016) 78:23–44. doi: 10.1146/annurev-physiol-021115-105045
43. Patil NK, Parajuli N, MacMillan-Crow LA, Mayeux PR. Inactivation of Renal Mitochondrial Respiratory Complexes and Manganese Superoxide Dismutase During Sepsis: Mitochondria- Targeted Antioxidant Mitigates Injury. *Am J Physiol Renal Physiol* (2014) 306(7):F734–43. doi: 10.1152/ajprenal.00643.2013
44. Escobar DA, Botero-Quintero AM, Kautza BC, Luciano J, Loughran P, Darwiche S, et al. Adenosine Monophosphate-Activated Protein Kinase Activation Protects Against Sepsis-Induced Organ Injury and Inflammation. *J Surg Res* (2015) 194(1):262–72. doi: 10.1016/j.jss.2014.10.009
45. Cheng SC, Scicluna BP, Arts RJ, Gresnigt MS, Lachmandas E, Giamarellos-Bourboulis EJ, et al. Broad Defects in the Energy Metabolism of Leukocytes Underlie Immunoparalysis in Sepsis. *Nat Immunol* (2016) 17(4):406–13. doi: 10.1038/ni.3398
46. Novakovic B, Habibi E, Wang SY, Arts RJW, Davar R, Megchelenbrink W, et al. β-Glucan Reverses the Epigenetic State of LPS-Induced Immunological Tolerance. *Cell* (2016) 167(5):1354–68.e14. doi: 10.1016/j.cell.2016.09.034
47. Vachharajani VT, Liu T, Brown CM, Wang X, Buechler NL, Wells JD, et al. SIRT1 Inhibition During the Hypoinflammatory Phenotype of Sepsis Enhances Immunity and Improves Outcome. *J Leukoc Biol* (2014) 96(5):785–96. doi: 10.1189/jlb.3MA0114-034RR
48. Howell MD, Davis AM. Management of Sepsis and Septic Shock. *JAMA* (2017) 317(8):847–8. doi: 10.1001/jama.2017.0131
49. Tumlin JA, Murugan R, Deane AM, Ostermann M, Busse LW, Ham KR, et al. Outcomes in Patients With Vasodilatory Shock and Renal Replacement Therapy Treated With Intravenous Angiotensin Ii. *Crit Care Med* (2018) 46(6):949–57. doi: 10.1097/CCM.0000000000003092
50. Gordon AC, Mason AJ, Thirunavukkarasu N, Perkins GD, Cecconi M, Cepkova M, et al. Effect of Early Vasopressin vs Norepinephrine on Kidney Failure in Patients With Septic Shock: The VANISH Randomized Clinical Trial. *JAMA* (2016) 316(5):509–18. doi: 10.1001/jama.2016.10485
51. Khanna A, English SW, Wang XS, Ham K, Tumlin J, Szerlip H, et al. Angiotensin II for the Treatment of Vasodilatory Shock. *N Engl J Med* (2017) 377(5):419–30. doi: 10.1056/NEJMoa1704154
52. Pickkers P, Mehta RL, Murray PT, Joannidis M, Molitoris BA, Kellum JA, et al. Effect of Human Recombinant Alkaline Phosphatase on 7-Day Creatinine Clearance in Patients With Sepsis-Associated Acute Kidney Injury: A Randomized Clinical Trial. *JAMA* (2018) 320(19):1998–2009. doi: 10.1001/jama.2018.14283
53. Moskowitz A, Andersen LW, Cocchi MN, Karlsson M, Patel PV, Donnino MW. Thiamine as a Renal Protective Agent in Septic Shock. A Secondary Analysis of a Randomized, Double-Blind, Placebo-Controlled Trial. *Ann Am Thorac Soc* (2017) 14(5):737–41. doi: 10.1513/AnnalsATS.201608-656BC
54. Lee SY, Lee YS, Choi HM, Ko YS, Lee HY, Jo SK, et al. Distinct Pathophysiologic Mechanisms of Septic Acute Kidney Injury: Role of Immune Suppression and Renal Tubular Cell Apoptosis in Murine Model of Septic Acute Kidney Injury. *Crit Care Med* (2012) 40(11):2997–3006. doi: 10.1097/CCM.0b013e31825b912d
55. Pannu N, Gibney RN. Renal Replacement Therapy in the Intensive Care Unit. *Ther Clin Risk Manag* (2005) 1(2):141–50. doi: 10.2147/tcrm.1.2.141.62908
56. RENAL Replacement Therapy Study Investigators, Bellomo R, Cass A, Cole L, Finfer S, Gallagher M, et al. Intensity of Continuous Renal-Replacement Therapy in Critically Ill Patients. *N Engl J Med* (2009) 361(17):1627–38. doi: 10.1056/NEJMoa0902413
57. Agapito Fonseca J, Gameiro J, Marques F, Lopes JA. Timing of Initiation of Renal Replacement Therapy in Sepsis-Associated Acute Kidney Injury. *J Clin Med* (2020) 9(5):1413. doi: 10.3390/jcm9051413
58. Yadav SP. The Wholeness in Suffix -Omics, -Omes, and the Word Om. *J Biomol Tech* (2007) 18(5):277.
59. Olivier M, Asmis R, Hawkins GA, Howard TD, Cox LA. The Need for Multi-Omics Biomarker Signatures in Precision Medicine. *Int J Mol Sci* (2019) 20(19):4781. doi: 10.3390/ijms20194781
60. Frank AJ, Sheu CC, Zhao Y, Chen F, Su L, Gong MN, et al. BCL2 Genetic Variants are Associated With Acute Kidney Injury in Septic Shock. *Crit Care Med* (2012) 40(7):2116–23. doi: 10.1097/CCM.0b013e3182514bca
61. Vilander LM, Kaunisto MA, Vaara ST, Pettilä VFINNAKI study group. Genetic Variants in SERPINA4 and SERPINA5, But Not BCL2 and SIK3 are Associated With Acute Kidney Injury in Critically Ill Patients With Septic Shock. *Crit Care* (2017) 21(1):47. doi: 10.1186/s13054-017-1631-3
62. Genga KR, Trinder M, Kong HJ, Li X, Leung AKK, Shimada T, et al. CETP Genetic Variant Rs1800777 (Allele A) is Associated With Abnormally Low HDL-C Levels and Increased Risk of AKI During Sepsis. *Sci Rep* (2018) 8(1):16764. doi: 10.1038/s41598-018-35261-2
63. Vilander LM, Vaara ST, Donner KM, Lakkisto P, Kaunisto MA, Pettilä V, et al. Heme Oxygenase-1 Repeat Polymorphism in Septic Acute Kidney Injury. *PLoS One* (2019) 14(5):e0217291. doi: 10.1371/journal.pone.0217291

64. Sun J, Cai X, Shen J, Jin G, Xie Q. Correlation Between Single Nucleotide Polymorphisms at the 3'-UTR of the NFKB1 Gene and Acute Kidney Injury in Sepsis. *Genet Test Mol Biomarkers* (2020) 24(5):274–84. doi: 10.1089/gtmb.2019.0222
65. Tran M, Tam D, Bardia A, Bhasin M, Rowe GC, Kher A, et al. PGC-1α Promotes Recovery After Acute Kidney Injury During Systemic Inflammation in Mice. *J Clin Invest* (2011) 121(10):4003–14. doi: 10.1172/JCI58662
66. Basu RK, Standage SW, Cvijanovich NZ, Allen GL, Thomas NJ, Freishtat RJ, et al. Identification of Candidate Serum Biomarkers for Severe Septic Shock-Associated Kidney Injury *via* Microarray. *Crit Care* (2011) 15(6):R273. doi: 10.1186/cc10554
67. Ge QM, Huang CM, Zhu XY, Bian F, Pan SM. Differentially Expressed miRNAs in Sepsis-Induced Acute Kidney Injury Target Oxidative Stress and Mitochondrial Dysfunction Pathways. *PLoS One* (2017) 12(3):e0173292. doi: 10.1371/journal.pone.0173292
68. Hultström M, Becirovic-Agic M, Jönsson S. Comparison of Acute Kidney Injury of Different Etiology Reveals in-Common Mechanisms of Tissue Damage. *Physiol Genomics* (2018) 50(3):127–41. doi: 10.1152/physiolgenomics.00037.2017
69. Tod P, Róka B, Kaucsár T, Szatmári K, Vizovišek M, Vidmar R, et al. Time-Dependent miRNA Profile During Septic Acute Kidney Injury in Mice. *Int J Mol Sci* (2020) 21(15):5316. doi: 10.3390/ijms21155316
70. Holly MK, Dear JW, Hu X, Schechter AN, Gladwin MT, Hewitt SM, et al. Biomarker and Drug-Target Discovery Using Proteomics in a New Rat Model of Sepsis-Induced Acute Renal Failure. *Kidney Int* (2006) 70(3):496–506. doi: 10.1038/sj.ki.5001575
71. Maddens B, Ghesquière B, Vanholder R, Demon D, Vanmassenhove J, Gevaert K, et al. Chitinase-Like Proteins are Candidate Biomarkers for Sepsis-Induced Acute Kidney Injury. *Mol Cell Proteomics* (2012) 11(6):M111.013094. doi: 10.1074/mcp.M111.013094
72. Wu F, Dong XJ, Li YY, Zhao Y, Xu QL, Su L. Identification of Phosphorylated MYL12B as a Potential Plasma Biomarker for Septic Acute Kidney Injury Using a Quantitative Proteomic Approach. *Int J Clin Exp Pathol* (2015) 8(11):14409–16.
73. Hinkelbein J, Böhm L, Braunecker S, Adler C, De Robertis E, Cirillo F. Decreased Tissue COX5B Expression and Mitochondrial Dysfunction During Sepsis-Induced Kidney Injury in Rats. *Oxid Med Cell Longev* (2017) 2017:8498510. doi: 10.1155/2017/8498510
74. Hashida T, Nakada TA, Satoh M, Tomita K, Kawaguchi R, Nomura F, et al. Proteome Analysis of Hemofilter Adsorbates to Identify Novel Substances of Sepsis: A Pilot Study. *J Artif Organs* (2017) 20(2):132–7. doi: 10.1007/s10047-016-0936-3
75. Li Y, Long J, Chen J, Zhang J, Qin Y, Zhong Y, et al. Analysis of Spatiotemporal Urine Protein Dynamics to Identify New Biomarkers for Sepsis-Induced Acute Kidney Injury. *Front Physiol* (2020) 11:139. doi: 10.3389/fphys.2020.00139
76. Lin YH, Platt MP, Fu H, Gui Y, Wang Y, Gonzalez-Juarbe N, et al. Global Proteome and Phosphoproteome Characterization of Sepsis-Induced Kidney Injury. *Mol Cell Proteomics* (2020) 19(12):2030–47. doi: 10.1074/mcp.RA120.002235
77. Waltz P, Carchman E, Gomez H, Zuckerbraun B. Sepsis Results in an Altered Renal Metabolic and Osmolyte Profile. *J Surg Res* (2016) 202(1):8–12. doi: 10.1016/j.jss.2015.12.011
78. Li P, Liao ST, Wang JS, Zhang Q, Xu DQ, Lv Y, et al. Protection by Huang-Lian-Jie-Du Decoction and its Constituent Herbs of Lipopolysaccharide-Induced Acute Kidney Injury. *FEBS Open Bio* (2017) 7(2):221–36. doi: 10.1002/2211-5463.12178
79. Rodrigues FAP, Santos ADDC, de Medeiros PHQS, Prata MMG, Santos TCS, da Silva JA, et al. Gingerol Suppresses Sepsis-Induced Acute Kidney Injury by Modulating Methylsulfonylmethane and Dimethylamine Production. *Sci Rep* (2018) 8(1):12154. doi: 10.1038/s41598-018-30522-6
80. Izquierdo-Garcia JL, Nin N, Cardinal-Fernandez P, Rojas Y, de Paula M, Granados R, et al. Identification of Novel Metabolomic Biomarkers in an Experimental Model of Septic Acute Kidney Injury. *Am J Physiol Renal Physiol* (2019) 316(1):F54–62. doi: 10.1152/ajprenal.00315.2018
81. Ping F, Guo Y, Cao Y, Shang J, Yao S, Zhang J, et al. Metabolomics Analysis of the Renal Cortex in Rats With Acute Kidney Injury Induced by Sepsis. *Front Mol Biosci* (2019) 6:152. doi: 10.3389/fmolb.2019.00152
82. Lin SH, Fan J, Zhu J, Zhao YS, Wang CJ, Zhang M, et al. Exploring Plasma Metabolomic Changes in Sepsis: A Clinical Matching Study Based on Gas Chromatography-Mass Spectrometry. *Ann Transl Med* (2020) 8(23):1568. doi: 10.21037/atm-20-3562
83. Hasson D, Goldstein SL, Standage SW. The Application of Omic Technologies to Research in Sepsis- Associated Acute Kidney Injury. *Pediatr Nephrol* (2021) 36(5):1075–86. doi: 10.1007/s00467-020-04557-9
84. Binnie A, Walsh CJ, Hu P, Dwivedi DJ, Fox-Robichaud A, Liaw PC, et al. Epigenetic Profiling in Severe Sepsis: A Pilot Study of DNA Methylation Profiles in Critical Illness. *Crit Care Med* (2020) 48(2):142–50. doi: 10.1097/CCM.0000000000004097
85. Zhang W, Guan Y, Bayliss G, Zhuang S. Class IIa HDAC Inhibitor TMP195 Alleviates Lipopolysaccharide- Induced Acute Kidney Injury. *Am J Physiol Renal Physiol* (2020) 319(6):F1015–26. doi: 10.1152/ajprenal.00405.2020
86. Ha ZL, Yu ZY. Downregulation of miR-29b-3p Aggravates Podocyte Injury by Targeting HDAC4 in LPS-Induced Acute Kidney Injury. *Kaohsiung J Med Sci* (2021) 37(12):1069–76. doi: 10.1002/kjm2.12431
87. Assis A, Oliveira E, Donate P, Giuliatti S, Nguyen C, Passos G. What Is the Transcriptome and How it is Evaluated? In: G Passos, editor. *Transcriptomics in Health and Disease*. Springer, Cham (2014). doi: 10.1007/978-3-319-11985-4_1
88. Washburn MP, Koller A, Oshiro G, Ulaszek RR, Plouffe D, Deciu C, et al. Protein Pathway and Complex Clustering of Correlated mRNA and Protein Expression Analyses in Saccharomyces Cerevisiae. *Proc Natl Acad Sci USA* (2003) 100(6):3107–12. doi: 10.1073/pnas.0634629100
89. Sharma NK, Salomao R. Sepsis Through the Eyes of Proteomics: The Progress in the Last Decade. *Shock* (2017) 47(1S Suppl 1):17–25. doi: 10.1097/SHK.0000000000000698
90. Marx D, Metzger J, Pejchinovski M, Gil RB, Frantzi M, Latosinska A, et al. Proteomics and Metabolomics for AKI Diagnosis. *Semin Nephrol* (2018) 38(1):63–87. doi: 10.1016/j.semnephrol.2017.09.007
91. Dona AC, Jiménez B, Schäfer H, Humpfer E, Spraul M, Lewis MR, et al. Precision High-Throughput Proton NMR Spectroscopy of Human Urine, Serum, and Plasma for Large-Scale Metabolic Phenotyping. *Anal Chem* (2014) 86(19):9887–94. doi: 10.1021/ac5025039
92. Forcisi S, Moritz F, Kanawati B, Tziotis D, Lehmann R, Schmitt-Kopplin P. Liquid Chromatography-Mass Spectrometry in Metabolomics Research: Mass Analyzers in Ultra High Pressure Liquid Chromatography Coupling. *J Chromatogr A* (2013) 1292:51–65. doi: 10.1016/j.chroma.2013.04.017
93. Husain-Syed F, Slutsky AS, Ronco C. Lung-Kidney Cross-Talk in the Critically Ill Patient. *Am J Respir Crit Care Med* (2016) 194(4):402–14. doi: 10.1164/rccm.201602-0420CP
94. Husain-Syed F, McCullough PA, Birk HW, Renker M, Brocca A, Seeger W, et al. Cardio-Pulmonary-Renal Interactions: A Multidisciplinary Approach. *J Am Coll Cardiol* (2015) 65(22):2433–48. doi: 10.1016/j.jacc.2015.04.024
95. Husain-Syed F, Rosner MH, Ronco C. Distant Organ Dysfunction in Acute Kidney Injury. *Acta Physiol (Oxf)* (2020) 228(2):e13357. doi: 10.1111/apha.13357
96. Harris PL, Umberger RA. Long-Term Renal Outcomes in Adults With Sepsis-Induced Acute Kidney Injury: A Systematic Review. *Dimens Crit Care Nurs* (2020) 39(5):259–68. doi: 10.1097/DCC.0000000000000432
97. Kaballo MA, Elsayed ME, Stack AG. Linking Acute Kidney Injury to Chronic Kidney Disease: The Missing Links. *J Nephrol* (2017) 30(4):461–75. doi: 10.1007/s40620-016-0359-5
98. Basile DP, Bonventre JV, Mehta R, Nangaku M, Unwin R, Rosner MH, et al. Progression After AKI: Understanding Maladaptive Repair Processes to Predict and Identify Therapeutic Treatments. *J Am Soc Nephrol* (2016) 27(3):687–97. doi: 10.1681/ASN.2015030309
99. McCullough PA, Shaw AD, Haase M, Bouchard J, Waikar SS, Siew ED, et al. Diagnosis of Acute Kidney Injury Using Functional and Injury Biomarkers: Workgroup Statements From the Tenth Acute Dialysis Quality Initiative Consensus Conference. *Contrib Nephrol* (2013) 182:13–29. doi: 10.1159/000349963
100. Chawla LS, Seneff MG, Nelson DR, Williams M, Levy H, Kimmel PL, et al. Elevated Plasma Concentrations of IL-6 and Elevated APACHE II Score Predict Acute Kidney Injury in Patients With Severe Sepsis. *Clin J Am Soc Nephrol* (2007) 2(1):22–30. doi: 10.2215/CJN.02510706
101. Tao X, Chen C, Luo W, Zhou J, Tian J, Yang X, et al. Combining Renal Cell Arrest and Damage Biomarkers to Predict Progressive AKI in Patient With Sepsis. *BMC Nephrol* (2021) 22(1):415. doi: 10.1186/s12882-021-02611-8

102. Dai X, Zeng Z, Fu C, Zhang S, Cai Y, Chen Z. Diagnostic Value of Neutrophil Gelatinase-Associated Lipocalin, Cystatin C, and Soluble Triggering Receptor Expressed on Myeloid Cells-1 in Critically Ill Patients With Sepsis-Associated Acute Kidney Injury. *Crit Care* (2015) 19(1):223. doi: 10.1186/s13054-015-0941-6
103. Hall E, Brookes ZL. Angiopoietin-1 Increases Arteriolar Vasoconstriction to Phenylephrine During Sepsis. *Regul Pept* (2005) 131(1-3):34–7. doi: 10.1016/j.regpep.2005.06.006
104. Giuliano JSJr, Lahni PM, Harmon K, Wong HR, Doughty LA, Carcillo JA, et al. Admission Angiopoietin Levels in Children With Septic Shock. *Shock* (2007) 28(6):650–4.
105. Kümpers P, Hafer C, David S, Hecker H, Lukasz A, Fliser D, et al. Angiopoietin-2 in Patients Requiring Renal Replacement Therapy in the ICU: Relation to Acute Kidney Injury, Multiple Organ Dysfunction Syndrome and Outcome. *Intensive Care Med* (2010) 36(3):462–70. doi: 10.1007/s00134-009-1726-7
106. Yu WK, McNeil JB, Wickersham NE, Shaver CM, Bastarache JA, Ware LB. Vascular Endothelial Cadherin Shedding is More Severe in Sepsis Patients With Severe Acute Kidney Injury. *Crit Care* (2019) 23(1):18. doi: 10.1186/s13054-019-2315-y
107. Katayama S, Nunomiya S, Koyama K, Wada M, Koinuma T, Goto Y, et al. Markers of Acute Kidney Injury in Patients With Sepsis: The Role of Soluble Thrombomodulin. *Crit Care* (2017) 21(1):229. doi: 10.1186/s13054-017-1815-x
108. Bagshaw SM, Bennett M, Haase M, Haase-Fielitz A, Egi M, Morimatsu H, et al. Plasma and Urine Neutrophil Gelatinase-Associated Lipocalin in Septic Versus non-Septic Acute Kidney Injury in Critical Illness. *Intensive Care Med* (2010) 36(3):452–61. doi: 10.1007/s00134-009-1724-9
109. Zhang CF, Wang HJ, Tong ZH, Zhang C, Wang YS, Yang HQ, et al. The Diagnostic and Prognostic Values of Serum and Urinary Kidney Injury Molecule-1 and Neutrophil Gelatinase-Associated Lipocalin in Sepsis Induced Acute Renal Injury Patients. *Eur Rev Med Pharmacol Sci* (2020) 24(10):5604–17. doi: 10.26355/eurrev_202005_21346
110. Aydoğdu M, Gürsel G, Sancak B, Yeni S, Sarı G, Taşyürek S, et al. The Use of Plasma and Urine Neutrophil Gelatinase Associated Lipocalin (NGAL) and Cystatin C in Early Diagnosis of Septic Acute Kidney Injury in Critically Ill Patients. *Dis Markers* (2013) 34(4):237–46. doi: 10.3233/DMA-130966
111. Mårtensson J, Martling CR, Oldner A, Bell M. Impact of Sepsis on Levels of Plasma Cystatin C in AKI and non-AKI Patients. *Nephrol Dial Transplant* (2012) 27(2):576–81. doi: 10.1093/ndt/gfr358
112. Li Y, Li X, Zhou X, Yan J, Zhu X, Pan J, et al. Impact of Sepsis on the Urinary Level of Interleukin-18 and Cystatin C in Critically Ill Neonates. *Pediatr Nephrol* (2013) 28(1):135–44. doi: 10.1007/s00467-012-2285-7
113. Honore PM, Nguyen HB, Gong M, Chawla LS, Bagshaw SM, Artigas A, et al. Urinary Tissue Inhibitor of Metalloproteinase-2 and Insulin-Like Growth Factor-Binding Protein 7 for Risk Stratification of Acute Kidney Injury in Patients With Sepsis. *Crit Care Med* (2016) 44(10):1851–60. doi: 10.1097/CCM.0000000000001827
114. Mårtensson J, Bellomo R. The Rise and Fall of NGAL in Acute Kidney Injury. *Blood Purif* (2014) 37(4):304–10. doi: 10.1159/000364937
115. Zhang A, Cai Y, Wang PF, Qu JN, Luo ZC, Chen XD, et al. Diagnosis and Prognosis of Neutrophil Gelatinase-Associated Lipocalin for Acute Kidney Injury With Sepsis: A Systematic Review and Meta-Analysis. *Crit Care* (2016) 20:41. doi: 10.1186/s13054-016-1212-x
116. Kim S, Kim HJ, Ahn HS, Song JY, Um TH, Cho CR, et al. Is Plasma Neutrophil Gelatinase- Associated Lipocalin a Predictive Biomarker for Acute Kidney Injury in Sepsis Patients? A Systematic Review and Meta-Analysis. *J Crit Care* (2016) 33:213–23. doi: 10.1016/j.jcrc.2016.02.014
117. Yamashita T, Doi K, Hamasaki Y, Matsubara T, Ishii T, Yahagi N, et al. Evaluation of Urinary Tissue Inhibitor of Metalloproteinase-2 in Acute Kidney Injury: A Prospective Observational Study. *Crit Care* (2014) 18 (6):716. doi: 10.1186/s13054-014-0716-5
118. Kashani K, Al-Khafaji A, Ardiles T, Artigas A, Bagshaw SM, Bell M, et al. Discovery and Validation of Cell Cycle Arrest Biomarkers in Human Acute Kidney Injury. *Crit Care* (2013) 17(1):R25. doi: 10.1186/cc12503
119. Fiorentino M, Xu Z, Smith A, Singbartl K, Palevsky PM, Chawla LS, et al. Serial Measurement of Cell-Cycle Arrest Biomarkers [TIMP-2]•[IGFBP7] and Risk for Progression to Death, Dialysis or Severe Acute Kidney Injury in Patients With Septic Shock. *Am J Respir Crit Care Med* (2020) 202(9):1262–70. doi: 10.1164/rccm.201906-1197OC
120. da Hora Passos R, Ramos JG, Mendonça EJ, miRanda EA, Dutra FR, Coelho MF, et al. A Clinical Score to Predict Mortality in Septic Acute Kidney Injury Patients Requiring Continuous Renal Replacement Therapy: The HELENICC Score. *BMC Anesthesiol* (2017) 17(1):21. doi: 10.1186/s12871-017-0312-8
121. Kurczewski L, Sweet M, McKnight R, Halbritter K. Reduction in Time to First Action as a Result of Electronic Alerts for Early Sepsis Recognition. *Crit Care Nurs Q* (2015) 38(2):182–7. doi: 10.1097/CNQ.0000000000000060
122. Wilson FP, Shashaty M, Testani J, Aqeel I, Borovskiy Y, Ellenberg SS, et al. Automated, Electronic Alerts for Acute Kidney Injury: A Single-Blind, Parallel-Group, Randomised Controlled Trial. *Lancet* (2015) 385 (9981):1966–74. doi: 10.1016/S0140-6736(15)60266-5
123. Micheel CM, Nass SJ, Omenn GS. *Committee on the Review of Omics-Based Tests for Predicting Patient Outcomes in Clinical Trials; Board on Health Care Services; Board on Health Sciences Policy; Evolution of Translational Omics: Lessons Learned and the Path Forward*. Washington, DC: National Academies Press US (2012).
124. Papadopoulos T, Krochmal M, Cisek K, Fernandes M, Husi H, Stevens R, et al. Omics Databases on Kidney Disease: Where They can be Found and How to Benefit From Them. *Clin Kidney J* (2016) 9(3):343–52. doi: 10.1093/ckj/sfv155
125. Hasin Y, Seldin M, Lusis A. Multi-Omics Approaches to Disease. *Genome Biol* (2017) 18(1):83. doi: 10.1186/s13059-017-1215-1
126. Langley RJ, Tsalik EL, van Velkinburgh JC, Glickman SW, Rice BJ, Wang C, et al. An Integrated Clinico-Metabolomic Model Improves Prediction of Death in Sepsis. *Sci Transl Med* (2013) 5(195):195ra95. doi: 10.1126/scitranslmed.3005893
127. Hato T, Zollman A, Plotkin Z, El-Achkar TM, Maier BF, Pay SL, et al. Endotoxin Preconditioning Reprograms S1 Tubules and Macrophages to Protect the Kidney. *J Am Soc Nephrol* (2018) 29(1):104–17. doi: 10.1681/ASN.2017060624
128. Alexander MP, Mangalaparthi KK, Madugundu AK, Moyer AM, Adam BA, Mengel M, et al. Acute Kidney Injury in Severe COVID-19 Has Similarities to Sepsis-Associated Kidney Injury: A Multi-Omics Study. *Mayo Clin Proc* (2021) 96(10):2561–75. doi: 10.1016/j.mayocp.2021.07.001
129. Islam S, Kjällquist U, Moliner A, Zajac P, Fan JB, Lönnerberg P, et al. Characterization of the Single-Cell Transcriptional Landscape by Highly Multiplex RNA-Seq. *Genome Res* (2011) 21(7):1160–7. doi: 10.1101/gr.110882.110
130. Papalexi E, Satija R. Single-Cell RNA Sequencing to Explore Immune Cell Heterogeneity. *Nat Rev Immunol* (2018) 18(1):35–45. doi: 10.1038/nri.2017.76
131. Yip SH, Sham PC, Wang J. Evaluation of Tools for Highly Variable Gene Discovery From Single-Cell RNA-Seq Data. *Brief Bioinform* (2019) 20 (4):1583–9. doi: 10.1093/bib/bby011
132. Saviano A, Henderson NC, Baumert TF. Single-Cell Genomics and Spatial Transcriptomics: Discovery of Novel Cell States and Cellular Interactions in Liver Physiology and Disease Biology. *J Hepatol* (2020) 73(5):1219–30. doi: 10.1016/j.jhep.2020.06.004
133. Longo SK, Guo MG, Ji AL, Khavari PA. Integrating Single-Cell and Spatial Transcriptomics to Elucidate Intercellular Tissue Dynamics. *Nat Rev Genet* (2021) 22(10):627–44. doi: 10.1038/s41576-021-00370-8
134. Melo Ferreira R, Sabo AR, Winfree S, Collins KS, Janosevic D, Gulbronson CJ, et al. Integration of Spatial and Single-Cell Transcriptomics Localizes Epithelial Cell-Immune Cross-Talk in Kidney Injury. *JCI Insight* (2021) 6 (12):e147703. doi: 10.1172/jci.insight.147703
135. Janosevic D, Myslinski J, McCarthy TW, Zollman A, Syed F, Xuei X, et al. The Orchestrated Cellular and Molecular Responses of the Kidney to Endotoxin Define a Precise Sepsis Timeline. *Elife* (2021) 10:e62270. doi: 10.7554/eLife.62270
136. Purkayastha S, Gichoya JW, Addepally SA. Implementation of a Single Sign-on System Between Practice, Research and Learning Systems. *Appl Clin Inform* (2017) 8(1):306–12. doi: 10.4338/ACI-2016-10-CR-0171
137. Bali J, Garg R, Bali RT. Artificial Intelligence (AI) in Healthcare and Biomedical Research: Why a Strong Computational/AI Bioethics

Framework is Required? *Indian J Ophthalmol* (2019) 67(1):3–6. doi: 10.4103/ijo.IJO_1292_18
138. Van Laere D, Meeus M, Beirnaert C, Sonck V, Laukens K, Mahieu L, et al. Machine Learning to Support Hemodynamic Intervention in the Neonatal Intensive Care Unit. *Clin Perinatol* (2020) 47(3):435–48. doi: 10.1016/j.clp.2020.05.002
139. Miotto R, Wang F, Wang S, Jiang X, Dudley JT. Deep Learning for Healthcare: Review, Opportunities and Challenges. *Brief Bioinform* (2018) 19(6):1236–46. doi: 10.1093/bib/bbx044
140. Schinkel M, Paranjape K, Nannan Panday RS, Skyttberg N, Nanayakkara PWB. Clinical Applications of Artificial Intelligence in Sepsis: A Narrative Review. *Comput Biol Med* (2019) 115:103488. doi: 10.1016/j.compbiomed.2019.103488
141. Chaudhary K, Vaid A, Duffy Á, Paranjpe I, Jaladanki S, Paranjpe M, et al. Utilization of Deep Learning for Subphenotype Identification in Sepsis-Associated Acute Kidney Injury. *Clin J Am Soc Nephrol* (2020) 15(11):1557–65. doi: 10.2215/CJN.09330819
142. Fleuren LM, Klausch TLT, Zwager CL, Schoonmade LJ, Guo T, Roggeveen LF, et al. Machine Learning for the Prediction of Sepsis: A Systematic Review and Meta-Analysis of Diagnostic Test Accuracy. *Intensive Care Med* (2020) 46(3):383–400. doi: 10.1007/s00134-019-05872-y

Conflict of Interest: The authors declare that the research was conducted in the absence of any commercial or financial relationships that could be construed as a potential conflict of interest.

Publisher's Note: All claims expressed in this article are solely those of the authors and do not necessarily represent those of their affiliated organizations, or those of the publisher, the editors and the reviewers. Any product that may be evaluated in this article, or claim that may be made by its manufacturer, is not guaranteed or endorsed by the publisher.

frontiers | Frontiers in Immunology

ORIGINAL RESEARCH
published: 12 July 2022
doi: 10.3389/fimmu.2022.925494

Influence of the Initial Neutrophils to Lymphocytes and Platelets Ratio on the Incidence and Severity of Sepsis-Associated Acute Kidney Injury: A Double Robust Estimation Based on a Large Public Database

Wenyan Xiao[1,2†], Zongqing Lu[1,2†], Yu Liu[3,4], Tianfeng Hua[1,2], Jin Zhang[1,2], Juanjuan Hu[1,2], Hui Li[1,2], Yaohua Xu[3,4] and Min Yang[1,2]*

[1] The 2nd Department of Intensive Care Unit, the Second Affiliated Hospital of Anhui Medical University, Hefei, China, [2] The Laboratory of Cardiopulmonary Resuscitation and Critical Care Medicine, The Second Affiliated Hospital of Anhui Medical University, Hefei, China, [3] Key Laboratory of Intelligent Computing and Signal Processing, Anhui University, Ministry of Education, Hefei, China, [4] School of Integrated Circuits, Anhui University, Hefei, China

OPEN ACCESS

Edited by:
Alessandra Stasi, University of Bari Aldo Moro, Italy

Reviewed by:
Gianvito Caggiano, University of Bari Aldo Moro, Italy
Ling Liu, Southeast University, China
Jun Lyu, First Affiliated Hospital of Jinan University, China

***Correspondence:**
Min Yang
yangmin@ahmu.edu.cn

[†]These authors have contributed equally to this work

Specialty section:
This article was submitted to Inflammation, a section of the journal Frontiers in Immunology

Received: *21 April 2022*
Accepted: *16 June 2022*
Published: *12 July 2022*

Citation:
Xiao W, Lu Z, Liu Y, Hua T, Zhang J, Hu J, Li H, Xu Y and Yang M (2022) Influence of the Initial Neutrophils to Lymphocytes and Platelets Ratio on the Incidence and Severity of Sepsis-Associated Acute Kidney Injury: A Double Robust Estimation Based on a Large Public Database. Front. Immunol. 13:925494. doi: 10.3389/fimmu.2022.925494

Background: Acute kidney injury (AKI) is a frequent consequence of sepsis and has been linked to poor prognosis. In critically ill patients, the ratio of neutrophils to lymphocytes and platelets (N/LP) has been confirmed as an inflammation-related marker connected with the development of renal dysfunction. However, the effect of the N/LP ratio on the initiation and development of AKI in patients with sepsis remained unclear. The purpose of this study was to determine if the N/LP ratio on intensive care unit (ICU) admission was associated with the occurrence of sepsis-associated AKI (S-AKI) and severe AKI.

Methods: Adult septic patients from the Medical Information Mart for Intensive Care-IV database were screened and classified into three categories (low, middle, or high) based on their N/LP ratio quartiles. The Cox proportional hazard and competing risk models were used to determine the risk of S-AKI in various N/LP groups, whilst the logistic regression model and restricted cubic splines (RCS) analysis were employed to investigate the link between N/LP ratios and the occurrence of severe AKI. Finally, we did a doubly robust estimation, a subgroup analysis, and a sensitivity analysis to determine the findings' robustness.

Results: We categorized 485, 968, and 485 septic patients into three groups based on their N/LP ratios: low, intermediate, and high. According the Cox proportional hazard model, the hazard rate (95% CI) for those in the middle and high N/LP groups on the incidence of S-AKI were 1.30(1.07, 1.58) and 1.27(1.02, 1.59), respectively, as compared to those in the low N/LP group. And the Fine-Gray proportional subdistribution hazards model indicated that mortality was not a substantial competing risk for S-AKI. Additionally, multivariate logistic regression revealed that the risk of severe AKI increased 1.83 fold in the high group compared to the low group. The RCS result also suggested that the

probability of severe AKI rose significantly when N/LP > 9.5. The consistency of these findings was confirmed using doubly robust estimation. However, subgroup and sensitivity analyses revealed that the association between N/LP and the incidence of S-AKI, severe AKI varied considerably between different populations and diagnostic criteria.

Conclusion: A raised initial N/LP level may induce the development of S-AKI and severe AKI within 7 days after ICU admission in septic patients. These influences were enhanced in elder, male, septic shock, and those with poor health condition. Furthermore, high NLP was more strongly connected to the risk of S-AKI and severe AKI in sepsis patients on the urine output-based AKI criteria than on the serum creatinine-based criteria.

Keywords: sepsis, neutrophils to lymphocytes and platelets ratio, acute kidney injury, competing risk model, double robust estimation

INTRODUCTION

According to the latest Sepsis 3.0 criteria (1), sepsis is defined as multiple organ dysfunction caused by an uncontrolled immune response to infection. Despite significant research efforts, sepsis continues to be one of the most challenging tasks for the healthcare system, with high morbidity and death globally. Based on evidence from previous epidemiological research, the worldwide incidence of sepsis is around 270 per 100,000 person-years (2). And the in-hospital mortality ranges from 17% to 26% (2), depending on the severity of the condition. As a common complication in sepsis patients, acute kidney damage (AKI) is usually results from tissue hypoperfusion, immune-inflammatory response dysregulation, and others (3, 4), with a incidence as high as 50% (5) and a 6-8 fold increased mortality compared to those with sepsis alone (6). As a result, it is necessary to initiate the early diagnosis and risk stratification of AKI in sepsis patients, which would contribute to effective interventions and a favorable prognosis.

Serum creatinine concentrations (SCr) and urine output (UO) are critical for clinical diagnosis of sepsis-associated AKI (S-AKI). However, due to its unique peak period and enhanced tubular secretion under stress, SCr appears to be an insensitive marker of AKI (7). At the same time, the UO is also particularly susceptible to varying factors other than the kidney, such as the circulating blood volume, urethral obstruction, and the use of diuretics. Thus, neither SCr nor UO are ideal and reliable indicators for S-AKI. Furthermore, numerous emerging technologies and approaches, including as machine learning (8, 9) and a series of novel biomarkers (7, 10), have been employed for S-AKI prediction and diagnosis. Nevertheless, it is regrettable that their actual effectiveness still requires extensive external validation and preclinical investigation. As noted previously, systemic inflammatory responses are intimately connected to the onset and development of S-AKI. The neutrophils to lymphocytes and platelets ratio (N/LP) is a low-cost indicator that can be obtained simply through routine blood tests and has been frequently applied in reflecting the body's inflammatory state. Its utility as a predictor of COVID-19 prognosis (11) and AKI occurrence following abdominal and cardiovascular surgery has already been demonstrated (12, 13). A recent retrospective study also demonstrated that higher N/LP ratios were significantly associated with an increased risk of in-hospital mortality among S-AKI patients (14). However, the relationship between the initial N/LP ratio and the development or severity of AKI in sepsis patients remained unclear. Besides, a large cohort research by Bianchi NA et al. revealed discrepancy between SCr and UO criteria for AKI diagnosis and prognosis (15). And the most appropriate diagnostic criteria that satisfied the clinical application of the N/LP are likewise undefined.

Accordingly, this study intended to determine whether elevated N/LP is causally linked with S-AKI risk and severity within seven days after ICU admission by using several statistical methods in a large cohort of adult sepsis patients. Additionally, we further explored the consistency of these associations on specific population subgroups and different diagnostic criteria for AKI to provide a basis for application scenarios.

Abbreviations: N/LP, neutrophils to lymphocytes and platelets; NLR, neutrophil-to-lymphocyte ratio; AKI, acute kidney injury; ICU, intensive care unit; S-AKI, sepsis-associated acute kidney injury; RCS, restricted cubic splines; SCr, serum creatinine; UO, urine output; MIMIC-IV, Medical Information Mart for Intensive Care IV; ICD, International Classification of Diseases; WBC, white blood cell count; BUN, blood urea nitrogen; AG, anion gap; SAPS II, Simplify the Acute Physiological Scores II; SOFA, Sequential Organ Failure Assessment; CRRT, continuous renal replacement therapy; MV, mechanical ventilation; KDIGO, Kidney Disease: Improving Global Outcomes Clinical Practice Guidelines; VIF, variance inflation factors; IPTW, inverse probability treatment weighting; SMD, standardized mean difference; K-M, Kaplan-Meier.

METHODS

Data Sources

The data for this study were obtained from the Medical Information Mart for Intensive Care IV (v1.0) (MIMIC-IV 1.0) database, which is a large, open-access database. The MIMIC-IV contained electronic data from 382, 278 patients admitted to the Beth Israel Deaconess Medical Center in Boston, Massachusetts, between 2008 and 2019 (16), including demographics, vital signs, laboratory results, imaging examinations, microbial culture results, medication and procedure records, survival information, and a data dictionary. This critical care database

has been approved by the Massachusetts Institute of Technology's Institutional Review Boards and released on March 16, 2021. Despite the fact that a substantial amount of research has been done based on MIMIC-IV, it was necessary to obtain authorization prior to the using. We have completed the Collaborative Institution Training Initiative Program Course offered by the National Institutes of Health in the United States and obtained certification (Record ID: 38455175, 39691989). Since the MIMIC database is a publicly available anonymized database, approval for the ethical committee was exempted.

Population Selection Criteria

Patients who met the criteria for sepsis at the time of ICU admission were eligible for enrollment. Sepsis and septic shock were defined according to the Third International Consensus Definitions for Sepsis and Septic Shock (Sepsis-3) (1), which included patients with a confirmed or suspected infection and a total SOFA score of 2 points. Simultaneously, suspected infection was defined as cases in which empiric antibiotic therapy was administered prior to or within three days of culture collection. Only data from the patient's first admission was used if they had multiple admission records. Minors (those under the age of 18) and those who were discharged or died within 24 hours of ICU admission were excluded. To avoid bias, patients with the following conditions were also excluded: (1) those with a blood system disease, such as aplastic anemia or various acute leukemia; (2) those with major immune diseases, including lymphoma, acquired immune deficiency syndrome, solid metastatic tumor, malignant tumor, and systemic lupus erythematosus; (3) those with pre-existing end-stage renal disease; (4) those with cirrhosis-induced hypersplenism; (5) those who received an acute renal damage diagnosis within the first 24 hours of ICU admission. When the patient was discharged, all associated comorbidities were identified using the International Classification of Diseases, Ninth Revision (ICD-9) and Tenth Revision (ICD-10) diagnosis codes.

Data Collection and Classification

Clinical data for the included patients were extracted from MIMIC IV using PostgreSQL programming (v4.21). Following that, STATA software (v15.1) was used to integrate, process, and classify the data based on the particular hadm id or stay id code. These clinical data included demographic information, associated comorbidities, infection locations, illness severity score, laboratory test variables, therapies administered, and endpoints, as following: age, gender, ethnic origin, type of care unit, presence of myocardial infarction, congestive heart failure, cirrhosis combined with non-hypersplenism, chronic obstructive pulmonary disease, or diabetes, presence of lower respiratory infection, genitourinary tract infection, intra-abdominal infection, bacteremia, skin and soft tissue infection, musculoskeletal infection, biliary tract infection, fungal infection, platelet count, neutrophil absolute value, lymphocyte absolute value, white blood cell count (WBC), serum creatinine (SCr), blood urea nitrogen (BUN), glucose, serum potassium, sodium, chloride, serum anion gap (AG), serum bicarbonate, Simplify the Acute Physiological Scores II (SAPS II), the Sequential Organ Failure Assessment (SOFA) excluding the coagulation system, the Charlson comorbidity index, the duration of ICU stay, the use of vasoactive medication, continuous renal replacement therapy (CRRT), or invasive mechanical ventilation (MV) during the follow-up period, the length of ICU stay, the 7-day mortality, the 28-day mortality, all-cause ICU mortality, the incidence of AKI, and the AKI stage. Except for neutrophils, lymphocytes, and platelet count, the lowest values of the aforesaid laboratory markers were retrieved within 24 hours of ICU admission. Patients with any missing values were discarded; values falling below the 1st percentile or above the 99th percentile were deemed outliers and were deleted before analysis. The formula for calculating N/LP was previously described as [Neutrophil count(10^9/L)*100]/[Lymphocyte count(10^9/L)*Platelet count(10^9/L)] (11). The mean of neutrophils, lymphocytes, and platelet count within the first 24 h after ICU admission were adopted in N/LP the computational process. Following that, all participants were classified into three categories based on their N/LP quartile range: low (N/LP=2.8718, 25th), middle (N/LP=10.4128, 25th-75th), and high (N/LP>10.4128, >75th).

Outcomes

The study's objectives were to determine the potential connection of different initial N/LP levels with the prevalence of S-AKI and severe AKI within 7 days after ICU admission in sepsis patients. Primary outcome was the S-AKI incidence; the secondary outcome was the risk of severe AKI. The duration of follow-up was defined as the period from ICU admission to the onset of AKI or death. While the overall time of follow-up for patients who survived without developing AKI was seven days. AKI was defined by the 2012 Kidney Disease: Improving Global Outcomes Clinical Practice Guidelines (KDIGO) as an elevated in serum creatinine of 0.3 mg/dL within 48 hours or a raise of at least 1.5 times the baseline level in the preceding seven days, or a decrease in UO to less than 0.5 ml/kg/h for more than 6 hours (17). If one or more of these criteria were met, AKI could be diagnosed; the highest stage among the SCr and UO criteria would be considered the final stage for those who met both criteria (15). And severe AKI was defined as stages 2 and 3 of AKI.

Independent Variable and Covariates

The independent variable was the varying levels of N/LP. Any significant variables associated with the outcomes through univariate analyses as well as those variables that seemed clinically important were considered as modifying covariates for subsequent multivariate analysis. Finally, age, gender, initial SAPS II, SOFA scores excluding coagulation system, Charlson comorbidity index, serum AG, serum bicarbonate, glucose, serum potassium, serum sodium, serum chloride, BUN, SCr, and usage of vasoactive medicine, CRRT, and invasive-MV were considered as confounders by statistical analyses and clinical judgment.

Statistical Analysis

We performed a normality test (*Agostino tests*), followed by a descriptive data analysis. Continuous variables were expressed as mean (standard deviation), while nonparametric variables were expressed as the median (interquartile ranges, IQR) and were compared using the one-way *ANOVA test* or nonparametric *Kruskal-Wallis test*. Categorical variables are expressed as a frequency (percentage) and were compared using the X^2 or *Rank-Sum test*.

We used the Kaplan-Meier (K-M) method to calculate the cumulative incidence rates and corresponding 95% confidence intervals (CIs) for each N/LP group and then plotted the cumulative incidence curves with the log-rank test for significance. The influence of the initial N/LP on AKI risk was then investigated using three Cox proportional hazard models with varied degrees of covariate adjustment. Firstly, a univariate analysis was conducted in Model 1 without adjusting for any covariates. Secondly, Model 2 modified with all sixteen factors discussed previously. Thirdly, in order to select the ideal model, we used a stepwise backward approach in multivariate analysis based on the Akaike information criteria and evaluated the possibility of collinearity in Model 3 by variance inflation factors (VIF). Additionally, variables with a VIF greater than 5 were excluded (15). Considering the death as a competing risk for the S-AKI occurrence, the cumulative incidence functions according to the Fine-Gray test was utilized to calculate the cumulative incidence for each of three groups in competing risk models and in turn, assess the stability of Cox proportional hazard model results (18). Similarly, we drew the cumulative incidence curve using the R package 'cmprsk' and then conducted Gray's test to compare the AKI risk between the N/LP groups.

Logistic regression model was implied to assess the influence of different initial N/LP levels on the severity of AKI. Additionally, given the inevitable information loss and change of dose-response relationship when artificially stratifying continuous variables, we modeled the potential nonlinear effect of N/LP at the continuity level using restricted cubic splines analysis (RCS) (19). We used RCS with five knot corresponding to 5th, 35th, 50th, 65th, and 95th percentile after adjusting all 16 covariates. The reference point was set at the 2.8718 (25th).

To further validate the aforementioned findings, double robust estimation models were performed. Sixteen covariates were included in the propensity scoring model to obtain the propensity scores using logistic regression. We then re-weighted the observations across the N/LP groups using inverse probability treatment weighting (IPTW) to create three groups that were similar for all covariates (20). The standardized mean difference of effect sizes (SMDs) were calculated to reflect the differences between the original and the IPTW cohorts, and an SMD with an absolute value greater than 0.1 after propensity scores weighting could be considered evidence of imbalance. Weighted regression on all the confounders included in the propensity scoring model was conducted, thereby obtaining double robust estimators in different N/LP groups.

Subgroup analyses according to age (<65, or ≥65 years), gender (male, or female), septic shock (yes, or no), SOFA scores (<5, or ≥5), SAPS II (<35, or ≥35), and Charlson comorbidity index (<5, or ≥5) were conducted respectively to examine the strata effect and potential interactions. Finally, considering the significant inconsistency between SCr and urine output criteria in AKI diagnosing and grading, sensitivity analysis was performed to re-evaluate the association of the initial N/LP Levels with the AKI and severe AKI occurrence in individual AKI criteria (SCr or UO criteria). All statistical analyses were performed using STATA 15.1 (College Station, Texas) and R 3.6.2 (Chicago, Illinois) software. The primary R package used in this study included *survival, survminer, cmprsk, tableone, foreign, ipw, twang, MatchIt, Hmisc, rms, glmnet, MASS, VIM, ggplot2*. The p values with < 0.05 were taken as statistically significant (two-sided).

RESULTS

Characteristics of Included Sepsis Participants

With in MIMIC-IV database, a total of 12274 patients met the Sepsis 3.0 criteria; and finally, 1938 patients were included in this study (**Figure 1**). The 25% quantile, median, and 75% quantile of the N/LP were given by 2.8718, 5.2734, and 10.4128 respectively. Of those enrolled, 485 patients were assigned to the low N/LP group, 968 to the middle N/LP group, and 485 to the high N/LP group using predefined grouping criteria. The baseline characteristics of participants were given in **Table 1** according

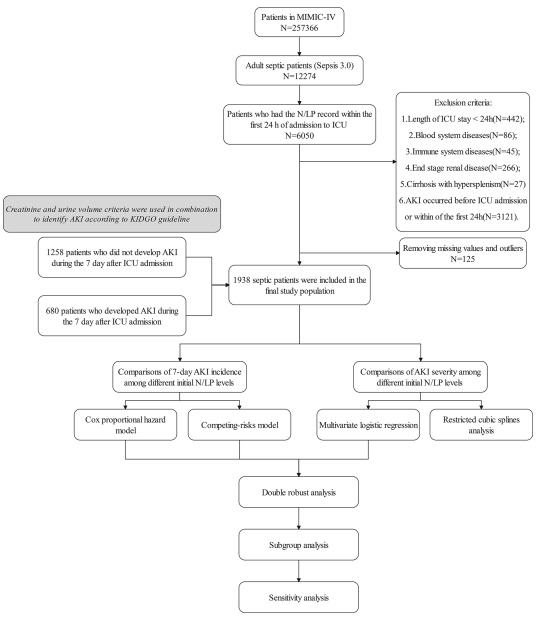

FIGURE 1 | Flowchart for analysis of the current study.

TABLE 1 | Baseline demographic and clinical characteristics by different N/LP level in sepsis patients.

Variables	Overall	Low group (N/LP<=2.8718)	Middle group (2.8718<N/LP<10.4128)	High group (N/LP>=10.4128)	*P*
N	1938	485	968	485	
Age (year)	65.99 [54.48, 78.37]	66.44 [53.29, 77.98]	65.96 [54.78, 78.45]	65.34 [54.71, 78.40]	0.688
Gender (%)					0.018
Female	1054 (54.4)	241 (49.7)	528 (54.5)	285 (58.8)	
Male	884 (45.6)	244 (50.3)	440 (45.5)	200 (41.2)	
Ethnicity (%)					0.002
AMERICAN INDIAN/ALASKA NATIVE	6 (0.3)	3 (0.6)	1 (0.1)	2 (0.4)	
ASIAN	75 (3.9)	18 (3.7)	32 (3.3)	25 (5.2)	
BLACK/AFRICAN AMERICAN	160 (8.3)	57 (11.8)	75 (7.7)	28 (5.8)	
HISPANIC/LATINO	71 (3.7)	25 (5.2)	27 (2.8)	19 (3.9)	
WHITE	1290 (66.6)	302 (62.3)	649 (67.0)	339 (69.9)	
UNKNOWN	230 (11.9)	50 (10.3)	134 (13.8)	46 (9.5)	
OTHER	106 (5.5)	30 (6.2)	50 (5.2)	26 (5.4)	
First_careunit (%)					<0.001
CVICU	267 (13.8)	89 (18.4)	166 (17.1)	12 (2.5)	
CCU	107 (5.5)	34 (7.0)	55 (5.7)	18 (3.7)	
MICU	617 (31.8)	137 (28.2)	292 (30.2)	188 (38.8)	
MICU/SICU	579 (29.9)	131 (27.0)	270 (27.9)	178 (36.7)	
Neuro Intermediate	35 (1.8)	14 (2.9)	10 (1.0)	11 (2.3)	
Neuro Stepdown	16 (0.8)	5 (1.0)	9 (0.9)	2 (0.4)	
Neuro SICU	28 (1.4)	8 (1.6)	17 (1.8)	3 (0.6)	
SICU	170 (8.8)	40 (8.2)	87 (9.0)	43 (8.9)	
Trauma SICU TSICU	119 (6.1)	27 (5.6)	62 (6.4)	30 (6.2)	
Comorbidity (%)					
Myocardial infarction	267 (13.8)	53 (10.9)	155 (16.0)	59 (12.2)	0.015
Congestive heart failure	438 (22.6)	106 (21.9)	221 (22.8)	111 (22.9)	0.902
Peripheral vascular disease	164 (8.5)	39 (8.0)	91 (9.4)	34 (7.0)	0.282
Cerebrovascular disease	220 (11.4)	74 (15.3)	94 (9.7)	52 (10.7)	0.006
COPD	478 (24.7)	130 (26.8)	230 (23.8)	118 (24.3)	0.438
Cirrhosis without hypersplenism	135 (7.0)	21 (4.3)	65 (6.7)	49 (10.1)	0.002
Diabetes	498 (25.7)	135 (27.8)	246 (25.4)	117 (24.1)	0.4
Infection sites (%)					
Lower respiratory infection	528 (27.2)	106 (21.9)	251 (25.9)	171 (35.3)	<0.001
Genitourinary tract infection	373 (19.2)	82 (16.9)	175 (18.1)	116 (23.9)	0.009
Intra abdominal infection	67 (3.5)	4 (0.8)	38 (3.9)	25 (5.2)	0.001
Bacteremia	65 (3.4)	19 (3.9)	28 (2.9)	18 (3.7)	0.522
Skin and skin structure infection	99 (5.1)	13 (2.7)	55 (5.7)	31 (6.4)	0.017
Musculoskeletal infection	18 (0.9)	6 (1.2)	5 (0.5)	7 (1.4)	0.158
Biliary tract infection	13 (0.7)	2 (0.4)	6 (0.6)	5 (1.0)	0.48
Systemic fungal infection	98 (5.1)	18 (3.7)	46 (4.8)	34 (7.0)	0.053
Other infection	923 (47.6)	271 (55.9)	489 (50.5)	163 (33.6)	<0.001
Laboratory tests[a]					
Platelet_mean (K/uL)	166.75 [119.50, 236.00]	215.00 [149.33, 287.00]	167.75 [123.92, 236.08]	128.50 [87.00, 183.50]	<0.001
Lymphocytes_mean (K/uL)	29.50 [1.21, 103.96]	69.03 [2.10, 154.28]	50.30 [1.26, 107.73]	2.80 [0.52, 44.66]	<0.001
Neutrophils_mean (K/uL)	288.47 [10.24, 990.07]	181.26 [7.27, 655.20]	415.75 [10.67, 1071.57]	200.00 [13.41, 1191.08]	<0.001
WBC_max (K/uL)	13.90 [9.60, 19.10]	11.40 [7.70, 15.50]	14.30 [10.30, 19.00]	16.10 [11.20, 23.00]	<0.001
Aniongap_max	16.00 [13.00, 19.00]	15.00 [13.00, 18.00]	16.00 [13.00, 19.00]	17.00 [14.00, 20.00]	<0.001
Bicarbonate_min (mEq/L)	21.00 [18.00, 23.00]	21.00 [19.00, 24.00]	21.00 [18.00, 23.00]	20.00 [17.00, 23.00]	<0.001
Bun_max (mg/dL)	21.00 [14.00, 36.00]	18.00 [13.00, 32.00]	20.50 [14.00, 34.00]	26.00 [17.00, 43.00]	<0.001
Chloride_max (mEq/L)	107.00 [103.00, 111.00]	107.00 [104.00, 110.00]	108.00 [103.00, 111.00]	107.00 [103.00, 111.00]	0.222
Creatinine_max (μmol/L)	1.10 [0.80, 1.60]	1.00 [0.70, 1.50]	1.10 [0.80, 1.50]	1.10 [0.80, 1.70]	<0.001
Glucose_max (mg/dl)	141.00 [115.00, 189.00]	135.00 [110.00, 176.00]	140.50 [115.00, 191.00]	149.00 [122.00, 200.00]	<0.001
Sodium_max (mEq/L)	140.00 [137.00, 143.00]	140.00 [137.00, 142.00]	140.00 [137.00, 142.00]	140.00 [137.00, 143.00]	0.866
Potassium_max (K/uL)	4.40 [4.00, 4.80]	4.40 [4.10, 4.90]	4.40 [4.00, 4.90]	4.30 [3.90, 4.70]	<0.001
Severity scoring					
SAPS II	35.00 [28.00, 43.00]	34.00 [26.00, 41.00]	35.00 [28.00, 42.25]	37.00 [30.00, 45.00]	<0.001
SOFA_exclude platelet	4.00 [3.00, 7.00]	4.00 [3.00, 6.00]	4.00 [3.00, 7.00]	5.00 [3.00, 7.00]	0.001
Charlson comorbidity index	5.00 [3.00, 7.00]	5.00 [3.00, 7.00]	5.00 [3.00, 7.00]	6.00 [4.00, 8.00]	0.028
Treatments					
Vasoactive drug (%)	864 (44.6)	201 (41.4)	447 (46.2)	216 (44.5)	0.231
Invasive ventilation (%)	666 (34.4)	159 (32.8)	354 (36.6)	153 (31.5)	0.115
CRRT (%)	7 (0.4)	1 (0.2)	3 (0.3)	3 (0.6)	0.525

(Continued)

TABLE 1 | Continued

Variables	Overall	Low group (N/LP<=2.8718)	Middle group (2.8718<N/LP<10.4128)	High group (N/LP>=10.4128)	*P*
Endpoints					
AKI (%)	680 (35.1)	141 (29.1)	360 (37.2)	179 (36.9)	0.006
AKI_stage (%)					0.004
Stage 1	260 (13.4)	62 (12.8)	145 (15.0)	53 (10.9)	
Stage 2	339 (17.5)	66 (13.6)	172 (17.8)	101 (20.8)	
Stage 3	81 (4.2)	13 (2.7)	43 (4.4)	25 (5.2)	
Length of ICU stay (day)	2.43 [1.63, 4.18]	2.23 [1.53, 3.67]	2.45 [1.63, 4.04]	2.73 [1.70, 5.14]	0.001
Mortality_ICU (%)	96 (5.0)	17 (3.5)	46 (4.8)	33 (6.8)	0.056
Mortality_ICU7 (%)	77 (4.0)	13 (2.7)	38 (3.9)	26 (5.4)	0.101
Mortality_ICU28 (%)	148 (7.6)	21 (4.3)	74 (7.6)	53 (10.9)	0.001

Categorical data were presented as frequency (percentage), parametric continuous data were presented as median (interquartile ranges), whereas non-parametric continuous data were presented as median (interquartile ranges);

CVICU, Cardiac Vascular Intensive Care Unit; CCU, Coronary Care Unit; MICU, Medical Intensive Care Unit; MICU/SICU, Medical/Surgical Intensive Care Unit; SICU, Surgical Intensive Care Unit; COPD, Chronic Obstructive Pulmoriary Disease; SOFA, Sequential Organ Failure Assessment; SAPS II, Simplified acute physiology score II; AKI, Acute kidney injury; CRRT, continuous renal replacement therapy; ICU, intensive care unit.

to respective N/LP groups. We found that the high N/LP group had a greater proportion of female (P=0.018), Caucasian (P=0.002), cirrhosis without hypersplenism (P=0.002) compared to other groups. With regard to the source of infection, the principal sites of the infection in high N/LP group were lower respiratory (P<0.001), genitourinary tract (P=0.009), intra-abdominal (P=0.001), skin and skin structure infection (P=0.017). Furthermore, the length of ICU stay (P=0.001) and 28-day mortality (P=0.001) increased significantly in high N/LP group.

The characteristics of patients in whom S-AKI occurred and patients in whom S-AKI did not occur were summarized in **Supplementary Table 1**. Patients with AKI were elder, and had more comorbidities such as cardio-cerebrovascular disease and chronic obstructive pulmonary disease. Besides, a higher proportion of lower respiratory infection and organ dysfunction were also observed in those not developing AKI.

The Incidence of S-AKI in Various N/LP Groups

AKI occurred in 680 (35.1%) of 1938 septic patients within seven days of ICU admission. As displayed in **Table 1**, the incidence of AKI varied significantly within each N/LP group. As compared to the low N/LP group, the middle and high N/LP groups had a significantly increased incidence of AKI (P<0.001) (**Figure 2A**). Additionally, the cumulative incidence curve calculated using the K-M method and the log-rank test result (P=0.0047) (**Figure 3A**) all followed the same trend as the above-mentioned founding. **Table 2** summarized the results of Cox proportional hazard models. Three statistical models with various adjusted confounders revealed that the hazard ratio (HR) and 95% confidence interval (CI) for both middle and high groups were larger than 1.0, indicating a higher incidence of AKI than the low N/LP group. In Model 2, after adjusting for all sixteen covariates, the HR (95%CI) for the middle and high groups was 1.30 (1.07, 1.58) (P=0.008) and 1.27 (1.02, 1.59) (P=0.034), respectively. It is important to note that the risk of AKI did not vary between the middle and high groups.

On the other hand, only 31 (1.60%) individuals died during the first week after ICU admission without developing AKI. Additionally, the *Fine-Gray* test revealed that an early death was not a significant competing risk factor for the development of AKI (P=0.105). Thus, the cumulative incidence curve and trend of the competing-risks model were similar to those plotted by the *K-M* method (**Figure 3B**). **Table 2** presents the results of univariate and multivariate *Fine-Gray* competing-risks regression models. Moreover, no significant differences between competing-risks and Cox proportional hazard models were observed. Then, these findings revealed that an elevated initial N/LP level was related with an increased risk of early AKI in septic patients.

The Relationship Between N/LP Ratios and Severe AKI

Among 680 sepsis patients with S-AKI, 260 (38.24%), 339 (49.85%), and 81 (11.91%) patients were diagnosed as stage 1, stage 2, and stage 3 based on both SCr and UO criteria. As illustrated in **Figure 2B**, severe AKI (stages 2 and 3) accounted for a greater proportion of the groups with a middle or high N/LP ratio. Besides, as the N/LP ratio increased, the proportion of patients with severe AKI risen substantially (**Figure 2C**).

The influence of varying N/LP levels on the occurrence of severe AKI in septic patients was then investigated by univariate and multivariate logistic regression. Each of the three models demonstrated a similar tendency (**Figure 4A**). When compared to the low N/LP group, a significant difference in the risk of severe AKI occurred only in the high N/LP group (aOR 1.83; 95%CI 1.12, 3.03), despite the fact that the odds ratio (OR) increased. RCS drew the N/LP dose-response curve and determined that the OR and 95%CI were greater than the dashed line on the Y-axis (Y = 1) only if the N/LP was more than around 9.5. (**Figure 5**). This finding was also consistent with logistic regression results.

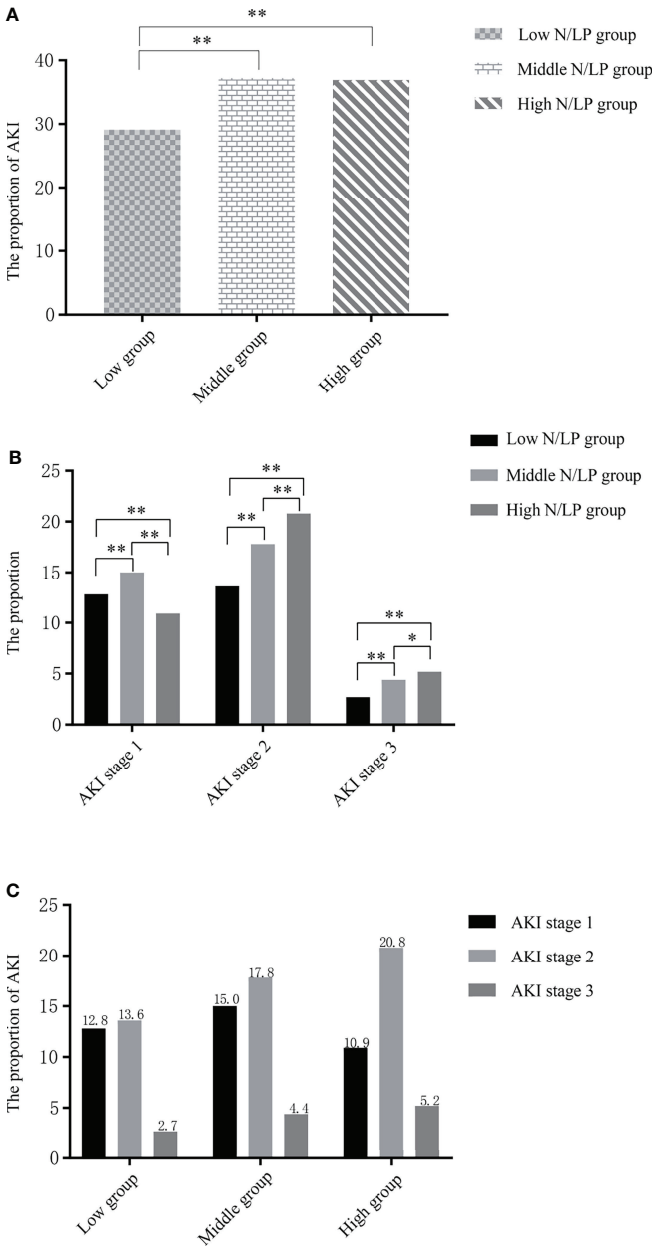

FIGURE 2 | **(A)** The incidence of sepsis-associated acute kidney injury (S-AKI) in each N/LP group were 29.1% (low N/LP group), 37.2% (middle N/LP group) and 36.9% (high N/LP group), respectively (*P*=0.006); **(B)** the comparison in the proportion of each N/LP level in different AKI stages, the rates of stages 1, 2, 3 were 12.8%, 13.6, 2.7% in low N/LP group, and 15%, 17.8%, 4.4% in middle N/LP group, and 10.9%, 20.8%, 5.2%; **(C)** the proportion of each AKI stage in different N/LP groups. AKI and corresponding stage are diagnosed based on serum creatinine and urine output criteria. Statistical analysis by *Rank-Sum test;* *, *P*<0.05; **, *P*<0.001.

Double Robust Estimation

Prior to performing double robust estimation, we conducted IPTW to balance the baseline among three N/LP groups. **Supplementary Figure 1** shown the SMD of all 16 covariates before and after propensity score matching. The serious disequilibrium problem in original data has been well-resolved by IPTW based on multinomial logistic regression.

Regarding S-AKI incidence, whether K-M methods or univariate Cox analysis after IPTW or double robust estimation regressed all 16 covariates included in the IPTW, a significantly increased risk of S-AKI was observed in middle and high N/LP groups compared with the low group (**Figure 6**). However, no difference was observed between the middle and high N/LP groups. When comparing the high N/LP group with

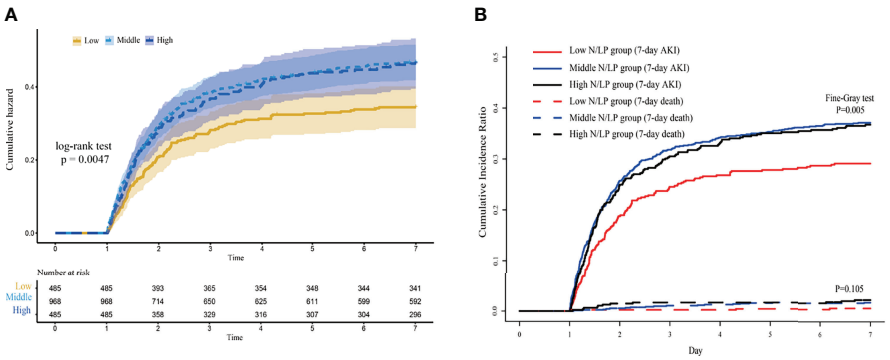

FIGURE 3 | The cumulative incidence curve of sepsis acute kidney injury **(AKI)** plotted by **(A)** Kaplan-Meier method; **(B)** and competing risk model. AKI was diagnosed based on serum creatinine and urine output criteria.

the low N/LP group, univariate logistic analysis showed a nearly doubled risk of severe AKI (OR 1.90; 95%CI 1.20, 3.03) after IPTW. And, the double robust estimation adjusted for all 16 covariates also yielded a similar result (OR 1.94; 95%CI 1.21, 3.14) (**Figure 4B**).

Subgroup Analysis

Tables 3, **4** summarized the results of subgroup analysis. Interaction tests with age, gender, septic shock, SOFA, SAPS II score, and Charlson comorbidity index were all non-significant for the risk of AKI (*P*=0.878, 0.674, 0.22, 0.455, 0.553, and 0.742) and severe AKI (*P*=0.213, 0.634, 0.355, 0.877, 0.543, and 0.674). Even so, we noticed that higher N/LP levels had a considerable impact on elder, male, septic shock patients, and those with poor health condition.

Sensitivity Analysis

In sensitivity analyses, SCr criteria or UO criteria were separately used for AKI identification rather than in combination. When only SCr criteria was applied, we found that elevated N/LP levels would still increased the risk of S-AKI (**Supplementary Figure 2**); however, statistical significance merely appeared in the high N/LP groups, whether proved by the univariate or multivariate Cox proportional hazard model or competing-risks model (**Supplementary Table 2**), or even the double robust analysis regressed all covariates after the IPTW (**Supplementary Figure 3** and **Supplementary Figure 4**). In contrast, the N/LP levels were no longer associated with the risk of severe AKI (**Supplementary Figure 5** and **Supplementary Figure 6**).

While under UO criteria, the results were consistent with those obtained by previous analysis based on two indicators (SCr and UO) combination. In brief, the septic patients with an initial N/LP level greater than 2.8718 have a higher incidence of AKI, and the risk of severe AKI also significantly increased when N/LP was greater than 10.4128 (aOR 2.30; 95%CI 1.31, 4.08). **Supplementary Figure 7** showed the cumulative incidence curve drawn by the K-M method and univariate competing-risks regression model about AKI occurrence. **Supplementary Figure 8** presented the differences between each N/LP group in the original and the IPTW cohort, and **Supplementary Table 3**, **Supplementary Figure 9** presented the results of the Cox

TABLE 2 | The results of Cox proportional hazards models and competing risk analyses.

Group	Model 1		Model 2		Model3	
	HR (95% CI)	*P*	HR (95% CI)	*P*	HR (95% CI)	*P*
Cox proportional hazard models						
Low N/LP group	Ref	1	Ref	1	Ref	1
Middle N/LP group	1.37 (1.13, 1.66)	0.001	1.30 (1.07, 1.58)	0.008	1.31 (1.08, 1.59)	0.007
High N/LP group	1.34 (1.08, 1.68)	0.009	1.27 (1.02, 1.59)	0.034	1.28 (1.03, 1.60)	0.029
Competing risk analyses						
Low N/LP group	Ref	1	Ref	1	Ref	1
Middle N/LP group	1.36 (1.12, 1.66)	0.002	1.30 (1.07, 1.58)	0.008	1.30 (1.07, 1.58)	0.008
High N/LP group	1.33 (1.07, 1.66)	0.011	1.26 (1.01, 1.58)	0.038	1.27 (1.02, 1.58)	0.036

Model 1: univariate analysis; Model 2: adjusted for age, gender, initial SAPS II, SOFA scores excluding coagulation system, Charlson comorbidity index, serum AG, serum bicarbonate, glucose, serum potassium, serum sodium, serum chloride, BUN, SCr, the use of vasoactive medication, CRRT, and invasive-MV; Model 3: adjusted for age, serum chloride, SCr, sodium, SOFA scores excluding coagulation system, vasoactive medication, and invasive-MV; SOFA, Sequential Organ Failure Assessment; SAPS II, Simplified acute physiology score II; AKI, Acute kidney injury; CRRT, Continuous Renal Replacement Therapy; MV, machine ventilation; SCr, Serum Creatinine; BUN, Blood Urea Nitrogen; N/LP, Neutrophil-to-Lymphocyte Platelet.

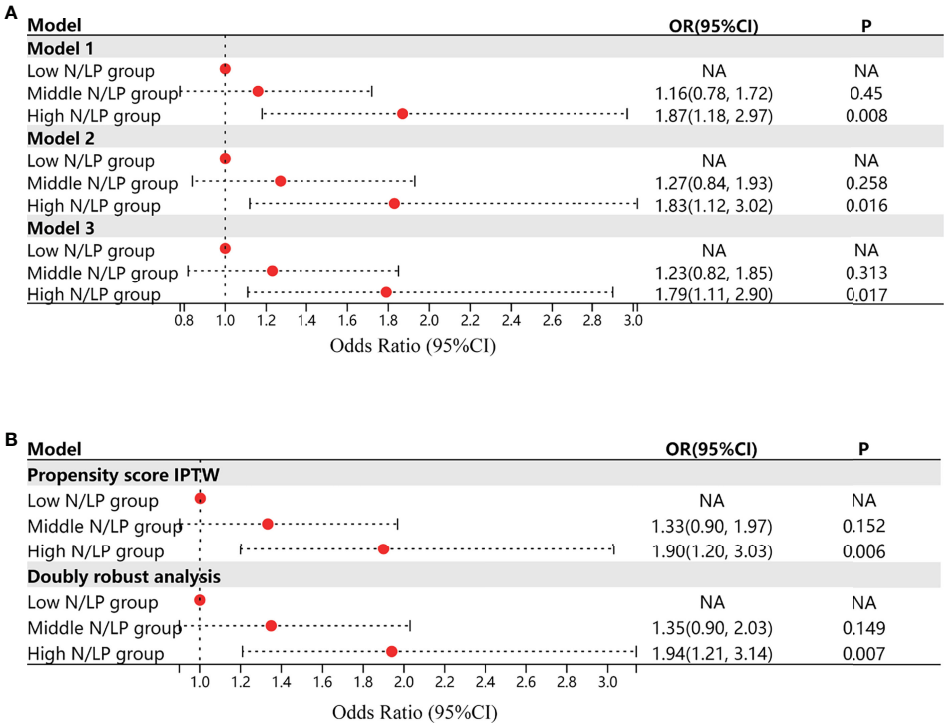

FIGURE 4 | **(A)** The results of univariate and multivariate logistic regression when analysed the influence of varying N/LP levels on the occurrence of severe AKI in septic patients; Model 1 represented the univariate analysis; Model 2 represented the multivariate analysis adjusting all covariates; Model 3 represented the multivariate analysis adjusting gender, serum bicarbonate, serum chloride, serum creatinine, serum sodium, SOFA scores excluding coagulation system, Charlson comorbidity index based on the results of stepwise backward approach and collinearity analysis; **(B)** the results of univariate logistic analysis after inverse probability treatment weighting and the double robust estimation. Acute kidney injury was diagnosed based on serum creatinine and urine output criteria.

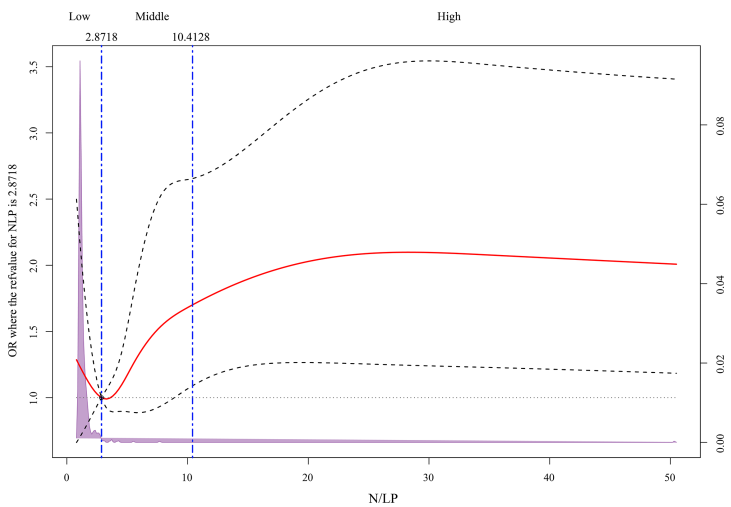

FIGURE 5 | Multivariable adjusted odds ratios for severe acute kidney injury (AKI) occurrence according to initial N/LP on a continuous scale. Solid red lines were multivariable-adjusted odds ratios, with dashed bold lines showing 95% confidence intervals derived from restricted cubic spline regressions with five knots. Reference lines for no association were indicated by the black dashed lines at a hazard ratio of 1.0 and the reference knot setted at 2.8718. Purple regions indicated the fraction of the population with different levels of N/LP. All 16 covariates were adjusted. AKI and corresponding stage were diagnosed based on serum creatinine and urine output criteria.

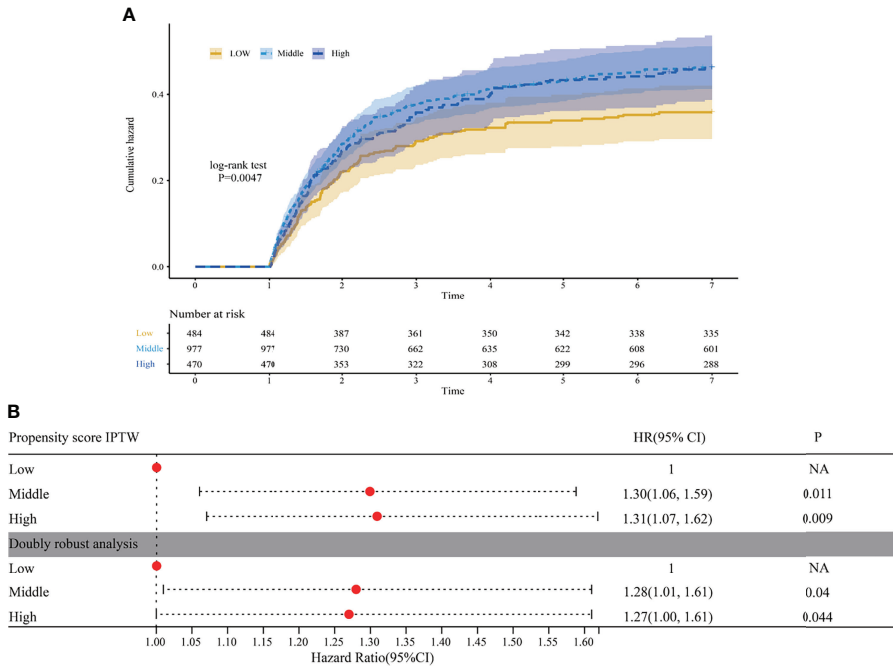

FIGURE 6 | **(A)** Cumulative incidence curve of sepsis acute kidney injury (S-AKI) in each N/LP groups were plotted by Kaplan-Meier method after inverse probability treatment weighting (IPTW); **(B)** the results of univariate Cox proportional hazard model after IPTW and double robust estimation regressed all 16 covariates. AKI was diagnosed based on serum creatinine and urine output criteria.

proportional hazard model and double robust analysis. Furthermore, **Supplementary Figure 10** and **Supplementary Figure 11** assessed the effect of high N/LP on the risk of severe AKI at different adjusting levels.

The sensitivity analysis results indicated that the UO criteria might be more suitable than SCr criteria when exploring the connection between the initial N/LP level with the occurrence of S-AKI and severe AKI.

DISCUSSION

Key Findings

In the present study, various methods, such as competing risks models and double robust estimation, have been employed to evaluate the association between initial N/LP levels with the incidence of S-AKI and severe AKI in sepsis patients. We found that elevated N/LP would lead to increases in the risk of S-AKI

TABLE 3 | Subgroup analysis regarding the influence of different N/LP level in the S-AKI occurrence. .

Subgroups	No.AKI/No.patients	Low N/LP group	Middle N/LP group	*P1*	High N/LP group	*P2*	*P* for interaction
Age							0.878
<65	303/920	Ref	1.20 (0.90, 1.61)	0.217	1.20 (0.85, 1.70)	0.302	
>=65	375/1018	Ref	1.40 (1.08, 1.83)	0.012	1.55 (1.14, 2.04)	0.005	
Gender							0.674
Female	288/884	Ref	1.27 (0.95, 1.69)	0.108	1.28 (0.90, 1.82)	0.164	
Male	390/1054	Ref	1.36 (1.04, 1.78)	0.026	1.42 (1.07, 1.89)	0.017	
Septic shock							0.22
NO	297/1074	Ref	1.14 (0.88, 1.48)	0.306	1.06 (0.78, 1.45)	0.705	
YES	381/864	Ref	1.51 (1.11, 2.05)	0.008	1.60 (1.13, 2.27)	0.008	
SOFA_exclude_platelet							0.455
<5	243/971	Ref	1.24 (0.91, 1.69)	0.182	1.25 (0.86, 1.83)	0.242	
>=5	435/967	Ref	1.31 (1.01, 1.67)	0.04	1.33 (1.12, 1.75)	0.015	
SAPS II							0.553
<35	262/928	Ref	1.14 (0.84, 1.54)	0.407	1.22 (0.84, 1.76)	0.303	
>=35	416/1010	Ref	1.39 (1.07, 1.81)	0.013	1.42 (1.11, 1.96)	0.007	
Charlson comorbidity index							0.742
<5	250/780	Ref	1.30 (0.94, 1.78)	0.108	1.26 (0.85, 1.86)	0.25	
>=5	428 /1158	Ref	1.29 (1.01, 1.66)	0.044	1.37(1.05, 1.81)	0.009	

P1: Middle N/LP group vs Low N/LP group; P2: High N/LP group vs Low N/LP group;
S-AKI, Sepsis associated acute kidney injury; N/LP, Neutrophil-to-Lymphocyte Platelet; SOFA, Sequential Organ Failure Assessment; SAPS II, Simplified acute physiology II.

TABLE 4 | Subgroup analysis regarding the influence of different N/LP level in the severe AKI occurrence.

Subgroups	No.AKI/No.patients	Low N/LP group	Middle N/LP group	*P1*	High N/LP group	*P2*	*P* for interaction
Age							0.213
<65	188/305	Ref	0.86(0.46, 1.61)	0.646	1.35 (0.64, 2.88)	0.428	
>=65	232/375	Ref	1.52 (0.86, 2.71)	0.153	2.13 (1.07, 4.28)	0.032	
Gender							0.634
Female	193/289	Ref	1.07 (0.57, 2.02)	0.835	1.16 (0.53, 2.55)	0.706	
Male	227/391	Ref	1.43 (0.80, 2.57)	0.228	2.49 (1.27, 4.93)	0.008	
Septic shock							0.355
NO	188/298	Ref	1.41 (0.72, 2.73)	0.316	1.18 (0.55, 2.53)	0.66	
YES	232/382	Ref	1.17 (0.67, 2.04)	0.541	2.69 (1.36, 5.43)	0.005	
SOFA_exclude_platelet							0.877
<5	145/244	Ref	1.49 (0.75, 2.99)	0.259	2.11 (0.88, 5.21)	0.1	
>=5	275/436	Ref	1.18 (0.69, 2.02)	0.547	1.69 (1.09, 3.14)	0.025	
SAPS II							0.543
<35	151/263	Ref	0.73 (0.38, 1.38)	0.335	1.61 (0.72, 3.67)	0.253	
>=35	269/417	Ref	1.91 (1.08, 3.38)	0.026	2.16 (1.15, 4.12)	0.018	
Charlson comorbidity index							0.674
<5	138/251	Ref	0.79 (0.40, 1.56)	0.504	1.33 (0.58, 3.10)	0.498	
>=5	282/429	Ref	1.79 (1.04, 3.09)	0.036	2.23 (1.18, 4.23)	0.014	

P1, Middle N/LP group vs Low N/LP group; P2m High N/LP group vs Low N/LP group; the severe AKI refers to the stage 2 and stage 3 AKI; AKI, Acute kidney injury; N/LP, Neutrophil-to-Lymphocyte Platelet; SOFA, Sequential Organ Failure Assessment; SAPS II, Simplified acute physiology II.

and severe AKI within 7 days after ICU admission. Furthermore, these influences above were strengthened among males, elder, septic shock patients, and those with a poor health conditions. Finally, high NLP was more strongly connected to the risk and severity of AKI in sepsis patients on the UO-based criteria than on the SCr-based AKI criteria.

Comparisons With Previous Studies

S-AKI is a common complication in critical septic patients and is associated with high morbidity and mortality (21). Due to the difficulty in prevention, early recognition of S-AKI is essential for timely intervention and improving prognosis. According to recent evidence, inflammatory response, microvascular dysfunction, and metabolic reprogramming may be the underlying mechanisms responsible for causing S-AKI (22). Since sepsis triggers a systemic cytokine-chemokine response, it would result in an extensive activation and dysfunction of the immune system, manifested as neutrophilia and lymphocytopenia (23). Thus, the neutrophil-to-lymphocyte ratio (NLR), calculated from whole blood counts, was proposed as a surrogate indicator to reflect the relative relationship between the inflammatory response and immune status (24). Previous studies have demonstrated that NLR may be valuable for predicting the disease outcome in multiple diseases, such as cardiovascular disease (25, 26), cancer (27), and sepsis (28, 29).

Although NLR had been reported to predict the development of AKI in sepsis, its sensitivity and specificity were limited (24). The possible reason is the complex interaction between immune mechanisms, inflammatory cascade activation, and coagulation pathway disorders. Subsequently, these interactions would result in microvascular dysfunction, leukocyte/platelet activation, and microthrombi formation, ultimately inducing renal tubular epithelial cell injury (30). Because of the intimate association between coagulation and the inflammatory response, platelets have been considered a critical factor in the initiation and progression of AKI development in sepsis (31). Hence, N/LP, suggested as a surrogate indicator for NLR, can shed light on the relationship between systemic inflammation, immunity, and coagulation disorders comprehensively (13). Moreover, recent research presented that the levels of postoperative N/LP were significantly associated with AKI after abdominal and cardiovascular surgery (12, 13, 32). In addition, several retrospective studies have also indicated that a rising N/LP ratio is an efficient predictor of the risk of in-hospital mortality in patients with S-AKI and those undergoing emergency surgery (14, 33). However, no study has reported the relationship between N/LP and the occurrence and severity of AKI in sepsis patients. In the present study, we found that elevated N/LP in sepsis patients was associated with an increased risk of AKI. Furthermore, we also demonstrated that the risk of severe AKI (KDIGO stages 2 and 3) increased more than 2-fold when N/LP was over 10. These findings suggest that early N/LP elevation may serve as a potential predictor of the occurrence and severity of AKI in sepsis patients.

KDIGO guideline considers SCr and/or oliguria to have equal prognostic power for diagnosing AKI. Nevertheless, it is difficult to accurately obtain the baseline value when using the SCr criteria for AKI diagnosing due to the lack of uniform delineation criteria (34). UO is also insensitive and easily influenced by many factors (15). Several studies have shown poor consistency between SCr and UO criteria in AKI diagnosing and the corresponding staging (35–37). A sizeable single-center retrospective study with 32, 045 critically ill patients found that UO-based and SCr-based criteria have different diagnostic power for AKI (36). In another retrospective study of 6637 patients undergoing cardiac surgery, the incidence of AKI increased from 38.6% to 81.2%

after considering UO criteria (37). Similarly, using the SCr criteria alone may miss approximately 20% of AKI patients and lead to AKI grade misclassification (34, 36). Bianchi et al. (15) proved that oliguria lasting longer than 12 hours (KDIGO stage 2 and 3) was significantly diagnostic of AKI in 15, 620 patients and was not accompanied by elevated SCr levels. In this study, high N/LP was more strongly associated with the risk of S-AKI and severe AKI among sepsis patients based on UO-based rather than SCr-based AKI criteria. A previous study found that enhanced monitoring of UO improved detection of AKI and reduced 30-day mortality in patients with AKI (38). Therefore, we suggest that enhanced monitoring of UO and N/LP may be more useful in guiding clinical decision-making in S-AKI, especially in some special populations (elder, male, septic shock, and patients with a poor health condition).

Strengths and Limitations

This study has several strengths. The relationship between N/LP and the risk and severity of S-AKI was investigated for the first time, and the effect of N/LP on S-AKI was analyzed by Cox proportional risk model, competing risk model, and double robust estimation. The results are reliable and stable and provide a basis for clinical diagnosis and intervention in S-AKI. Notably, high N/LP based on UO criteria more strongly correlated with the risk of S-AKI and severe AKI in patients with sepsis compared with KDIGO AKI criteria. Thus, enhanced monitoring of UO and N/LP would be more helpful in guiding ICU physicians' clinical decision-making regarding S-AKI. However, this study has several limitations. First, MIMIC-IV is a single-center database, and selection bias exists in this study, limiting our conclusions' extrapolation. Second, we only discussed the influence of single indicator N/LP on the occurrence and development of S-AKI. Finally, our study only examined N/LP values within 24 hours of ICU admission in patients with sepsis and failed to evaluate the dynamic effect of N/LP, which was related to the absence of relevant information in the MIMIC database. In future studies, the predictive value of N/LP for S-AKI can be further evaluated by its dynamic changes.

CONCLUSIONS

Early assessment and intervention are crucial for managing S-AKI patients in the ICU. An initial elevated N/LP level may induce the development of S-AKI and severe AKI within 7 days after ICU admission in septic patients. These influences were enhanced in elder, males, septic shock, and those with a poor health condition. Furthermore, high NLP was more strongly connected to the risk of S-AKI and severe AKI in sepsis patients on the UO-based AKI criteria than on the SCr-based criteria. Therefore, enhanced monitoring of UO and N/LP would be more helpful in guiding clinical decisions about S-AKI. Of course, the effectiveness of N/LP in guiding the treatment of AKI in sepsis needs to be further investigated.

DATA AVAILABILITY STATEMENT

The original contributions presented in the study are included in the article/**Supplementary Material**, further inquiries can be directed to the corresponding author/s.

ETHICS STATEMENT

MIMIC-IV database is a publicly available anonymized database, approval for the ethical committee was not necessary.

AUTHOR CONTRIBUTIONS

XW and YM designed the study. LZ and LY extracted the data. XW, LZ and HT conducted data quality management and statistical analysis and drafted the manuscript. ZJ and HJ participated in the literature search. LH, XY and YM critically revised the manuscript. All authors contributed to the article and approved the submitted version.

FUNDING

This study was supported by a research grant from the National Natural Science Foundation of China (No. 82072134) and the National Natural Science Foundation Youth Science Foundation (No. 81601661).

ACKNOWLEDGMENTS

We thanks all participants in the Second Affiliated Hospital of Anhui Medical University and AnHui University.

SUPPLEMENTARY MATERIAL

The Supplementary Material for this article can be found online at: https://www.frontiersin.org/articles/10.3389/fimmu.2022.925494/full#supplementary-material

Supplementary Figure 1 | SMD of all 16 covariables before and after IPTW in (A) 1938 included sepsis patients, (B) and 680 patients with acute kidney injury diagnosed by SCr and UO criteria. SMD, standardized mean difference; IPTW, inverse probability of treatment weighting; LR, logistic regression; SAPS II, simplified acute physiology score II; SOFA, sequential organ failure assessment; CRRT, continuous renal replacement therapy; BUN, blood urea nitrogen; SCr, serum creatinine; UO, urine output.

Supplementary Figure 2 | The cumulative incidence curve of sepsis acute kidney injury (S-AKI) plotted by (A) Kaplan-Meier method, (B) and competing risk model. AKI is diagnosed based on serum creatinine criteria only.

Supplementary Figure 3 | (A) The cumulative incidence curve of sepsis acute kidney injury (S-AKI) plotted by Kaplan-Meier method after inverse probability treatment weighting (IPTW); (B) the results of univariate Cox proportional hazard

model after IPTW and double robust estimation regressed all 16 covariates. AKI is diagnosed based on serum creatinine criteria only.

Supplementary Figure 4 | SMD of all 16 covariables before and after IPTW in sensitivity analysis; (A) all sepsis patients with SCr records; (B) those who fulfill the SCr criteria in acute kidney injury diagnosing. SMD, standardized mean difference; IPTW, inverse probability of treatment weighting; LR, logistic regression; SAPS II, simplified acute physiology score II; SOFA, sequential organ failure assessment; CRRT, continuous renal replacement therapy; BUN, blood urea nitrogen; SCr, serum creatinine.

Supplementary Figure 5 | (A) The results of univariate and multivariate logistic regression. Model 1 represents the univariate analysis; Model 2 represents the multivariate analysis adjusting all covariates; Model 3 represents the multivariate analysis adjusting serum chloride, serum creatinine, SOFA scores excluding coagulation system, Charlson comorbidity index, the use of vasoactive medication, and invasive machine ventilation based on the results of stepwise backward approach and collinearity analysis; (B) the results of univariate logistic analysis after inverse probability treatment weighting and the double robust estimation. Acute kidney injury is diagnosed based on serum creatinine criteria only.

Supplementary Figure 6 | Multivariable adjusted odds ratios for severe acute kidney injury (AKI) occurrence according to initial N/LP on a continuous scale by using restricted cubic splines analysis. AKI and corresponding stage are diagnosed based on serum creatinine criteria only.

Supplementary Figure 7 | The cumulative incidence curve of sepsis acute kidney injury (S-AKI) plotted by (A) Kaplan-Meier method, and (B) competing risk model. AKI is diagnosed based on urine output criteria only.

Supplementary Figure 8 | SMD of all 16 covariables before and after IPTW in sensitivity analysis based; (A) all sepsis patients with urine output (UO) records; (B) those who fulfill the UO criteria in acute kidney injury diagnosing. SMD, standardized mean difference; IPTW, inverse probability of treatment weighting; LR, logistic regression; SAPS II, simplified acute physiology score II; SOFA, sequential organ failure assessment; CRRT, continuous renal replacement therapy; BUN, blood urea nitrogen; UO, urine output.

Supplementary Figure 9 | (A) The cumulative incidence curve of sepsis acute kidney injury (S-AKI) plotted by Kaplan-Meier method after inverse probability treatment weighting (IPTW); (B) the results of univariate Cox proportional hazard model after IPTW and double robust estimation regressed all 16 covariates. AKI is diagnosed based on urine output criteria only.

Supplementary Figure 10 | (A) The results of univariate and multivariate logistic regression. Model 1 represents the univariate analysis; Model 2 represents the multivariate analysis adjusting all covariates; Model 3 represents the multivariate analysis adjusting gender, serum bicarbonate, serum sodium, SOFA scores excluding coagulation system, Charlson comorbidity index, and the use of vasoactive medication based on the results of stepwise backward approach and collinearity analysis; (B) the results of univariate logistic analysis after inverse probability treatment weighting and the double robust estimation. Acute kidney injury is diagnosed based on urine output criteria only.

Supplementary Figure 11 | Multivariable adjusted odds ratios for severe acute kidney injury (AKI) occurrence according to initial N/LP on a continuous scale by using restricted cubic splines analysis. AKI and corresponding stage are diagnosed based on urine output criteria only.

REFERENCES

1. Rhodes A, Evans LE, Alhazzani W, Levy MM, Antonelli M, Ferrer R, et al. Surviving Sepsis Campaign: International Guidelines for Management of Sepsis and Septic Shock: 2016. *Crit Care Med* (2017) 45(3):486–552. doi: 10.1097/CCM.0000000000002255
2. Fleischmann C, Scherag A, Adhikari NK, Hartog CS, Tsaganos T, Schlattmann P, et al. Assessment of Global Incidence and Mortality of Hospital-Treated Sepsis. Current Estimates and Limitations. *Am J Respir Crit Care Med* (2016) 193(3):259–72. doi: 10.1164/rccm.201504-0781OC
3. Mårtensson J, Bellomo R. Pathophysiology of Septic Acute Kidney Injury. *Contrib Nephrol* (2016) 187:36–46. doi: 10.1159/000442363
4. Gomez H, Ince C, De Backer D, Pickkers P, Payen D, Hotchkiss J, et al. A Unified Theory of Sepsis-Induced Acute Kidney Injury: Inflammation, Microcirculatory Dysfunction, Bioenergetics, and the Tubular Cell Adaptation to Injury. *Shock* (2014) 41(1):3–11. doi: 10.1097/SHK.0000000000000052
5. Uchino S, Kellum JA, Bellomo R, Doig GS, Morimatsu H, Morgera S, et al. Acute Renal Failure in Critically Ill Patients: A Multinational, Multicenter Study. *JAMA* (2005) 294(7):813–8. doi: 10.1001/jama.294.7.813
6. Gómez H, Kellum JA. Sepsis-Induced Acute Kidney Injury. *Curr Opin Crit Care* (2016) 22(6):546–53. doi: 10.1097/MCC.0000000000000356
7. Coca SG, Yalavarthy R, Concato J, Parikh CR. Biomarkers for the Diagnosis and Risk Stratification of Acute Kidney Injury: A Systematic Review. *Kidney Int* (2008) 73(9):1008–16. doi: 10.1038/sj.ki.5002729
8. He J, Lin J, Duan M. Application of Machine Learning to Predict Acute Kidney Disease in Patients With Sepsis Associated Acute Kidney Injury. *Front Med (Lausanne)* (2021) 8:792974. doi: 10.3389/fmed.2021.792974
9. Luo XQ, Yan P, Zhang NY, Luo B, Wang M, Deng YH, et al. Machine Learning for Early Discrimination Between Transient and Persistent Acute Kidney Injury in Critically Ill Patients With Sepsis. *Sci Rep* (2021) 11 (1):20269. doi: 10.1038/s41598-021-99840-6
10. Manrique-Caballero CL, Del Rio-Pertuz G, Gomez H. Sepsis-Associated Acute Kidney Injury. *Crit Care Clin* (2021) 37(2):279–301. doi: 10.1016/j.ccc.2020.11.010
11. Cakir Guney B, Hayiroglu M, Senocak D, Cicek V, Cinar T, Kaplan M. Evaluation of N/LP Ratio as a Predictor of Disease Progression and Mortality in COVID-19 Patients Admitted to the Intensive Care Unit. *Medeni Med J* (2021) 36(3):241–8. doi: 10.5222/MMJ.2021.95676
12. Gameiro J, Fonseca JA, Dias JM, Milho J, Rosa R, Jorge S, et al. Neutrophil, Lymphocyte and Platelet Ratio as a Predictor of Postoperative Acute Kidney Injury in Major Abdominal Surgery. *BMC Nephrol* (2018) 19(1):320. doi: 10.1186/s12882-018-1073-4
13. Koo CH, Eun Jung D, Park YS, Bae J, Cho YJ, Kim WH, et al. Neutrophil, Lymphocyte, and Platelet Counts and Acute Kidney Injury After Cardiovascular Surgery. *J Cardiothorac Vasc Anesth* (2018) 32(1):212–22. doi: 10.1053/j.jvca.2017.08.033
14. Gameiro J, Fonseca JA, Jorge S, Gouveia J, Lopes JA. Neutrophil, Lymphocyte and Platelet Ratio as a Predictor of Mortality in Septic-Acute Kidney Injury Patients. *Nefrol (Engl Ed)* (2020) 40(4):461–8. doi: 10.1016/j.nefro.2019.11.006
15. Bianchi NA, Stavart LL, Altarelli M, Kelevina T, Faouzi M, Schneider AG. Association of Oliguria With Acute Kidney Injury Diagnosis, Severity Assessment, and Mortality Among Patients With Critical Illness. *JAMA Netw Open* (2021) 4(11):e2133094. doi: 10.1001/jamanetworkopen.2021.33094
16. Johnson A, Bulgarelli L, Pollard T, et al. *MIMIC-IV (Version 1.0) PhysioNet* (2021). Available at: https://physionet.org/content/mimiciv/1.0/.
17. Kidney Disease: Improving Global Outcomes (KDIGO) Acute Kidney Injury Work Group. KDIGO Clinical Practice Guideline for Acute Kidney Injury. *Kidney Inter* (2012) 2(Suppl):1–138. doi: 10.1038/kisup.2012.1
18. Yamada S, Taniguchi M, Tokumoto M, Yoshitomi R, Yoshida H, Tatsumoto N, et al. Modified Creatinine Index and the Risk of Bone Fracture in Patients Undergoing Hemodialysis: The Q-Cohort Study. *Am J Kidney Dis* (2017) 70 (2):270–80. doi: 10.1053/j.ajkd.2017.01.052
19. Lee DH, Keum N, Hu FB, Orav EJ, Rimm EB, Willett WC, et al. Predicted Lean Body Mass, Fat Mass, and All Cause and Cause Specific Mortality in Men: Prospective US Cohort Study. *BMJ* (2018) 362:k2575. doi: 10.1136/bmj.k2575
20. Bernier-Jean A, Wong G, Saglimbene V, Ruospo M, Palmer SC, Natale P, et al. Self-Reported Physical Activity and Survival in Adults Treated With

Hemodialysis: A DIET-HD Cohort Study. *Kidney Int Rep* (2021) 6(12):3014–25. doi: 10.1016/j.ekir.2021.09.002
21. Hoste EA, Bagshaw SM, Bellomo R, Cely CM, Colman R, Cruz DN, et al. Epidemiology of Acute Kidney Injury in Critically Ill Patients: The Multinational AKI-EPI Study. *Intensive Care Med* (2015) 41(8):1411–23. doi: 10.1007/s00134-015-3934-7
22. Peerapornratana S, Manrique-Caballero CL, Gómez H, Kellum JA. Acute Kidney Injury From Sepsis: Current Concepts, Epidemiology, Pathophysiology, Prevention and Treatment. *Kidney Int* (2019) 96(5):1083–99. doi: 10.1016/j.kint.2019.05.026
23. Heffernan DS, Monaghan SF, Thakkar RK, Machan JT, Cioffi WG, Ayala A. Failure to Normalize Lymphopenia Following Trauma is Associated With Increased Mortality, Independent of the Leukocytosis Pattern. *Crit Care* (2012) 16(1):R12. doi: 10.1186/cc11157
24. Bu X, Zhang L, Chen P, Wu X. Relation of Neutrophil-to-Lymphocyte Ratio to Acute Kidney Injury in Patients With Sepsis and Septic Shock: A Retrospective Study. *Int Immunopharmacol* (2019) 70:372–7. doi: 10.1016/j.intimp.2019.02.043
25. Seropian IM, Romeo FJ, Pizarro R, Vulcano NO, Posatini RA, Marenchino RG, et al. Neutrophil-To-Lymphocyte Ratio and Platelet-to-Lymphocyte Ratio as Predictors of Survival After Heart Transplantation. *ESC Heart Fail* (2018) 5(1):149–56. doi: 10.1002/ehf2.12199
26. Wada H, Dohi T, Miyauchi K, Shitara J, Endo H, Doi S, et al. Pre-Procedural Neutrophil-to-Lymphocyte Ratio and Long-Term Cardiac Outcomes After Percutaneous Coronary Intervention for Stable Coronary Artery Disease. *Atherosclerosis* (2017) 265:35–40. doi: 10.1016/j.atherosclerosis.2017.08.007
27. Yodying H, Matsuda A, Miyashita M, Matsumoto S, Sakurazawa N, Yamada M, et al. Prognostic Significance of Neutrophil-To-Lymphocyte Ratio and Platelet-To-Lymphocyte Ratio in Oncologic Outcomes of Esophageal Cancer: A Systematic Review and Meta-Analysis. *Ann Surg Oncol* (2016) 23(2):646–54. doi: 10.1245/s10434-015-4869-5
28. Hwang SY, Shin TG, Jo IJ, Jeon K, Suh GY, Lee TR, et al. Neutrophil-To-Lymphocyte Ratio as a Prognostic Marker in Critically-Ill Septic Patients. *Am J Emerg Med* (2017) 35(2):234–9. doi: 10.1016/j.ajem.2016.10.055
29. Riché F, Gayat E, Barthélémy R, Le Dorze M, Matéo J, Payen D. Reversal of Neutrophil-to-Lymphocyte Count Ratio in Early Versus Late Death From Septic Shock. *Crit Care* (2015) 19:439. doi: 10.1186/s13054-015-1144-x
30. Fani F, Regolisti G, Delsante M, Cantaluppi V, Castellano G, Gesualdo L, et al. Recent Advances in the Pathogenetic Mechanisms of Sepsis-Associated Acute Kidney Injury. *J Nephrol* (2018) 31(3):351–9. doi: 10.1007/s40620-017-0452-4
31. Greco E, Lupia E, Bosco O, Vizio B, Montrucchio G. Platelets and Multi-Organ Failure in Sepsis. *Int J Mol Sci* (2017) 18(10):2200. doi: 10.3390/ijms18102200
32. Li Y, Zou Z, Zhang Y, Zhu B, Ning Y, Shen B, et al. Dynamics in Perioperative Neutrophil-to-Lymphocyte*Platelet Ratio as a Predictor of Early Acute Kidney Injury Following Cardiovascular Surgery. *Ren Fail* (2021) 43 (1):1012–9. doi: 10.1080/0886022X.2021.1937220
33. Chae YJ, Lee J, Park JH, Han DG, Ha E, Yi IK. Late Mortality Prediction of Neutrophil-To-Lymphocyte and Platelet Ratio in Patients With Trauma Who Underwent Emergency Surgery: A Retrospective Study. *J Surg Res* (2021) 267:755–61. doi: 10.1016/j.jss.2020.11.088
34. Poston JT, Koyner JL. Sepsis Associated Acute Kidney Injury. *BMJ* (2019) 364: k4891. doi: 10.1136/bmj.k4891
35. Prowle JR, Liu YL, Licari E, Bagshaw SM, Egi M, Haase M, et al. Oliguria as Predictive Biomarker of Acute Kidney Injury in Critically Ill Patients. *Crit Care* (2011) 15(4):R172. doi: 10.1186/cc10318
36. Kellum JA, Sileanu FE, Murugan R, Lucko N, Shaw AD, Clermont G. Classifying AKI by Urine Output Versus Serum Creatinine Level. *J Am Soc Nephrol* (2015) 26(9):2231–8. doi: 10.1681/ASN.2014070724
37. Priyanka P, Zarbock A, Izawa J, Gleason TG, Renfurm RW, Kellum JA. The Impact of Acute Kidney Injury by Serum Creatinine or Urine Output Criteria on Major Adverse Kidney Events in Cardiac Surgery Patients. *J Thorac Cardiovasc Surg* (2021) 162(1):143–51.e7. doi: 10.1016/j.jtcvs.2019.11.137
38. Jin K, Murugan R, Sileanu FE, Foldes E, Priyanka P, Clermont G, et al. Intensive Monitoring of Urine Output Is Associated With Increased Detection of Acute Kidney Injury and Improved Outcomes. *Chest* (2017) 152(5):972–9. doi: 10.1016/j.chest.2017.05.011

Conflict of Interest: KS is employed by Daiichi Sankyo Co., Ltd.

The remaining authors declare that the research was conducted in the absence of any commercial or financial relationships that could be construed as a potential conflict of interest.

Publisher's Note: All claims expressed in this article are solely those of the authors and do not necessarily represent those of their affiliated organizations, or those of the publisher, the editors and the reviewers. Any product that may be evaluated in this article, or claim that may be made by its manufacturer, is not guaranteed or endorsed by the publisher.

frontiers | Frontiers in Immunology

TYPE Original Research
PUBLISHED 14 July 2022
DOI 10.3389/fimmu.2022.895018

OPEN ACCESS

EDITED BY
Alessandra Stasi,
University of Bari Aldo Moro, Italy

REVIEWED BY
Davide Medica,
University of Eastern Piedmont, Italy
Gianvito Caggiano,
University of Bari Aldo Moro, Italy

*CORRESPONDENCE
Daoxin Wang
wangdaoxin@hospital.cqmu.edu.cn
Di Qi
qidi@hospital.cqmu.edu.cn

†These authors have contributed equally to this work

SPECIALTY SECTION
This article was submitted to Inflammation, a section of the journal Frontiers in Immunology

RECEIVED 12 March 2022
ACCEPTED 27 June 2022
PUBLISHED 14 July 2022

CITATION
Peng J, Tang R, Yu Q, Wang D and Qi D (2022) No sex differences in the incidence, risk factors and clinical impact of acute kidney injury in critically ill patients with sepsis. *Front. Immunol.* 13:895018. doi: 10.3389/fimmu.2022.895018

No sex differences in the incidence, risk factors and clinical impact of acute kidney injury in critically ill patients with sepsis

Junnan Peng†, Rui Tang†, Qian Yu, Daoxin Wang* and Di Qi*

Department of Respiratory and Critical Care Medicine, Second Affiliated Hospital of Chongqing Medical University, Chongqing, China

Background: Sex-stratified medicine is an important aspect of precision medicine. We aimed to compare the incidence and risk factors of acute kidney injury (AKI) for critically ill men and women with sepsis. Furthermore, the short-term mortality was compared between men and women with sepsis associated acute kidney injury (SA-AKI).

Method: This was a retrospective study based on the Medical Information Mart for Intensive Care IV database. We used the multivariable logistic regression analysis to evaluate the independent effect of sex on the incidence of SA-AKI. We further applied three machine learning methods (decision tree, random forest and extreme gradient boosting) to screen for the risk factors associated with SA-AKI in the total, men and women groups. We finally compared the intensive care unit (ICU) and hospital mortality between men and women with SA-AKI using propensity score matching.

Results: A total of 6463 patients were included in our study, including 3673 men and 2790 women. The incidence of SA-AKI was 83.8% for men and 82.1% for women. After adjustment for confounders, no significant association was observed between sex and the incidence of SA-AKI (odds ratio (OR), 1.137; 95% confidence interval (CI), 0.949-1.361; p=0.163). The machine learning results revealed that body mass index, Oxford Acute Severity of Illness Score, diuretic, Acute Physiology Score III and age were the most important risk factors of SA-AKI, irrespective of sex. After propensity score matching, men had similar ICU and hospital mortality to women.

Conclusions: The incidence and associated risk factors of SA-AKI are similar between men and women, and men and women with SA-AKI experience comparable rates of ICU and hospital mortality. Therefore, sex-related effects may play a minor role in developing SA-AKI. Our study helps to contribute to the knowledge gap between sex and SA-AKI.

KEYWORDS

sepsis, AKI, sex, intensive care, critically ill

Introduction

Sepsis is one of the most common critical diseases treated in the intensive care unit (ICU) (1). In the United States, the annual incidence of sepsis was 82.7 to 240.4 per 100,000 population (2), while the estimated worldwide incidence was up to 437 per 100,000 population years (3). Sepsis frequently leads to multiorgan dysfunction, and kidney involvement is usual (4). More than half of patients with sepsis develop acute kidney injury (AKI) during hospitalization, and this condition adversely affects patient outcomes (5). Despite years of research, sepsis associated acute kidney injury (SA-AKI) remains an important concern and clinical burden, and the identification of risk factors for SA-AKI is still essential so that targeted strategies may be implemented (6).

Sex-stratified medicine is an important aspect of precision medicine (7). The impact of patient sex on clinical outcomes is an area of intense interest. A large retrospective study of 261,255 critically ill patients revealed that women less than 50 years of age had lower adjusted mortality than men (8). Moreover, different disease processes and outcomes between men and women were also found in some specific disease groups, like coronary artery disease (9), acute ischemic stroke (10) and coronavirus disease 2019 (11). This may be associated with the influence of sex hormones on the modulation of inflammation during immune responses (12). Sexual dimorphism exists in immune processes, leading to the differences in immunomodulation of the cytokine network during inflammatory responses (13, 14). It has been found that excessive inflammation and immune suppression are involved in developing SA-AKI (6, 15). Therefore, the role of sex in SA-AKI should be drawn further attention. Until present, relevant studies are mainly about the effect of sex on mortality of SA-AKI patients, and data on the association between sex and the incidence as well as risk factors of SA-AKI are very scarce.

The primary goal of our study was to assess sex-specific effects on the incidence of AKI in critical patients with sepsis. We further investigated if men and women had differential risk factors associated with SA-AKI, which indicates the non-homogenous management strategies for them. We also aimed to compare the short-term clinical outcomes between men and women with SA-AKI. Our hypothesis was that sex would affect the incidence of SA-AKI, and the risk factors as well as clinical impact of SA-AKI were not similar between men and women.

Method

Study design

This study is reported following the REporting of studies Conducted using Observational Routinely collected health Data (RECORD) statement (16). Medical ethical approval and the informed consent were exempted due to the retrospective study design and anonymous information collection.

We extracted patient data from the Medical Information Mart for Intensive Care IV (MIMIC-IV) database (https://mimic.physionet.org/about/mimic/). The description of MIMIC-IV database is available elsewhere (17). In brief, the MIMIC-IV database is a large and publicly available database comprising more than 70,000 patients in the ICU of the Beth Israel Deaconess Medical Center in Boston, MA, USA, between 2008 and 2019. All data were collected before the coronavirus disease 2019 outbreak. To apply for access to the database, we have passed the National Institutes of Health Web-based training course and Protecting Human Research Participants examination (No. 9555299). Data extraction was performed in the Structured Query Language with Navicat Premium (version 15).

Selection of patients

In the present study, patients older than 18 years of age admitted to the ICU with an ICU length of stay longer than 72 hours were screened for possible inclusion. Since one patient may be admitted to the ICU multiple times, we only counted the first ICU admission due to non-independence of the outcome among subsequent ICU admissions. Patients were included if they met the Sepsis-3.0 definition upon ICU admission. The details of sepsis-3.0 definition include the presence of an infection with signs of organ dysfunction, which are represented by an increase in the Sequential [Sepsis-related] Organ Failure Assessment (SOFA) score of two points or more (18). Infection was identified from the international classification of diseases (ICD)-9 or ICD-10 code in the MIMIC-IV database. We excluded patients if they developed AKI before ICU admission or after 7 days of ICU admission.

Outcomes

We defined the occurrence of AKI within the first 7 days after ICU admission as the primary outcome of interest. Included patients for whom AKI occurred within 7 days after ICU admission were classified as the AKI group, and the rest of the patients comprised the non-AKI group. The AKI was diagnosed according to the Kidney Disease: Improving Global Outcomes (KDIGO) criteria. KDIGO criteria are as follows (19): increase in serum creatinine (SCr) to ≥ 1.5 times baseline must have occurred within the prior 7 days, or an increase of SCR ≥ 0.3 mg/dl within 48 hours, or urine volume < 0.5 ml/kg/hour for 6 h or more. We used the admission SCr as a baseline value, in accordance with previous studies (20, 21). Patients were

categorized into the AKI group (KDIGO stage 3) if they received continuous renal replacement therapy (CRRT) within the first 7 days after ICU admission. Severe AKI was defined as KDIGO stage 2 or higher, otherwise it was defined as mild AKI (22, 23). Secondary outcomes included the ICU and hospital mortality, which were defined as the occurrence of death during the ICU and hospital stay, respectively.

Sensitivity and subgroup analyses

We did several sensitivity and subgroup analyses for the primary outcomes. First, given the considerable impact of age on sex hormones (7), we conducted a stratified analysis according to age in decades (≤40, (40–50], (50–60], (60–70], (70–80], (80–90] and>90 years). Second, to determine whether the illness severity of AKI would influence the results, we further compared patients without AKI to those with mild AKI or with severe AKI. Lastly, we also performed analyses adjusted for the presence of comorbidities.

Data extraction

Baseline characteristics within the first 24 h after ICU admission were collected, including age, sex, body mass index (BMI), ethnicity and admission type. Comorbidities including hypertension, coronary atherosclerosis, heart failure, diabetes mellitus, chronic obstructive pulmonary disease (COPD), cerebral infarction, chronic liver disease, chronic kidney disease, and tumors were also collected for analysis based on the recorded ICD-9 or ICD-10 codes in the MIMIC-IV database. The severity as measured by the Sequential Organ Failure Assessment (SOFA) score, the Acute Physiology Score III (APS III) and the Oxford Acute Severity of Illness Score (OASIS) were calculated upon ICU admission. The use of vasopressor, mechanical ventilation, diuretic, aminoglycoside, statin and angiotensin-converting enzyme inhibitors/angiotensin receptor blockers were also recorded. For the AKI group, an intervention was considered positive if conducted before the onset of AKI and negative otherwise; for the non-AKI group, it was based on the records within 7 days of ICU admission. Vital signs included the heart rate, mean arterial pressure, respiratory rate, temperature and peripheral blood oxygen saturation (SpO_2). Laboratory findings including white blood cell, hemoglobin, platelet, pondus hydrogenii, bicarbonate, blood urea nitrogen, creatinine, potassium, sodium, chloride, glucose, prothrombin time, activated partial thromboplastin time and lactate were measured during the first 24 h in the ICU. If a variable was recorded more than once, we only used the first value for analysis. Detailed information on missing data is available in **Supplementary Table S1**. The random Forest-based imputation method was used to impute missing values for these variables (24). The random forest algorithm was implemented using the R package "missForest" (version 1.4; https://CRAN.R-project.org/package=missForest).

Statistical analysis

We performed the statistical analysis and created pictures by using R statistical software (version 3.6.1, https://cran.r-project.org/), GraphPad Prizm (version 8.0, San Diego, CA, https://www.graphpad.com/scientific-software/prism/) or SPSS software (version 26.0, IBM, USA, https://www.ibm.com/analytics/spss-statistics-software). For continuous variables, we first investigated the normality using the Kolmogorov-Smirnov test. Normally distributed variables are expressed as mean ± standard deviation (SD) and were compared using Student's t-test. Non-normally distributed variables are presented as the median and interquartile range (IQR) and were analyzed using the non-parametric Mann–Whitney U test. Categorical variables are expressed as count with percentage (%) and were compared with the chi-square test or Fisher's exact test as appropriate. All tests were two-tailed. A p-value <0.05 was considered significant.

We then used the multivariable logistic regression analyses to assess the independent association between sex and the incidence of SA-AKI. Five different models were built. The first one only included sex, and the second model included sex, age, BMI, ethnicity and admission type. In the third model, we further included comorbidities as covariates. The fourth model additionally included other exposure variables with p-value <0.1 in univariate analyses for multivariable analysis, due to their potential influence on the patient's primary outcome. In the final model, all baseline variables were included in order to provide a comprehensive assessment. In all models, the effect of sex (women=referent) on primary outcome was presented as an odds ratio (OR) with a 95% confidence interval (95%CI).

Further, we applied three machine learning models to screen for the risk factors: decision tree model, random forest model and Extreme Gradient Boosting (XGBoost) model. A decision tree algorithm is a basic classification method that constructs a model based on the feature of data using a tree structure (25). Feature selection, tree generation, and pruning are the basic steps of building decision trees, and an object-relational mapping relationship was eventually generated (26). In this study, we used the Classification and Regression Tree method with the rpart package (version 4.1.16, https://CRAN.R-project.org/package=rpart) for constructing the decision tree in the R language. Random forest is an ensemble algorithm that combines multiple decision trees, and there is no correlation between each decision tree (27). The voting method is used to discriminate and classify data, and the maximum number of votes is taken as the final classification result (28). In this study, we used the RandomForest package (version 4.7-1, https://CRAN.R-project.org/package=randomForest) in the R

language for analysis. XGBoost is an ensemble algorithm composed of multiple decision trees and a gradient boost machine (29). The main advantage of XGBoost is to combine multithreading, data compression, and fragmentation methods to improve the efficiency of the algorithm as much as possible (30). In this study, XGBoost was implemented using the xgboost package (version 1.5.2.1, https://CRAN.R-project.org/package=xgboost) in the R language. Machine learning models have exhibited several advantages over conventional statistical methods, and are gradually used in recent studies (31, 32).

Lastly, we estimated the effect of sex on ICU and hospital mortality for patients with SA-AKI. We used propensity score matching (PSM) to balance baseline variables between men and women. Specifically, matching was performed using R package 'matching' (version 4.9-11, https://CRAN.R-project.org/package=Matching), with a ratio of 1:1 and a caliper width of 0.1 without replacement. We considered a standardized mean difference (SMD) of less than 0.1 as acceptable. After propensity matching, differences in ICU and hospital mortality were compared between the two groups. This method has been widely used to compare the mortality between different groups, due to its excellent ability to control measured confounding in observational studies (33, 34).

Results

Baseline characteristics

The process of patient selection is shown in **Figure 1**. Finally, a total of 6463 patients were included in our study. Of them, 3673 (56.8%) were men and 2790 (43.2%) were women, with mean age of 66.42 ± 16.58 years. The most common comorbidity was hypertension, followed by heart failure, diabetes mellitus and chronic kidney disease. Men were younger, less likely to have hypertension, heart failure, COPD and cerebral infarction than women; however, men were more likely to have coronary atherosclerosis and chronic kidney disease. Men had lower OASIS and higher SOFA scores than women, but the APS III score was similar between them. In terms of the interventions, more men had mechanical ventilation and statin, while fewer men had diuretic use. The overall incidence of SA-AKI was 83.1% (5368/6463), and men had a slightly higher but not significant incidence than women (83.8% *vs.* 82.1%, $p = 0.068$). The detailed information about baseline characteristics of the total cohort, men and women are shown in **Table 1**.

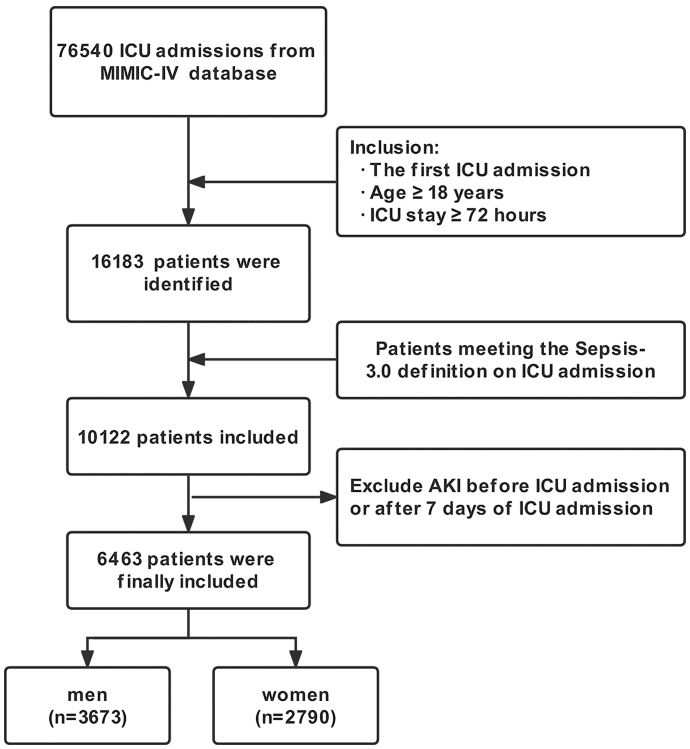

FIGURE 1
Flow chart of this study. MIMIC-IV, Medical Information Mart for Intensive Care IV database; ICU, Intensive care unit; AKI, Acute kidney injury.

10.3389/fimmu.2022.895018

TABLE 1 Baseline characteristics of patients.

Variables	Total (n=6463)	Men (n=3673)	Women (n=2790)	*p*-value
Age (years)	66.42 ± 16.58	64.86 ± 16.38	68.48 ± 16.61	<0.001
BMI (kg/m^2)	29.65 ± 7.50	29.52 ± 7.26	29.82 ± 7.80	0.113
Ethnicity, n (%)				0.119
White	4217 (65.2)	2367 (64.4)	1850 (66.3)	
Non-white	2246 (34.8)	1306 (35.6)	940 (33.7)	
Admission type, n (%)				0.715
Emergency	4003 (61.9)	2282 (62.1)	1721 (61.7)	
Non-emergency	2460 (38.1)	1391 (37.9)	1069 (38.3)	
Comorbidities, n (%)				
Hypertension	2671 (41.3)	1477 (40.2)	1194 (42.8)	0.037
Coronary atherosclerosis	1098 (17.1)	687 (18.7)	411 (14.7)	<0.001
Heart failure	2048 (31.7)	1124 (30.6)	924 (33.1)	0.031
Diabetes mellitus	1708 (26.4)	977 (27.1)	711 (25.5)	0.134
COPD	561 (8.7)	290 (7.9)	271 (9.7)	0.01
Cerebral infarction	673 (10.4)	353 (9.6)	320 (11.5)	0.015
Chronic liver disease	98 (1.5)	61 (1.7)	37 (1.3)	0.276
Chronic kidney disease	1412 (21.8)	858 (23.4)	554 (19.9)	0.001
Tumor	1109 (17.2)	619 (16.9)	490 (17.6)	0.453
Severity scale (at admission)				
APS III	64.89 ± 27.57	64.59 ± 27.91	65.30 ± 27.12	0.307
OASIS	39.24 ± 9.19	38.77 ± 9.14	39.86 ± 9.21	<0.001
SOFA	3 (2–5)	3 (2-5)	3 (2-4)	<0.001
Interventions, n (%)				
Vasopressor use	473 (7.3)	278 (7.6)	195 (7.0)	0.376
Mechanical ventilation	4087 (63.2)	2391 (65.1)	1696 (60.8)	<0.001
Diuretic	1616 (25.0)	837 (22.8)	779 (27.9)	<0.001
Aminoglycoside	135 (2.1)	79 (2.2)	56 (2.0)	0.689
Statin	1836 (28.4)	1084 (29.5)	752 (27.0)	0.024
ACEI/ARBs	662 (10.2)	367 (10.0)	295 (10.6)	0.445
Vital signs				
Heart rate (beats/min)	92.45 ± 21.17	91.99 ± 21.31	93.05 ± 20.97	0.047
MAP (mmHg)	82.50 ± 19.57	82.80 ± 18.93	82.10 ± 20.38	0.155
RR (times/min)	20.28 ± 6.32	20.12 ± 6.26	20.50 ± 6.39	0.018
Temperature (°C)	36.73 ± 1.00	36.76 ± 1.01	36.69 ± 1.00	0.005
SpO2 (%)	98 (95-100)	98 (95-100)	98 (95-100)	0.927
Laboratory findings				
WBC (k/uL)	12.3 (8.6-17.2)	12.3 (8.6-17.2)	12.2 (8.5-17.2)	0.692
Hemoglobin (g/L)	10.60 ± 2.30	10.92 ± 2.41	10.18 ± 2.07	<0.001
Platelet (k/uL)	202.50 ± 114.86	194.30 ± 111.88	213.30 ± 117.81	<0.001
PH	7.35 ± 0.10	7.35 ± 0.10	7.35 ± 0.11	0.022
Bicarbonate (mEq/L)	22.21 ± 5.14	22.23 ± 4.84	22.18 ± 5.51	0.662
BUN (mg/dL)	22 (15-36)	22 (15-37)	21 (14-34)	<0.001
Creatinine (mg/dL)	1.1 (0.8-1.7)	1.2 (0.9-1.8)	0.9 (0.7-1.5)	<0.001
Potassium (mEq/L)	4.24 ± 0.80	4.33 ± 0.81	4.12 ± 0.77	<0.001
Sodium (mEq/L)	138.79 ± 5.85	138.71 ± 5.73	138.89 ± 6.01	0.213
Chloride (mEq/L)	104.64 ± 7.18	104.48 ± 7.05	104.83 ± 7.33	0.056
Glucose (mg/dL)	155.44 ± 82.87	155.75 ± 82.84	155.01 ± 82.93	0.721
PT (s)	17.20 ± 9.94	17.21 ± 9.53	17.18 ± 10.45	0.918

(Continued)

TABLE 1 Continued

Variables	Total (n=6463)	Men (n=3673)	Women (n=2790)	*p*-value
APTT (s)	38.97 ± 23.67	39.08 ± 23.56	38.83 ± 23.83	0.672
Lactate (mmol/L)	1.9 (1.3-2.9)	1.9 (1.3-2.9)	1.8 (1.3-2.8)	0.004
AKI	5368 (83.1)	3078 (83.8)	2290 (82.1)	0.068

Data were presented as mean ± standard deviation or median (interquartile range) or numbers (percentages).
ACEI/ARBs, Angiotensin-converting enzyme inhibitors/angiotensin receptor blockers; AKI, Acute kidney injury; APS III, Acute Physiology Score III; APTT, Activated partial thromboplastin time; BMI, Body mass index; BUN, Blood urea nitrogen; COPD, Chronic obstructive pulmonary disease; OASIS, Oxford Acute Severity of Illness Score; PT, Prothrombin time; SOFA, Sequential Organ Failure Assessment; RR, Respiratory rate; WBC, White blood cell.

Comparison between aki and non-aki groups

In order to search for factors that might influence the incidence of SA-AKI, we compared the baseline characteristics between patients with and without SA-AKI. As shown in **Table 2**, we found that the AKI group was older, had a higher BMI, and was more likely to be admitted from the emergency department. The proportion of patients with heart failure, diabetes mellitus, COPD, chronic liver disease and chronic kidney disease were higher in the AKI group, while more patients had tumors in the non-AKI group. In addition, patients with SA-AKI had higher severity scores on admission when compared to those without SA-AKI, including APS III, OASIS and SOFA scores. Patients with SA-AKI were more likely to have vasopressor use and mechanical ventilation when

TABLE 2 Comparison between AKI group and non-AKI group.

Variables	non-AKI group (n=1095)	AKI group (n=5368)	*p*-value
Age (years)	61.01 ± 18.98	67.52 ± 15.82	<0.001
Sex (males, %)	595 (54.3)	3078 (57.3)	0.068
BMI (kg/m2)	25.71 ± 4.15	30.46 ± 7.77	<0.001
Ethnicity, n (%)			0.056
White	687 (62.7)	3530 (65.8)	
Non-white	408 (37.3)	1838 (34.2)	
Admission type, n (%)			<0.001
Emergency	356 (32.5)	2104 (39.2)	
Non-emergency	739 (67.5)	3264 (60.8)	
Comorbidities, n (%)			
Hypertension	423 (38.6)	2248 (41.9)	0.047
Coronary atherosclerosis	119 (10.9)	979 (18.2)	<0.001
Heart failure	177 (16.2)	1871 (34.9)	<0.001
Diabetes mellitus	197 (18.0)	1511 (28.1)	<0.001
COPD	67 (6.1)	494 (9.2)	0.001
Cerebral infarction	99 (9.0)	574 (10.7)	0.103
Chronic liver disease	8 (0.7)	90 (1.7)	0.02
Chronic kidney disease	116 (10.6)	1296 (24.1)	<0.001
Tumor	222 (20.3)	887 (16.5)	0.003
Severity scale (at admission)			
APS III	47.98 ± 19.32	68.34 ± 27.73	<0.001
OASIS	32.84 ± 7.72	40.55 ± 8.91	<0.001
SOFA	3 (2-4)	3 (2-5)	<0.001
Interventions, n (%)			
Vasopressor use	51 (4.7)	422 (7.9)	<0.001
Mechanical ventilation use	560 (51.1)	3527 (65.7)	<0.001
Diuretic	506 (46.2)	1110 (20.7)	<0.001
Aminoglycoside	58 (5.3)	77 (1.4)	<0.001

(Continued)

TABLE 2 Continued

Variables	non-AKI group (n=1095)	AKI group (n=5368)	*p*-value
Statin	340 (31.1)	1496 (27.9)	0.033
ACEI/ARBs	253 (23.1)	409 (7.6)	<0.001
Vital signs			
Heart rate (beats/min)	92.65 ± 20.74	92.41 ± 21.25	0.736
MAP (mmHg)	81.15 ± 18.01	82.16 ± 19.86	0.001
RR (times/min)	20.08 ± 5.88	20.32 ± 6.41	0.219
Temperature (°C)	36.88 ± 0.90	36.70 ± 1.02	<0.001
SpO2 (%)	98 (96-100)	98 (95-100)	0.311
Laboratory findings			
WBC (k/uL)	11.4 (7.8-15.8)	12.5 (8.8-17.5)	<0.001
Hemoglobin (g/L)	10.64 ± 2.13	10.59 ± 2.33	0.529
Platelet (k/uL)	208.86 ± 112.72	201.21 ± 115.26	0.045
PH	7.38 ± 0.81	7.35 ± 0.11	<0.001
Bicarbonate (mEq/L)	22.70 ± 4.82	22.11 ± 5.20	<0.001
BUN (mg/dL)	16 (11-27)	23 (15-37)	<0.001
Creatinine (mg/dL)	0.8 (0.6-1.1)	1.1 (0.8-1.8)	<0.001
Potassium (mEq/L)	4.02 ± 0.66	4.28 ± 0.81	<0.001
Sodium (mEq/L)	139.13 ± 5.87	138.72 ± 5.84	0.035
Chloride (mEq/L)	105.11 ± 7.13	104.54 ± 7.18	0.016
Glucose (mg/dL)	141.06 ± 69.98	158.37 ± 84.97	<0.001
PT (s)	15.34 ± 6.55	17.57 ± 10.46	<0.001
APTT (s)	34.59 ± 18.37	39.87 ± 24.52	<0.001
Lactate (mmol/L)	1.7 (1.3-2.3)	1.9 (1.3-3)	<0.001

Data were presented as mean ± standard deviation or median (interquartile range) or numbers (percentages).
ACEI/ARBs, Angiotensin-converting enzyme inhibitors/angiotensin receptor blockers; AKI, Acute kidney injury; APS III, Acute Physiology Score III; APTT, Activated partial thromboplastin time; BMI, Body mass index; BUN, Blood urea nitrogen; COPD, Chronic obstructive pulmonary disease; OASIS, Oxford Acute Severity of Illness Score; PT, Prothrombin time; SOFA, Sequential Organ Failure Assessment; RR, Respiratory rate; WBC, White blood cell.

compared to those without SA-AKI; however, a lower proportion of patients in the AKI group had diuretic, aminoglycoside, statin and ACEI/ARBs. Patients with SA-AKI had significantly higher ICU and hospital mortality rates, compared with the patients without SA-AKI (ICU mortality, 19.84% *vs.* 3.65, $p<0.001$; hospital mortality, 25.09% *vs.* 7.76%, $p<0.001$).

Association between sex and SA-AKI

We examined the association between sex and SA-AKI in univariate and extended logistic regression models. We found that men were associated with a higher likelihood of having SA-AKI, but this association became insignificant in the full adjusted model (OR, 1.137; 95% CI, 0.949-1.361; $p = 0.163$; **Table 3**). Similarly, multiple logistic regression revealed that no significant differences in SA-AKI incidence between sexes when comparing patients without SA-AKI to those with mild SA-AKI or with severe SA-AKI (non-AKI *vs.* mild AKI, OR 1.161, 95% CI 0.962-1.402, $p = 0.120$, **Table S2**; non-AKI *vs.* severe AKI, OR 1.175; 95% CI 0.912-1.513; $p = 0.211$, **Table S3**). Then, we examined the effect of age on sex-related outcomes. When age was stratified per decade, there was no association between sexes and SA-AKI incidence except for higher rates for men in those aged 50 to 60 years (men *vs.* women, 19.23% *vs.* 20.66%, $p = 0.196$; **Figure 2**). However, in logistic regression adjusted for all baseline variables, the SA-AKI incidence in men and women was approximately the same for all ages (**Figure 3**). Additionally, we conducted a series of subgroup analyses to determine the effect of comorbidity on the incidence of SA-AKI. The results remained consistent except for patients with cerebral infarction (men *vs.* women, OR 2.062, 95%CI 1.088-3.905, $p=0.026$, **Table S4**).

Risk factors for patients with SA-AKI

We used three machine learning methods (decision tree model, random forest model and XGBoost model) to evaluate risk factors of SA-AKI in patients with sepsis. Of all patients, BMI, OASIS, diuretic, APS III and age had the five highest values in importance of the models (**Figures 4A–C**). Similar results were also found in men (**Figures 5A–C**) and women (**Figures 6A–C**).

TABLE 3 Multivariate logistic regression analysis of sex for SA-AKI.

Model	OR (95%CI)	*p*-value
Model 1	1.129 (0.991-1.287)	0.068
Model 2	1.266 (1.100-1.457)	0.001
Model 3	1.230 (1.067-1.419)	0.004
Model 4	1.126 (0.943-1.344)	0.190
Model 5	1.137 (0.949-1.361)	0.163

Adjusted covariates: Model 1= sex (women=referent).
Model 2= Model 1 + age, BMI, ethnicity and admission type.
Model 3=Model 2 + comorbidities (hypertension, coronary atherosclerosis, heart failure, diabetes mellitus, COPD, cerebral infarction, chronic liver disease, chronic kidney disease, tumor).
Model 4=Model 3 + other variables with p<0.1 in the univariate analysis (APS III, OASIS, SOFA, MAP, temperature, WBC, platelet, PH, bicarbonate, BUN, creatinine, potassium, sodium, chloride, glucose, PT, APTT, lactate, vasopressor use, mechanical ventilation use, diuretic, aminoglycoside, statin, ACEI/ARBs).
Model 5 was adjusted for all baseline variables.
ACEI/ARBs, Angiotensin-converting enzyme inhibitors/angiotensin receptor blockers; APS III, Acute Physiology Score III; APTT, Activated partial thromboplastin time; BMI, Body mass index; BUN, Blood urea nitrogen; CI, Confidence interval; COPD, Chronic obstructive pulmonary disease; OASIS, Oxford Acute Severity of Illness Score; OR, Odds ratio; PT, Prothrombin time; SA-AKI, Sepsis associated acute kidney injury; SOFA, Sequential Organ Failure Assessment; RR, Respiratory rate; WBC, White blood cell.

Sex-related short-term mortality in patients with SA-AKI

We finally assessed the effect of sex on in-hospital and ICU mortality in patients with SA-AKI. Before propensity-score matching, age, the proportion of patients with coronary atherosclerosis, OASIS, SOFA, the proportion of mechanical ventilation and diuretic usage, hemoglobin, platelet, BUN, creatinine and potassium were different between the men and women groups (**Table 4**). We found that men had lower but not statistically significant ICU and hospital mortality than women (ICU mortality, men *vs.* women, 19.23% *vs.* 20.66%, $p = 0.196$, **Figure 7A**; hospital mortality, men *vs.* women, 24.20% *vs.* 26.29%, $p = 0.082$, **Figure 7C**). With the use of propensity-score matching (1:1 matching ratio), 1866 pairs of matched SA-AKI patients were created. After matching, we found no significant imbalance between the two groups, with the standardized mean difference being<0.1 for all variables (**Figure S1**; **Table 4**). No differences in ICU and hospital mortality between men and women were found (ICU mortality, men *vs.* women, 19.72% *vs.* 20.42%, $p = 0.595$, **Figure 7B**; hospital mortality, men *vs.* women, 25.62% *vs.* 25.77%, $p = 0.991$, **Figure 7D**).

Discussion

In this large retrospective study, we compared the incidence of SA-AKI and risk factors associated with SA-AKI for critically ill men and women with sepsis. The sex-specific clinical outcomes were also examined in men versus women with SA-AKI. To our surprise, we found that men and women had similar SA-AKI incidence, and the association between sex and the incidence of SA-AKI was insignificant in the full-adjusted

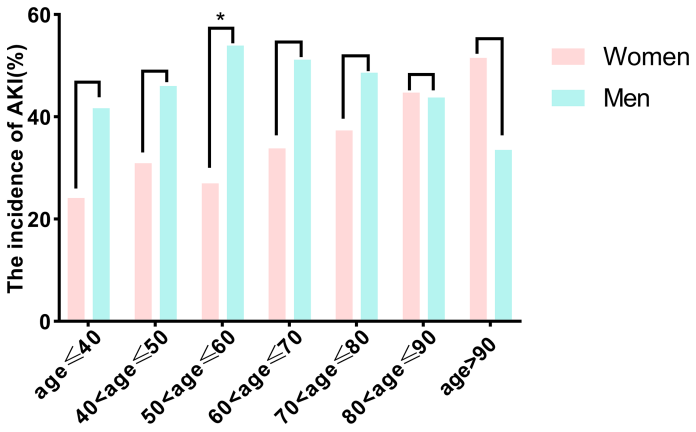

FIGURE 2
Comparison of the incidence of acute kidney injury between men and women according to age in decades. *p<0.05. AKI, Acute kidney injury.

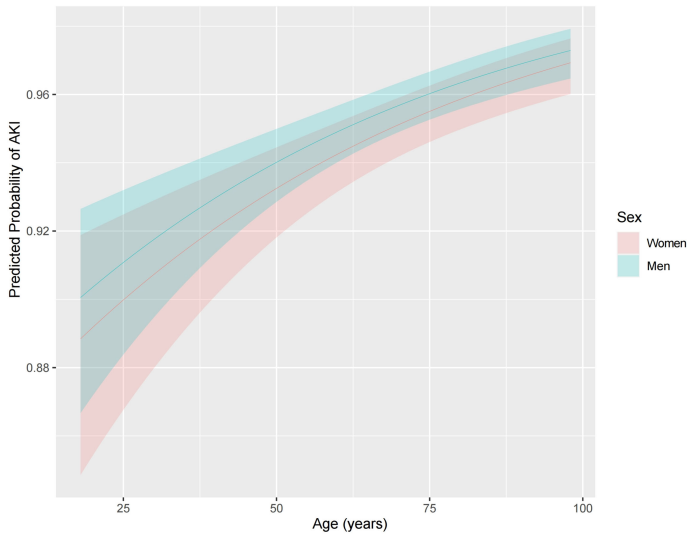

FIGURE 3
Effect of age on the adjusted incidence of acute kidney injury in men and women. Models were adjusted for all variables, including age, BMI, ethnicity, admission type, hypertension, coronary atherosclerosis, heart failure, diabetes mellitus, COPD, cerebral infarction, chronic liver disease, chronic kidney disease, tumor, APS III, OASIS, SOFA, heart rate, MAP, RR, temperature, SpO2, WBC, hemoglobin, platelet, PH, bicarbonate, BUN, creatinine, potassium, sodium, chloride, glucose, PT, APTT, lactate, vasopressor use, mechanical ventilation use, diuretic, aminoglycoside, statin, ACEI/ARBs. ACEI/ARBs, Angiotensin-converting enzyme inhibitors/angiotensin receptor blockers; AKI, Acute kidney injury; APS III, Acute Physiology Score III; APTT, Activated partial thromboplastin time; BMI, Body mass index; BUN, Blood urea nitrogen; COPD, Chronic obstructive pulmonary disease; OASIS, Oxford Acute Severity of Illness Score; PT, Prothrombin time; SA-AKI, Sepsis associated acute kidney injury; SOFA, Sequential Organ Failure Assessment; RR, Respiratory rate; WBC, White blood cell.

model. The risk factors of SA-AKI in men were almost consistent with those in women. The ICU and hospital mortality were comparable between men and women with SA-AKI. Therefore, the main results were contrary to our original hypothesis. Our study suggested that sex may not act as an essential factor of SA-AKI, and the clinical management of SA-AKI could be the same for men and women.

Knowledge of sex differences is an essential ingredient in developing precision medicine (7). It has been found that sex could affect the manifestation and pathophysiology of many diseases (9–11). The impact of sex on outcomes in patients with sepsis has been widely investigated, yielding conflicting results (35–38). It has been found that women generally have more advantageous immunological responses compared to men by the

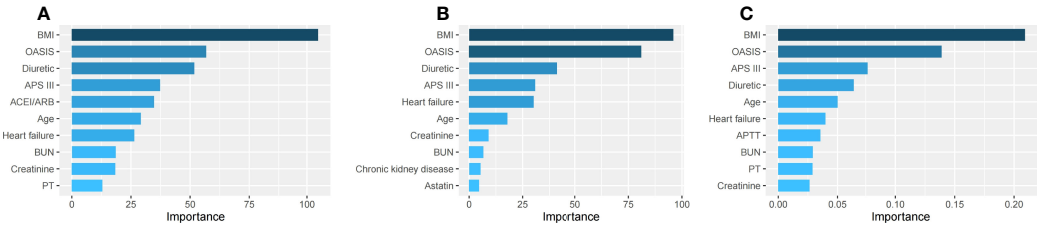

FIGURE 4
The top ten important factors of SA-AKI for the entire cohort in the decision tree model **(A)**, random forest model **(B)** and extreme gradient boosting model **(C)**. Models were adjusted for all variables, including age, BMI, ethnicity, admission type, hypertension, coronary atherosclerosis, heart failure, diabetes mellitus, COPD, cerebral infarction, chronic liver disease, chronic kidney disease, tumor, APS III, OASIS, SOFA, heart rate, MAP, RR, temperature, SpO2, WBC, hemoglobin, platelet, PH, bicarbonate, BUN, creatinine, potassium, sodium, chloride, glucose, PT, APTT, lactate, vasopressor use, mechanical ventilation use, diuretic, aminoglycoside, statin, ACEI/ARBs. ACEI/ARBs, Angiotensin-converting enzyme inhibitors/angiotensin receptor blockers; AKI, Acute kidney injury; APS III, Acute Physiology Score III; APTT, Activated partial thromboplastin time; BMI, Body mass index; BUN, Blood urea nitrogen; COPD, Chronic obstructive pulmonary disease; OASIS, Oxford Acute Severity of Illness Score; PT, Prothrombin time; SA-AKI, Sepsis associated acute kidney injury; SOFA, Sequential Organ Failure Assessment; RR, Respiratory rate; WBC, White blood cell.

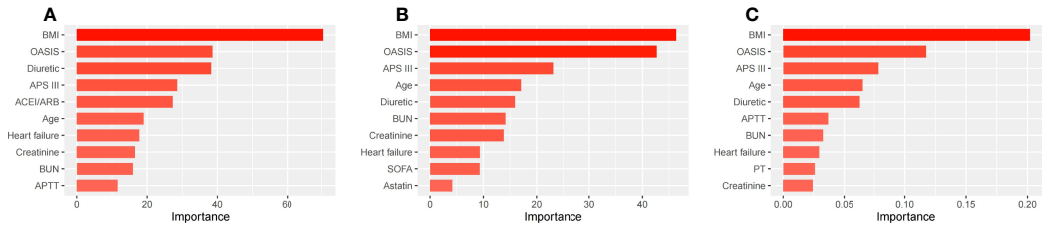

FIGURE 5
The top ten important factors of SA-AKI for men in the decision tree model **(A)**, random forest model **(B)** and extreme gradient boosting model **(C)**. Models were adjusted for all variables, including age, BMI, ethnicity, admission type, hypertension, coronary atherosclerosis, heart failure, diabetes mellitus, COPD, cerebral infarction, chronic liver disease, chronic kidney disease, tumor, APS III, OASIS, SOFA, heart rate, MAP, RR, temperature, SpO2, WBC, hemoglobin, platelet, PH, bicarbonate, BUN, creatinine, potassium, sodium, chloride, glucose, PT, APTT, lactate, vasopressor use, mechanical ventilation use, diuretic, aminoglycoside, statin, ACEI/ARBs. ACEI/ARBs, Angiotensin-converting enzyme inhibitors/angiotensin receptor blockers; AKI, Acute kidney injury; APS III, Acute Physiology Score III; APTT, Activated partial thromboplastin time; BMI, Body mass index; BUN, Blood urea nitrogen; COPD, Chronic obstructive pulmonary disease; OASIS, Oxford Acute Severity of Illness Score; PT, Prothrombin time; SA-AKI, Sepsis associated acute kidney injury; SOFA, Sequential Organ Failure Assessment; RR, Respiratory rate; WBC, White blood cell.

effect of their sexual hormones (13, 39). Animal studies have demonstrated that testosterone depletion or estrogen supplementation exerts beneficial effects on sepsis (40). Sexual immunomodulation modulates the release of pro-inflammatory and anti-inflammatory cytokines, which is associated with the subsequent multiorgan failure (14, 40). Moreover, ischemia–reperfusion injury is another common source of AKI. Experimental studies suggested that sex hormones regulate cellular pathways involved in kidney ischemia–reperfusion injury and have been implicated in defining AKI susceptibility (41, 42). Kidney is the organ most often involved in sepsis, therefore the effect of sex in SA-AKI should be further explored.

In univariate analysis, we found that the incidence of SA-AKI was lower in women than that in men, but this difference did not reach statistical significance. After adjusting for relevant confounders, we could not determine the significant sex-specific difference in SA-AKI incidence. The results were consistent and stable in patients with different age groups and the degree of disease severity. Moreover, in the analysis of patients with or without different comorbidities, men and women still had similar incidences of SA-AKI except for those with cerebral infarction. One potential explanation for this may include the sample size is relatively small, thus increasing the chance of false-positive outcomes. Future studies specifically designed to avoid sample bias are needed to validate this result. It is generally assumed that men had a higher incidence of sepsis, but the research about the relationship between sex and sepsis prognosis failed to reach consistent conclusions (35–38). Ponce-Alonso et al. found that men with sepsis had worse clinical characteristics when admitted to the ICU, but sex had no influence on mortality (35). They compared their results with the last 15 years'

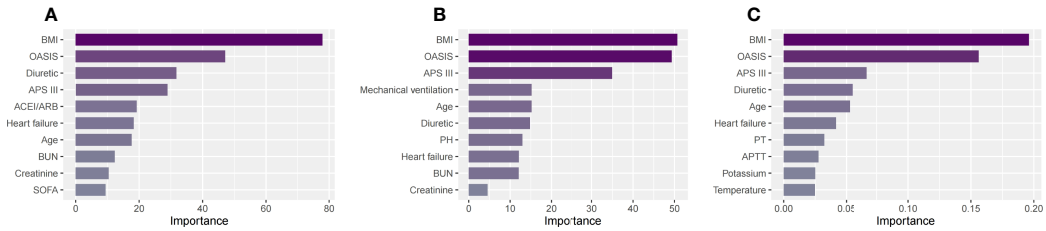

FIGURE 6
The top ten important factors of SA-AKI for women in the decision tree model **(A)**, random forest model **(B)** and extreme gradient boosting model **(C)**. Models were adjusted for all variables, including age, BMI, ethnicity, admission type, hypertension, coronary atherosclerosis, heart failure, diabetes mellitus, COPD, cerebral infarction, chronic liver disease, chronic kidney disease, tumor, APS III, OASIS, SOFA, heart rate, MAP, RR, temperature, SpO2, WBC, hemoglobin, platelet, PH, bicarbonate, BUN, creatinine, potassium, sodium, chloride, glucose, PT, APTT, lactate, vasopressor use, mechanical ventilation use, diuretic, aminoglycoside, statin, ACEI/ARBs. ACEI/ARBs, Angiotensin-converting enzyme inhibitors/angiotensin receptor blockers; AKI, Acute kidney injury; APS III, Acute Physiology Score III; APTT, Activated partial thromboplastin time; BMI, Body mass index; BUN, Blood urea nitrogen; COPD, Chronic obstructive pulmonary disease; OASIS, Oxford Acute Severity of Illness Score; PT, Prothrombin time; SA-AKI, Sepsis associated acute kidney injury; SOFA, Sequential Organ Failure Assessment; RR, Respiratory rate; WBC, White blood cell.

TABLE 4 Comparisons of baseline SA-AKI patient characteristics before and after propensity score matching.

Variables	Before propensity score matching			After propensity score matching		
	Men (n=3078)	Women (n=2290)	SMD	Men (n=1866)	Women (n=1866)	SMD
Age (years)	65.95 ± 15.70	69.65 ± 15.73	0.235	68.55 ± 15.10	68.66 ± 16.19	0.007
BMI (kg/m^2)	30.22 ± 7.54	30.77 ± 8.06	0.07	30.44 ± 7.98	30.46 ± 7.50	0.003
Ethnicity, n (%)			0.013			0.009
White	2016 (65.5)	1514 (66.1)		1243 (66.6)	1235 (66.2)	
Non-white	1062 (34.5)	776 (33.9)		623 (33.4)	631 (33.8)	
Admission type, n (%)			0.002			0.007
Emergency	1205 (39.1)	899 (39.3)		732 (39.2)	726 (38.9)	
Non-emergency	1873 (60.9)	1391 (60.7)		1134 (60.8)	1140 (61.1)	
Comorbidities, n (%)						
Hypertension	1261 (41.0)	987 (43.1)	0.043	771 (41.3)	796 (42.7)	0.027
Coronary atherosclerosis	612 (19.9)	367 (16.0)	0.101	300 (16.1)	325 (17.4)	0.036
Heart failure	1034 (33.6)	837 (36.6)	0.062	669 (35.9)	652 (34.9)	0.019
Diabetes mellitus	881 (28.6)	630 (27.5)	0.025	533 (28.6)	534 (28.6)	0.001
COPD	252 (8.2)	242 (10.6)	0.082	179 (9.6)	183 (9.8)	0.007
Cerebral infarction	306 (9.9)	268 (11.7)	0.057	208 (11.1)	207 (11.1)	0.002
Chronic liver disease	56 (1.8)	34 (1.5)	0.026	30 (1.6)	30 (1.6)	<0.001
Chronic kidney disease	790 (25.7)	506 (22.1)	0.084	450 (24.1)	440 (23.6)	0.013
Tumor	493 (16.0)	394 (17.2)	0.032	318 (17.0)	315 (16.9)	0.004
Severity scale (at admission)						
APS III	68.00 ± 28.03	68.80 ± 27.32	0.029	68.81 ± 27.26	68.28 ± 27.51	0.019
OASIS	40.02 ± 8.86	41.26 ± 8.93	0.139	40.84 ± 8.72	40.70 ± 8.91	0.016
SOFA	3 (2-5)	3 (2-5)	0.13	3 (2-5)	3 (2-5)	0.034
Interventions, n (%)						
Vasopressor use	252 (8.2)	170 (7.4)	0.028	136 (7.3)	142 (7.6)	0.012
Mechanical ventilation	2085 (67.7)	1442 (63.0)	0.1	1191 (63.8)	1215 (65.1)	0.027
Diuretic	579 (18.8)	531 (23.2)	0.108	417 (22.3)	410 (22.0)	0.009
Aminoglycoside	49 (1.6)	28 (1.2)	0.031	20 (1.1)	26 (1.4)	0.029
Statin	894 (29.0)	602 (26.3)	0.062	518 (27.8)	514 (27.5)	0.005
ACEI/ARBs	229 (7.4)	180 (7.9)	0.016	136 (7.3)	142 (7.6)	0.012
Vital signs						
Heart rate (beats/min)	91.95 ± 21.40	93.03 ± 21.04	0.051	92.47 ± 21.45	92.28 ± 70.70	0.009
MAP (mmHg)	82.55 ± 19.27	81.64 ± 20.63	0.045	81.82 ± 18.94	81.91 ± 20.52	0.004
RR (times/min)	20.16 ± 6.34	20.54 ± 6.50	0.058	20.37 ± 6.50	20.43 ± 6.47	0.01
Temperature (°C)	36.73 ± 1.03	36.66 ± 1.02	0.072	36.68 ± 1.05	36.68 ± 1.03	0.006
SpO2 (%)	98 (95-100)	98 (95-100)	0.005	99 (95-100)	98 (95-100)	0.028
Laboratory findings						
WBC (k/uL)	12.5 (8.8-17.5)	12.4 (8.7-17.5)	0.007	12.4 (8.7-17.4)	12.4 (8.7-17.4)	0.013
Hemoglobin (g/L)	10.91 ± 2.45	10.16 ± 2.09	0.333	10.32 ± 2.29	10.38 ± 2.08	0.028
Platelet (k/uL)	192.59 ± 111.05	212.79 ± 119.73	0.175	199.50 ± 121.63	202.08 ± 107.13	0.022
PH	7.34 ± 0.11	7.35 ± 0.11	0.037	7.35 ± 0.10	7.35 ± 0.11	0.021
Bicarbonate (mEq/L)	22.10 ± 4.87	22.11 ± 5.61	0.002	22.18 ± 4.85	22.10 ± 5.56	0.016
BUN (mg/dL)	24 (16-39)	22 (14-35)	0.137	24 (16-37)	22 (14-36)	0.087
Creatinine (mg/dL)	1.2 (0.9-1.9)	1 (0.7-1.6)	0.231	1.2 (0.9-1.7)	1 (0.7-1.7)	0.032
Potassium (mEq/L)	4.36 ± 0.83	4.17 ± 0.78	0.24	4.23 ± 0.73	4.21 ± 0.80	0.025
Sodium (mEq/L)	138.65 ± 5.72	138.80 ± 6.00	0.025	138.71 ± 5.91	138.83 ± 6.01	0.02
Chloride (mEq/L)	104.38 ± 7.08	104.75 ± 7.32	0.05	104.59 ± 7.15	104.75 ± 7.34	0.022

(Continued)

TABLE 4 Continued

Variables	Before propensity score matching			After propensity score matching		
	Men (n=3078)	Women (n=2290)	SMD	Men (n=1866)	Women (n=1866)	SMD
Glucose (mg/dL)	159.12 ± 85.96	157.36 ± 83.63	0.021	155.56 ± 82.71	157.99 ± 83.72	0.029
PT (s)	17.56 ± 9.96	17.59 ± 11.1	0.003	17.60 ± 9.74	17.40 ± 10.60	0.02
APTT (s)	40.07 ± 24.48	39.59 ± 24.58	0.02	40.10 ± 24.83	39.69 ± 24.97	0.017
Lactate (mmol/L)	1.9 (1.4-3)	1.9 (1.3-3)	0.054	1.9 (1.3-2.9)	1.9 (1.3-3)	<0.001

Data were presented as mean ± standard deviation or median (interquartile range) or numbers (percentages).
ACEI/ARBs, Angiotensin-converting enzyme inhibitors/angiotensin receptor blockers; AKI, Acute kidney injury; APS III, Acute Physiology Score III; APTT, Activated partial thromboplastin time; BMI, Body mass index; BUN, Blood urea nitrogen; COPD, Chronic obstructive pulmonary disease; OASIS, Oxford Acute Severity of Illness Score; PT, Prothrombin time; SA-AKI, Sepsis associated acute kidney injury; SMD, Standardized mean difference; SOFA, Sequential Organ Failure Assessment; RR, Respiratory rate; WBC, White blood cell.

relevant published studies, and indicated that geographic location and case definitions were important confounders. Our study was a single-center study with consistent disease definitions, which could minimize the effects of the above factors. A recent study of 17,146 septic patients also reported similar findings (36). The role of sex in kidney disease remains a topic of broad interest. Population-based studies indicated that women have a higher prevalence of chronic kidney disease overall, but men were more likely to experience adverse cardiovascular events and death (43–45). Moreover, men were twice as likely to develop kidney cancer than women and had a higher mortality rate (46). These findings could be partly explained by the difference in sex hormones and the diseases mentioned above are chronic conditions. Additionally, exogenous hormone therapy was associated with the incidence of AKI in patients with prostate cancer (47). Therefore, the sex-related effects may play a minor role in the clinical course of SA-AKI due to the acute situation in patients with sepsis and AKI. Based on our study design, this finding must remain descriptive, and the explanation of the causes remains speculative.

Interestingly, the risk factor analysis showed a strong positive association between BMI and the incidence of SA-AKI. A study of almost 15,000 critically ill patients suggested that each 5 kg/m2 increase in body mass index was associated with a 10% risk of more severe AKI (48). And morbidly obese (defined as BMI >40) has been demonstrated to be an independent risk factor for AKI (49). The following reasons could be attributed (49, 50): First, obesity would increase renal blood flow and induce glomerular hyperfiltration, leading to structural changes in glomerular cells and thus increasing the risk of SA-AKI. Second, higher sympathetic and renin-angiotensin-system activities were found in obese patients, which could enhance kidney damage. Finally, adipose tissue secretes various pro- and anti-inflammatory adipokines that may influence the balance of prostaglandins and thromboxane in the kidney. The biological behavior of the mesangial cells may accordingly change, and thereby partially responsible for the development of SA-AKI.

OASIS and APS III are common scoring systems used to quantify the severity of illness across hospitalized patients (51, 52). Wang et al. have found that OASIS presented good discrimination and calibration in predicting prognosis of AKI (52). Indeed, these scoring systems contain rich clinical information and have been validated in various studies. Our study further supports their predictive value in SA-AKI. Although many studies have explored the effect of diuretic on the development or progression of AKI, no consistent conclusion has been achieved (53). Victor et al. observed that the need for diuretic was positively associated with AKI, and they suggested that this was due to the diuretic use may be a reflection of more severe forms of AKI (e.g., oliguric/anuric AKI) instead of a direct cause of AKI (54). More targeted research is needed in this area for a more definitive account. In addition, previous studies have proven that older age was associated with a significantly higher incidence of AKI (6). There are many reasons for this, but the primary one is the increased vulnerability of the kidney to stressors and insults with increasing age (55).

In the present study, it was not unexpected to observe that SA-AKI was associated with increased ICU and hospital mortality in patients with sepsis, regardless of sex. Therefore, we further compared the short-term mortality between men and women with SA-AKI. Our results revealed that men and women had similar ICU and hospital mortality after propensity score matching. To date, few studies have explored the risk factors of mortality in SA-AKI. Passos et al. found that norepinephrine utilization, liver failure, medical condition, lactate level, and pre-dialysis creatinine level were associated with early mortality in SA-AKI patients treated with CRRT (56). Two other studies also revealed that comorbidities, disease severity and certain drugs are the main risk factors for mortality in SA-AKI (57, 58). Taken together, sex is not a predominant factor affecting the prognosis of patients with SA-AKI.

Some limitations pertain to our study. First, our study was an observational retrospective design that precludes any definitive inference about causality. Second, the care of patients with sepsis may have changed during the study period, which might have

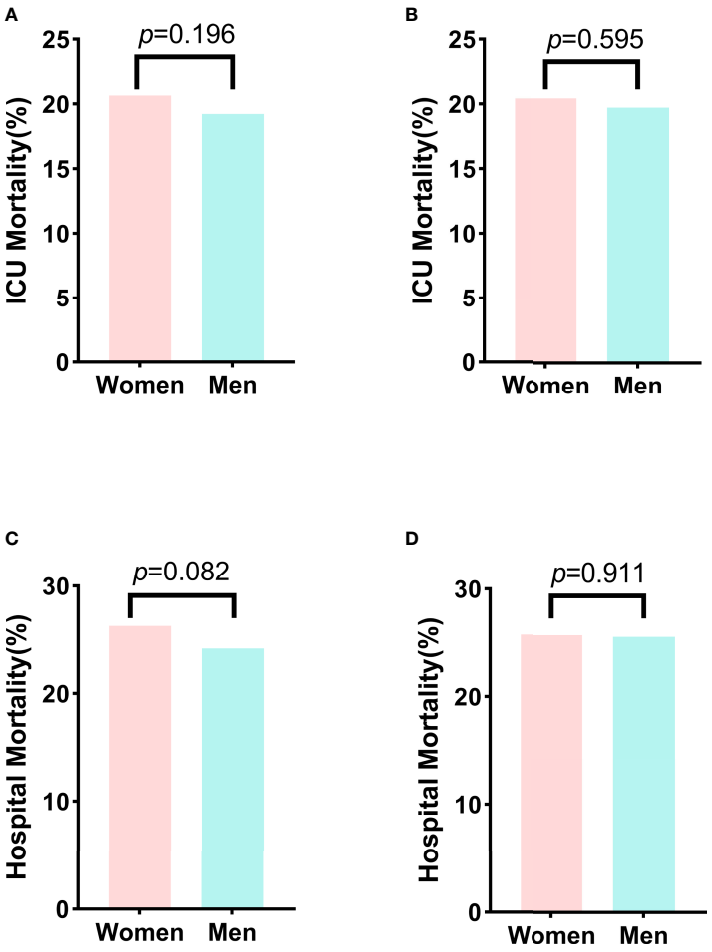

FIGURE 7
Comparison of the ICU and hospital mortality between men and women before matching and after matching. **(A)** The ICU mortality between men and women before matching. **(B)** The ICU mortality between men and women after matching. **(C)** The hospital mortality between men and women before matching. **(D)** The hospital mortality between men and women after matching. ICU, Intensive care unit.

affected the incidence of SA-AKI in these patients. Third, we only considered traditional parameters and did not include some sex-specific variables, such as hormone levels, which may help explain the potential mechanism of our results. Fourth, our study only included ICU patients, thus caution should be taken when attempting to generalize our findings to the whole population. These limitations could be overcome by more in-depth, large-scale, and prospective studies in the future.

Conclusions

In this study, we could not detect the significant sex-specific difference in SA-AKI incidence based on data from critically ill patients with sepsis. BMI, OASIS, diuretic, APS III and age are all the most common risk factors of SA-AKI for the total, men and women groups. The ICU and hospital mortality are comparable between men and women with SA-AKI. Therefore, our study indicates that sex plays a minor role in the clinical course of SA-AKI, and further prospective studies are needed to validate our findings.

Data availability statement

The raw data supporting the conclusions of this article will be made available by the authors, without undue reservation.

Ethics statement

Ethical review and approval was not required for the study on human participants in accordance with the local legislation and institutional requirements. Written informed consent for

participation was not required for this study in accordance with the national legislation and the institutional requirements.

Author contributions

Conceptualization and supervision: DW and DQ. Methodology and software: JP and RT. Writing-Original draft preparation: JP, RT and QY. Writing- Reviewing and Editing: all authors. Final approval for publication: all authors

Funding

This research was funded by National Natural Science Foundation of Chongqing, China(Grant NO. CQYC2020020321).

Acknowledgments

To the team of the Laboratory for Computational Physiology from the Massachusetts Institute of Technology who work to keep the MIMIC-IV database available.

Conflict of interest

The authors declare that the research was conducted in the absence of any commercial or financial relationships that could be construed as a potential conflict of interest.

Publisher's note

Supplementary material

The Supplementary Material for this article can be found online at: https://www.frontiersin.org/articles/10.3389/fimmu.2022.895018/full#supplementary-material

References

1. SepNet Critical Care Trials Group. Incidence of severe sepsis and septic shock in German intensive care units: the prospective, multicentre INSEP study. *Intensive Care Med* (2016) 42:1980–9. doi: 10.1007/s00134-016-4504-3

2. Martin GS, Mannino DM, Eaton S, Moss M. The epidemiology of sepsis in the united states from 1979 through 2000. *N Engl J Med* (2003) 348:1546–54. doi: 10.1056/NEJMoa022139

3. Fleischmann C, Scherag A, Adhikari NK, Hartog CS, Tsaganos T, Schlattmann P, et al. Assessment of global incidence and mortality of hospital-treated sepsis. current estimates and limitations. *Am J Respir Crit Care Med* (2016) 193:259–72. doi: 10.1164/rccm.201504-0781OC

4. Lelubre C, Vincent JL. Mechanisms and treatment of organ failure in sepsis. *Nat Rev Nephrol* (2018) 14:417–27. doi: 10.1038/s41581-018-0005-7

5. Mehta RL, Bouchard J, Soroko SB, Ikizler TA, Paganini EP, Chertow GM, et al. Sepsis as a cause and consequence of acute kidney injury: program to improve care in acute renal disease. *Intensive Care Med* (2011) 37:241–8. doi: 10.1007/s00134-010-2089-9

6. Poston JT, Koyner JL. Sepsis associated acute kidney injury. *BMJ* (2019) 364: k4891. doi: 10.1136/bmj.k4891

7. Westergaard D, Moseley P, Sørup FKH, Baldi P, Brunak S. Population-wide analysis of differences in disease progression patterns in men and women. *Nat Commun* (2019) 10:666. doi: 10.1038/s41467-019-08475-9

8. Mahmood K, Eldeirawi K, Wahidi MM. Association of gender with outcomes in critically ill patients. *Crit Care* (2012) 16:R92. doi: 10.1186/cc11355

9. Chichareon P, Modolo R, Kerkmeijer L, Tomaniak M, Kogame N, Takahashi K, et al. Association of sex with outcomes in patients undergoing percutaneous coronary intervention: a subgroup analysis of the GLOBAL LEADERS randomized clinical trial. *JAMA Cardiol* (2020) 5:21–9. doi: 10.1001/jamacardio.2019.4296

10. Manwani B, Fall P, Zhu L, O'Reilly MR, Conway S, Staff I, et al. Increased P450 aromatase levels in post-menopausal women after acute ischemic stroke. *Biol Sex Differ* (2021) 12:8. doi: 10.1186/s13293-020-00357-w

11. Beltrame A, Salguero P, Rossi E, Conesa A, Moro L, Bettini LR, et al. Association between sex hormone levels and clinical outcomes in patients with COVID-19 admitted to hospital: an observational, retrospective, cohort study. *Front Immunol* (2022) 13:834851. doi: 10.3389/fimmu.2022.834851

12. Zellweger R, Wichmann MW, Ayala A, Stein S, DeMaso CM, Chaudry IH. Females in proestrus state maintain splenic immune functions and tolerate sepsis better than males. *Crit Care Med* (1997) 25:106–10. doi: 10.1097/00003246-199701000-00021

13. Sperry JL, Nathens AB, Frankel HL, Vanek SL, Moore EE, Maier RV, et al. Characterization of the gender dimorphism after injury and hemorrhagic shock: are hormonal differences responsible? *Crit Care Med* (2008) 36:1838–45. doi: 10.1097/CCM.0b013e3181760c14

14. Diodato MD, Knöferl MW, Schwacha MG, Bland KI, Chaudry IH. Gender differences in the inflammatory response and survival following haemorrhage and subsequent sepsis. *Cytokine* (2001) 14:162–9. doi: 10.1006/cyto.2001.0861

15. Kimura T, Isaka Y, Yoshimori T. Autophagy and kidney inflammation. *Autophagy* (2017) 13:997–1003. doi: 10.1080/15548627.2017.1309485

16. Benchimol EI, Smeeth L, Guttmann A, Harron K, Moher D, Petersen I, et al. The REporting of studies conducted using observational routinely-collected health data (RECORD) statement. *PLoS Med* (2015) 12:e1001885. doi: 10.1371/journal.pmed.1001885

17. Johnson A, Bulgarelli L, Pollard T, Horng S, Celi LA, Mark R. MIMIC-IV (version 1.0), in: *PhysioNet* (2021) (Accessed 25 January 2022).

18. Singer M, Deutschman CS, Seymour CW, Shankar-Hari M, Annane D, Bauer M, et al. The third international consensus definitions for sepsis and septic shock (Sepsis-3). *JAMA* (2016) 315:801–10. doi: 10.1001/jama.2016.0287

19. Khwaja A. KDIGO clinical practice guidelines for acute kidney injury. *Nephron Clin Pract* (2012) 120:c179–84. doi: 10.1159/000339789

20. Dépret F, Amzallag J, Pollina A, Fayolle-Pivot L, Coutrot M, Chaussard M, et al. Circulating dipeptidyl peptidase-3 at admission is associated with circulatory failure, acute kidney injury and death in severely ill burn patients. *Crit Care* (2020) 24:168. doi: 10.1186/s13054-020-02888-5

21. Molina Barragan AM, Pardo E, Galichon P, Hantala N, Gianinazzi AC, Darrivere L, et al. SARS-CoV-2 renal impairment in critical care: an observational study of 42 cases (Kidney COVID). *J Clin Med* (2021) 10:1571. doi: 10.3390/jcm10081571

22. Dépret F, Hoffmann C, Daoud L, Thieffry C, Monplaisir L, Creveaux J, et al. Association between hydroxocobalamin administration and acute kidney injury after smoke inhalation: a multicenter retrospective study. *Crit Care* (2019) 23:421. doi: 10.1186/s13054-019-2706-0

23. Stanski NL, Stenson EK, Cvijanovich NZ, Weiss SL, Fitzgerald JC, Bigham MT, et al. PERSEVERE biomarkers predict severe acute kidney injury and renal

recovery in pediatric septic shock. *Am J Respir Crit Care Med* (2020) 201:848–55. doi: 10.1164/rccm.201911-2187OC

24. Pantanowitz A, Marwala T. Advances in intelligent and soft computing. In: W Yu and EN Sanchez, editors. *Advances in computational intelligence*, vol. vol 116 . Berlin, Heidelberg: Springer (2009). doi: 10.1007/978-3-642-03156-4_6

25. Barros RC, Basgalupp MP, de Carvalho ACPLF, Freitas AA. A survey of evolutionary algorithms for decision-tree induction. *IEEE Trans Syst Man Cybern C* (2012) 42(3):291–312. doi: 10.1109/tsmcc.2011.2157494

26. Akter S, Xu D, Nagel SC, Bromfield JJ, Pelch K, Wilshire GB, et al. Machine learning classifiers for endometriosis using transcriptomics and methylomics data. *Front Genet* (2019) 10:766. doi: 10.3389/fgene.2019.00766

27. Paul A, Mukherjee DP, Das P, Gangopadhyay A, Chintha AR, Kundu S. Improved random forest for classification. *IEEE Trans image Process Publ IEEE Signal Process Soc* (2018) 27:4012–24. doi: 10.1109/tip.2018.2834830

28. Simeon S, Jongkon N. Construction of quantitative structure activity relationship (QSAR) models to predict potency of structurally diversed janus kinase 2 inhibitors. *Molecules* (2019) 24:4393. doi: 10.3390/molecules24234393

29. Wu TE, Chen HA, Jhou MJ, Chen YN, Chang TJ, Lu CJ. Evaluating the effect of topical atropine use for myopia control on intraocular pressure by using machine learning. *J Clin Med* (2020) 10:111. doi: 10.3390/jcm10010111

30. Qiang X, Chen H, Ye X, Su R, Wei L. M6AMRFS: robust prediction of N6-methyladenosine sites with sequence-based features in multiple species. *Front Genet* (2018) 9:495. doi: 10.3389/fgene.2018.00495

31. Morris KL, Perna FM. Decision tree model vs traditional measures to identify patterns of sun-protective behaviors and sun sensitivity associated with sunburn. *JAMA Dermatol* (2018) 154:897–902. doi: 10.1001/jamadermatol.2018.1646

32. Raita Y, Goto T, Faridi MK, Brown DFM, Camargo CAJr., Hasegawa K. Emergency department triage prediction of clinical outcomes using machine learning models. *Crit Care* (2019) 23:64. doi: 10.1186/s13054-019-2351-7

33. Goto Y, Koyama K, Katayama S, Tonai K, Shima J, Koinuma T, et al. Influence of contrast media on renal function and outcomes in patients with sepsis-associated acute kidney injury: a propensity-matched cohort study. *Crit Care* (2019) 23:249. doi: 10.1186/s13054-019-2517-3

34. Feng M, McSparron JI, Kien DT, Stone DJ, Roberts DH, Schwartzstein RM, et al. Transthoracic echocardiography and mortality in sepsis: analysis of the MIMIC-III database. *Intensive Care Med* (2018) 44:884–92. doi: 10.1007/s00134-018-5208-7

35. Ponce-Alonso M, Fernández-Félix BM, Halperin A, Rodríguez-Domínguez M, Sánchez-Díaz AM, Cantón R, et al. Propensity-score analysis reveals that sex is not a prognostic factor for mortality in intensive care unit-admitted patients with septic bacteremia. *Int J Infect Dis* (2021) 110:36–44. doi: 10.1016/j.ijid.2021.07.034

36. Wernly B, Bruno RR, Mamandipoor B, Jung C, Osmani V. Sex-specific outcomes and management in critically ill septic patients. *Eur J Intern Med* (2021) 83:74–7. doi: 10.1016/j.ejim.2020.10.009

37. Kondo Y, Miyazato A, Okamoto K, Tanaka H. Impact of sex differences on mortality in patients with sepsis after trauma: a nationwide cohort study. *Front Immunol* (2021) 12:678156. doi: 10.3389/fimmu.2021.678156

38. Papathanassoglou E, Middleton N, Benbenishty J, Williams G, Christofi MD, Hegadoren K. Systematic review of gender- dependent outcomes in sepsis. *Nurs Crit Care* (2017) 22:284–92. doi: 10.1111/nicc.12280

39. Klein SL, Jedlicka A, Pekosz A. The xs and y of immune responses to viral vaccines. *Lancet Infect Dis* (2010) 10:338–49. doi: 10.1016/s1473-3099(10)70049-9

40. Angele MK, Pratschke S, Hubbard WJ, Chaudry IH. Gender differences in sepsis: cardiovascular and immunological aspects. *Virulence* (2014) 5:12–9. doi: 10.4161/viru.26982

41. Viñas JL, Porter CJ, Douvris A, Spence M, Gutsol A, Zimpelmann JA, et al. Sex diversity in proximal tubule and endothelial gene expression in mice with ischemic acute kidney injury. *Clin Sci (Lond)* (2020) 134:1887–909. doi: 10.1042/cs20200168

42. Hutchens MP, Fujiyoshi T, Komers R, Herson PS, Anderson S. Estrogen protects renal endothelial barrier function from ischemia-reperfusion *in vitro* and in vivo. *Am J Physiol Renal Physiol* (2012) 303:F377–85. doi: 10.1152/ajprenal.00354.2011

43. Swartling O, Rydell H, Stendahl M, Segelmark M, Trolle Lagerros Y, Evans M. CKD progression and mortality among men and women: a nationwide study in Sweden. *Am J Kidney Dis* (2021) 78:190–9.e1. doi: 10.1053/j.ajkd.2020.11.026

44. Jung CY, Heo GY, Park JT, Joo YS, Kim HW, Lim H, et al. Sex disparities and adverse cardiovascular and kidney outcomes in patients with chronic kidney disease: results from the KNOW-CKD. *Clin Res Cardiol* (2021) 110:1116–27. doi: 10.1007/s00392-021-01872-5

45. Carrero JJ, Hecking M, Chesnaye NC, Jager KJ. Sex and gender disparities in the epidemiology and outcomes of chronic kidney disease. *Nat Rev Nephrol* (2018) 14:151–64. doi: 10.1038/nrneph.2017.181

46. Peired AJ, Campi R, Angelotti ML, Antonelli G, Conte C, Lazzeri E, et al. Sex and gender differences in kidney cancer: clinical and experimental evidence. *Cancers (Basel)* (2021) 13:4588. doi: 10.3390/cancers13184588

47. Lapi F, Azoulay L, Niazi MT, Yin H, Benayoun S, Suissa S. Androgen deprivation therapy and risk of acute kidney injury in patients with prostate cancer. *JAMA* (2013) 310:289–96. doi: 10.1001/jama.2013.8638

48. Danziger J, Chen KP, Lee J, Feng M, Mark RG, Celi LA, et al. Obesity, acute kidney injury, and mortality in critical illness. *Crit Care Med* (2016) 44:328–34. doi: 10.1097/ccm.0000000000001398

49. Bucaloiu ID, Perkins RM, DiFilippo W, Yahya T, Norfolk E. Acute kidney injury in the critically ill, morbidly obese patient: diagnostic and therapeutic challenges in a unique patient population. *Crit Care Clin* (2010) 26:607–24. doi: 10.1016/j.ccc.2010.06.005

50. Kambham N, Markowitz GS, Valeri AM, Lin J, D'Agati VD. Obesity-related glomerulopathy: an emerging epidemic. *Kidney Int* (2001) 59:1498–509. doi: 10.1046/j.1523-1755.2001.0590041498.x

51. Chen Q, Zhang L, Ge S, He W, Zeng M. Prognosis predictive value of the Oxford acute severity of illness score for sepsis: a retrospective cohort study. *PeerJ* (2019) 7:e7083. doi: 10.7717/peerj.7083

52. Wang N, Wang M, Jiang L, Du B, Zhu B, Xi X. The predictive value of the oxford acute severity of illness score for clinical outcomes in patients with acute kidney injury. *Ren Fail* (2022) 44:320–8. doi: 10.1080/0886022x.2022.2027247

53. Hegde A. Diuretics in acute kidney injury. *Indian J Crit Care Med* (2020) 24: S98–s9. doi: 10.5005/jp-journals-10071-23406

54. Ortiz-Soriano V, Donaldson K, Du G, Li Y, Lambert J, Cleland D, et al. Incidence and cost of acute kidney injury in hospitalized patients with infective endocarditis. *J Clin Med* (2019) 8:927. doi: 10.3390/jcm8070927

55. Coca SG. Acute kidney injury in elderly persons. *Am J Kidney Dis* (2010) 56:122–31. doi: 10.1053/j.ajkd.2009.12.034

56. da Hora Passos R, Ramos JG, Mendonça EJ, Miranda EA, Dutra FR, Coelho MF, et al. A clinical score to predict mortality in septic acute kidney injury patients requiring continuous renal replacement therapy: the HELENICC score. *BMC Anesthesiol* (2017) 17:21. doi: 10.1186/s12871-017-0312-8

57. Wang H, Ji X, Wang AY, Wu PK, Liu Z, Dong L, et al. Epidemiology of sepsis-associated acute kidney injury in Beijing, China: a descriptive analysis. *Int J Gen Med* (2021) 14:5631–49. doi: 10.2147/ijgm.S320768

58. Hu H, Li L, Zhang Y, Sha T, Huang Q, Guo X, et al. A prediction model for assessing prognosis in critically ill patients with sepsis-associated acute kidney injury. *Shock* (2021) 56:564–72. doi: 10.1097/shk.0000000000001768

frontiers | Frontiers in Immunology

TYPE Mini Review
PUBLISHED 05 August 2022
DOI 10.3389/fimmu.2022.956448

OPEN ACCESS

EDITED BY
Alessandra Stasi,
University of Bari Aldo Moro, Italy

REVIEWED BY
Tianxin Chen,
First Affiliated Hospital of Wenzhou Medical University, China
Yu-Lei Gao,
Tianjin Medical University General Hospital, China
Gianvito Caggiano,
University of Bari Aldo Moro, Italy

*CORRESPONDENCE
Jiang Zheng
zhengj99219@163.com
Xin Liu
liux0704@tmmu.edu.cn

SPECIALTY SECTION
This article was submitted to Inflammation, a section of the journal Frontiers in Immunology

RECEIVED 30 May 2022
ACCEPTED 12 July 2022
PUBLISHED 05 August 2022

CITATION
Wang N, Lu Y, Zheng J and Liu X (2022) Of mice and men: Laboratory murine models for recapitulating the immunosuppression of human sepsis. *Front. Immunol.* 13:956448. doi: 10.3389/fimmu.2022.956448

Of mice and men: Laboratory murine models for recapitulating the immunosuppression of human sepsis

Ning Wang[1], Yongling Lu[2], Jiang Zheng[2]* and Xin Liu[2]*

[1]West China Biopharm Research Institute, West China Hospital, Sichuan University, Chengdu, China, [2]Medical Research Center, Southwest Hospital, Army Military Medical University, Chongqing, China

Prolonged immunosuppression is increasingly recognized as the major cause of late phase and long-term mortality in sepsis. Numerous murine models with different paradigms, such as lipopolysaccharide injection, bacterial inoculation, and barrier disruption, have been used to explore the pathogenesis of immunosuppression in sepsis or to test the efficacy of potential therapeutic agents. Nonetheless, the reproducibility and translational value of such models are often questioned, owing to a highly heterogeneric, complex, and dynamic nature of immunopathology in human sepsis, which cannot be consistently and stably recapitulated in mice. Despite of the inherent discrepancies that exist between mice and humans, we can increase the feasibility of murine models by minimizing inconsistency and increasing their clinical relevance. In this mini review, we summarize the current knowledge of murine models that are most commonly used to investigate sepsis-induced immunopathology, highlighting their strengths and limitations in mimicking the dysregulated immune response encountered in human sepsis. We also propose potential directions for refining murine sepsis models, such as reducing experimental inconsistencies, increasing the clinical relevance, and enhancing immunological similarities between mice and humans; such modifications may optimize the value of murine models in meeting research and translational demands when applied in studies of sepsis-induced immunosuppression.

KEYWORDS

sepsis, immunosuppression, murine models, immunopathy, preclinical study, LPS tolerance

Introduction

Sepsis is defined as a life-threatening organ dysfunction caused by a dysregulated host response to infection (1). As a leading cause of death in intensive care units (ICUs), sepsis affected an estimated 48.9 million people in 2017, with a death toll surpassing 10 million (2). Due to advances in supportive care, the in-hospital mortality during the early stages of sepsis has been significantly reduced, resulting in a dramatic increase in late-phase sepsis patients and sepsis survivors (3). Persistent immunosuppression is a hallmark of late-phase sepsis and post-sepsis syndrome, which disrupts the host's antimicrobial response against secondary infection, culminating in organ dysfunction and death (4). Notably, patients are increasingly admitted to hospital with concomitant diseases or immune compromised conditions, which increases their risk of developing sepsis (5) or is associated with poor prognosis post-sepsis (6, 7). Consequently, extensive studies have been performed to uncover the mechanisms that drive immunosuppression in sepsis (8). Moreover, immunostimulatory strategies that aim to reverse the immunocompromised status for patients suffering sepsis, are also being increasingly appraised in experimental animals or in human subjects (9).

Many insights into the pathogenesis of sepsis, including the development of immunosuppression, were first derived from animal models (7, 10, 11). The pharmacological evaluation of immunostimulatory agents has always been initiated in preclinical studies (9). However, the reproducibility and translational feasibility of animal studies are often questioned due to inherent immunological discrepancies between animals and humans (11). Inconsistencies in modeling procedures may further broaden the gaps between modeled and clinical sepsis. Despite of their inevitable deficiencies, the validity and clinical relevance of preclinical sepsis models can be improved by standardizing the modeling procedures and refining the modeling strategies. In this mini review, we describe the major types of animal models used to mimic the immunosuppression observed in human sepsis, highlighting their strengths and limitations. We also propose potential directions for improving the quality and value of preclinical models of sepsis. Given that most studies of sepsis are performed in mice (due to numerous advantages such as ease of accessibility and handling, convenience of examining the immune response, and feasibility of genetical manipulation) (11), this mini review exclusively discusses the use of laboratory murine models used to specifically recapitulate the immunosuppression observed in human sepsis.

Immunopathogenesis in sepsis

Compelling experimental and clinical evidence has indicated that elements of both pro-inflammatory and anti-inflammatory responses occur early and simultaneously in sepsis (12, 13). Typically, a rapid onset of pro-inflammatory reactions, including the excessive release of pro-inflammatory cytokines and the hyperactivation of the complement system, the coagulation system and the endothelial system, are provoked by the activation of PAMPs and DAMPs, giving rise to life-threatening organ injuries at the early stage of sepsis (14, 15). Meanwhile, an adaptive anti-inflammatory phenotype is also upregulated which alters the status of innate immune cells and induce apoptosis and anergy in lymphocytes, leading to a long-term immunosuppression that characterize late sepsis or post-sepsis sequelae (15). Of note, the signs of immunoparalysis are much early or even appear first after sepsis in immunocompromised patients (15). Given that the majority of patients are likely to survive the early stage of sepsis while an expansion of aging people or other population predisposing to an immunosuppressive status tend to be more prone to sepsis, increasing awareness has been given to understanding the mechanisms that drive sepsis-induced immunosuppression (7). A number of key events, such as transcriptional reprogramming, epigenetic modifications and metabolic disorders, have been demonstrated to promote leukocyte tolerance (reduced cytokine production and impaired antigen presentation), increase the expression of inhibitory checkpoint molecules (e.g., programmed cell death protein 1 (PD-1), programmed cell death ligand 1 (PD-L1), and cytotoxic T - lymphocyte antigen 4 CTLA-1) or suppressive immune cells (e.g., regulatory T cells (Tregs) and myeloid-derived suppressor cells (MDSCs)) and induce anergy or death in lymphocytes (8, 14). Meanwhile, the inevitable use of immunosuppressive agents, such as norepinephrine and hydrocortisone, may further deteriorate the immunocompromised status in sepsis (12). Consequently, a broad and persistent dysfunction occurs in host immune responses, leading to increased susceptibility for low-virulent bacterial, fungal and viral pathogens (15). This results in unresolved septic foci, incapability to combat secondary or nosocomial infections and other multiple complications that cause multiple organ dysfunction syndromes (MODS), extend hospital length of stay, and may even leads to death in the late phase or after discharge (12).

Murine models use to recapitulate immunosuppression in sepsis

Sepsis is characterized by a profound shift from an overwhelmingly hyperinflammatory state towards a broad defect in both innate and adaptive immunity (8). Therefore, experimental studies are performed in murine models, allowing a natural course of sepsis-induced immunosuppression (16). Given the susceptibility of immunocompromised patients to secondary infection, microbial insults are often additionally

imposed on septic animals; the resulting models are termed 'two-hit' or 'double-hit' models (17). In some cases, a pre-sepsis insult (e.g., trauma, burns, hyperoxia, ischemia, or hemorrhage) or other post-sepsis challenges (e.g., stress, lipopolysaccharide (LPS) exposure, immunization, or organ injury) may also be involved to create a model with more than 'two-hit'. To understand specific features of sepsis-associated immunosuppression, murine models with special features are sometimes developed. A good example is the use of the LPS tolerance model to reveal alterations reminiscent of leukocyte reprogramming in human sepsis (8). Further, compelling evidence has suggested an obvious immunological gap in the pre-sepsis stage between animal models and human sepsis (7). Therefore, sepsis is modeled in mice under different immunological conditions, such as memory mice, dirty mice, aged mice, and mice with genetic or gender-specific differences. Considering that human sepsis is often associated with the use of immunosuppressants or the presence of concomitant diseases, sepsis is also modeled in mice primed with immunosuppressant or bearing comorbidities. An overview of the models used to specifically recapitulate sepsis-induced immunosuppression, is provided in Figure 1. The key steps involved in establishing these models, along with their main advantages and disadvantages, are addressed in detail below and summarized in Tables 1 and 2.

The 'one-hit' model

The one-hit model is an exactly routine sepsis model, which can be simply categorized into injection models and surgical models by the way sepsis is recapitulated. The injection models are established by giving an exogenous toxin (e.g. lipopolysaccharide (LPS), a viable pathogen (e.g. *Escherichia coli*), and feces or other pathogen containing materials (18). The surgical models are made by disrupting the endogenous barriers *via* surgery, which thereby induces local infection and sepsis. Cecal ligation and puncture (CLP) model and colon ascendens stent peritonitis (CASP) model are typical surgical models that reproduce abdominal sepsis *via* intra-abdominal surgery (18). Despite similar lethality in these models, intravenous injection of lethal doses of toxins or live pathogens induces a rapid and severe systemic proinflammatory response rather than a low-grade inflammation, accompanied with persistent immunosuppression (19). In contrast, local infection models established by injection, implantation or surgery demonstrate attenuated inflammatory response and increased tendency to develop immunosuppression (20, 21). Typically, the CLP model is most widely used to demonstrate ongoing immune suppression, including splenocyte apoptosis (22), lymphopenia (23) and expansion of Tregs (24) and MDSCs (25). Immunosuppression can be directly evaluated by using one-hit models, allowing a natural sepsis course without other modeling methods. However, a diversified inflammatory and immune profiles may exist with different modeling strategies. Moreover, the lack of a secondary insult makes them insufficient to reflect host response in an immunosuppressive state.

The 'two-hit' model

To induce immunosuppression following sepsis, model mice are first made to develop sepsis (the first hit) and then challenged with a secondary infection (the second hit). Indeed, two-hit mice are demonstrated to exhibit increased bacterial load and lower inflammatory resolution, thereby recapitulating the nosocomial infection observed at the prolonged immunosuppressive stage post-sepsis (26, 27). The first hit is typically performed using

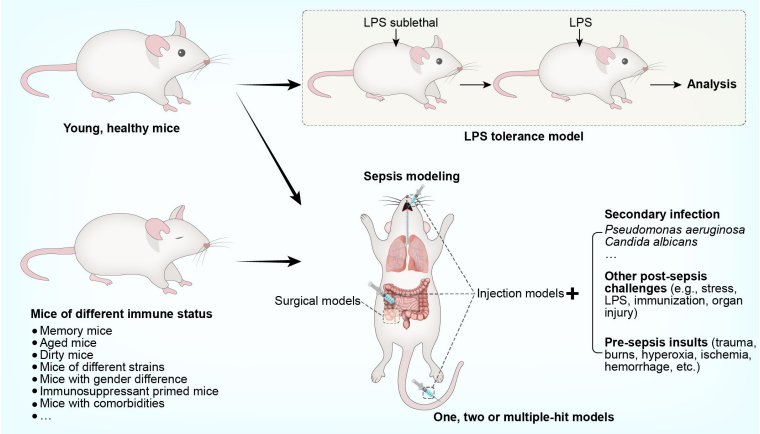

FIGURE 1
Murine models that recapitulate immunosuppression in human sepsis.

TABLE 1 Comparison of major modeling methodologies used to generate murine models of sepsis-associated immunosuppression.

Model type	Modeling methods	Clinical relevant manifestations	Features of immunosuppression	Model strengths	Model weaknesses
The one-hit model	• Intranasal or intraperitoneal pathogen inoculum • Intraperitoneal feces injection • CLP or CASP	• Clinically relevant to late sepsis from abdominal or lung infection • Sublethal or low-mortality • Low-grade or persistent cytokine production, moderate hypotension and organ injury, splenic myelopoiesis and prolonged immunosuppression (PICS)	• Immune anergy • Lymphopenia • Elevated inhibitory markers (e.g., PD-L1) • Elevated suppressive immune cells (e.g., Treg, MDSCs, etc.)	• Requiring no other modeling methods • Mimicking a natural development of immunosuppression in sepsis	• Diversified inflammatory and immune profiles after modeling • Without secondary insult to reflect immunosuppression
The two-hit model	• First hit: sublethal septic insult (CLP most commonly) • Second hit: Bacterial (e.g., *P. aeruginosa, S. aureus*) or fungal (e.g. *C. albicans*) infection or other post-sepsis challenges (e.g., stress, LPS, immunization, organ injury)	• Clinically relevant to sepsis with secondary infection • First hit: Similar mortality, cytokines, and organ injury to one-hit models • Second hit: Increased pathogen load, reduced cytokine production, worsened organ injury, and elevated mortality	• Similar to one-hit models • Susceptible to secondary infection	• Recapitulating immunosuppression in mice surviving early sepsis • Similar to secondary infection or other immune deficiencies in human sepsis	• Different status after the first hit • Lack of standardized second hit method (e.g., microbial species, time course, and dosage)
The more than two-hit model	• Two-hit models with pre-sepsis insult (trauma, burns, hyperoxia, ischemia, hemorrhage, etc.)	• Clinically relevant to sepsis secondary to multiple injuries • Stronger inflammation, organ injury than one-hit or two-hit models	• Worse immunosuppression than one-hit or two-hit models	• Mimicking immunosuppression by both combined injury and sepsis	• Higher modeling inconsistency • Heterogeneous immune responses created by different insults
The LPS tolerance	• Priming: repeated exposure to sublethal LPS • Re-challenge: lethal dosage of LPS	• Clinically relevant to endotoxemia • Reprogrammed cytokines (proinflammatory ↓, anti-inflammatory ↑) • Organ mildly injured in priming while protected in re-challenge • Susceptible to secondary infection	• Monocyte exhaustion (phagocytosis↑, antigen presentation↓, bacterial killing↓) • Elevated inhibitory markers and suppressive cells	• Recapitulating leukocyte reprogramming in human sepsis	• Focusing on monocytes and macrophages only • Different from immunosuppression in human sepsis (IL-10↓, phagocytosis↓)

CLP, cecal ligation and puncture; CASP, colon ascendens stent peritonitis; PICS, persistent inflammation, immunosuppression and catabolism syndrome; Tregs, regulatory T-cells; MDSCs, myeloid-derived suppressor cells.

10.3389/fimmu.2022.956448

TABLE 2 Summary of mouse models with specific immunologically characteristics to study immunosuppression in sepsis.

Model type	Background	Immune status	Manifestations in sepsis modeling
Memory mice	• Pathogenic or antigenic pre-exposure to develop immune memory	• Trained immunity • Enhanced antigen-specific memory T-cells • Reprogramming of myeloid cells	• Clinically relevant to reinfection or vaccination • Augmented inflammatory response • Enhanced protection against secondary infection
Aged mice	• >18 months old	• Immune cell senescence • Chronic inflammation, persistent immunosuppression	• Clinically relevant to sepsis in the elderly • Insufficient myeloid response, T-cell exhaustion • Heavier organ dysfunction and reduced survival
Dirty mice	• Exposure to microbes by co-housing, sequential infection, microbiota transfer, and rewilding	• Experienced immunity (memory, differentiation in T-cells) • Natural microbiota and pathogens	• Better recapitulation of human immunity in sepsis • Enhanced inflammation and protection against infection
Mice from different strains	• Genetic variation (Th1 vs. Th2) • Genetic heterogeneity (inbred vs. outbred)	• Higher immunosuppression in Th2 (BALB/c, etc.) than in Th1 (C57BL/6, etc.) strains due to genetic variation • Lower immunosuppression in outbred (CD-1, etc.) than in inbred (C57BL/6J, etc.) strains due to genetic heterogeneity	• More unresolved inflammation, impaired bacterial clearance and susceptibility to infection in Th2 strains than in Th2 strains • Lower Th1 cytokines and more susceptible to infection in inbred than in outbred strains
Mice with gender difference	• Male vs. female	• Depressed cellular immune responses in males while unchanged or enhanced in females under stress conditions • Immunosuppressive male sex hormones vs. immunostimulatory female sex hormones	• Clinically relevant to gender-associated variations in sepsis • Higher inflammation and sustained immune response, enhanced bacterial killing and increased survival in female than male mice
Immunosuppressant-primed mice	• Preconditioning with immunosuppressants (e.g., glucocorticoids, calcineurin inhibitors, and fingolimod)	• Endotoxin tolerance (glucocorticoids) • Lymphopenia and T-cell dysfunction (calcineurin inhibitors, fingolimod)	• Clinically relevant to predisposed immunosuppression • Decreased inflammatory cytokine release • Heavier organ damage and higher bacterial load
Mice with comorbidities	• Preconditioned illness (autoimmunity disease, obesity, cancer, and NAFLD) before sepsis modeling	• Pronounced T-cell apoptosis and Treg expansion	• Clinically relevant to sepsis with comorbidities • Elevated morbidity and mortality • Increased gut permeability, persistent inflammation, aggravated organ injury, and more prone to immunosuppression

routine sepsis modeling methods, either by extrinsic pathogen inoculation or surgical approaches that establish intrinsic infection. During the second hit procedure, a clinically relevant pathogen is commonly injected into mice to mimic the secondary infection encountered in human sepsis.

Specifically, sublethal or low-lethal intraperitoneal surgery in the form of cecal ligation and puncture (CLP) is most widely applied to perform the first hit. Then a secondary pneumonia or systemic infection is established *via* the administration of *Pseudomonas aeruginosa*, *Candida albicans* or other opportunistic pathogens that are non-lethal in healthy or sham mice but induce high mortality in the model mice (26, 28). Generally, the first-hit by CLP creates a similarly immunosuppressive status in mice, which consistently renders them more susceptible to secondary infection by either *Pseudomonas aeruginosa*, *Staphylococcus aureus* or *Candida albicans*. However, bacterial infection is preferentially given *via* the intranasal route which is clinically relevant of hospital-acquired pneumonia secondary to abdominal sepsis or injuries. In contrast, fungal pathogens are commonly injected intravenously to mimic disseminated infection in human sepsis (29). In addition to secondary infection, post-CLP mice may suffer LPS injection or daily chronic stress to induce an aggravated inflammation response that recapitulates persistent inflammation, immunosuppression, and catabolism syndrome (PICS) after sepsis (30, 31). Other secondary insult, such as antigen immunization is also given after CLP to evaluate the adaptive immunosuppression, including Treg expansion and reduced memory CD4+ T cells (32, 33). Moreover, CLP mice are subjected to second challenge of organ injury or wound, which reflects either the impaired organ protection or wound healing due to immunosuppressive state (34, 35). Given that pneumonia is a leading cause of sepsis, the first hit is sometimes performed by intratracheal bacterial inoculation to replicate a natural immunodeficient state that develops in pneumonia-induced sepsis. A second hit of bacterial or viral infection is then administered *via* inoculated to examine the paralyzed immune state characteristic of the post-sepsis period (36).

Two-hit models mimic the natural course of immunosuppression development in sepsis, and therefore, they best characterize the systemic immunopathology of human sepsis. However, two-hit mouse models can be generated under varying conditions and the first hit can be created using different methods. Additionally, the microbial species used, as well as the time course and dosage of second hit have not been standardized, which may further increase the inconsistency of outcomes and hinder comparisons between different laboratories. In some experiments, two-hit models are coupled with pre-sepsis insult, such as trauma, burns, hyperoxia, ischemia and hemorrhage (37–39). These models may refer as 'more than two-hit' models, with stronger inflammation and organ injury are demonstrated in these models compared with one-hit or two-hit models. These models are clinically relevant to sepsis secondary to multiple injuries. However, they may display higher modeling inconsistency due to more heterogeneous immune responses by different pre-sepsis insults.

The LPS tolerance model

The injection of LPS is extensively used to induce sepsis in experimental models. However, studies using lethal dosages of LPS are no longer convincing due to the rapid kinetics, extreme inflammation, and immediate cardiovascular collapse, which are dramatically different from human sepsis that originates from localized infection (18). Nevertheless, the LPS tolerance model, which is induced by repeated exposure with sublethal doses of LPS, resembles a key feature of innate immune system paralysis in human sepsis, known as leukocyte reprogramming (40). Leukocyte reprogramming defines an adaptive immune response that is associated with a decline in proinflammatory cytokine production and the downregulation of surface HLA-DR expression on leukocytes upon stimulation with microbial agonists like LPS; this phenomenon is also known as LPS tolerance. Leukocyte reprogramming can also be detected in LPS-tolerant mice (14). Therefore, this model is valuable for exploring the mechanisms of long-term adaptation of innate immune cells following excessive inflammation to immunosuppression in sepsis, such as epigenetic reprogramming, autophagy impairment, decrease in the levels of activating cell surface molecules and the upregulation of negative regulatory factors (40, 41). However, some studies suggest that the phagocytic function and pathogen killing capacity of monocytes/macrophages in this model are enhanced while the anti-inflammatory mediators such as interleukin (IL)-10 are upregulated (8). These phenotypes differ from clinical observations of immunosuppression in human sepsis, which is overall aberrant in cytokine production and is associated with a refractory response to secondary infection (4). Furthermore, the immune state observed in the murine LPS tolerance model arises specifically in response to LPS stimulation rather than recapitulating the immunosuppression observed in human sepsis, which is a consequence of polymicrobial infection.

The use of mice with specific immunological features to model the immunosuppression observed in human sepsis

Unlike young, healthy, naïve mice that are often used to recapitulate human sepsis, patients with sepsis have heterogeneous characteristics such as discrepant age, gender, living environment, genetic background, and immunological status. Therefore, attempts have been made to increase the clinical relevance of murine models by modifying their immunological profiles or considering different immunological backgrounds. For example, standard laboratory mice are hygienic and lack effector-differentiated and mucosal memory T-cells, due to being housed under specific pathogen-free conditions (42). Therefore, memory mice are made to develop immune memory by pre-exposure to specific pathogenic or antigenic stimuli. Memory mice are also clinically relevant models for the study of reinfection or vaccination. They display raised inflammatory responses and a higher level of protection against secondary infection following sepsis induction. Likewise, dirty mouse models are also introduced by exposure to microbes *via* co-housing, sequential infection, the transfer of microbiota, and rewilding. Dirty mice have an experienced immune system and are exposed to naturally-occurring microbiota and pathogens, meaning that their inflammatory response and protection against infection are more relevant to human immunity during sepsis. Interspecies immune discrepancies are ascribed to genetic variations of laboratory mice that profoundly affect the responsiveness of immunity in sepsis., mice with genetic variations (Th1 vs. Th2) or genetic heterogeneity (Inbred vs. outbred) differ in their immune response to sepsis. Typically, higher levels of immunosuppression can be detected in Th2 mice (e.g., BALB/c) than in Th1 (e.g., C57BL/6) strains due to genetic variations (43). In addition, lower-level immunosuppression is found in outbred (e.g., CD-1) than in inbred (e.g., C57BL/6J) strains, due to genetic heterogeneity (44). Therefore, it is necessary to consider these variations when recapitulating sepsis in murine models.

Animals uses as models are typically normal in their immunological status prior sepsis modeling. However, patients are more likely to suffer from the effects of sepsis when they are either already immunodeficient or develop early immunosuppression post-infection. The immunological susceptibility to sepsis has prompted attempts to establish pre-sepsis immunosuppression in model animals *via* the administration of immunosuppressants. Indeed,

immunosuppressants such as cyclophosphamide or cyclosporine were given to mice to induce a pre-existing immunosuppressive state. When pathogens were injected into these mice, the animals developed sepsis in similar fashion to immunocompromised patients (45, 46). However, pre-existing immunosuppressive status may not accurately replicate the natural course and severity of sepsis-induced immunoparalysis. The release of proinflammatory mediators, for instance, remains persistently low in this type of model, and the transition from hyperinflammation towards immunosuppression, as seen in human sepsis, is not observed (45). Moreover, cyclosporine mainly impairs T lymphocyte activity, rather than suppress the overall immune response, which also differs from the immunopathy encountered in sepsis (45).

Sepsis is often associated with co-morbidities (e.g., trauma, obesity, and cancer), causing patients to become more predisposed to immunosuppression in sepsis (47, 48). Therefore, researchers have modeled sepsis in animals bearing these co-morbidities. For instance, traumatic hemorrhage was induced in mice prior to CLP to examine its impact on the immune status and the ability to survive the subsequent onset of sepsis (49). Other studies have modelled sepsis-associated immunosuppression in obese mice (50) or tumor-bearing mice (51, 52), which were designed to evaluate the impact of co-morbidities on the development of sepsis and sepsis-associated immunoparalysis. Such studies are important for broadening our understanding of the heterogeneity of sepsis but are not ideal for delineating the mechanisms of immunosuppression, which can be attributed to sepsis or the comorbidity. In addition, animals with pre-existing diseases often produce more heterogenous experimental outcomes, thereby demanding more standardized and elaborate modeling procedures.

Strengths and limitations of modeling sepsis-induced immunosuppression in mice

How do murine models accurately replicate the immunological alterations in human sepsis?

Mice and humans share a highly homologous genetic background (>80% conserved synteny), meaning that the discovery of murine genes and corresponding phenotypes often applicable to humans (53–55). Shay et al. (56) compared the genome-wide transcriptional compendia of humans and mice, and founds that the resting and activated immune cells of both organisms shared a conserved transcriptional program and associated regulatory mechanisms. An earlier collaborative research program termed Glue Grant, which addressed how murine models mirror human disease in sepsis and trauma (57), described more specifically the similarities in both species upon endotoxin challenge, including the appearance of lymphopenia, which characterizes immunosuppression in sepsis (58). A series of subsequent studies further compared interspecies data derived from Glue Grant or other databases (e.g., the Immunological Genome Project). Although the overall transcriptomic association between mouse injury models and human inflammatory diseases (such as trauma, burns and sepsis) was weak (59, 60), the signaling pathways involved in early inflammation and innate/adaptive immunity were similar in both species (60). In addition, a number of pathways/biogroups that reflect both excessive inflammation and immunosuppression, such as enhanced cytokine signaling and suppressed lymphocyte differentiation, are altered in both mice and humans consistently (61). A more recent study further demonstrated that the gene expression patterns in LPS-stimulated mouse peritoneal cells, including genes associated with immunosuppression, are similar to genes upregulated in human cells stimulated with LPS *in vitro* or cells isolated from septic patients (62). These findings suggest the feasibility of murine models to accurately replicate the immunological alterations in human sepsis.

Specific murine models reflect the features of immunosuppression in human sepsis, either in part or in whole. For example, a mixture of both pro- and anti-inflammatory reactions, accompanied with subsequent dysfunction of adaptive immune responses that characterize the immunosuppression of human sepsis, has been demonstrated in murine CLP models (28, 63). Moreover, the phenomenon of leukocyte reprogramming in human sepsis, as indicated by diminished cytokine release and impaired antigen presentation, can also be similarly detected in murine LPS tolerance model (40). Other similarities due to the influence by different immunological backgrounds, such as age and gender, have also been identified in both mice and humans. For example, the increased production of immunosuppressive cytokines and the impaired CD4+ T cell proliferation were similarly detected in elderly sepsis patients and CLP mice (64). Furthermore, clinical and experimental studies have both indicated that female mice and patients are immunologically more competent than male subjects upon sepsis insult, which renders the transition towards immunosuppression and decreases the susceptibility to secondary infection (65).

How do murine models advance our understanding of immunosuppression in sepsis?

First, the principal immunological players involved in sepsis were predominantly discovered in mice and only later identified in humans (55). For instance, toll-like receptor 4 (TLR4) was initially characterized in mice as the pattern recognition receptor

(PRR) for LPS, and represents a significant milestone in improving our understanding of the immunopathology of sepsis (66). Likewise, the discovery of the metabolic and epigenetic rewiring mechanism that drives the shift towards immunosuppression in sepsis was also initially made using mouse models (67, 68). Other major immunological breakthroughs in sepsis, such as the characterization of immunosuppressive cells (e.g., regulatory T-cells, Tregs; and myeloid-derived suppressor cells, MDSCs) and immune checkpoints (e.g., programmed cell death protein-1, PD-1; and cytotoxic T-lymphocyte antigen 4, CTLA-4), occurred initially in models, before further verification of their importance in human sepsis (69–71). Second, our knowledge of sepsis immunology in humans is almost exclusively derived from studies using blood samples. However, increasing importance has been attributed to the roles of tissue and organ immunology in sepsis (7). In this regard, it may be more valuable to examine immunological profiles at the site of infection rather than solely in the blood (72). A variety of sample types can be extracted from murine models, thereby facilitating the characterization of compartment-specific immunopathy in sepsis. For instance, the functionality of alveolar macrophages and microglial cells are primed or unaltered, respectively, in the LPS injection or CLP models, compared to the tolerance induction observed in peritoneal cells and splenocytes (7). In addition, Komegae et al. (73) recently reported the site-specific responsiveness of alveolar, peritoneal, and adipose-associated macrophages to bacterial LPS, as indicated by the different tumor necrosis factor alpha (TNF-α)/IL-10 ratios that are indicative of the immunosuppressive status. Such results cannot be obtained *via* the study of peripheral blood samples alone.

Third, murine models are extensively used preclinical studies to inform future clinical trials or support the implementation guidelines for the management of sepsis survivors (74). In particular, attempts have been made in animal models to reverse the immunocompromised status or boost immunity with immunostimulants by means of cytokines, peptides, small molecule compounds, and cell transfer strategies (14). For example, pharmacological or genetic approaches to suppressing lymphocyte apoptosis have been verified in experimental models, aiming to evaluate the potential of reducing sepsis lethality by targeting apoptosis in lymphocytes (14).

How to understand the limitation of using murine models in studying immunosuppression in sepsis?

Mouse models have improved our understanding of the immune profiles that exist in sepsis. However, there are a number of discrepancies that interfere with the recapitulation of the immunosuppression observed in human sepsis. Of note, these discrepancies may either result from their inherently-distinct immune responses or otherwise are induced by inappropriate experimental procedures during sepsis modeling.

First, the precise immunological changes are not consistent between murine models and human sepsis (75). In fact, the dynamics of the immunological response is much more rapid and intense in murine sepsis models, and lead to a short course of disease. However, human sepsis is often chronic and immunological alterations, including the onset of immunosuppression, is persistent or repeated. Further, murine models that recapitulate sepsis induced by a certain kind of insult or at a specific infection site can only model a subtype of sepsis or demonstrate one aspect of the pathophysiological changes that are encountered in human sepsis. To illustrate, induction of LPS tolerance may only mimic compartmentalized immunological changes in sepsis. However, a modeling strategy that induces sepsis by targeting different tissue sites may significantly affect the immune response in sepsis (20). Similarly, the administration of IL-10, an immunosuppressive cytokine, has been shown to protect model mice from abdominal sepsis but led to the deterioration of mice with pulmonary sepsis (20). In this regard, when investigating the pathology or treatment of immunosuppression in sepsis, results from different models should be interpreted with caution.

Second, various methodological factors may dramatically alter the immune profiles of model mice. For example, it has been demonstrated that immunosuppression is well reproduced in the CLP model (11, 18) whereas other polymicrobial peritonitis models, such as the CASP model and the cecal slurry model, have ongoing proinflammatory responses that do not reach an immunosuppressive state (18, 76). Moreover, murine models are established in young, healthy, homogeneous, and pathogen-free animals, compared to the heterogeneous background conditions of human sepsis. Therefore, the common establishment of sepsis in these animals cannot fully replicate those of human sepsis, which occurs predominantly in a heterogeneous aging population, with existing comorbidities. Furthermore, individuals with sepsis harbor commensal microbiota or acquired infections that may dramatically affect their immunological state. These differences make it hard to replicate the exact features of immunosuppression in human sepsis by using standardized murine models. With regards to the comparison of murine models to human sepsis, another considerable discrepancy exists in post-sepsis interventions. Human patients with sepsis always receive supportive care, such as surgical resection, antibiotics, analgesia, and organ support. However, these interventions are absent or inconsistently performed during the care of human patients or in mouse models. Taking the use of analgesics as an example, opioids like buprenorphine, hydromorphone, oxycodone, and tramadol are less immunosuppressive than morphine and fentanyl, which suggests that different choices of analgesics may cause variations in the immune status of animals thereby

affecting their immunological phenotypes during the modeling of sepsis (77). Finally, the design and execution of animal experiments lack inter-lab consistency, with sufficiently powered, randomized, or blinded analyses being rarely conducted (74). Therefore, positive outcomes are more likely to be reported, leading to a biased interpretation that limits the success of translation into human subjects (78). A brief description of strengths and limitations is depicted in Figure 2.

Future directions to narrow the gaps between murine models and human sepsis

Reducing experimental inconsistency

Standardized sepsis models are necessary to minimize discordant results between models and reduce discrepancies between animal and human sepsis (79). The recently published minimum quality threshold in pre-clinical sepsis studies (MQTiPSS), which was published by a consortium of experts from various research institutions, proposed a set of guidelines to enhance the consistency and translational value of sepsis models *via* the development of standardized technical procedures (80). In addition, we and other researchers have reported attempts to improve the consistency of CLP or CASP models by standardizing surgical procedures and the application of specialized surgical tools (81, 82). Nevertheless, we are some distance from creating standardized animal models that mimic the immunosuppression of human sepsis. Further research is thus needed to comprehensively document the immunological profiles of different septic models, such as the factors that predispose to immunosuppression development, the kinetics of immunological events, organ-specific immunological alterations and their association with organ dysfunction (7, 73). For example, a scoring system could be devised for predicting or evaluating the immunological parameters in sepsis, serving to reduce the inconsistencies in modeling and enable better comparisons between different experiments or laboratories (79).

Increasing clinical relevance

Sepsis is highly heterogeneous in terms of pathogen species, genetics, age, gender, and comorbidities. It is therefore challenging to predict the progression from sepsis onset to immunosuppression. The complexity of sepsis calls for the development of a precision medicine approach, which requires more individualized and clinically compatible models for the recapitulation of sepsis-associated immunosuppression. For instance, the pathogen species used in current murine sepsis models are neither polymicrobial in nature nor clinically relevant. Therefore, a possible way of refining these models is to instead perform polymicrobial inoculation with clinical strains of microbes (83), or otherwise rebuild the microbiota of lab mice by introducing environmental pathogens prior to sepsis modeling (42). Additionally, most existing studies use young and healthy animals to model sepsis. Recently, attempts have been made to model sepsis in elderly mice, demonstrating remarkable

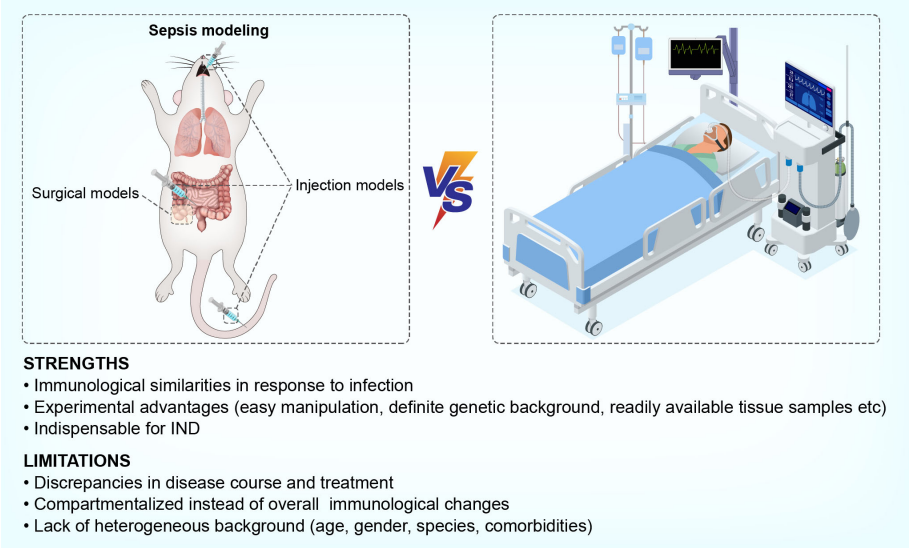

FIGURE 2
Strengths and limitations of using murine models to mimic sepsis-induced immunosuppression in humans.

differences in the immune response and disease outcomes when compared with their young counterparts (84, 85). In addition to considering the influence of age on sepsis pathology, future studies should aim to model sepsis in animals of different gender, or having a pre-existing illness (e.g., obesity and diabetes).

Sepsis often induces prolonged immunosuppression, which is associated with an increased risk of chronic dysfunction, such as weakness, secondary infection, and cancer (86). However, animals used to model septic often die too early for the onset of long-term consequences to be observed. The development of intensive care unit (ICU)-like murine facilities has already been shown prolong the survival of mice with sepsis and allow for longitudinal studies (87, 88).

Finally, translational research sepsis research to narrow the gaps when addressing therapeutic interventions for sepsis. Two recent systematic reviews have outlined recommendations for the design of preclinical studies to ensure clinical relevance (74, 89). Thus, in addition to the refinement of existing models, other experimental factors such as appropriate cohort selection, randomization, blinding, the timing of the intervention, as well as the use of powerful statistical analyses (i.e., using appropriate power and sample size), should be considered when designing clinically-relevant models of sepsis.

Improving immunological similarities between mice and humans

In addition to the approaches outlined in earlier sections of this mini review, research is being carried out into improving the immunological similarities between mice and humans, thus narrowing the gap between these species for the study of sepsis. Sepsis is increasingly recognized as a syndrome of immunoparalysis rather than a cytokine storm-driven condition. A recent study reported that the switch from uncontrolled inflammation to ordered hypoinflammation and immunosuppression could be achieved by priming with a diverse pool of antigens to induce the activation of immunological memory (90). In this model, short-term mortality was reduced allowing for the long-term investigation of sepsis survivors, which may better resemble the course of sepsis-associated immunosuppression observed in humans (90). Environmental factors such as the microbiota also greatly affect the immune status of laboratory mice. To address this issue, a recent study created wildling mice by transferring C57BL/6 embryos into wild mice. These wildling mice demonstrated phenocopied human immune responses, and are therefore more suitable as candidate animals for investigating immunosuppression in sepsis (91).

Although sepsis modeling is predominantly performed in mice, translational gaps exist between mice and humans due to differences in their immune systems (92). To solve this issue, mice with a reconstituted human immune system or bearing active human immunogens have been created. These 'humanized mice' have been successfully utilized to study viral infection and transplantation and are expected to bridge the translational gap between mice and humans. Some recent studies have demonstrated that features of immunosuppression in sepsis, including bone marrow suppression (93), reduced cell surface marker expression (94), and increased apoptosis (95), are better replicated in humanized mice after CLP modeling. Although limitations exist and humanized mice cannot fully replicate human immunology in sepsis, this model may offer an alternative approach for the study of immunosuppression in sepsis. Given that the microbiome shapes human immunity and affects the outcomes of clinical sepsis, another approach would be to recreate a humanized microbiome in model mice, thereby increasing the utility of mice as a model organism by populating them with the same pathogens that are present in the human microbiome during sepsis (96).

Conclusions

Mice remain the organism of choice for modelling sepsis. However, questions and doubts continue to be raised regarding the reliability of murine models in sepsis research, due to conflicting reports and negative translational outcomes. Sepsis is a heterogeneous syndrome, rendered even more complex by the period of immunosuppression that follows early-stage disease. Given that an ideal modeling strategy has not yet been developed, efforts should focus on refining current murine models to reduce inconsistency and increase clinical relevance; these improved murine models will be invaluable tools for study of the complex immunopathology of human sepsis.

Author contributions

NW and XL reviewed literatures and wrote the manuscript. NW prepared figures and tables. YL reviewed literature and help to prepare figures. JZ and XL conceived the review article and made substantial revision before submission. All authors contributed to the article and approved the submission.

Funding

This work was supported by grants from the National Natural Science Foundation (81873955, 81772137).

Conflict of interest

The authors declare that the research was conducted in the absence of any commercial or financial relationships that could be construed as a potential conflict of interest.

Publisher's note

References

1. Singer M, Deutschman CS, Seymour CW, Shankar-Hari M, Annane D, Bauer M, et al. The third international consensus definitions for sepsis and septic shock (Sepsis-3). *JAMA* (2016) 315(8):801–10. doi: 10.1001/jama.2016.0287

2. Rudd KE, Johnson SC, Agesa KM, Shackelford KA, Tsoi D, Kievlan DR, et al. Global, regional, and national sepsis incidence and mortality, 1990-2017: analysis for the global burden of disease study. *Lancet* (2020) 395(10219):200–11. doi: 10.1016/S0140-6736(19)32989-7

3. Cecconi M, Evans L, Levy M, Rhodes A. Sepsis and septic shock. *Lancet* (2018) 392(10141):75–87. doi: 10.1016/S0140-6736(18)30696-2

4. Boomer JS, To K, Chang KC, Takasu O, Osborne DF, Walton AH, et al. Immunosuppression in patients who die of sepsis and multiple organ failure. *JAMA* (2011) 306(23):2594–605. doi: 10.1001/jama.2011.1829

5. Warny M, Helby J, Nordestgaard BG, Birgens H, Bojesen SE. Lymphopenia and risk of infection and infection-related death in 98,344 individuals from a prospective Danish population-based study. *PloS Med* (2018) 15(11):e1002685. doi: 10.1371/journal.pmed.1002685

6. Yende S, Kellum JA, Talisa VB, Peck PO, Chang CH, Filbin MR, et al. Long-term host immune response trajectories among hospitalized patients with sepsis. *JAMA Netw Open* (2019) 2(8):e198686. doi: 10.1001/jamanetworkopen.2019.8686

7. Rubio I, Osuchowski MF, Shankar-Hari M, Skirecki T, Winkler MS, Lachmann G, et al. Current gaps in sepsis immunology: new opportunities for translational research. *Lancet Infect Dis* (2019) 19(12):e422–36. doi: 10.1016/S1473-3099(19)30567-5

8. van der Poll T, Shankar-Hari M, Wiersinga WJ. The immunology of sepsis. *Immunity* (2021) 54(11):2450–64. doi: 10.1016/j.immuni.2021.10.012

9. Patil NK, Bohannon JK, Sherwood ER. Immunotherapy: A promising approach to reverse sepsis-induced immunosuppression. *Pharmacol Res* (2016) 111:688–702. doi: 10.1016/j.phrs.2016.07.019

10. Kieslichova E, Rocen M, Merta D, Kudla M, Splichal I, Cap J, et al. The effect of immunosuppression on manifestations of sepsis in an animal model of cecal ligation and puncture. *Transplant Proc* (2013) 45(2):770–7. doi: 10.1016/j.transproceed.2012.07.159

11. Hu SB, Zider A, Deng JC. When host defense goes awry: Modeling sepsis-induced immunosuppression. *Drug Discovery Today Dis Models* (2012) 9(1):e33–8. doi: 10.1016/j.ddmod.2011.09.001

12. Torres LK, Pickkers P, van der Poll T. Sepsis-induced immunosuppression. *Annu Rev Physiol* (2022) 84:157–81. doi: 10.1146/annurev-physiol-061121-040214

13. Peters VTA, Kox M, Abdo WF, Pickkers P. Precision immunotherapy for sepsis. *Front Immunol* (2018) 9:1926. doi: 10.3389/fimmu.2018.01926

14. van der Poll T, van de Veerdonk FL, Scicluna BP, Netea MG. The immunopathology of sepsis and potential therapeutic targets. *Nat Rev Immunol* (2017) 17(7):407–20. doi: 10.1038/nri.2017.36

15. Hamers L, Kox M, Pickkers P. Sepsis-induced immunoparalysis: mechanisms, markers, and treatment options. *Minerva Anestesiol* (2015) 81(4):426–39.

16. Buras JA, Holzmann B, Sitkovsky M. Animal models of sepsis: setting the stage. *Nat Rev Drug Discovery* (2005) 4(10):854–65. doi: 10.1038/nrd1854

17. Restagno D, Venet F, Paquet C, Freyburger L, Allaouchiche B, Monneret G, et al. Mice survival and plasmatic cytokine secretion in a "Two hit" model of sepsis depend on intratracheal pseudomonas aeruginosa bacterial load. *PloS One* (2016) 11(8):e162109. doi: 10.1371/journal.pone.0162109

18. Stortz JA, Raymond SL, Mira JC, Moldawer LL, Mohr AM, Efron PA. Murine models of sepsis and trauma: Can we bridge the gap? *Ilar J* (2017) 58(1):90–105. doi: 10.1093/ilar/ilx007

19. Remick DG, Ward PA. Evaluation of endotoxin models for the study of sepsis. *Shock* (2005) 24 Suppl 1:7–11. doi: 10.1097/01.shk.0000191384.34066.85

20. Chen P, Stanojcic M, Jeschke MG. Differences between murine and human sepsis. *Surg Clin North Am* (2014) 94(6):1135–49. doi: 10.1016/j.suc.2014.08.001

21. Ayala A, Song GY, Chung CS, Redmond KM, Chaudry IH. Immune depression in polymicrobial sepsis: the role of necrotic (injured) tissue and endotoxin. *Crit Care Med* (2000) 28(8):2949–55. doi: 10.1097/00003246-200008000-00044

22. Grailer JJ, Fattahi F, Dick RS, Zetoune FS, Ward PA. Cutting edge: critical role for C5aRs in the development of septic lymphopenia in mice. *J Immunol* (2015) 194(3):868–72. doi: 10.4049/jimmunol.1401193

23. Durand M, Hagimont E, Louis H, Asfar P, Frippiat JP, Singer M, et al. The beta1-adrenergic receptor contributes to sepsis-induced immunosuppression through modulation of regulatory T-cell inhibitory function. *Crit Care Med* (2022). doi: 10.1097/CCM.0000000000005503

24. de Lima M, Hiroki CH, de Fatima BV, Cebinelli G, Santos J, Rosa MH, et al. Sepsis-induced immunosuppression is marked by an expansion of a highly suppressive repertoire of FOXP3+ T-regulatory cells expressing TIGIT. *J Infect Dis* (2022) 225(3):531–41. doi: 10.1093/infdis/jiab405

25. Ruan WS, Feng MX, Xu J, Xu YG, Song CY, Lin LY, et al. Early activation of myeloid-derived suppressor cells participate in sepsis-induced immune suppression *via* PD-L1/PD-1 axis. *Front Immunol* (2020) 11:1299. doi: 10.3389/fimmu.2020.01299

26. Muenzer JT, Davis CG, Dunne BS, Unsinger J, Dunne WM, Hotchkiss RS. Pneumonia after cecal ligation and puncture: a clinically relevant "two-hit" model of sepsis. *Shock* (2006) 26(6):565–70. doi: 10.1097/01.shk.0000235130.82363.ed

27. Wang Z, Pu Q, Lin P, Li C, Jiang J, Wu M. Design of cecal ligation and puncture and intranasal infection dual model of sepsis-induced immunosuppression. *J Vis Exp* (2019) 148. doi: 10.3791/59386

28. Dejager L, Pinheiro I, Dejonckheere E, Libert C. Cecal ligation and puncture: the gold standard model for polymicrobial sepsis? *Trends Microbiol* (2011) 19(4):198–208. doi: 10.1016/j.tim.2011.01.001

29. Davis CG, Chang K, Osborne D, Walton AH, Dunne WM, Muenzer JT. Increased susceptibility to candida infection following cecal ligation and puncture. *Biochem Biophys Res Commun* (2011) 414(1):37–43. doi: 10.1016/j.bbrc.2011.09.017

30. Chen X, Li X, Lu H, Xu Y, Wei Y, Cao K, et al. Mouse model of critical persistent inflammation, immunosuppression, and catabolism syndrome. *Shock* (2022) 57(2):238–45. doi: 10.1097/SHK.0000000000001878

31. Efron PA, Darden DB, Wang Z, Nacionales DC, Lopez MC, Hawkins RB, et al. Transcriptomic responses from improved murine sepsis models can better mimic human surgical sepsis. *FASEB J* (2021) 35(2):e21156. doi: 10.1096/fj.202002150R

32. Schmoeckel K, Mrochen DM, Huhn J, Potschke C, Broker BM. Polymicrobial sepsis and non-specific immunization induce adaptive immunosuppression to a similar degree. *PloS One* (2018) 13(2):e192197. doi: 10.1371/journal.pone.0192197

33. Sjaastad FV, Kucaba TA, Dileepan T, Swanson W, Dail C, Cabrera-Perez J, et al. Polymicrobial sepsis impairs antigen-specific memory CD4 T cell-mediated immunity. *Front Immunol* (2020) 11:1786. doi: 10.3389/fimmu.2020.01786

34. Portella VG, Silva-Filho JL, Landgraf SS, de Rico TB, Vieira MA, Takiya CM, et al. Sepsis-surviving mice are more susceptible to a secondary kidney insult. *Crit Care Med* (2013) 41(4):1056–68. doi: 10.1097/CCM.0b013e3182746696

35. Davis FM, Schaller MA, Dendekker A, Joshi AD, Kimball AS, Evanoff H, et al. Sepsis induces prolonged epigenetic modifications in bone marrow and peripheral macrophages impairing inflammation and wound healing. *Arterioscler Thromb Vasc Biol* (2019) 39(11):2353–66. doi: 10.1161/ATVBAHA.119.312754

36. Roquilly A, Jacqueline C, Davieau M, Molle A, Sadek A, Fourgeux C, et al. Alveolar macrophages are epigenetically altered after inflammation, leading to long-term lung immunoparalysis. *Nat Immunol* (2020) 21(6):636–48. doi: 10.1038/s41590-020-0673-x

37. Drechsler S, Weixelbaumer KM, Redl H, van Griensven M, Bahrami S, Osuchowski MF. Experimentally approaching the ICU: monitoring outcome-based responses in the two-hit mouse model of posttraumatic sepsis. *J BioMed Biotechnol* (2011) 2011:357926. doi: 10.1155/2011/357926

38. Bastarache JA, Smith K, Jesse JJ, Putz ND, Meegan JE, Bogart AM, et al. A two-hit model of sepsis plus hyperoxia causes lung permeability and inflammation.

Am J Physiol Lung Cell Mol Physiol (2022) 322(2):L273–82. doi: 10.1152/ajplung.00227.2021

39. Bauhofer A, Lorenz W, Kohlert F, Torossian A. Granulocyte colony-stimulating factor prophylaxis improves survival and inflammation in a two-hit model of hemorrhage and sepsis. *Crit Care Med* (2006) 34(3):778–84. doi: 10.1097/01.ccm.0000201900.01000.6b

40. Biswas SK, Lopez-Collazo E. Endotoxin tolerance: new mechanisms, molecules and clinical significance. *Trends Immunol* (2009) 30(10):475–87. doi: 10.1016/j.it.2009.07.009

41. Liu D, Cao S, Zhou Y, Xiong Y. Recent advances in endotoxin tolerance. *J Cell Biochem* (2019) 120(1):56–70. doi: 10.1002/jcb.27547

42. Beura LK, Hamilton SE, Bi K, Schenkel JM, Odumade OA, Casey KA, et al. Normalizing the environment recapitulates adult human immune traits in laboratory mice. *Nature* (2016) 532(7600):512–6. doi: 10.1038/nature17655

43. Sans-Fons MG, Yeramian A, Pereira-Lopes S, Santamaria-Babi LF, Modolell M, Lloberas J, et al. Arginine transport is impaired in C57Bl/6 mouse macrophages as a result of a deletion in the promoter of Slc7a2 (CAT2), and susceptibility to leishmania infection is reduced. *J Infect Dis* (2013) 207(11):1684–93. doi: 10.1093/infdis/jit084

44. Carreras E, Velasco DAM, Orta-Mascaro M, Simoes IT, Catala C, Zaragoza O, et al. Discordant susceptibility of inbred C57BL/6 versus outbred CD1 mice to experimental fungal sepsis. *Cell Microbiol* (2019) 21(5):e12995. doi: 10.1111/cmi.12995

45. Kong X, Zhang J, Huo J, Wang L, Guo L, Liu Y, et al. A systematic investigation on animal models of cyclosporine a combined with escherichia coli to simulate the immunosuppressive status of sepsis patients before onset. *Int Immunopharmacol* (2018) 62:67–76. doi: 10.1016/j.intimp.2018.05.031

46. Manepalli S, Gandhi JA, Ekhar VV, Asplund MB, Coelho C, Martinez LR. Characterization of a cyclophosphamide-induced murine model of immunosuppression to study acinetobacter baumannii pathogenesis. *J Med Microbiol* (2013) 62(Pt 11):1747–54. doi: 10.1099/jmm.0.060004-0

47. Frydrych LM, Bian G, O'Lone DE, Ward PA, Delano MJ. Obesity and type 2 diabetes mellitus drive immune dysfunction, infection development, and sepsis mortality. *J Leukoc Biol* (2018) 104(3):525–34. doi: 10.1002/JLB.5VMR0118-021RR

48. Sinapidis D, Kosmas V, Vittoros V, Koutelidakis IM, Pantazi A, Stefos A, et al. Progression into sepsis: an individualized process varying by the interaction of comorbidities with the underlying infection. *BMC Infect Dis* (2018) 18(1):242. doi: 10.1186/s12879-018-3156-z

49. Knoferl MW, Angele MK, Diodato MD, Schwacha MG, Ayala A, Cioffi WG, et al. Female sex hormones regulate macrophage function after trauma-hemorrhage and prevent increased death rate from subsequent sepsis. *Ann Surg* (2002) 235(1):105–12. doi: 10.1097/00000658-200201000-00014

50. Xu W, Pepper D, Sun J, Welsh J, Cui X, Eichacker PQ. The effects of obesity on outcome in preclinical animal models of infection and sepsis: A systematic review and meta-analysis. *J Obes* (2020) 2020:1508764. doi: 10.1155/2020/1508764

51. Lyons JD, Chen CW, Liang Z, Zhang W, Chihade DB, Burd EM, et al. Murine pancreatic cancer alters T cell activation and apoptosis and worsens survival after cecal ligation and puncture. *Shock* (2019) 51(6):731–9. doi: 10.1097/SHK.0000000000001203

52. Zhang W, Anyalebechi JC, Ramonell KM, Chen CW, Xie J, Liang Z, et al. TIGIT modulates sepsis-induced immune dysregulation in mice with preexisting malignancy. *JCI Insight* (2021) 6(11):e139823. doi: 10.1172/jci.insight.139823

53. Breschi A, Gingeras TR, Guigo R. Comparative transcriptomics in human and mouse. *Nat Rev Genet* (2017) 18(7):425–40. doi: 10.1038/nrg.2017.19

54. Waterston RH, Lindblad-Toh K, Birney E, Rogers J, Abril JF, Agarwal P, et al. Initial sequencing and comparative analysis of the mouse genome. *Nature* (2002) 420(6915):520–62. doi: 10.1038/nature01262

55. Masopust D, Sivula CP, Jameson SC. Of mice, dirty mice, and men: Using mice to understand human immunology. *J Immunol* (2017) 199(2):383–8. doi: 10.4049/jimmunol.1700453

56. Shay T, Jojic V, Zuk O, Rothamel K, Puyraimond-Zemmour D, Feng T, et al. Conservation and divergence in the transcriptional programs of the human and mouse immune systems. *Proc Natl Acad Sci U.S.A.* (2013) 110(8):2946–51. doi: 10.1073/pnas.1222738110

57. Calvano SE, Xiao W, Richards DR, Felciano RM, Baker HV, Cho RJ, et al. A network-based analysis of systemic inflammation in humans. *Nature* (2005) 437(7061):1032–7. doi: 10.1038/nature03985

58. Copeland S, Warren HS, Lowry SF, Calvano SE, Remick D. Acute inflammatory response to endotoxin in mice and humans. *Clin Diagn Lab Immunol* (2005) 12(1):60–7. doi: 10.1128/CDLI.12.1.60-67.2005

59. Seok J, Warren HS, Cuenca AG, Mindrinos MN, Baker HV, Xu W, et al. Genomic responses in mouse models poorly mimic human inflammatory diseases. *Proc Natl Acad Sci U.S.A.* (2013) 110(9):3507–12. doi: 10.1073/pnas.1222878110

60. Gentile LF, Nacionales DC, Lopez MC, Vanzant E, Cuenca A, Cuenca AG, et al. A better understanding of why murine models of trauma do not recapitulate the human syndrome. *Crit Care Med* (2014) 42(6):1406–13. doi: 10.1097/CCM.0000000000000222

61. Takao K, Miyakawa T. Genomic responses in mouse models greatly mimic human inflammatory diseases. *Proc Natl Acad Sci U.S.A.* (2015) 112(4):1167–72. doi: 10.1073/pnas.1401965111

62. Rosier F, Nunez NF, Torres M, Loriod B, Rihet P, Pradel LC. Transcriptional response in a sepsis mouse model reflects transcriptional response in sepsis patients. *Int J Mol Sci* (2022) 23(2):821. doi: 10.3390/ijms23020821

63. Osuchowski MF, Welch K, Siddiqui J, Remick DG. Circulating cytokine/inhibitor profiles reshape the understanding of the SIRS/CARS continuum in sepsis and predict mortality. *J Immunol* (2006) 177(3):1967–74. doi: 10.4049/jimmunol.177.3.1967

64. Inoue S, Suzuki K, Komori Y, Morishita Y, Suzuki-Utsunomiya K, Hozumi K, et al. Persistent inflammation and T cell exhaustion in severe sepsis in the elderly. *Crit Care* (2014) 18(3):R130. doi: 10.1186/cc13941

65. McPeak MB, Youssef D, Williams DA, Pritchett CL, Yao ZQ, McCall CE, et al. Frontline science: Myeloid cell-specific deletion of cebpb decreases sepsis-induced immunosuppression in mice. *J Leukoc Biol* (2017) 102(2):191–200. doi: 10.1189/jlb.4HI1216-537R

66. Poltorak A, He X, Smirnova I, Liu MY, Van Huffel C, Du X, et al. Defective LPS signaling in C3H/HeJ and C57BL/10ScCr mice: mutations in Tlr4 gene. *Science* (1998) 282(5396):2085–8. doi: 10.1126/science.282.5396.2085

67. Cheng SC, Scicluna BP, Arts RJ, Gresnigt MS, Lachmandas E, Giamarellos-Bourboulis EJ, et al. Broad defects in the energy metabolism of leukocytes underlie immunoparalysis in sepsis. *Nat Immunol* (2016) 17(4):406–13. doi: 10.1038/ni.3398

68. Binnie A, Tsang J, Hu P, Carrasqueiro G, Castelo-Branco P, Dos SC. Epigenetics of sepsis. *Crit Care Med* (2020) 48(5):745–56. doi: 10.1097/CCM.0000000000004247

69. Sharma P, Allison JP. The future of immune checkpoint therapy. *Science* (2015) 348(6230):56–61. doi: 10.1126/science.aaa8172

70. Delano MJ, Scumpia PO, Weinstein JS, Coco D, Nagaraj S, Kelly-Scumpia KM, et al. MyD88-dependent expansion of an immature GR-1(+)CD11b(+) population induces T cell suppression and Th2 polarization in sepsis. *J Exp Med* (2007) 204(6):1463–74. doi: 10.1084/jem.20062602

71. Martin MD, Badovinac VP, Griffith TS. CD4 T cell responses and the sepsis-induced immunoparalysis state. *Front Immunol* (2020) 11:1364. doi: 10.3389/fimmu.2020.01364

72. Stearns-Kurosawa DJ, Osuchowski MF, Valentine C, Kurosawa S, Remick DG. The pathogenesis of sepsis. *Annu Rev Pathol* (2011) 6:19–48. doi: 10.1146/annurev-pathol-011110-130327

73. Komegae EN, Fonseca MT, Da SCS, Turato WM, Filgueiras LR, Markus RP, et al. Site-specific reprogramming of macrophage responsiveness to bacterial lipopolysaccharide in obesity. *Front Immunol* (2019) 10:1496. doi: 10.3389/fimmu.2019.01496

74. Lamontagne F, Briel M, Duffett M, Fox-Robichaud A, Cook DJ, Guyatt G, et al. Systematic review of reviews including animal studies addressing therapeutic interventions for sepsis. *Crit Care Med* (2010) 38(12):2401–8. doi: 10.1097/CCM.0b013e3181fa0468

75. Mestas J, Hughes CC. Of mice and not men: differences between mouse and human immunology. *J Immunol* (2004) 172(5):2731–8. doi: 10.4049/jimmunol.172.5.2731

76. Gentile LF, Nacionales DC, Lopez MC, Vanzant E, Cuenca A, Szpila BE, et al. Host responses to sepsis vary in different low-lethality murine models. *PloS One* (2014) 9(5):e94404. doi: 10.1371/journal.pone.0094404

77. Nemzek JA, Hugunin KM, Opp MR. Modeling sepsis in the laboratory: merging sound science with animal well-being. *Comp Med* (2008) 58(2):120–8.

78. Bebarta V, Luyten D, Heard K. Emergency medicine animal research: does use of randomization and blinding affect the results? *Acad Emerg Med* (2003) 10(6):684–7. doi: 10.1111/j.1553-2712.2003.tb00056.x

79. Remick DG, Ayala A, Chaudry IH, Coopersmith CM, Deutschman C, Hellman J, et al. Premise for standardized sepsis models. *Shock* (2019) 51(1):4–9. doi: 10.1097/SHK.0000000000001164

80. Osuchowski MF, Ayala A, Bahrami S, Bauer M, Boros M, Cavaillon JM, et al. Minimum quality threshold in pre-clinical sepsis studies (MQTiPSS): An international expert consensus initiative for improvement of animal modeling in sepsis. *Shock* (2018) 50(4):377–80. doi: 10.1097/SHK.0000000000001212

81. Liu X, Wang N, Wei G, Fan S, Lu Y, Zhu Y, et al. Consistency and pathophysiological characterization of a rat polymicrobial sepsis model *via* the improved cecal ligation and puncture surgery. *Int Immunopharmacol* (2016) 32:66–75. doi: 10.1016/j.intimp.2015.12.041

82. Utiger JM, Glas M, Levis A, Prazak J, Haenggi M. Description of a rat model of polymicrobial abdominal sepsis mimicking human colon perforation. *BMC Res Notes* (2021) 14(1):14. doi: 10.1186/s13104-020-05438-y

83. Hou X, Zhang X, Zhao W, Zeng C, Deng B, McComb DW, et al. Vitamin lipid nanoparticles enable adoptive macrophage transfer for the treatment of multidrug-resistant bacterial sepsis. *Nat Nanotechnol* (2020) 15(1):41–6. doi: 10.1038/s41565-019-0600-1

84. Goswami DG, Walker WE. Aged IRF3-KO mice are protected from sepsis. *J Inflammation Res* (2021) 14:5757–67. doi: 10.2147/JIR.S335203

85. Stortz JA, Hollen MK, Nacionales DC, Horiguchi H, Ungaro R, Dirain ML, et al. Old mice demonstrate organ dysfunction as well as prolonged inflammation, immunosuppression, and weight loss in a modified surgical sepsis model. *Crit Care Med* (2019) 47(11):e919–29. doi: 10.1097/CCM.0000000000003926

86. Mirouse A, Vigneron C, Llitjos JF, Chiche JD, Mira JP, Mokart D, et al. Sepsis and cancer: An interplay of friends and foes. *Am J Respir Crit Care Med* (2020) 202(12):1625–35. doi: 10.1164/rccm.202004-1116TR

87. Owen AM, Patel SP, Smith JD, Balasuriya BK, Mori SF, Hawk GS, et al. Chronic muscle weakness and mitochondrial dysfunction in the absence of sustained atrophy in a preclinical sepsis model. *Elife* (2019) 8:e49920. doi: 10.7554/eLife.49920

88. Guillon A, Preau S, Aboab J, Azabou E, Jung B, Silva S, et al. Preclinical septic shock research: why we need an animal ICU. *Ann Intensive Care* (2019) 9 (1):66. doi: 10.1186/s13613-019-0543-6

89. Lewis AJ, Lee JS, Rosengart MR. Translational sepsis research: Spanning the divide. *Crit Care Med* (2018) 46(9):1497–505. doi: 10.1097/CCM.0000000000003271

90. Nowill AE, Fornazin MC, Spago MC, Dorgan NV, Pinheiro V, Alexandre S, et al. Immune response resetting in ongoing sepsis. *J Immunol* (2019) 203(5):1298–312. doi: 10.4049/jimmunol.1900104

91. Rosshart SP, Herz J, Vassallo BG, Hunter A, Wall MK, Badger JH, et al. Laboratory mice born to wild mice have natural microbiota and model human immune responses. *Science* (2019) 365(6452):eaaw4361. doi: 10.1126/science.aaw4361

92. Laudanski K, Stentz M, DiMeglio M, Furey W, Steinberg T, Patel A. Potential pitfalls of the humanized mice in modeling sepsis. *Int J Inflam* (2018) 2018:6563454. doi: 10.1155/2018/6563454

93. Lapko N, Zawadka M, Polosak J, Worthen GS, Danet-Desnoyers G, Puzianowska-Kuznicka M, et al. Long-term monocyte dysfunction after sepsis in humanized mice is related to persisted activation of macrophage-colony stimulation factor (M-CSF) and demethylation of PU.1, and it can be reversed by blocking m-CSF *In vitro* or by transplanting naive autologous stem cells *In vivo*. *Front Immunol* (2017) 8:401. doi: 10.3389/fimmu.2017.00401

94. Skirecki T, Drechsler S, Hoser G, Jafarmadar M, Siennicka K, Pojda Z, et al. The fluctuations of leukocytes and circulating cytokines in septic humanized mice vary with outcome. *Front Immunol* (2019) 10:1427. doi: 10.3389/fimmu.2019.01427

95. Zhao ZZ, Wang XL, Xie J, Chen LP, Li Q, Wang XX, et al. Therapeutic effect of an anti-human programmed death-ligand 1 (PD-L1) nanobody on polymicrobial sepsis in humanized mice. *Med Sci Monit* (2021) 27:e926820. doi: 10.12659/MSM.926820

96. Alverdy JC, Keskey R, Thewissen R. Can the cecal ligation and puncture model be repurposed to better inform therapy in human sepsis? *Infect Immun* (2020) 88(9):e00942–19. doi: 10.1128/IAI.00942-19

frontiers | Frontiers in Immunology

TYPE Original Research
PUBLISHED 20 September 2022
DOI 10.3389/fimmu.2022.987916

OPEN ACCESS

EDITED BY
Alessandra Stasi,
University of Bari Aldo Moro, Italy

REVIEWED BY
Dipendra Khadka,
Wonkwang University School of Medicine, South Korea
Chenyu Li,
Ludwig Maximilian University of Munich, Germany

*CORRESPONDENCE
Jiaojiao Zhou
zhoujiaojiao@wchscu.cn

SPECIALTY SECTION
This article was submitted to Inflammation, a section of the journal Frontiers in Immunology

RECEIVED 06 July 2022
ACCEPTED 29 August 2022
PUBLISHED 20 September 2022

CITATION
Wang S, Yang L, Zhou J, Yang J, Wang X, Chen X and Ji L (2022) A prediction model for acute kidney injury in adult patients with hemophagocytic lymphohistiocytosis. *Front. Immunol.* 13:987916. doi: 10.3389/fimmu.2022.987916

A prediction model for acute kidney injury in adult patients with hemophagocytic lymphohistiocytosis

Siwen Wang[1,2], Lichuan Yang[1], Jiaojiao Zhou[3]*, Jia Yang[1], Xin Wang[4], Xuelian Chen[1] and Ling Ji[1]

[1]Department of Nephrology, West China Hospital Sichuan University, Chengdu, China, [2]Department of Occupational Disease and Toxicosis/Nephrology, West China Fourth Hospital Sichuan University, Chengdu, China, [3]Department of Ultrasound, West China Hospital Sichuan University, Chengdu, China, [4]Department of Pediatric Nephrology, West China Second Hospital Sichuan University, Chengdu, China

Background and aims: Hemophagocytic lymphohistiocytosis is a clinical syndrome resulting from abnormally active immune cells and a cytokine storm, with the accompanying phagocytosis of blood cells. Patients with hemophagocytic lymphohistiocytosis often suffer acute kidney injury during hospitalization, which usually signifies poor prognosis. We would like to establish a prediction model for the occurrence of acute kidney injury in adult patients with hemophagocytic lymphohistiocytosis for risk stratification.

Method: We extracted the electronic medical records of patients diagnosed with hemophagocytic lymphohistiocytosis during hospitalization from January 2009 to July 2019. The observation indicator is the occurrence of acute kidney injury within 28 days of hospitalization. LASSO regression was used to screen variables and modeling was performed by COX regression.

Results: In the present study, 136 (22.7%) patients suffered from acute kidney injury within 28 days of hospitalization. The prediction model consisted of 11 variables, including vasopressor, mechanical ventilation, disseminated intravascular coagulation, admission heart rate, hemoglobin, baseline cystatin C, phosphorus, total bilirubin, lactic dehydrogenase, prothrombin time, and procalcitonin. The risk of acute kidney injury can be assessed by the sum of the scores of each parameter on the nomogram. For the development and validation groups, the area under the receiver operating characteristic curve was 0.760 and 0.820, and the C-index was 0.743 and 0.810, respectively.

Conclusion: We performed a risk prediction model for the development of acute kidney injury in patients with hemophagocytic lymphohistiocytosis,

10.3389/fimmu.2022.987916

which may help physicians to evaluate the risk of acute kidney injury and prevent its occurrence.

KEYWORDS

acute kidney injury, hemophagocytic lymphohistiocytosis (HLH), risk factors, prediction model, risk assessment

Introduction

Hemophagocytic lymphohistiocytosis (HLH) is a life-threatening syndrome caused by an abnormally active immune system. The major players involved are immunocytes such as cytotoxic T lymphocytes and natural killer cells, as well as inflammatory factors, including interferon-γ (IFN-γ), interleukin (IL)-1β, and IL-18. Hemophagocytosis is an important feature of HLH. Primary HLH is caused by genetic defect, while secondary HLH is mainly triggered by malignant tumors, infections, and immune factors (1, 2). The detection of hemophagocytes in the bone marrow is a characteristic of HLH, but not specific, and it is common in other tissues (such as liver, spleen, lymph nodes, etc) of critically ill patients (3). HLH is clinically difficult to diagnose, progresses rapidly, and is susceptible to multi-organ failure, including kidney failure. Clinicians face great challenges in the diagnosis and treatment of HLH and the management of its complications.

Acute kidney injury (AKI) is a clinical syndrome with a rapid increase in serum creatinine and/or a rapid decrease in urine output within a short period of time (4). AKI is common in hospitalized patients and has a high mortality rate. AKI, often secondary to extra-renal events, is an increasingly common problem for physicians and surgeons. In addition, the present view suggests that AKI promotes the development of chronic kidney disease and is a risk factor for cardiovascular disease (5). However, most patients with AKI have no noticeable clinical manifestations and AKI often co-exists with other syndromes, making it easy for clinicians to overlook it, leading to delay in diagnosis and treatment.

In recent years, an increasing number of researchers have focused on renal diseases complicated by HLH, especially AKI in HLH. Some scholars observed intraglomerular hemophagocytosis and erythrophagocytic macrophages in the tubular lumen (6, 7). However, the knowledge and expertise of researchers and clinicians on AKI in HLH are still far from enough. The AKI caused by HLH is mostly reported in some cases, which presented pathologic and speculated about the cause of AKI (7, 8). At present only one retrospective cohort study in this field analyzed the characteristics of AKI, kidney disease outcome and factors of mortality. And the study showed a high incidence of AKI in the course of HLH of up to 62% and the mortality risk is significantly higher in patients combined with AKI (9). AKI in HLH diminishes patients' quality of life and is strongly associated with high mortality. Therefore, there is a strong need to develop an appropriate model to predict AKI in patients with HLH to facilitate disease management by clinicians.

In the present study, we aimed to leverage available data to identify risk factors for AKI in HLH patients, establish a predictive model and evaluate the model to elucidate its accuracy and clinical practicality.

Materials and methods

Study population

We first filtered out 669 patients diagnosed with HLH at West China Hospital of Sichuan University from January 2009 to July 2019. Patients with HLH who fulfilled the diagnostic criteria proposed by the Histocyte Society in 2004 were then enrolled (10). Patients were required to fulfill 5 of the following 8 criteria: 1) fever; 2) splenomegaly; 3) cytopenia affecting at least 2 of 3 lineages in the peripheral blood; 4) hypertriglyceridemia (triglyceride ≥3.0 mmol/L) and/or hypofibrinogenemia (fibrinogen ≤1.5 g/L); 5) hemophagocytosis in bone marrow or spleen or lymph nodes; 6) low or absent NK-cell activity; 7) ferritin ≥500 ng/ml; and 8) soluble CD25 (i.e., soluble IL-2 receptor) ≥2,400 U/ml. We did ' t adopt gene standard in the diagnosis of HLH because genetic testing is not generally recommended in adult patients (11). The exclusion criteria include the following: patients younger than 18 years old, kidney transplant recipients, dialysis within the past 1 month, kidney malignancy, chronic kidney disease stage 4-5 and missing data. A total of 669 individuals were included in this study, and after the screening process, we analyzed 600 patients who met the requirements. Patients were split randomly into development and validation groups in a 7:3 ratio, with 419 individuals in the development group and 181 in the validation group (Figure 1). The outcome indicator of interest is whether the patient experienced AKI from the start of admission to the 28th day of hospitalization.

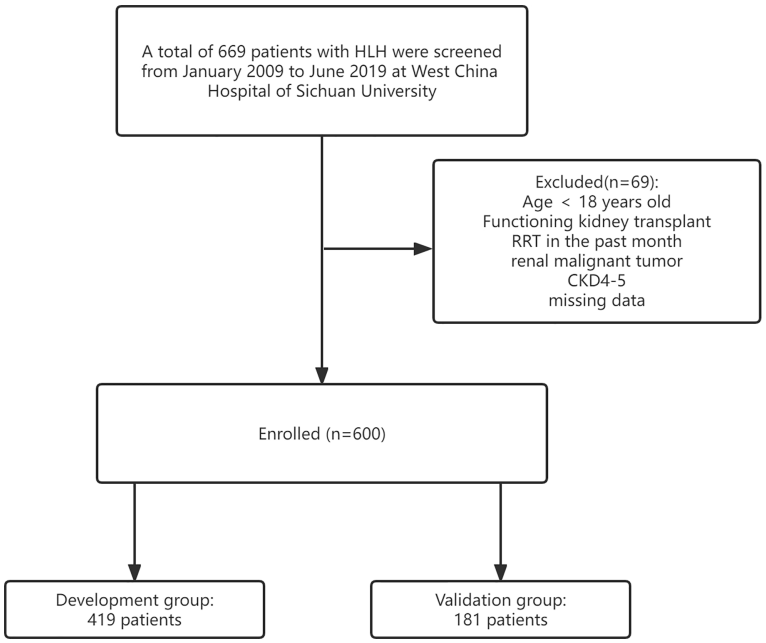

FIGURE 1
Research flowchart.

Clinical and biochemical data acquisition

We retrospectively gathered patients' information from the electronic medical record database established at our hospital. Demographic characteristics included gender, age, and history of tobacco and alcohol use. Treatment modalities consisted of therapy for HLH and some supportive therapy. The main triggers of HLH were infection, tumor, and autoimmune disease (1). If a specific trigger of HLH cannot be found, it is defined as "Undetermined". We also collected some comorbidities such as hypertension, diabetes mellitus, and heart failure. HLH-related clinical manifestations like fever, hepatosplenomegaly, and lymph node enlargement were also potential variables for our study. Laboratory based data were platelets, white blood cells, hemoglobin, baseline creatinine, baseline cystatin C, bilirubin, albumin, triglycerides, cholesterol, fibrinogen, etc. The lowest creatinine of patients within 2 days before admission was used as the baseline creatinine. If creatinine within 2 days before hospital admission was not available, the first creatinine tested after admission would be considered as the baseline creatinine.

Definitions employed

The updates made to the organization Kidney Disease Improving Global Outcomes (KDIGO)'s diagnostic criteria in 2012 defined AKI as an increase in the serum creatinine of ≥ 0.3 mg/dl (≥ 26.5μmol/l) within 48 h, ≥ 1.5 times the baseline within the previous 7 days, or a urine volume ≤ 0.5 ml/kg/h for 6 h. Since it was not convenient to obtain the patients' urine volume, AKI was diagnosed on the basis of the creatinine level change (12). Fever was measured as axillary temperature of 37.3°C or higher. Physical Examination and imaging were used to evaluate whether the patient had enlarged lymph nodes and hepatosplenomegaly. The recognition of edema is mainly depending on clinical signs. Vasopressors included norepinephrine, dopamine, epinephrine, phenylephrine, and vasopressin.

Statistical analysis

This analysis of data was performed using R software (version 4.0.3; The R Foundation for Statistical Computing), and $P<0.05$ was considered statistically significant for this study. Continuous variables were expressed as mean ± standard deviation, and categorical variables were expressed as frequencies and percentages. Independent samples t-test (normal distribution for continuous variables), Wilcoxon rank-sum test (skewed distribution for continuous variables), and Pearson chi-square test (categorical variables) were used to determine statistical differences between the AKI and non-AKI groups, respectively.

Because of the large number of predictor variables in this study, it is appropriate to adopt least absolute shrinkage and selection operator (LASSO) regression screening variables (glmnet package) in the development group. LASSO regression filters lambda by Ten-fold cross-validation (13). The initial screening variables after lasso regression were screened for colinearity before modeling, and the exclusion criteria were those with variance inflation factor (VIF) values ≥ 5. Cox regression was then applied to build the model and regression coefficients, standard error values, hazard ratio (HR), 95% confidence intervals (CI) and p-values were calculated for each variable in the model. For clinical convenience, we plotted nomogram following the relative weights of the variables in the model. According to the magnitude of the regression coefficients of each influence factor in the model, a score is assigned to each value level of each influence factor, and then the individual scores are summed to obtain the total score.

The area under the receiver operating characteristic (ROC) curve (AUC) and the concordance index (Harrell's concordance index/C-index) were used for model discrimination evaluation in the development and validation groups. Calculation of integrated discrimination improvement (IDI) to represent the role of baseline cystatin C in the model.

Results

Baseline characteristics of patients with HLH

During the 28 days of hospitalization, 136 (22.7%) patients developed AKI. Baseline characteristics of patients were shown in Table 1, including demographics, laboratory data, treatment regimens and clinical manifestations. There were 266 (57.33%) males in the non-AKI group and 79 (58.09%) males in the AKI group. The mean age of patients in the two groups was 41.56 ± 16.49 and 44.75 ± 17.30, respectively. Baseline creatinine was 69.12 ± 41.47 and 57.83 ± 23.12 umol/L, and baseline cystatin C was 1.57 ± 0.71 and 1.34 ± 0.46 mg/L for patients in the AKI and non-AKI groups, respectively.

Risk factors for the development of AKI in patients and Model building

We performed univariate cox regression analysis on all 600 patients and identified several factors that were highly associated with the occurrence of AKI (Table 2). To build the optimal AKI risk prediction model, we conducted LASSO regression analysis of all variables. The LASSO screening variable was calculated based on the maximum lambda corresponding to the selection error mean within 1 standard deviation of the minimum, i.e., lambda = 0.0565 and log(lambda) = -2.8734 (Figure 2). Twelve variables were obtained by lasso screening: vasopressor, mechanical ventilation, DIC, admission heart rate, hemoglobin (HGB), baseline cystatin C, phosphorus, total bilirubin, direct bilirubin, LDH, PT, and PCT (Figure 3). After covariate screening, direct bilirubin was excluded and the remaining 11 variables were combined to create a risk prediction model for AKI through COX regression. Modeling equations: Logit(Y)=0.28706*(vasopressor=1) +0.97581*(mechanical ventilation=1) +0.31892*(DIC=1) +0.02007*admission heart rate, -0.00676*HGB + 0.64382* baseline cystatin C +0.04119*phosphorus +0.00198* total bilirubin +0.00003*LDH +0.00392*PT+0.01527*PCT. The detailed parameters of each variable in the prediction model are shown in Table 3. Baseline cystatin C is an independent risk factor for AKI. We then plotted the nomogram based on the results of the COX regression (Figure 4).

Model evaluation

The model exhibited good predictive ability with AUC =0.760 for the development group and AUC =0.820 for the validation group (Figure 5). C-indexes were calculated in both the development (0.743) and validation set (0.810), indicating the reasonable accuracy of this model. The development group with baseline cystatin C had 4.2% higher predictive power compared with the one without baseline cystatin C (IDI=0.0420, 95%CI 0.0090~ 0.0780, P=0.0070). The validation group model prediction capability also improved by 7.3% (IDI=0.0730, 95% CI 0.0080~0.1570, P=0.0130).

Discussion

We derived and internally validated a predictive model for the development of AKI in patients hospitalized with HLH. Clinical prediction models (also 'risk scores') predict the incidence of a specific disease or mortality by combining multiple risk factors. Risk scores for a multitude of diseases were already clinically applicable to risk-stratify patients and guide treatments (14). Although some shortcomings, there were many other predictive models for secondary AKI that contributed to the improvement of the outcome of AKI patients to some extent (15, 16).

AKI is a clinical syndrome that is susceptible to multiple critical illnesses and usually signals a poor prognosis for the patients. Susantitaphong et al. investigated and found the prevalence of AKI in adults to be about 21.6% (17), which is consistent with our study (22.7%). However, sometimes AKI has an insidious clinical onset and there are no reliable diagnostic and prognostic markers for AKI in patients with HLH at present (2). The delay in AKI diagnosis worsens the severity and prognosis of AKI. Our predictive model can assist physicians in diagnosing AKI on time.

In our prediction model, patients with poor baseline renal function, rapid heart rate on admission, complicated DIC, lower hemoglobin, higher total bilirubin, LDH and PCT, serum

10.3389/fimmu.2022.987916

TABLE 1 Baseline characteristics of the AKI and non-AKI groups.

Variables	Non-AKI n = 464	AKI n = 136	P
AKI stage I		50 (36.76%)	
AKI stage II		44 (32.35%)	
AKI stage III		42 (30.88%)	
Age	41.56 ± 16.49	44.75 ± 17.30	0.051
Gender			0.875
Male (%)	266 (57.33%)	79 (58.09%)	
Female (%)	198 (42.67%)	57 (41.91%)	
Tobacco use (%)	141 (30.39%)	35 (25.74%)	0.295
Alcohol (%)	118 (25.43%)	40 (29.41%)	0.354
Glucocorticoid (%)	417 (89.87%)	122 (89.71%)	0.955
Etoposide (%)	215 (46.34%)	52 (38.24%)	0.095
Nephrotoxic drugs (%)	228 (49.14%)	67 (49.26%)	0.979
Chemotherapy (%)	136 (29.31%)	37 (27.21%)	0.634
Immunosuppressant (%)	159 (34.27%)	37 (27.21%)	0.123
Vasopressor (%)	84 (18.10%)	73 (53.68%)	<0.001
Mechanical ventilation (%)	44 (9.48%)	54 (39.71%)	<0.001
monoclonal antibodies (%)	32 (6.90%)	9 (6.62%)	0.91
Triggers of HLH			
Infection (%)	227 (48.92%)	60 (44.12%)	0.324
Tumor (%)	242 (52.16%)	74 (54.41%)	0.643
Autoimmune disease (%)	25 (5.39%)	9 (6.62%)	0.585
Undetermined (%)	21 (4.53%)	15 (11.03%)	0.005
≥2 causes (%)	61 (13.15%)	12 (8.82%)	0.175
Disease history			
Tuberculous (%)	11 (2.37%)	3 (2.21%)	0.911
Tumor lysis syndrome (%)	3 (0.65%)	8 (5.88%)	<0.001
Hypertension (%)	28 (6.03%)	14 (10.29%)	0.087
Diabetes (%)	16 (3.45%)	5 (3.68%)	0.899
Heart failure (%)	21 (4.53%)	20 (14.71%)	<0.001
Viral hepatitis (%)	51 (10.99%)	13 (9.56%)	0.634
Clinical manifestations of HLH			
Lymph nodes enlargement (%)	271 (58.41%)	85 (62.50%)	0.393
Splenomegaly (%)	347 (74.78%)	96 (70.59%)	0.328
Hepatomegaly (%)	164 (35.34%)	44 (32.35%)	0.519
Fever (%)	446 (96.12%)	133 (97.79%)	0.350
Edema (%)	165 (35.56%)	69 (50.74%)	0.001
DIC (%)	66 (14.22%)	46 (33.82%)	<0.001
Maximum body temperature during hospitalization (°C)	39.32 ± 1.00	39.44 ± 0.91	0.197
Admission heart rate (Times /min)	98.02 ± 18.11	104.60 ± 18.15	<0.001
Blood pressure			
Systolic pressure (mmHg)	110.97 ± 15.95	113.17 ± 16.10	0.16
Diastolic pressure (mmHg)	68.61 ± 11.79	70.63 ± 12.92	0.086
PLT ($\times 10^9$/L)	27.39 ± 33.41	17.14 ± 20.39	0.002
HGB (g/L)	65.14 ± 19.62	55.88 ± 14.66	<0.001
WBC ($\times 10^9$/L)	1.43 ± 1.77	1.42 ± 1.58	0.528
Baseline Scr (umol/L)	57.83 ± 23.12	69.12 ± 41.47	0.004
Baseline Cystatin C (mg/L)	1.34 ± 0.46	1.57 ± 0.71	<0.001
Calcium (mmol/L)	1.76 ± 0.20	1.68 ± 0.23	<0.001

(Continued)

TABLE 1 Continued

Variables	Non-AKI n = 464	AKI n = 136	P
Phosphorus (mmol/L)	0.90 ± 0.40	1.18 ± 0.69	<0.001
Potassium (mmol/L)	3.14 ± 0.54	3.29 ± 1.02	0.018
Sodium (mmol/L)	128.34 ± 5.34	126.15 ± 7.07	<0.001
Total bilirubin (umol/L)	70.91 ± 89.27	132.48 ± 134.64	<0.001
Direct bilirubin (umol/L)	55.91 ± 78.73	108.99 ± 110.49	<0.001
Indirect bilirubin (umol/L)	14.29 ± 14.62	23.51 ± 32.32	0.023
Albumin (g/L)	23.73 ± 4.82	21.53 ± 3.95	<0.001
Triglyceride (mmol / L)	4.66 ± 3.00	5.72 ± 3.85	<0.001
Cholesterol (mmol / L)	3.22 ± 2.68	2.75 ± 2.06	0.014
ALT (IU/L)	254.40 ± 340.79	381.82 ± 661.37	0.042
AST (IU/L)	416.12 ± 968.78	1126.30 ± 2213.91	<0.001
LDH (IU/L)	1703.34 ± 2119.80	3745.49 ± 4759.27	<0.001
LDL-C (mmol/L)	2.90 ± 35.15	0.83 ± 1.37	<0.001
LDL-H (mmol/L)	0.60 ± 1.46	0.89 ± 2.08	0.027
APTT (s)	61.03 ± 34.69	78.17 ± 42.04	<0.001
D-dimer (mg/l FEU)	12.94 ± 11.69	15.78 ± 13.02	0.045
Fibrinogen (g / L)	1.24 ± 0.94	1.08 ± 0.79	0.055
PT (s)	21.47 ± 22.75	31.89 ± 31.51	<0.001
PCT (ng/ml)	4.02 ± 8.51	9.21 ± 16.28	<0.001
Urine protein			0.068
0	70 (15.09%)	14 (10.29%)	
+/-	97 (20.91%)	25 (18.38%)	
+	234 (50.43%)	66 (48.53%)	
++	55 (11.85%)	25 (18.38%)	
+++	8 (1.72%)	6 (4.41%)	
Ferritin (ng/ml)			0.211
>2000	388 (83.62%)	122 (89.71%)	
≥500,≤2000	72 (15.52%)	13 (9.56%)	
<500	4 (0.86%)	1 (0.74%)	

AKI, Acute kidney injury; HLH, Hemophagocytic lymphohistiocytosis; DIC, Disseminated intravascular coagulation; PLT, Platelet; HGB, Hemoglobin; WBC, White blood cell; Scr, Serum creatinine; ALT, Aspartate transaminase; AST, Aspartate aminotransferase; LDH, Lactic dehydrogenase; LDL-C, Low density lipoprotein; LDL-H, High density lipoprotein; APTT, Activated partial prothrombin time; PT, Prothrombin time; PCT, Procalcitonin; RRT, Renal replacement therapy.

phosphorus abnormalities, PT extension, needing for vasopressor and mechanical ventilation were at high risk of AKI. Patients with fast heart rates were more likely to experience AKI (HR 1.0203, 95%CI 1.0083-1.0324, P=0.0008), which has also been identified and applied to the model by other investigators (18, 19). This may be due to the effects of tachycardia on cardiac function and cardiac output, and consequently a decrement in renal perfusion levels (20). Baseline cystatin C was an independent risk factor for the development of AKI (HR 1.9037, 95%CI 1.4432-2.5112, P<0.0001) and enhanced the predictive power of the model. Previous studies have revealed that patients with underlying renal insufficiency tend to have a higher risk of AKI (5, 21), and our study also supported this opinion. Oxidative stress, mitochondrial dysfunction, inflammatory response, vascular dysfunction and other pathological changes in CKD contribute to the heightened sensitivity of AKI (22).

Mild elevation of serum bilirubin protects against renal tubular injury *via* inhibition of oxidative stress and apoptosis, thereby protecting renal function (23, 24). By contrast, high levels of serum bilirubin lead to a lowering of arterial pulse pressure and intraglomerular pressure, exerting direct toxic effects on renal tubule (25–27). Total bilirubin only protects the kidney at <1.2 mg/dl (20.52 umol/L) and promotes the progression of AKI at >2.0 mg/dl (34.20 umol/L) (28). Serum total bilirubin was 84.86 ± 104.45 umol/L, and an independent risk factor for AKI (HR 1.002, 95%CI 1.0001-1.0039, P=0.0418), which is consistent with previous studies. Mechanical ventilation was associated with an elevated risk of AKI in patients (HR 2.6533, 95%CI 1.4766-4.7679, P=0.0011). The pathological

10.3389/fimmu.2022.987916

TABLE 2 Univariate analysis of COX regression in patients with HLH.

	HR (95%CI)	P
Tobacco use (%)	0.85 (0.58-1.25)	0.4105
Alcohol (%)	1.19 (0.83-1.73)	0.3477
Glucocorticoid (%)	0.77 (0.44-1.35)	0.3655
Etoposide (%)	0.63 (0.44-0.89)	0.0090
Nephrotoxic drugs (%)	0.85 (0.60-1.19)	0.3309
Chemotherapy (%)	0.74 (0.51-1.08)	0.1216
Immunosuppressant (%)	0.63 (0.43-0.91)	0.0151
Vasopressor (%)	3.57 (2.55-5.01)	<0.0001
Mechanical ventilation (%)	4.05 (2.87-5.71)	<0.0001
monoclonal antibodies (%)	0.78 (0.40-1.54)	0.4819
Hypertension (%)	1.54 (0.88-2.67)	0.1288
Diabetes (%)	1.08 (0.44-2.63)	0.8711
Heart failure (%)	2.36 (1.47-3.79)	0.0004
DIC (%)	2.79 (1.95-3.98)	<0.0001
Age	1.01 (1.00-1.02)	0.0463
Admission heart rate (Times /min)	1.02 (1.01-1.03)	<0.0001
PLT ($\times10^9$/L)	0.99 (0.98-0.99)	0.0014
HGB (g/L)	0.98 (0.97-0.99)	<0.0001
WBC ($\times10^9$/L)	1.03 (0.94-1.13)	0.5784
Baseline Scr (umol/L)	1.01 (1.01-1.01)	<0.0001
Baseline Cystatin C (mg/L)	2.08 (1.63-2.64)	<0.0001
Calcium(mmol/L)	0.37 (0.20-0.68)	0.0014
Phosphorus(mmol/L)	1.81 (1.46-2.25)	<0.0001
Potassium(mmol/L)	1.42 (1.16-1.73)	0.0007
Sodium(mmol/L)	0.96 (0.93-0.98)	<0.0001
Total bilirubin(umol/L)	1.00 (1.00-1.00)	<0.0001
Direct bilirubin(umol/L)	1.00 (1.00-1.01)	<0.0001
Indirect bilirubin(umol/L)	1.01 (1.01-1.02)	<0.0001
Albumin(g/L)	0.92 (0.89-0.96)	<0.0001
Triglyceride (mmol / L)	1.06 (1.02-1.11)	0.0051
Cholesterol (mmol / L)	0.92 (0.84-1.00)	0.0392
ALT (IU/L)	1.00 (1.00-1.00)	0.0054
AST (IU/L)	1.00 (1.00-1.00)	<0.0001
LDH (IU/L)	1.00 (1.00-1.00)	<0.0001
LDL-C (mmol/L)	0.81 (0.70-0.94)	0.0064
LDL-H (mmol/L)	1.08 (0.99-1.17)	0.0981
APTT(s)	1.01 (1.01-1.01)	<0.0001
D-dimer (mg/l FEU)	1.01 (1.00-1.03)	0.0363
Fibrinogen (g / L)	0.82 (0.66-1.03)	0.0829
PT(s)	1.01 (1.01-1.02)	<0.0001
PCT (ng/ml)	1.02 (1.01-1.03)	<0.0001

HLH, Hemophagocytic lymphohistiocytosis; DIC, Disseminated intravascular coagulation; PLT, Platelet; HGB, Hemoglobin; WBC, White blood cell; Scr, Serum creatinine; ALT, Aspartate transaminase; AST, Aspartate aminotransferase; LDH, Lactic dehydrogenase; LDL-C, Low density lipoprotein; LDL-H, High density lipoprotein; APTT, Activated partial prothrombin time; PT, Prothrombin time; PCT, Procalcitonin.

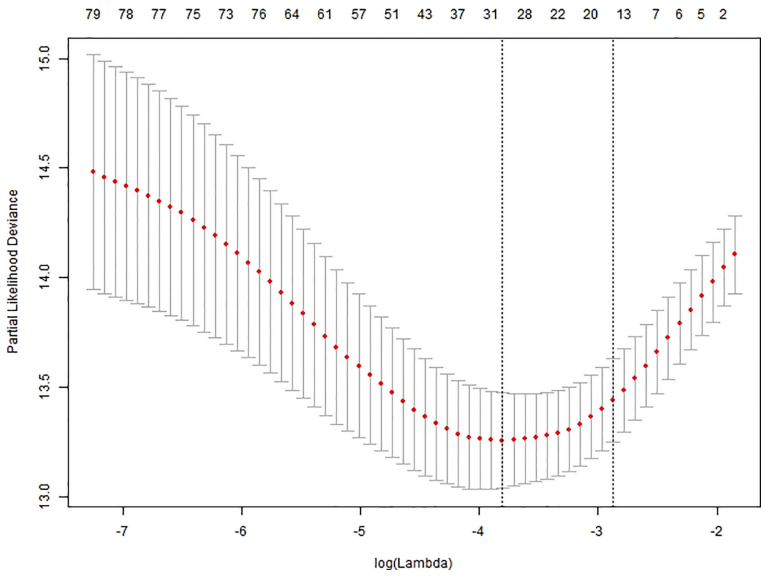

FIGURE 2
LASSO regression lambda filter graph. The horizontal coordinate is log(lambda) and the vertical coordinate is the mean and standard error of the deviance obtained from Ten-fold cross-validation.

mechanism is compatible with mechanical ventilation enhancing the action of inflammatory mediators, leading to epithelial cell apoptosis in the kidney and causing renal dysfunction (29).

To the best of our knowledge, this is the first prediction model for AKI in patients with HLH. This proposed study used LASSO regression to check the variables, and then based on COX regression modeling with different threshold values

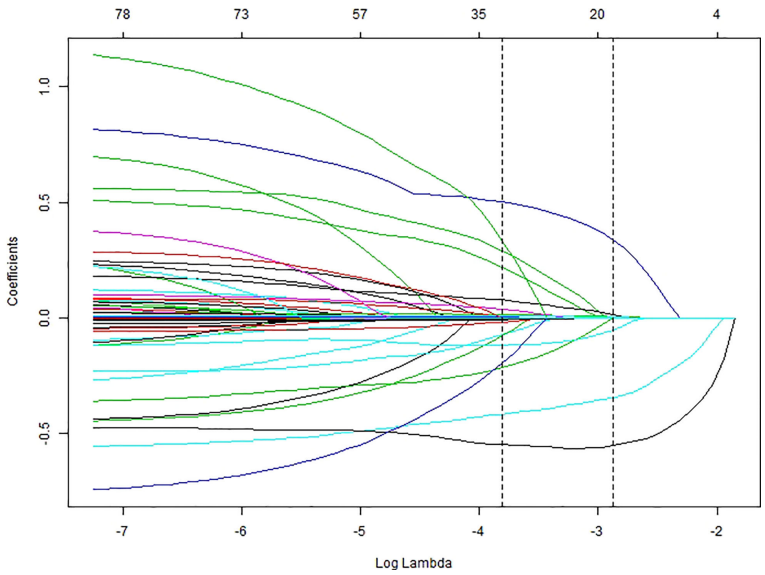

FIGURE 3
LASSO regression coefficients correspond to lambda values. The bottom scale of the horizontal coordinate is log(lambda), the top scale is the number of variables corresponding to the log(lambda) value, and the vertical coordinate is the lasso regression coefficient.

TABLE 3 Multivariate COX regression analysis of variables selected with LASSO for predicting AKI.

Variables	β	SE	HR	Lower 95%CI	Upper 95%CI	P
Vasopressor	0.2871	0.2968	1.3325	0.7448	2.384	0.3335
Mechanical ventilation	0.9758	0.299	2.6533	1.4766	4.7679	0.0011
DIC	0.3189	0.2745	1.3756	0.8033	2.3557	0.2452
Admission heart rate (Times /min)	0.0201	0.006	1.0203	1.0083	1.0324	0.0008
HGB (g/L)	-0.0068	0.0068	0.9933	0.9801	1.0066	0.3198
Baseline cystatin C(mg/L)	0.6438	0.1413	1.9037	1.4432	2.5112	<0.0001
Phosphorus(mmol/L)	0.0412	0.1549	1.0421	0.7692	1.4118	0.7903
Total bilirubin(umol/L)	0.002	0.001	1.002	1.0001	1.0039	0.0418
LDH(IU/L)	0	0	1	1	1.0001	0.2436
PT(s)	0.0039	0.0043	1.0039	0.9956	1.0123	0.3576
PCT (ng/ml)	0.0153	0.0084	1.0154	0.9988	1.0323	0.0697

DIC, Disseminated intravascular coagulation; HGB, Hemoglobin; LDH, Lactic dehydrogenase; PT, Prothrombin time; PCT, Procalcitonin; SE, Standard error; HR, Hazard ratio; CI, Confidence interval.

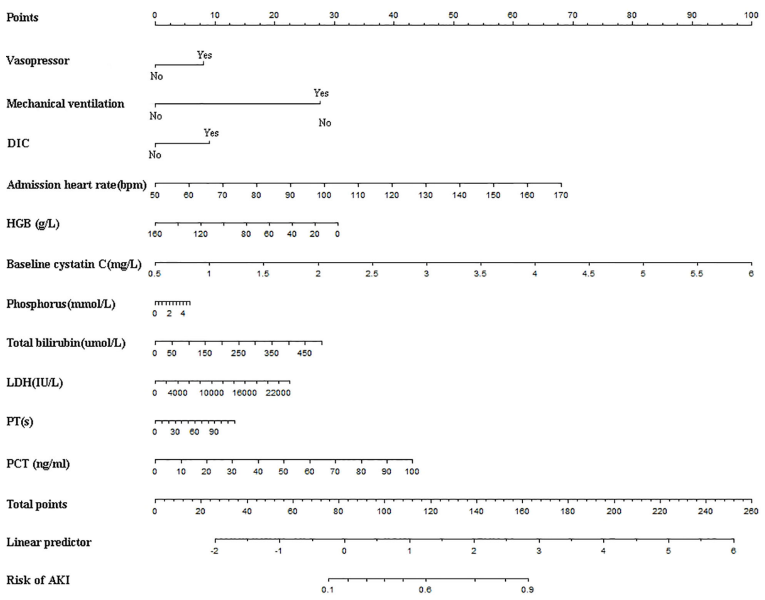

FIGURE 4
Nomogram for predicting the risk of AKI in patients with HLH. AKI, acute kidney injury; DIC, Disseminated intravascular coagulation; HGB, Hemoglobin; LDH, Lactic dehydrogenase; PT, Prothrombin time; PCT, Procalcitonin.

assigned to each variable. The design gives us the ability to evaluate the weighting of different variables in the diagnosis of AKI. The variables in our prediction model are common and easily accessible in clinical work, and the scoring system is simple and quick, making it easy for clinicians to quickly determine a patient's risk of AKI and take timely countermeasures. The strong predictive capability and accuracy of the model help us limit misdiagnosis and underdiagnosis.

This prediction model has some drawbacks as well. First, owing to the lack of urine volume, we diagnosed AKI based only on the level of creatinine change. Some patients suffering from AKI before admission may have been omitted. These may lead to underestimation of the incidence rates of AKI. Second, our study could not conclusively determine the cause of AKI occurrence. Retrospective cohort studies may be potentially subject to selection bias. Data for this study were obtained from a single center. Finally, our model was not externally validated, and in

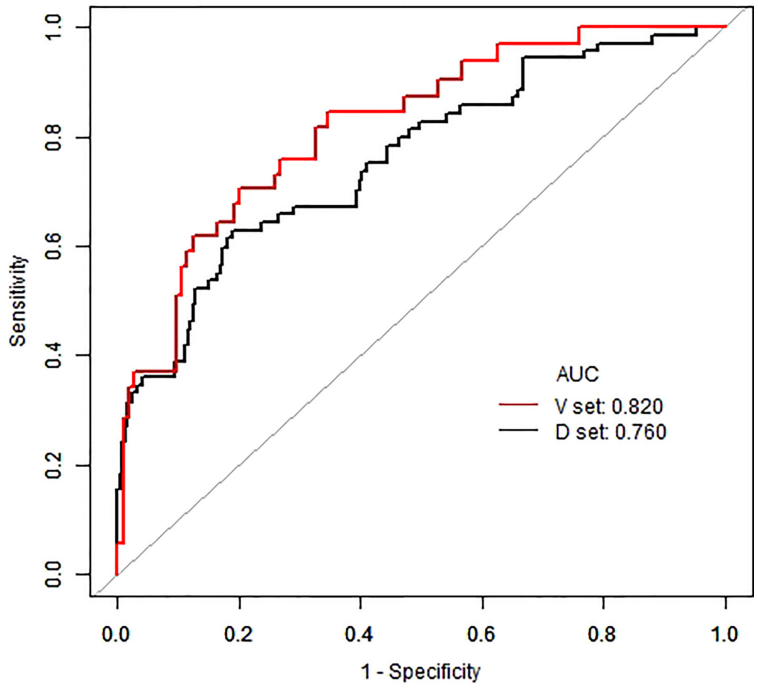

FIGURE 5
The ROC curves of development and validation set.

the future, we need to perform this work and assess its predictive power with long-term observation.

In conclusion, we developed a risk prediction model for AKI in HLH patients within 28 days of hospitalization. The model applies 11 predictive factors to stratify the risk of AKI occurrence. The predictive power and accuracy of the model are good, and the clinical application is convenient. These may facilitate closer monitoring and early treatment to prevent patients at imminent risk of AKI and heighten clinicians' alertness to patients at high risk of AKI.

Data availability statement

The datasets presented in this article are not readily available because the datasets were obtained from the database of West China Hospital and are available from the corresponding author on reasonable request. Requests to access the datasets should be directed to JZ, zhoujiaojiao@wchscu.cn.

Ethics statement

The studies involving human participants were reviewed and approved by the ethical committee of West China Hospital, Sichuan University. Written informed consent for participation was not required for this study in accordance with the national legislation and the institutional requirements.

Author contributions

SW and JZ formulated the experimental protocol. The authors SW, JY, XW, and XC collected and compiled relevant data. SW and JZ performed statistical analysis. SW wrote the manuscript and LY, JZ, and LJ revised and commented on the draft. LY and JZ supervised the whole process. JZ provided valuable advice and acquired funding. All authors contributed to the article and approved the submitted version.

Funding

This study was supported by grants from the National Natural Science Foundation of China [NO. 82102067] and 1·3·5 Project for Disciplines of Excellence–Clinical Research Incubation Project, West China Hospital, Sichuan University [NO. 2020HXFH049], Sichuan, China.

Acknowledgments

The authors are grateful to the West China Hospital of Sichuan University database for providing open access. We thank Spandidos Publications for the help in language polishing.

Conflict of interest

The authors declare that the research was conducted in the absence of any commercial or financial relationships that could be construed as a potential conflict of interest.

Publisher's note

All claims expressed in this article are solely those of the authors and do not necessarily represent those of their affiliated organizations, or those of the publisher, the editors and the reviewers. Any product that may be evaluated in this article, or claim that may be made by its manufacturer, is not guaranteed or endorsed by the publisher.

References

1. Al-Samkari H, Berliner N. Hemophagocytic lymphohistiocytosis. *Annu Rev Pathol: Mech Dis* (2018) 13(1):27–49. doi: 10.1146/annurev-pathol-020117-043625

2. Griffin G, Shenoi S, Hughes GC. Hemophagocytic lymphohistiocytosis: An update on pathogenesis, diagnosis, and therapy. *Best Pract Res Clin Rheumatol* (2020) 34(4):101515. doi: 10.1016/j.berh.2020.101515

3. Strauss R, Neureiter D, Westenburger B, Wehler M, Kirchner T, Hahn EG. Multifactorial risk analysis of bone marrow histiocytic hyperplasia with hemophagocytosis in critically ill medical patients–a postmortem clinicopathologic analysis. *Crit Care Med* (2004) 32(6):1316–21. doi: 10.1097/01.CCM.0000127779.24232.15

4. Ronco C, Bellomo R, Kellum JA. Acute kidney injury. *Lancet* (2019) 394 (10212):1949–64. doi: 10.1016/S0140-6736(19)32563-2

5. Chawla LS, Eggers PW, Star RA, Kimmel PL. Acute kidney injury and chronic kidney disease as interconnected syndromes. *N Engl J Med* (2014) 371 (1):58–66. doi: 10.1056/NEJMra1214243

6. Santoriello D, Hogan J, D'Agati VD. Hemophagocytic syndrome with histiocytic glomerulopathy and intraglomerular hemophagocytosis. *Am J Kidney Dis* (2016) 67(6):978–83. doi: 10.1053/j.ajkd.2015.11.017

7. Hashimoto H, Sugiura T, Matsushima H. Hemophagocytic syndrome with acute kidney injury accompanied by erythrophagocytic macrophages in the tubular lumen. *CEN Case Rep* (2019) 8(4):252–5. doi: 10.1007/s13730-019-00402-7

8. Bae MN, Kwak DH, Park SJ, Choi BS, Park CW, Choi YJ, et al. Acute kidney injury induced by thrombotic microangiopathy in a patient with hemophagocytic lymphohistiocytosis. *BMC Nephrology* (2016) 17(1):1–6. doi: 10.1186/s12882-015-0217-z

9. Aulagnon F, Lapidus N, Canet E, Galicier L, Boutboul D, Peraldi MN, et al. Acute kidney injury in adults with hemophagocytic lymphohistiocytosis. *Am J Kidney Dis* (2015) 65(6):851–9. doi: 10.1053/j.ajkd.2014.10.012

10. Henter JI, Horne A, Arico M, Egeler RM, Filipovich AH, Imashuku S, et al. HLH-2004: Diagnostic and therapeutic guidelines for hemophagocytic lymphohistiocytosis. *Pediatr Blood Cancer* (2007) 48(2):124–31. doi: 10.1002/pbc.21039

11. La Rosée P, Horne A, Hines M, von Bahr Greenwood T, Machowicz R, Berliner N, et al. Recommendations for the management of hemophagocytic lymphohistiocytosis in adults. *Blood J Am Soc Hematol* (2019) 133(23):2465–77. doi: 10.1182/blood.2018894618

12. Khwaja A. KDIGO clinical practice guidelines for acute kidney injury. *Nephron Clin Pract* (2012) 120(4):c179–184. doi: 10.1159/000339789

13. Tibshirani R. The lasso method for variable selection in the cox model. *Stat Med* (1997) 16(4):385–95. doi: 10.1002/(SICI)1097-0258(19970228)16:4<385::AID-SIM380>3.0.CO;2-3

14. Collins GS, Reitsma JB, Altman DG, Moons KG. Transparent reporting of a multivariable prediction model for individual prognosis or diagnosis (TRIPOD): the TRIPOD statement. *Br J Surg* (2015) 102(3):148–58. doi: 10.1002/bjs.9736

15. Patidar KR, Xu C, Shamseddeen H, Cheng YW, Ghabril MS, Mukthinuthalapati VVPK, et al. Development and validation of a model to predict acute kidney injury in hospitalized patients with cirrhosis. *Clin Transl Gastroenterol* (2019) 10(9):e00075. doi: 10.14309/ctg.0000000000000075

16. Zhou J, Bai Y, Wang X, Yang J, Fu P, Cai D, et al. A simple risk score for prediction of sepsis associated-acute kidney injury in critically ill patients. *J Nephrol* (2019) 32(6):947–56. doi: 10.1007/s40620-019-00625-y

17. Susantitaphong P, Cruz DN, Cerda J, Abulfaraj M, Alqahtani F, Koulouridis I, et al. World incidence of AKI: a meta-analysis. *Clin J Am Soc Nephrol.* (2013) 8 (9):1482–93. doi: 10.2215/CJN.00710113

18. Abusaada K, Yuan C, Sabzwari R, Butt K, Maqsood A. Development of a novel score to predict the risk of acute kidney injury in patient with acute myocardial infarction. *J Nephrol* (2017) 30(3):419–25. doi: 10.1007/s40620-016-0326-1

19. Queiroz RE, de Oliveira LS, de Albuquerque CA, Santana Cde A, Brasil PM, Carneiro LL, et al. Acute kidney injury risk in patients with ST-segment elevation myocardial infarction at presentation to the ED. *Am J Emerg Med* (2012) 30 (9):1921–7. doi: 10.1016/j.ajem.2012.04.011

20. Shacham Y, Leshem-Rubinow E, Gal-Oz A, Arbel Y, Keren G, Roth A, et al. Acute cardio-renal syndrome as a cause for renal deterioration among myocardial infarction patients treated with primary percutaneous intervention. *Can J Cardiol* (2015) 31(10):1240–4. doi: 10.1016/j.cjca.2015.03.031

21. Hsieh MJ, Chen YC, Chen CC, Wang CL, Wu LS, Wang CC. Renal dysfunction on admission, worsening renal function, and severity of acute kidney injury predict 2-year mortality in patients with acute myocardial infarction. *Circ J* (2013) 77(1):217–23. doi: 10.1253/circj.CJ-12-0539

22. He L, Wei Q, Liu J, Yi M, Liu Y, Liu H, et al. AKI on CKD: heightened injury, suppressed repair, and the underlying mechanisms. *Kidney Int* (2017) 92(5):1071–83. doi: 10.1016/j.kint.2017.06.030

23. Oh SW, Lee ES, Kim S, Na KY, Chae DW, Kim S, et al. Bilirubin attenuates the renal tubular injury by inhibition of oxidative stress and apoptosis. *BMC Nephrology* (2013) 14(1):1–12. doi: 10.1186/1471-2369-14-105

24. Chin HJ, Cho HJ, Lee TW, Na KY, Oh KH, Joo KW, et al. The mildly elevated serum bilirubin level is negatively associated with the incidence of end stage renal disease in patients with IgA nephropathy. *J Korean Med Sci* (2009) 24 (Suppl 1):S22–9. doi: 10.3346/jkms.2009.24.S1.S22

25. Boon AC, Bulmer AC, Coombes JS, Fassett RG. Circulating bilirubin and defense against kidney disease and cardiovascular mortality: mechanisms contributing to protection in clinical investigations. *Am J Physiol Renal Physiol* (2014) 307(2):F123–136. doi: 10.1152/ajprenal.00039.2014

26. Bhuiyan AR, Srinivasan SR, Chen W, Sultana A, Berenson GS. Association of serum bilirubin with pulsatile arterial function in asymptomatic young adults: the bogalusa heart study. *Metabolism* (2008) 57(5):612–6. doi: 10.1016/j.metabol.2007.12.003

27. van Slambrouck CM, Salem F, Meehan SM, Chang A. Bile cast nephropathy is a common pathologic finding for kidney injury associated with severe liver dysfunction. *Kidney Int* (2013) 84(1):192–7. doi: 10.1038/ki.2013.78

28. Wu YH, Wu CY, Cheng CY, Tsai SF. Severe hyperbilirubinemia is associated with higher risk of contrast-related acute kidney injury following contrast-enhanced computed tomography. *PloS One* (2020) 15(4):e0231264. doi: 10.1371/journal.pone.0231264

29. Imai Y, Parodo J, Kajikawa O, Imai Y, Parodo J, Kajikawa O, et al. Injurious mechanical ventilation and end-organ epithelial cell apoptosis and organ dysfunction in an experimental model of acute respiratory distress syndrome. *Jama* (2003) 289(16):2104–12. doi: 10.1001/jama.289.16.2104

frontiers | Frontiers in Immunology

TYPE Original Research
PUBLISHED 05 January 2023
DOI 10.3389/fimmu.2022.1074488

OPEN ACCESS

EDITED BY
Alessandra Stasi,
University of Bari Aldo Moro, Italy

REVIEWED BY
Vladimir M. Pisarev,
Federal Research and Clinical Center of Intensive Care Medicine and Rehabilitation, Russia
Ming-Jun Shi,
Department of Urology, Capital Medical University, China

*CORRESPONDENCE
Tongzu Liu
liutongzu@163.com
Xiaojie Bai
13476839931@163.com

†These authors have contributed equally to this work

SPECIALTY SECTION
This article was submitted to Inflammation, a section of the journal Frontiers in Immunology

RECEIVED 19 October 2022
ACCEPTED 15 December 2022
PUBLISHED 05 January 2023

CITATION
Cao Y, Bai C, Si P, Yan X, Zhang P, Yisha Z, Lu P, Tuoheti K, Guo L, Chen Z, Bai X and Liu T (2023) A novel model of urosepsis in rats developed by injection of Escherichia coli into the renal pelvis.
Front. Immunol. 13:1074488.
doi: 10.3389/fimmu.2022.1074488

A novel model of urosepsis in rats developed by injection of Escherichia coli into the renal pelvis

Yuanfei Cao[1†], Can Bai[1†], Penghui Si[1†], Xin Yan[1], Peng Zhang[2], Zuhaer Yisha[1†], Peixiang Lu[1], Kuerban Tuoheti[1], Linfa Guo[1], Zhao Chen[1], Xiaojie Bai[1*] and Tongzu Liu[1*]

[1]Department of Urology, Zhongnan Hospital of Wuhan University, Wuhan, China, [2]Institute of Hepatobiliary Diseases , Zhongnan Hospital of Wuhan University, Wuhan, China

Despite extensive research, urosepsis remains a life-threatening, high-mortality disease. Currently, animal models of urosepsis widely accepted by investigators are very scarce. This study aimed to establish a standardized and reproducible model of urosepsis in rats. Forty adult Wistar rats were randomly divided into four groups according to the concentration of injected E. coli suspensions: Sham, Sep 3×, Sep 6×, and Sep 12×. Because the ureter is so thin and fragile, no conventional needle can be inserted into the ureter, which is probably why rats are rarely used to develop models of urosepsis. To solve this problem, the left ureter was ligated in the first procedure. After 24 hours, the left ureter above the ligation was significantly dilated, then saline or different concentrations of E. coli at 3 ml/kg were injected into the left renal pelvis using a 30G needle. The left ureter was subsequently ligated again at a distance of 1 cm from the renal hilum to maintain high pressure in the renal pelvis. Following injection of E. coli or saline for 24 h, three rats from each group were sacrificed and their organs (lung, liver, and right kidney) were collected. In contrast, the remaining seven rats continued to be observed for survival. At 10 days after E. coli injection, rats in the sep12× group had a higher mortality rate (100%) compared to the sep3× group (28.6%) or the sep6× group (71.4%). The significant changes in peripheral blood WBC count, serum IL-6 and TNF-α levels were also in the sep12× group. In addition, rats in the sepsis group showed multi-organ dysfunction, including damage to the lungs, liver, and kidneys. The establishment of a standardized rat model of urosepsis may be of great value for studying the pathophysiological of urosepsis.

KEYWORDS

urosepsis, rats, animal model, *Escherichia coli*, upper urinary tract obstruction, pathophysiology

Introduction

Sepsis, a life-threatening organ dysfunction with rapid progression and high mortality (17-26%), is the leading cause of death in critically ill patients worldwide (1–3). Depending on the site of infection, infections originating in the urinary tract and/or male genital tract are referred to as urosepsis (4, 5). It is estimated that approximately 20-30% of all sepsis cases are urosepsis. In total, there are an estimated 31.5 million sepsis cases each year, representing a potential of up to 9.45 million cases of urosepsis (6). Therefore, sepsis and urosepsis have been recognized as very concerning problems by many hospitals and are made a global health priority by the World Health Organization. Despite many new research results in recent years, the pathophysiology of sepsis is still incompletely understood. Several animal models have been created that all seek to mimic the typical pathophysiological changes in septic patients to study the pathophysiological causes of sepsis.

Injection of endotoxin or bacteria, cecum ligation and puncture (CLP), and colonic ascending stent peritonitis (CASP) are the commonly used models of sepsis (7–9). Among these, the rodent cecum ligation and puncture (CLP) model of experimental sepsis has grown to be the most popular and is currently regarded as the gold standard for sepsis research (10–12). However, widely applied and standardized animal models of urosepsis are relatively rare. Some scholars have found that rabbits can be used to develop models of urosepsis by injecting E. coli into the renal pelvis (13–16). Rodents, the most widely used for experimental research, are rarely used to make models of urosepsis. Therefore, the establishment of a standardized rat model of urosepsis may rapidly advance the study of the pathophysiological mechanisms of urosepsis.

In this study, we attempted to utilize rats to produce a standardized and reproducible model of urosepsis by injecting E. coli into the renal pelvis. We evaluated the effectiveness of a rat model of urosepsis by observing survival rates and blood cultures, detecting changes in WBC and inflammatory factors, and verifying multi-organ damage to the lungs, liver, and kidneys. The establishment of a standardized rat model of urosepsis may be of great value for studying the pathophysiological of urosepsis.

Materials and methods

Animal

Adult Wistar rats of either sex (weight 250–300 g) were purchased from Beijing Speford Biotechnology Co. (Beijing, China). All experiments were performed at the Animal Research Institute of Zhongnan Hospital at Wuhan University. The animal study was evaluated and approved by the ethics committee of the Zhongnan Hospital at Wuhan University. Rats were raised at controlled temperature (21-25°C) and humidity (45-55%) with a 12-hour light/dark cycle for 7 days to acclimate to the environment.

Experimental procedures

Forty adult Wistar rats (250-300g) were randomly divided into four groups according to the concentration of injected E. coli suspensions: Sham (injected with saline), Sep 3× (injected with 3×10^8 cfu/mL E. coli), Sep 6× (injected with 6×10^8 cfu/mL E. coli), Sep 12× (injected with 12×10^8 cfu/mL E. coli).

Before the experiment, Wistar rats were fasted overnight but allowed to drink freely. All rats were anesthetized with intraperitoneally injected 30 mg/kg of 1% sodium pentobarbital. After anesthesia, the abdomen of the rats was shaved, and a 3 cm-long incision was performed on the left side of the abdomen. The abdominal cavity of the rats was opened to expose the left kidney, and the left ureter was carefully isolated. At a distance of 2 cm from the left renal hilus, we ligated the left ureter using 4-0 silk, placing the left kidney and intestine back into the abdominal cavity, closing the abdominal cavity, and suturing the skin. 24 h later, the rats were reanesthetized, and the abdominal cavity was reopened, showing that the left renal pelvis and left ureter were significantly dilated compared with those before ligation. Groups Sep3×, 6×, and 12× were injected with 3 ml/kg E. coli solution in the left ureter above the ligation at a concentration of 3×10^8, 6×10^8, and 12×10^8 cfu/ml, respectively. Saline was also injected into the left ureter of the sham group at 3 ml/kg. Subsequently, the left ureter was ligated again at a distance of 1 cm from the renal hilum to maintain a state of pelvic hypertension. The rats were then sutured and received postoperative analgesic meloxicam (1 mg/kg, s.c.).

Blood samples were collected at four postoperative time points (0h, 2h, 24h, and 48h). A portion of the fresh samples was utilized for routine blood testing (WBC count). Additional blood samples were processed at 3000 rpm for 20 minutes using a cryogenic centrifuge, and the supernatant was stored in a -80°C refrigerator for TNF-α and IL-6 assay.

Bacterial culture

Escherichia coli (E. coli) (ATCC 25922) was purchased from Guangdong Huankai Microbial Technology Co. and cultured on McConkey Agar (Solarbio Life Science Technology Co., Beijing, China) for 24h at 37°C to form individual colonies. Afterward, a single colony of bacteria was picked and inoculated in LB medium at 37°C with shaking at 200 rpm for 18-24h. The bacteria medium was precipitated by centrifugation at 2000g for 10 min and then resuspended in saline to a concentration of 3×10^8,6×10^8,12×10^8 cfu/mL. To ensure accurate concentration, bacterial suspensions were tested using a bacterial turbidimeter (Thermo Fisher Scientific, USA).

After injection of E. coli for 24h, blood samples were collected and inoculated onto MacConkey agar for 24h at 37°C. If pink colonies were found, E. coli in the blood was proven.

Clinical observations

After intrarenal pelvis injection of E. coli, rats were examined for general responses such as consciousness, activity, weakness, and mortality. Every 4-6 hours, rectal body temperature was measured (Thermometer type T15SGF; Panasonic, Japan), as well as respiratory rate, heart rate, and body weight. Rats were euthanized for humanitarian reasons when they reached a behavior score of 1, where 1 represented Moribund [adapted from Yang et (17)].

Measurement of WBC, Cytokines(IL-6, TNF-α), Serum CRE, BUN, AST, and ALT

White blood cell (WBC) counts were determined using an automatic hematology analyzer (Nihon Kohden, Japan). Rat serum concentrations of interleukin IL-6 and tumor necrosis factor-alpha (TNF-α) were determined by the Ellisa enzyme immunoassay kit (Wuhan antigene Biotechnology Co., Ltd. Wuhan, China) according to the manufacturer's protocol. Determination of markers of kidney function by BUN and CRE kits and changes in liver function by AST and ALT kits according to the manufacturer's instructions (Nanjing Jiancheng Institute of Biotechnology, Nanjing, China)

Real-time PCR

Under the manufacturer agreement, total RNA was extracted from bladder cancer cells using RaPure Total RNA Micro Kit (Magen, China). The RNA NanoPhotometer spectrophotometer (IMPLEN, Westlake Village, CA, USA) quantified the RNA at 260 nm/280 nm. Following the package recommendations, 2 μg of total RNA was reverse transcribed to cDNA utilizing ABScript II RT Master Mix (ABclonal, Wuhan, China). Using a Bio-Rad (Hercules, CA, USA) CFX96 system, qRT-PCR was used to ascertain the mRNA level of an interesting gene predicated upon SYBR green. The primer sequence is shown in Table S1. Each target gene's relative mRNA expression level was estimated using the 2–ΔΔCT method in conjunction with ACTB as an internal loading control.

Western blotting analysis

Cells were lysed sufficiently in RIPA that contained 1% protease inhibitor and 1% PMSF (all from Sigma-Aldrich, St. Louis, MO). 40 μg total protein was separated by 10–12.5% SDS-PAGE electrophoresis and transferred onto a polyvinylidene fluoride (PVDF) membrane (Millipore, cat# IPVH00010). After blocking with 5% skim milk at room temperature for 2 h, the membrane was first treated with the primary antibody (Table S2) at 4°C for an overnight period, followed by incubation with the secondary antibody—goat anti-rabbit IgG (Table S3)—at room temperature for an additional two hours. The bands on the membrane were monitored on a Tanon-5200 ECL imager (Tanon, Shanghai, China) and visualized by an enhanced chemiluminescence kit (Thermo Scientifisher, Waltham, MA, USA).

Immunohistochemical (IHC)

Formalin-fixed, paraffin-embedded tissue sections were first deparaffinized. And then, endogenous peroxidase activity was inhibited using H2O2. The indicated primary antibody (Table S2) and secondary antibody (Table S3) were added to the sections according to the suggested methods offered by the manufacturer. All the slides were examined under an inverted microscope at 200× magnification.

Statistical analysis

All experimental data were represented as the means ± standard error. Student t-tests or one-way ANOVA were employed to assess the statistical analyses, with $P < 0.05$ regarded as statistically significant.

Results

Surgical methods and critical points of the rat urosepsis model

To better investigate the mechanism of urosepsis, we tried to establish an animal model of urosepsis in rats. Briefly, we first ligated the left ureter, injected E. coli suspension into the dilated ureter after 24 h, and then ligated the left ureter again at 1 cm from the renal hilum to prevent the flow of E. coli out of the renal pelvis. Three rats in each group were killed at 24 h postoperatively, and the organs were collected, while the remaining seven rats continued to be observed for survival (Figure 1A). We found that the ureters of rats were very slim, not even more than 1 mm in diameter (Figure 1B), which made it extremely difficult to establish a model of urosepsis. After 24 h of ureteral ligation, the original slender ureter became significantly dilated, and its diameter could reach 3-4 mm (Figure 1C). We could easily inject E. coli into the dilated ureter using a syringe with a 30G needle (Figure 1D).

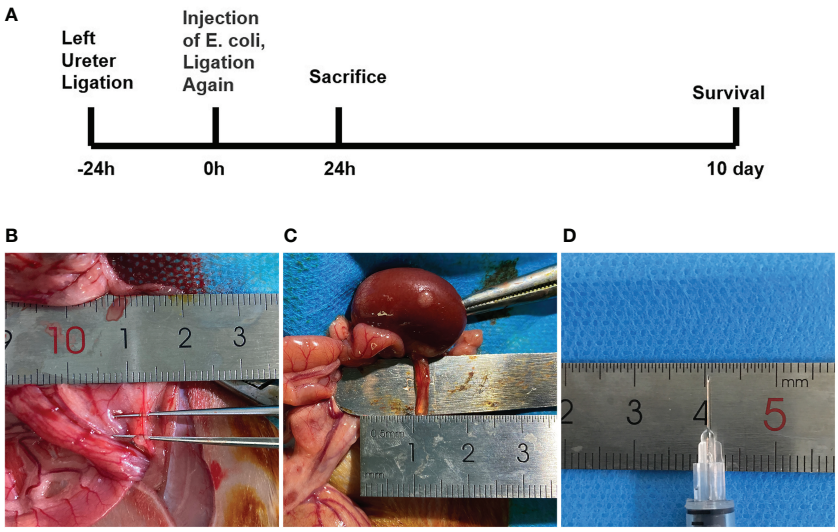

FIGURE 1
The experimental procedure and critical steps in the process of urinary sepsis model in rats.**(A)** Schematic diagram of the experimental procedure. **(B)** The ureter prior to ligation. **(C)** Dilated ureter after ligation for 24h. **(D)** 30G syringe needle.

Characterization of urosepsis in rats.

We detected that greater concentrations of E. coli led to higher mortality in rats at 10 days, with 28.6% mortality in the sep 3× group, 71.4% mortality in the sep 6× group, and 100% mortality in the sep 12× group (Figure 2A). After 24 h of E. coli or saline injection, all rats were tested by blood culture. Figure 2B showed that blood cultures were positive in the three sepsis groups while negative in the sham group. In addition, we collected blood samples at four-time points (0h, 2h, 24h, and 48h postoperatively) for WBC counts. And the data performed statistically significant changes in WBC of all rats 2h after renal pelvis injection of E. coli solution compared to preoperative values except for the control group. These changes were most

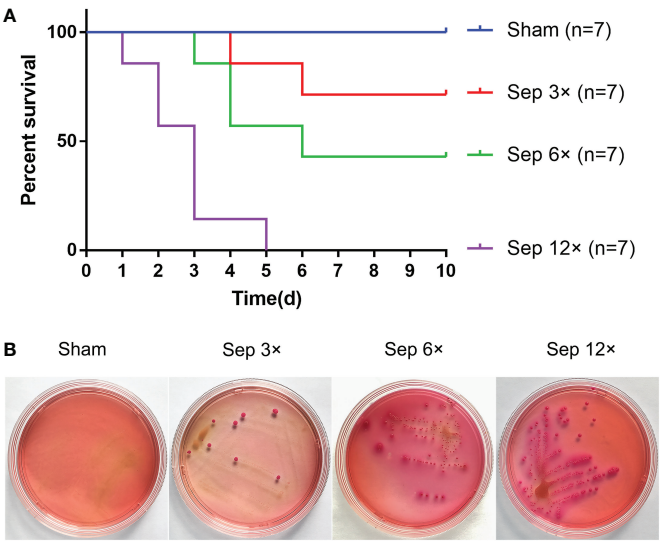

FIGURE 2
Survival analysis and Blood cultures after ureter ligation and inoculation of E coli. **(A)** Survival analysis after ureter ligation and inoculation of *E coli*. **(B)** Blood specimens were incubated on MacConkey agar at 37°C after 24h inoculation with *E coli*.

evident in the sep12× group with a mean ± SD WBC of 1.24 ± 0.47× 109/L (Figure 3A). Similarly, the changes in IL-6 and TNF-α levels were most remarkable in the sep12× group with mean± SD values of 114.78 ± 7.18 pg/mL and 531.46± 61.99 ng/L, respectively. It is important to note that the increase in IL6 and TNF-α concentrations occurred at 24h postoperatively instead of 2h (Figures 3B, C).

Lung injury in the rat model of urosepsis

The sep 6× group was selected as a representative of the sepsis groups compared with the sham group. HE staining examination (Figure 4A) showed that the alveolar wall was widened, and the alveolar lumen collapsed in most areas due to edema in the sepsis group. At the same time, the alveolar wall and alveolar lumen of the sepsis group also had a large number of inflammatory cell infiltrates and erythrocyte exudates. Immunohistochemical (IHC) analysis of paraffin-embedded lungs illustrated that the levels of IL-6 and TNF-α were considerably greater in the sepsis group than in the sham group (Figure 4A). As shown in Figure 4B, there was a statistically significant difference in the relative mRNA levels of IL-6 and TNF-α in the lung tissue of the sepsis group vs the sham group ($P<0.05$). Furthermore, compared with the sham group, Western blotting analysis of the collected lung tissues revealed that the expression levels of IL-6 and TNF-α proteins were increased in the model sepsis group (Figures 4C–E).

Liver injury in the rat model of urosepsis

Histopathological examination proved that liver sections from sepsis rats had features of liver injury, such as inflammatory infiltration, disorganized cell arrangement, vacuolated necrosis, and ductal hyperplasia(Figure 5A). And serum levels of ALT and AST were elevated (compared to sham surgery) due to sepsis-induced liver injury (Figures 5B, C). In addition, we also performed a reverse transcription-polymerase chain reaction (RT-PCR) analysis on the livers of rats (Figure 5D). The relative mRNA levels of IL-6 and TNF-α were significantly higher than those of the sham group ($P<0.01$). Immunohistochemistry and Western blotting analysis of liver tissue also revealed that the levels of IL-6 and TNF-α protein expression were considerably greater in the sepsis group (Figures 5A–G).

Kidney injury in the rat model of urosepsis

We performed HE staining of the right kidney tissue and discovered that renal tissue sections from the sepsis group had apparent features of renal injury, such as vacuolar degeneration of renal tubular epithelial cells, separation of renal tubular epithelial cells, and inflammatory cell infiltration (Figure 6A). Using measurements of serum biochemical parameters in rats, we demonstrated that serum Cre and BUN were significantly increased in the sepsis group 24 h after E. coli injection (Figures 6B, C). The most significant elevation of serum Cr and BUN was examined in the sep 12× group compared to the sham group. In addition, RT-PCR analysis of rat livers (Figure 6D) revealed that the relative mRNA levels of IL-6 and TNF-α were considerably greater than those in the sham group. Finally, we identified that IL-6 and TNF-α protein expression levels were significantly elevated in the sepsis group by immunohistochemistry and Western blotting analysis of renal tissues compared to the sham group (Figures 6A, 6E–G).

Discussion

This research depicts a standardized rat model of urosepsis with ligation of one ureter and consequent injection of Escherichia coli. The experimental results demonstrate our success in developing a standardized model of urosepsis in rats and confirm a significant correlation between the severity of urosepsis and the concentration of inoculated E. coli.

The incidence of urosepsis is increasing approximately 8.7% per year, which is closely linked to the widespread availability of upper urinary tract endoscopic procedures (18). In addition to stone co-infection and prolonged surgery, high intraoperative

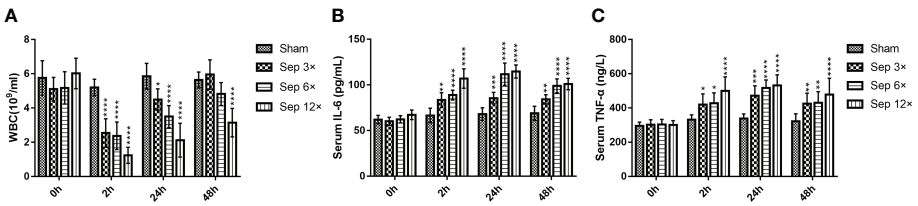

FIGURE 3
Changes in WBC **(A)**, serum IL-6 **(B)**, and serum TNF-α **(C)** in rats at different E coli concentrations and intervals. Values were shown as mean ± SD. *P < 0.05, **P < 0.01, ***P <0.001, and ****P < 0.0001 vs sham group.

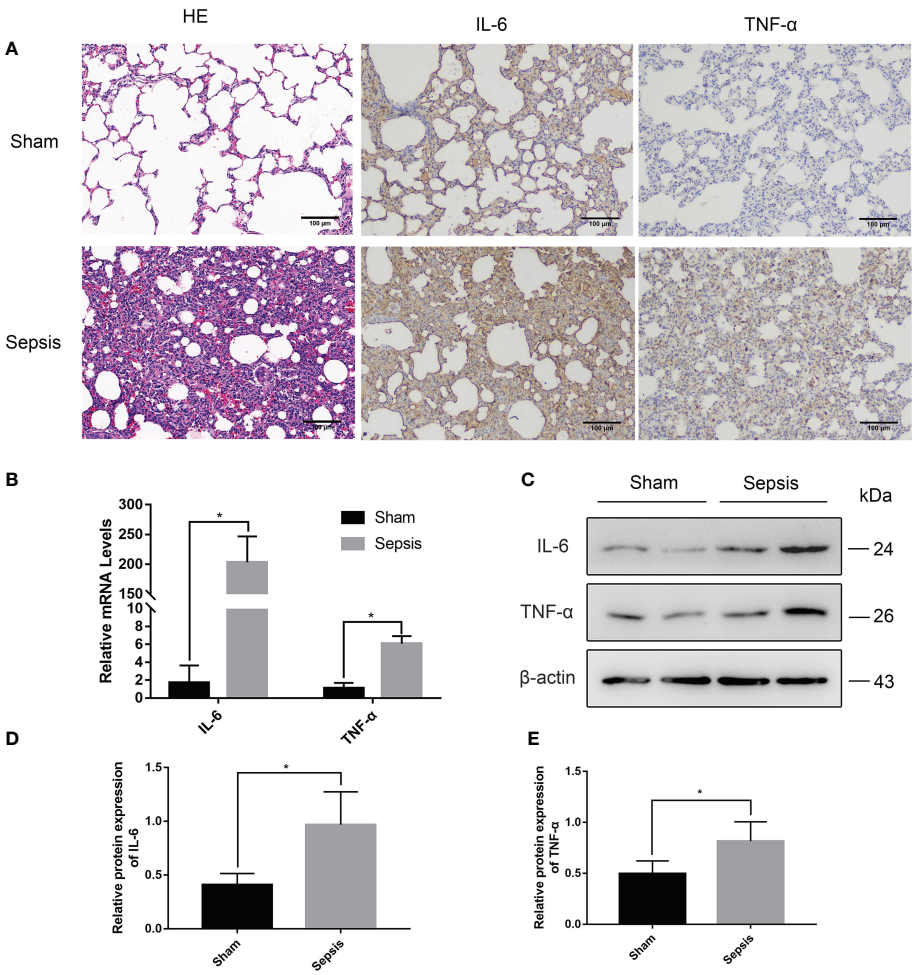

FIGURE 4
Lung injury in the rat model of urinary sepsis. **(A)** Representative images of hematoxylin and eosin **(H&E)** staining of lung tissue from the sham and sepsis groups, immunohistochemical analysis of IL-6 and TNF-α in lung tissue. **(B)** The relative mRNA levels of IL-6 and TNF-α in the lung tissue. **(C)** Expressions of IL-6 and TNF-α in lung tissue were tested by western blot, and β-actin was used as a loading control. **(D, E)** Quantitative data of the levels of IL-6 and TNF-α. The sep 6× group was selected as a representative of the sepsis groups. Values were shown as mean ± SD. *P < 0.05, vs sham group.

pelvic pressure leading to bacterial entry into the bloodstream is also a factor contributing to the development of urosepsis (19). Nguyen et al. (20) demonstrated that when the renal pelvic pressure exceeds 40 cm H_2O, the urine can reflux into the bloodstream carrying bacteria and metabolic waste products. Wu et al. (13) discovered that E. coli was injected into the renal pelvis at 2 ml/kg to maintain intrapelvic hypertension, leading to the development of a New Zealand rabbit model of urosepsis. In a preliminary pre-experiment, we observed low mortality in rats when 2 ml/kg of E. coli was injected into the renal pelvis. We hypothesized that intrapelvic injection of a small number of bacteria leads to a pyelonephritis model rather than a urosepsis model because of insufficient pressure in the renal pelvis. Gupta K et al. established pyelonephritis models by injecting small amounts of bacteria into the renal pelvis of rats or rabbits (21, 22), which confirmed our hypothesis. After several attempts, we finally chose to inject 3ml/kg of E. coli into the renal pelvis. Autopsy of the dead rats revealed that the left kidney was enlarged while renal parenchyma was thinned, and the renal capsule was intact without rupture, indicating that the injection dose of 3 ml/kg was safe. Therefore, we believe that maintaining renal pelvic hypertension is necessary for this urosepsis model.

CLP is similar to the clinical development of human sepsis, which is why it has been called the gold standard for sepsis research (23). The model features a pathogen from the host interior and mimics the pathogenesis of peritonitis (24). However, the severity of sepsis is not well standardized due to the difficulty of quantifying surgical operations, such as the percentage of cecum ligation and the dose of bacteria that enter the peritoneum after the puncture (25). Therefore, Rittirsch et al. renormalized the details of the CLP

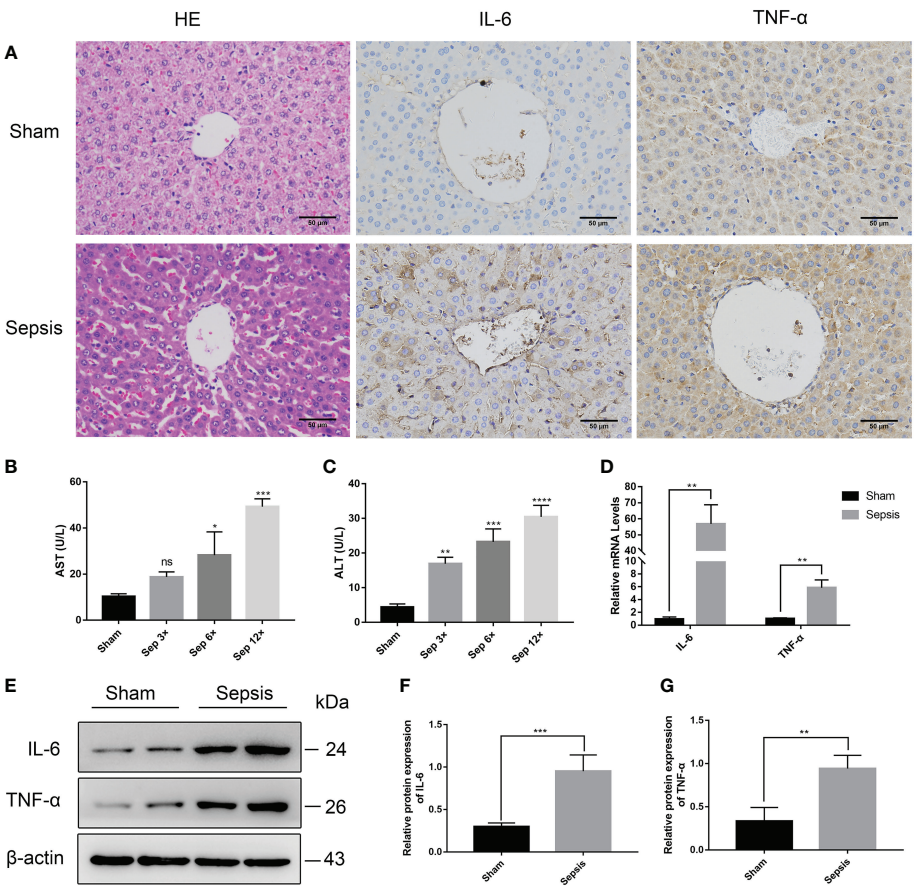

FIGURE 5
Liver injury in the rat model of urinary sepsis **(A)** Representative images of hematoxylin and eosin **(H&E)** staining of liver tissue from the sham and sepsis groups, immunohistochemical analysis of IL-6 and TNF-α in liver tissue (magnification, 200×; bar). **(B, C)** Serum AST and ALT levels in rats 24 hours after E. coli or saline inoculation of the renal pelvis. **(D)** The relative mRNA levels of IL-6 and TNF-α in the lung tissue. **(E)** Expressions of IL-6 and TNF-α in liver tissue were tested by western blot, and β-actin was used as a loading control. **(F, G)** Quantitative data of the levels of IL-6 and TNF-α. The sep 6× group was selected as a representative of the sepsis groups. Values were shown as mean ± SD. *P < 0.05, **P < 0.01, ***P <0.001, and ****P < 0.0001 vs sham group. "ns" means "not signifcant".

technique to control the severity of sepsis by the length of the ligated cecum and the size and/or the number of punctures (26). In our study, we obtained a similar mortality rate using ligation of the ureter 1 cm from the renal hilum to standardize the surgical procedure. Compared to the CLP technique of regulating the ligation site of the cecum, it is undoubtedly much simpler to adjust different concentrations of E. coli to achieve control of sepsis severity in our experiments.

The host inflammatory response might be seen as a balanced response between pro-inflammatory and anti-inflammatory mediators (27). In the early stages of sepsis, activation of the host's innate immune system leads to a massive release of pro-inflammatory mediators, the main ones including IL-6 and TNF-α, as well as chemokines (24, 28). In various animal models of sepsis, IL-6 and TNF-α expression were significantly elevated compared to the normal group (29–31). Besides, plasma IL-6 levels have been found to be potential indicators of the intensity of inflammation and mortality predictions (32). As the concentration of inoculated E. coli increased, we observed a significant increase in serum IL-6 and TNF-α levels, indicating that adjusting the concentration of E. coli could control the severity of sepsis in our study.

In contrast, peripheral blood WBC counts were significantly decreased in the Sep 12× group at 2 h postoperatively after E. coli inoculation. Wu et al. (13) revealed a decrease in WBC counts 2 h after formation in a New Zealand rabbit model of urosepsis, which is consistent with our results.

In 2016, sepsis was redefined as life-threatening organ dysfunction resulting from dysregulated host responses to infection (33). The severity of organ dysfunction is quantified using the Sequential Organ Failure Assessment (SOFA) score (34). Compared to the previous definition, the new version of the definition of sepsis places more emphasis on multi-organ damage. Our data suggested that the relative mRNA levels and protein levels of inflammatory factors (IL-6 and TNF-a)

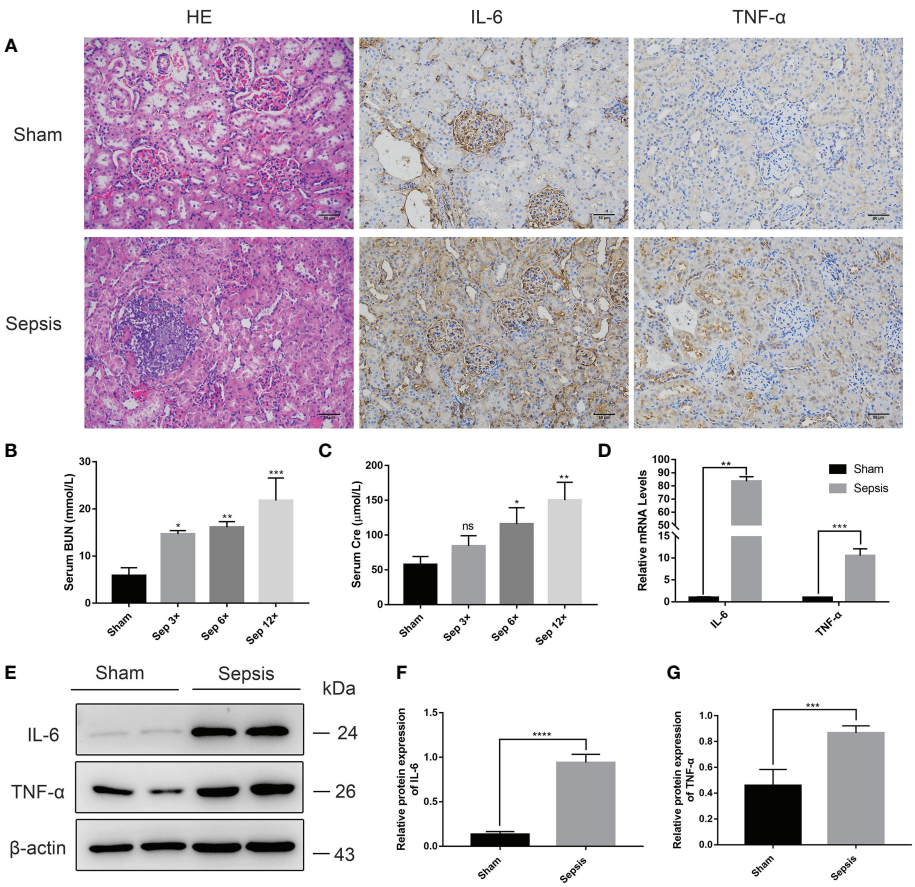

FIGURE 6
Kidney injury in the rat model of urinary sepsis **(A)** Representative images of hematoxylin and eosin **(H&E)** staining of kidney tissue from the sham and sepsis groups, immunohistochemical analysis of IL-6 and TNF-α in kidney tissue (magnification, 200×; bar, 50 μm). **(B, C)** Serum BUN and Cre levels in rats 24 hours after E. coli or saline inoculation of the renal pelvis. **(D)** The relative mRNA levels of IL-6 and TNF-α in kidney tissue. **(E)** Expressions of IL-6 and TNF-α in kidney tissue were tested by western blot, and β-actin was used as a loading control. **(F, G)** Quantitative data of the levels of IL-6 and TNF-α. The sep 6× group was selected as a representative of the sepsis groups. Values were shown as mean ± SD. *P < 0.05, **P < 0.01, ***P <0.001, and ****P < 0.0001 vs sham group. "ns" means "not signifcant".

extracted from three organs—the lung, liver, and kidney—were considerably greater in the sepsis group than in the sham group. Our rat urosepsis model confirmed three organ damages by HE staining, immunohistochemistry, RT-PCR, and Western blotting.

Conclusions

Current animal sepsis models do not fully replicate the pathophysiological process of human sepsis. In this study, our novel rat sepsis model simulates human urosepsis due to upper urinary tract obstruction combined with urinary tract infection. In addition, this model can manipulate the severity of sepsis by adjusting the concentration of E. coli suspensions. Therefore, this rat model may be an essential tool for studying the pathophysiological mechanisms of sepsis or urosepsis.

Data availability statement

The original contributions presented in the study are included in the article/Supplementary Material. Further inquiries can be directed to the corresponding authors.

Ethics statement

The animal study was reviewed and approved by Zhongnan Hospital of Wuhan University's Ethics Committee.

Author contributions

YC, CB, and PS designed the study, analyzed the data, and prepared the original draft. YC, XY, and PZ collected the data and conducted the statistical analysis. ZY, PL, and KT collected the data.

LG and ZC raised rats. YC wrote the paper. XB and TL designed and monitored the study, together with significant revisions to the manuscript. All authors have approved the final draft submitted.

Acknowledgments

We are very grateful to the laboratory staff at the Zhongnan Hospital of Wuhan University for their help in completing this study.

Conflict of interest

The authors declare that the research was conducted in the absence of any commercial or financial relationships that could be construed as a potential conflict of interest.

Publisher's note

Supplementary material

The Supplementary Material for this article can be found online at: https://www.frontiersin.org/articles/10.3389/fimmu.2022.1074488/full#supplementary-material

References

1. Rudd KE, Johnson SC, Agesa KM, Shackelford KA, Tsoi D, Kievlan DR, et al. Global, regional, and national sepsis incidence and mortality, 1990-2017: Analysis for the global burden of disease study. *Lancet.* (2020) 395(10219):200–11. doi: 10.1016/S0140-6736(19)32989-7

2. Dreger NM, Degener S, Ahmad-Nejad P, Wöbker G, Roth S. Urosepsis–etiology, diagnosis, and treatment. *Dtsch Arztebl Int* (2015) 112(49):837–47. doi: 10.3238/arztebl.2015.0837

3. Fleischmann C, Scherag A, Adhikari NKJ, Hartog CS, Tsaganos T, Schlattmann P, et al. Assessment of global incidence and mortality of hospital-treated sepsis. current estimates and limitations. *Am J Respir Crit Care Med* (2016) 193(3):259–72. doi: 10.1164/rccm.201504-0781OC

4. Bonkat G, Cai T, Veeratterapillay R, Bruyère F, Bartoletti R, Pilatz A, et al. Management of urosepsis in 2018. *Eur Urol Focus* (2019) 5(1):5–9. doi: 10.1016/j.euf.2018.11.003

5. Wagenlehner FME, Pilatz A, Weidner W. Urosepsis–from the view of the urologist. *Int J Antimicrob Agents* (2011) 38 Suppl:51–7. doi: 10.1016/j.ijantimicag.2011.09.007

6. Rhodes A, Evans LE, Alhazzani W, Levy MM, Antonelli M, Ferrer R, et al. Surviving sepsis campaign: International guidelines for management of sepsis and septic shock: 2016. *Intensive Care Med* (2017) 43(3):304–77. doi: 10.1007/s00134-017-4683-6

7. Fink MP. Animal models of sepsis. *Virulence.* (2014) 5(1):143–53. doi: 10.4161/viru.26083

8. Männel DN. Advances in sepsis research derived from animal models. *Int J Med Microbiol* (2007) 297(5):393–400. doi: 10.1016/j.ijmm.2007.03.005

9. van der Poll T. Preclinical sepsis models. *Surg Infect (Larchmt)* (2012) 13 (5):287–92. doi: 10.1089/sur.2012.105

10. Rittirsch D, Hoesel LM, Ward PA. The disconnect between animal models of sepsis and human sepsis. *J Leukoc Biol* (2007) 81(1):137–43. doi: 10.1189/jlb.0806542

11. Deitch EA. Rodent models of intra-abdominal infection. *Shock.* (2005) 24 Suppl 1:19–23. doi: 10.1097/01.shk.0000191386.18818.0a

12. Buras JA, Holzmann B, Sitkovsky M. Animal models of sepsis: Setting the stage. *Nat Rev Drug Discovery* (2005) 4(10):854–65. doi: 10.1038/nrd1854

13. Wu H, Zhu S, Yu S, Ding G, Xu J, Li T, et al. Early drastic decrease in white blood count can predict uroseptic shock induced by upper urinary tract endoscopic lithotripsy: a translational study. *J Urol* (2015) 193(6):2116–22. doi: 10.1016/j.juro.2015.01.071

14. Wu H, Wang Z, Zhu S, Rao D, Hu L, Qiao L, et al. Uroseptic shock can be reversed by early intervention based on leukocyte count 2 h post-operation: Animal model and multicenter clinical cohort study. *Inflammation.* (2018) 41(5):1835–41. doi: 10.1007/s10753-018-0826-3

15. Qiu H, Chen X, Luo Z, Zhao L, Zhang T, Yang N, et al. Inhibition of endogenous hydrogen sulfide production exacerbates the inflammatory response during urine-derived sepsis-induced kidney injury. *Exp Ther Med* (2018) 16 (4):2851–8. doi: 10.3892/etm.2018.6520

16. Ge G, Zheng Q, Sun Z, Wang H, Wang H, Ren K, et al. Proteomic signature of urosepsis: From discovery in a rabbit model to validation in humans. *J Proteome Res* (2021) 20(8):3889–99. doi: 10.1021/acs.jproteome.1c00189

17. Yang B, Bundkirchen K, Krettek C, Relja B, Neunaber C. Traumatic injury pattern is of equal relevance as injury severity for experimental (poly)trauma modeling. *Sci Rep* (2019) 9(1):5706. doi: 10.1038/s41598-019-42085-1

18. Martin GS, Mannino DM, Eaton S, Moss M. The epidemiology of sepsis in the united states from 1979 through 2000. *N Engl J Med* (2003) 348(16):1546–54. doi: 10.1056/NEJMoa022139

19. Mariappan P, Tolley DA. Endoscopic stone surgery: minimizing the risk of post-operative sepsis. *Curr Opin Urol* (2005) 15(2):101–5. doi: 10.1097/01.mou.0000160624.51484.60

20. Nguyen MJ, Higashi R, Ohta K, Nakamura KI, Hashitani H, Lang RJ. Autonomic and sensory nerve modulation of peristalsis in the upper urinary tract. *Auton Neurosci* (2016) 200:1–10. doi: 10.1016/j.autneu.2015.07.425

21. Gupta K, Donnola SB, Sadeghi Z, Lu L, Erokwu BO, Kavran M, et al. Intrarenal injection of escherichia coli in a rat model of pyelonephritis. *J Vis Exp* (2017) 125:54649. doi: 10.3791/54649

22. Giamarellos-Bourboulis EJ, Antonopoulou A, Raftogiannis M, Koutoukas P, Tsaganos T, Tziortzioti V, et al. Clarithromycin is an effective immunomodulator when administered late in experimental pyelonephritis by multidrug-resistant pseudomonas aeruginosa. *BMC Infect Dis* (2006) 6:31. doi: 10.1186/1471-2334-6-31

23. Wichterman KA, Baue AE, Chaudry IH. Sepsis and septic shock–a review of laboratory models and a proposal. *J Surg Res* (1980) 29(2):189–201. doi: 10.1016/0022-4804(80)90037-2

24. Dejager L, Pinheiro I, Dejonckheere E, Libert C. Cecal ligation and puncture: the gold standard model for polymicrobial sepsis? *Trends Microbiol* (2011) 19 (4):198–208. doi: 10.1016/j.tim.2011.01.001

25. Doi K, Leelahavanichkul A, Yuen PST, Star RA. Animal models of sepsis and sepsis-induced kidney injury. *J Clin Invest* (2009) 119(10):2868–78. doi: 10.1172/JCI39421

26. Rittirsch D, Huber-Lang MS, Flierl MA, Ward PA. Immunodesign of experimental sepsis by cecal ligation and puncture. *Nat Protoc* (2009) 4(1):31–6. doi: 10.1038/nprot.2008.214

27. Angus DC, van der Poll T. Severe sepsis and septic shock. *N Engl J Med* (2013) 369(9):840–51. doi: 10.1056/NEJMra1208623

28. Matsukawa A, Hogaboam CM, Lukacs NW, Lincoln PM, Strieter RM, Kunkel SL. Endogenous monocyte chemoattractant protein-1 (MCP-1) protects mice in a model of acute septic peritonitis: cross-talk between MCP-1 and leukotriene B4. *J Immunol* (1999) 163(11):6148–54.

29. Çakır M, Tekin S, Okan A, Çakan P, Doğanyiğit Z. The ameliorating effect of cannabinoid type 2 receptor activation on brain, lung, liver and heart damage in cecal ligation and puncture-induced sepsis model in rats. *Int Immunophar* (2020) 78:105978. doi: 10.1016/j.intimp.2019.105978

30. Sutherland RE, Olsen JS, McKinstry A, Villalta SA, Wolters PJ. Mast cell IL-6 improves survival from klebsiella pneumonia and sepsis by enhancing neutrophil killing. *J Immunol* (2008) 181(8):5598–605. doi: 10.4049/jimmunol.181.8.5598

31. Chou K-T, Cheng S-C, Huang S-F, Perng D-W, Chang S-C, Chen Y-M, et al. Impact of intermittent hypoxia on sepsis outcomes in a murine model. *Sci Rep* (2019) 9(1):12900. doi: 10.1038/s41598-019-49381-w

32. Remick DG, Bolgos GR, Siddiqui J, Shin J, Nemzek JA. Six at six: interleukin-6 measured 6 h after the initiation of sepsis predicts mortality over 3 days. *Shock*. (2002) 17(6):463–7. doi: 10.1097/00024382-200206000-00004

33. Singer M, Deutschman CS, Seymour CW, Shankar-Hari M, Annane D, Bauer M, et al. The third international consensus definitions for sepsis and septic shock (Sepsis-3). *JAMA*. (2016) 315(8):801–10. doi: 10.1001/jama.2016.0287

34. Cecconi M, Evans L, Levy M, Rhodes A. Sepsis and septic shock. *Lancet*. (2018) 392(10141):75–87. doi: 10.1016/S0140-6736(18)30696-2

Frontiers in Immunology

Explores novel approaches and diagnoses to treat immune disorders.

The official journal of the International Union of Immunological Societies (IUIS) and the most cited in its field, leading the way for research across basic, translational and clinical immunology.

Discover the latest Research Topics

See more →

Frontiers

Avenue du Tribunal-Fédéral 34
1005 Lausanne, Switzerland
frontiersin.org

Contact us

+41 (0)21 510 17 00
frontiersin.org/about/contact